



Durham E-Theses

Diethynylrhodacyclopentadienes: a new class of luminescent organometallics

Ward, Richard M.

How to cite:

Ward, Richard M. (2007) *Diethynylrhodacyclopentadienes: a new class of luminescent organometallics*, Durham theses, Durham University. Available at Durham E-Theses Online: <http://etheses.dur.ac.uk/2556/>

Use policy

The full-text may be used and/or reproduced, and given to third parties in any format or medium, without prior permission or charge, for personal research or study, educational, or not-for-profit purposes provided that:

- a full bibliographic reference is made to the original source
- a [link](#) is made to the metadata record in Durham E-Theses
- the full-text is not changed in any way

The full-text must not be sold in any format or medium without the formal permission of the copyright holders.

Please consult the [full Durham E-Theses policy](#) for further details.



Diethynylrhodacyclopentadienes: A new class of luminescent organometallics

The copyright of this thesis rests with the author or the university to which it was submitted. No quotation from it, or information derived from it may be published without the prior written consent of the author or university, and any information derived from it should be acknowledged.

Richard M. Ward



A thesis presented to Durham University in fulfillment of the thesis requirement for the degree of Doctor of Philosophy in Chemistry

Durham 2007

- 3 MAY 2007

Declaration

The work described in this thesis was carried out in the Department of Chemistry at Durham University between October 2003 and November 2006, under the supervision of Prof. Todd B. Marder. All the work is my own, unless otherwise stated, and has not been submitted previously for a degree at this or any other university.

Richard M. Ward

Statement of Copyright

The copyright of this thesis rests with the author. No quotation from it should be published without their prior consent and information derived from it should be acknowledged.

To mum and dad, for your continual love and support

Acknowledgments

First and foremost I would like to thank Prof. Todd Marder for giving me the opportunity to undertake a PhD under his supervision and in such an excellently equipped laboratory. For all the help and ideas I was offered on my research and the encouragement I was given when things didn't go the way we planned, I'm very grateful. Thank you also for the great help I was given with putting together my job applications and CV and also for the references I was given, which helped me get the horrible 'J' word.

I would like to thank Dr. Laurent Porrès and Dr. Andrew Beeby, as without their help, I could have never have managed to run all the optical experiments and collect all of the necessary data for my compounds. Thanks for collecting and solving the lifetime data too. To Lucas 'ASBO boy' Applegarth, cheers for collecting all of the Raman data for many compounds.

A big thank you to Dr. Andrei Batsanov and Dr. David Albesa-Jové for running all of the single crystal X-ray diffraction experiments that I have submitted over three years and for the many hours they have spent in working on the structures here in my thesis and also on the structures that have already been published. Andrei particularly is a genius at getting a good structure out of the poorest quality crystals....apparently.

Many thanks to all of the departmental services for all of the help I received and for the experiments I had run. Dr. Alan Kenwright, Catherine Heffernan and Ian McKeag for all the NMR work, Judith Magee and Jaroslava Dostal for the (countless) elemental analysis samples, Dr. Mike Jones and Lara Turner for the mass spectrometry work, Peter Coyne and Malcolm Richardson for fixing all of my broken glassware so quickly (especially the Young's Tap NMR tubes), and all of the technicians and lab attendants for their all round assistance.

Thank you to all of the Marder group and group visitors, past and present, for making the lab a nice place, with a good atmosphere to work in; Dr. Jon Collings, Dr. Dave Coventry, Dr. Tolu Fasina, Dr. Ibraheem Mkhaliid, Nathan Bell, Kitty Wongkhan, Maha Al-Haddad, Caroline Bridgens, Jonathan Barnard, Mengguan Tay, Magda van

Leeuwen, Alex Parsons, Michael Green, Oliver Dale, Jamie Siddle, Mark Sinkinson, Iris Poon, Jing Liu, Xunjin Zhu, Max Siebert, Thomas Herbst and Daniella Rais. I'd like to give a special thank you to Brian Hall for his selfless work for the group, for collecting our solvents, and particularly for his help with the glovebox. I'd like to also wish Mengguan good luck with his PhD continuing the work on the rhodacycles.

To mum and dad, for all of your support (emotionally and financially) and encouragement, not only during my PhD, but for all I've chosen to do in my life. Thank you for everything. Didn't I tell you before I did my GSCE's to relax, it'd be alright! Thank you also to Grandma, David and Elaine, Claire, Darren and Georgia for all of your support for me on my quest to become an eternal student.

To my girlfriend Hache, thank you so much for putting up with me (especially during the thesis writing "angst" stage) and for making PhD years two and three so much fun! I couldn't have done it without you, although, I possibly might have got more work done if I had...;)

To the list of friends who have been involved in my time at Durham, many of whom are still around the place, but also those who live in the world of work; (apologies if I've missed you off.....this could be embarrassing) Alex, Rich, Joe, Dave, Watters, Flynny, Andy, Seb, Lucas, Shelley, Victoria, Rachel, Mark, Claire, Steve, John, Jules, Ian, Kimmy, Aled, Matt, Helen, Liz, Donacadh, Mike, Robek, Ben, Mark, Pippa, Sara-Jayne, Howard and all of the Munky Punch boys and girls, thank you so much. I'm sure that without you lot, I'd now have a lot more money, a much healthier liver and a 3 volume thesis, however, that's just not the Chemistry way now, is it!

To anyone randomly reading this thesis, I hope you enjoy my PhD as much as I did!

Right. To the real world....And beyond!!!

Publications

Synthesis of New *mer,trans*-Rhodium(III) Hydrido-Bis(acetylide) Complexes: Structure of *mer,trans*-[(PMe₃)₃Rh(C≡C-C₆H₄-4-NMe₂)₂H].

X. Zhu, R. M. Ward, D. Albesa-Jové, J. A. K. Howard, L. Porrès, A. Beeby, P. J. Low, W. Wong, T. B. Marder. *Inorg. Chim. Acta.*, 2006, **359**, 2859.

Synthesis and Structure of an Unusual Di-Rhodium Diarylbutadiyne π -Complex Featuring a μ -(1,2- η^2):(3,4- η^2)-*p*-CF₃C₆H₄-C≡C-C≡C-C₆H₄-*p*-CF₃ Moiety.

R. M. Ward, A. S. Batsanov, J. A.K. Howard, T. B. Marder. *Inorg. Chim. Acta.*, 2006, **359**, 3671.

Crystal Engineering with Ethynylbenzenes 2: Structures of 4-Ethynyl-N,N-dimethylaniline with $Z' = 12$, and 4-Trimethylsilyethynyl-N,N-dimethylaniline.

A. S. Batsanov, J. C. Collings, R. M. Ward, A. E. Goeta, L. Porrès, A. Beeby, J. A. K. Howard, J. W. Steed, T. B. Marder, *CrystEngComm*, 2006, **8**, 622.

Synthesis, optical properties, crystal structures and phase behaviour of symmetric, conjugated ethynylarene-based rigid rods with terminal carboxylate groups.

T. M. Fasina, J. C. Collings, J. M. Burke, A. S. Batsanov, R. M. Ward, D. Albesa-Jové, L. Porrès, A. Beeby, J. A. K. Howard, A. J. Scott, W. Clegg, S. W. Watt, C. Viney, T. B. Marder. *J. Mater. Chem.*, 2005, **15**, 690.

Requirement for an oxidant in Pd/Cu co-catalyzed terminal alkyne homocoupling give symmetrical 1,4-disubstituted 1,3-diynes.

A. S. Batsanov, J. C. Collings, I. J. S. Fairlamb, J. P. Holland, J. A. K. Howard, Z. Y. Lin, T. B. Marder, A. C. Parsons, R. M. Ward, J. Zhu. *J. Org. Chem.*, 2005, **70**, 703.

Synthesis, photophysical properties and crystal and molecular structures of luminescent 2,5-bis(*p*-R-phenylethynyl)thiophenes and 2,5-bis(pentafluorophenylethynyl)thiophene.

J. S. Siddle, R. M. Ward, J. C. Collings, S. R. Rutter, L. Porrès, L. Applegarth, A. Beeby, A. S. Batsanov, A. L. Thompson, J. A. K. Howard, T. B. Marder, submitted.

The Synthesis, Optical Properties, Crystal Structures and Liquid Crystal Phase Behaviour of 9,10-bis(*p*-R-phenylethynyl)anthracenes.

P. Nguyen, S. Todd, D. van den Biggelaar, N. J. Taylor, J. C. Collings, R. M. Ward, R. Ll. Thomas, A. S. Batsanov, D. S. Yufit, A. L. Thompson, J. A. K. Howard, O. F. Koentjoro, D. P. Lydon, P. J. Low, S. R. Rutter, K. S. Findlay, L. Porrès, A. Beeby, A. S. Scott, W. Clegg, S. W. Watt, C. Viney, T. B. Marder, in preparation.

Research is what I'm doing when I don't know what I'm doing!

Dr. Wernher Magnus Maximilian von Braun

Abstract

A series of *mer,cis*-[tris(trimethylphosphine)-X-2,5-bis(4-R-phenylethynyl)-3,4-bis(4-R-phenyl)rhodacyclopenta-2,4-diene] compounds have been synthesised by the regiospecific reductive coupling of 1,4-bis(4-R-phenyl)buta-1,3-diyne with $\text{Rh}(\text{PMe}_3)_4\text{X}$ (where X = $-\text{C}\equiv\text{C}-\text{TMS}$, $-\text{C}\equiv\text{C}-\text{C}_6\text{H}_4-4-\text{NMe}_2$, $-\text{C}\equiv\text{C}-\text{C}\equiv\text{C}-\text{C}_6\text{H}_4-4-\text{NPh}_2$, and R = H, Me, OMe, SMe, CF_3 , CN, CO_2Me , NMe_2 , NO_2 , $\text{C}\equiv\text{C}-\text{TMS}$). The compounds absorb strongly in the range 453-544 nm, and are photoluminescent, in solution at room temperature, emitting in the range 496-631 nm with singlet lifetimes and quantum yields of 3-18 %. The photophysical properties are strongly influenced by the nature of R, but appear to be almost independent of the acetylide used; the latter is related to unfavourable steric interactions. Acceptor R groups red-shift both absorption and emission much more significantly than donor groups. A number of the structures have been solved by single crystal X-ray diffraction and the structures are compared and contrasted.

Analogous compounds with X = Me and Cl have also been prepared. The absorbance properties are similar to the acetylide-substituted derivatives, although absorption maxima are slightly shifted to lower energy. Also correlated with this are the values of $J_{\text{Rh-P}}$ for the sets of compounds which surprisingly suggest better donating ability of both Me and Cl over the acetylides. The Cl compound is luminescent, its emission maximum again shifted to lower energy from that of the acetylide examples. In stark contrast to the acetylide and Cl rhodacycle derivatives, the Me compounds are not emissive at room temperature in solution.

The rhodacycles react slowly, with additional diyne only under forcing conditions, to form highly substituted benzenes. It is shown that the rhodacycles can catalyse the regiospecific cyclotrimerisation of 1,4-bis(4-R-phenyl)buta-1,3-diyne to give 1,2,4-tris(4-R-phenylethynyl)-2,5,6-tri(4-R-phenyl)benzenes exclusively. The activity of the rhodacycles as catalysts for trimerisation are low, but due to the 2,5-selectivity of the rhodacycle formation, the reaction is regiospecific. The cyclotrimers are luminescent and the photophysical properties have been studied. The single-crystal X-ray structure for the parent cyclotrimer, 1,2,4-tris(phenylethynyl)-2,5,6-tri(phenyl)benzene, has been obtained and is discussed.

The mechanism for rhodacycle formation has been probed. A number of Rh-diyne π -complexes, in which one of the diyne $\text{C}\equiv\text{C}$ bonds is coordinated to Rh, which were

observed as intermediates during rhodacycle syntheses, have been isolated and characterised. ^1H , $^{19}\text{F}\{^1\text{H}\}$ and $^{31}\text{P}\{^1\text{H}\}$ NMR spectroscopy has been used to propose a general structure, and several related Rh- π -complexes of symmetrical and unsymmetrical tolans have been prepared to support this, some of which have been characterised by X-ray diffraction and are discussed. The crystal structures of two solvates of the unusual centrosymmetric bimetallic complex, $[\text{Rh}(\text{PMe}_3)_3(\text{Cl})]_2(\mu-(1,2-\eta^2):(3,4-\eta^2)-4-\text{F}_3\text{C}-\text{C}_6\text{H}_4-\text{C}\equiv\text{C}-\text{C}\equiv\text{C}-\text{C}_6\text{H}_4-4-\text{CF}_3)$ have also been obtained.

Abbreviations

Me	=	Methyl
Et	=	Ethyl
<i>i</i> Pr	=	<i>Iso</i> -Propyl
<i>t</i> Bu	=	<i>Tertiary</i> -butyl
Hex	=	n-Hexyl
Ar	=	Aryl
Ph	=	Phenyl
Tolyl	=	4-Me-C ₆ H ₄
Np	=	Naphthyl
OAc	=	Acetate
COE	=	Cyclooctene
COD	=	Cyclooctadiene
py	=	Pyridyl
en	=	Ethylenediamine
dtbpm	=	<i>t</i> Bu ₂ PCH ₂ P' <i>t</i> Bu ₂
dippe	=	<i>i</i> Pr ₂ PCH ₂ CH ₂ P' <i>i</i> Pr ₂
Cp	=	Cyclopentadienyl
Cp*	=	Pentamethylcyclopentadienyl
DCM	=	Dichloromethane
TMSA	=	Trimethylsilylacetylene
TMS	=	Trimethylsilyl
THF	=	Tetrahydrofuran
TMED	=	N,N,N',N'-tetramethylethylenediamine

bmim	=	1-butyl-3-methylimidazolium
DMI	=	1,3-dimethyl-2-imidazolidinone
DMF	=	N,N-dimethylformamide
Fc	=	Ferrocenyl
nm	=	Nanometre
ns	=	Nanosecond
μs	=	Microsecond
Å	=	Angstrom
mol	=	mole
wt	=	weight
NMR	=	Nuclear magnetic resonance
s	=	Singlet
d	=	Doublet
t	=	Triplet
q	=	Quartet
vt	=	Virtual triplet
dd	=	Doublets of doublets
dt	=	Doublets of triplets
ddd	=	Doublets of doublets of doublets
IR	=	Infra-red
UV	=	Ultra-violet
Vis	=	Visible
HOMO	=	Highest occupied molecular orbital
LUMO	=	Lowest unoccupied molecular orbital
EI	=	Electron impact

GC-MS = Gas chromatography - mass spectrometry
HPLC = High performance liquid chromatography
FT-IR = Fourier transform – Infra-red
PCC = Pyridinium chlorochromate
psi = Pounds per square inch

Table of Contents

Declaration.....	2
Statement of Copyright.....	2
Acknowledgments	4
Publications.....	6
Abstract.....	9
Abbreviations.....	11
Table of Contents.....	14
List of Figures.....	18
List of Tables	24
Preface	26
Chapter 1	27
1.1 Introduction.....	28
1.1.1 The Sonogashira Reaction: Catalytic formation of C-C bonds using Pd/Cu catalysis.....	28
1.2 Homocoupling of terminal alkynes to form buta-1,3-diyne.....	30
1.2.1 Examples of copper catalysis.....	30
1.2.2 Examples of palladium catalysis.....	31
1.2.3 Catalysis by other metal systems.....	32
1.2.4 Diyne synthesis from R-C≡C-X systems.....	34
1.2.5 Synthesis of unsymmetrical diynes.....	35
1.3 Crystal structures containing the buta-1,3-diyne moiety	37
1.4 Optical properties of 1,4-(4-R-phenyl)buta-1,3-diyne and related compounds	38
1.5 Substituted bis(4-R-phenyl)hex-3-ene-1,4-diyne.....	40
1.5.1 Synthesis of enediyne.....	40
1.5.2 Photophysical properties of bis(4-R-phenyl)hex-3-ene-1,4-diyne.....	41
1.6 Results and Discussion	42
1.6.1 Synthesis of terminal alkynes	42
1.6.2 Synthesis of butadiynes	45
1.7 Crystal structures	48
1.7.1 Crystal structures of alkyne precursor compounds.....	48

1.7.2 Crystal structures of buta-1,3-diyne	52
1.8 Synthesis of an enediyne.....	55
1.9 Photophysical properties of buta-1,3-diyne and an enediyne.....	56
1.9.1 Optical properties of buta-1,3-diyne	56
1.9.2 Optical properties of 1,6-bis(4-trifluoromethylphenyl)hex-3-ene-1,4-diyne	58
1.10 Conclusions.....	59
1.11 Experimental.....	60
1.11.1 General.....	60
1.11.2 Synthesis of TMS protected ethynylbenzenes.....	61
1.11.3 Synthesis of ethynylbenzenes	66
1.11.4 Synthesis of 1,4-bis(4-R-phenyl)buta-1,3-diyne and related compounds.....	72
1.11.5 Synthesis of 1,6-bis(4-trifluoromethylphenyl)hex-3-ene-1,4-diyne.....	79
1.12 References.....	80
Chapter 2	83
2.1 Introduction.....	84
2.1.1 Metallacyclopentadienes: MC ₄ metallacycles	84
2.2 Catalytic cyclotrimerisation of alkynes	84
2.3 Reductive coupling of buta-1,3-diyne	86
2.4 Metal biphenyl (bph) complexes	89
2.4.1 Direct insertion into biphenylene.....	89
2.4.2 Reactions of metal halides with lithiated biphenyls	92
2.4.3 Other routes.....	94
2.5 Catalysis by metal bph complexes.....	95
2.6 Luminescent transition metal biphenyl complexes.....	98
2.7 Metallacyclopentadiene containing polymers	99
2.8 Siloles: SiC ₄ main group analogues.....	102
2.9 Results and Discussion	105
2.9.1 Synthesis of TMSA rhodacyclopentadienes.....	105
2.9.2 Optical properties.....	109
2.9.3 Synthesis of Rh-C≡C-C ₆ H ₄ -4-NMe ₂ -based rhodacyclopentadienes	113
2.9.4 Optical properties of Me ₂ N-4-C ₆ H ₄ -substituted rhodacyclopentadienes.....	115
2.9.5 Crystal structures of acetylide substituted rhodacyclopentadienes.....	117
2.9.6 Synthesis of a Rh-C≡C-C≡C-NPh ₂ -based rhodacyclopentadiene	128

2.9.7 Optical properties.....	130
2.9.8 Comparison of rhodacycle optical properties with organic analogues.....	131
2.9.9 Synthesis of Rh-Me-based analogues.....	132
2.9.10 Crystal structure of 22	134
2.9.11 Rh-Cl-based rhodacycles.....	136
2.9.12 Optical properties of Rh-Me and Rh-Cl-based rhodacyclopentadienes.....	139
2.10 Cyclotrimerisation of buta-1,3-diyne.....	141
2.10.1 Introduction to transition metal catalysed cyclotrimerisation of buta-1,3-diyne.....	141
2.11 Cyclotrimerisation results and discussion.....	145
2.11.1 Cyclotrimer synthesis.....	145
2.11.2 Proposed catalytic cycle.....	147
2.11.3 Crystal structure of 25a	148
2.11.4 Optical properties of 25a-c	150
2.12 Experimental.....	154
2.12.1 General.....	155
2.12.2 Synthesis of Rh-C≡C-TMS-based rhodacyclopentadienes.....	156
2.12.3 Synthesis of Rh-C≡C-C ₆ H ₄ -NMe ₂ -based rhodacyclopentadienes.....	162
2.12.4 Synthesis of Rh-C≡C-C≡C-C ₆ H ₄ -NPh ₂ -based rhodacyclopentadienes and the related compound [RhH(PMe ₃) ₃ (C≡C-C≡C-Ph-NPh ₂) ₂].....	165
2.12.5 Synthesis of Rh-Me-based rhodacyclopentadienes.....	167
2.12.6 Synthesis of a Rh-Cl-based rhodacyclopentadiene.....	170
2.12.7 Synthesis of cyclotrimers.....	170
2.13 References.....	173

Chapter 3 179

3.1 Introduction.....	180
3.1.1 Mono-metallic complexes of buta-1,3-diyne.....	180
3.1.2 Bi-metallic complexes of buta-1,3-diyne.....	187
3.2 Results and Discussion.....	191
3.2.1 Intermediate π -complexes formed during Rh-Me-based rhodacycle synthesis.....	191
3.2.2 Crystal structure of 4	194
3.3.3 Proposed reaction mechanism.....	197

3.3.4 Intermediate π -complexes formed during attempts to synthesise a Rh-Cl-based rhodacycle.....	201
3.3.5 Crystal structure of 9	203
3.3.6 Synthesis of Rh(PMe ₃) ₃ Cl π -complexes.....	205
3.3.7 Crystal structure of 10	206
3.4 Conclusions.....	211
3.5 Experimental.....	212
3.5.1 General.....	212
3.5.2 Synthesis of Rh(PMe ₃) ₃ Me-diyne and -tolan π -complexes.....	213
3.5.3 Synthesis of Rh(PMe ₃) ₃ Cl-diyne and -tolan π -complexes.....	215
3.6 References.....	218
Chapter 4	221
4.1 Conclusions.....	222
4.2 Suggestions for future work.....	223

List of Figures

Chapter 1

Figure 1. General Sonogashira cross-coupling reaction.	28
Figure 2. Proposed cycle for the Sonogashira reaction.....	29
Figure 3. Reoxidation of Pd(0) to Pd(II) with Cu(II).	31
Figure 4. Example of a pyridine-based Pd catalyst used in diyne synthesis.....	32
Figure 5. Pd and Cu catalysts and their yield of reaction depending on ring size formed. .	33
Figure 6. Ag ⁺ as a promoter for Cu(II) catalysed homocoupling.	34
Figure 7. Route to unsymmetrical diyne <i>via</i> TMS-C≡C-C≡C-H.....	36
Figure 8. Formation of unsymmetrical butadiyne from terminal butadiynes and aryl iodides.	36
Figure 9. Novel route to unsymmetrical butadiynes without the need for Pd or Cu catalysis.	37
Figure 10. 3,6-dimethoxy-4,5-dimethylbenzene- and 4-benzoquinone-fused dehydroannulenes.	39
Figure 11. Pd/Cu catalysed formation of a <i>trans</i> -enediyne.	40
Figure 12. Enediyne synthesis involving a Ramberg-Bäcklund rearrangement.....	41
Figure 13. Acid catalysed formation of an unreported terminal alkyne containing imine, 26	45
Figure 14. The compound 1,4-bis[(3,5-bis(trifluoromethyl)phenyl)-4-ethynylphenylethynyl]buta-1,3-diyne.	47
Figure 15. Synthesis of 1,4-bis(4-dicyanovinylbenzene)buta-1,3-diyne, 43	47
Figure 16. Independent molecules in the asymmetric unit of compound 1	49
Figure 17. Molecular structure of 9	49
Figure 18. Molecular structure of 2-(4-ethynylphenylethynyl)thiophene, 21	52
Figure 19. Molecular structure of 1,4-bis(4-trifluoromethylphenyl)buta-1,3-diyne, 29	53
Figure 20. Molecular structure of 1,4-bis(4-carbomethoxyphenyl)buta-1,3-diyne, 32	53
Figure 21. Molecular structure of 38	54
Figure 22. Molecular structure of 39	55
Figure 23. Synthesis of 1,6-bis(4-trifluoromethylphenyl)hex-3-ene-1,4-diyne, 44	55
Figure 24. Normalised absorption spectra for luminescent diynes 36 , 37 , 38 , 40 and 43	57

Figure 25. Normalised emission spectra for luminescent diynes 36 , 37 , 38 , 40 and 43	588
Figure 26. Absorption and emission spectra of <i>E</i> -1,6-bis(4-trifluoromethylphenyl)hex-3-ene-1,4-diyne in CHCl ₃	59

Chapter 2

Figure 1. a) Metal diimine complex; b) metal bi-pyridine complex; c) metal 2-phenylpyridine complex; d) metal biphenyl complex.....	84
Figure 2. General catalytic cycle for the cyclotrimerisation of internal alkynes.....	85
Figure 3. Formation of three stereoisomers by reductive coupling of butadiynes; [Co] = CpCo(PPh ₃).....	86
Figure 4. Formation of regiospecific 2,5-bis(arylethynyl)rhodacyclopentadienes.....	87
Figure 5. Molecular structure of <i>mer, cis</i> -[tris(trimethylphosphine)trimethylsilylethynyl-2,5-bis(4-tolylethynyl)-3,4-bis(4-tolyl)rhodacyclopenta-2,4-diene]..	88
Figure 6. Molecular structure of bis(η^5 -cyclopentadienyl)-2,4-bis(trimethylsilylethynyl)-3,5-bis(trimethylsilyl)titanacyclopenta-2,4-diene.....	88
Figure 7. Formation of a metal bph complex from biphenylene.	89
Figure 8. Formation of a Rh bph complex from a bimetallic starting material.	90
Figure 9. Formation of fluorenone from a bimetallic bph Co complex.....	91
Figure 10. Formation of a dibenzoferrrole derivative.....	91
Figure 11. Formation of Fe ₂ (CO) ₅ (μ -CO)(μ - η^2 - η^4 -C ₆ H ₄) ₂	92
Figure 12. Examples of Pt(bph) complexes formed from Pt chloride salts and 2,2'-dilithiobiphenyl.....	93
Figure 13. Formation of Pt(bph)(dtbpm) by C-H activation of 4,4'-bis(trifluoromethyl)biphenyl.....	94
Figure 14. Synthesis of Ir(bph)Cp*(CO) by decarbonylation of sodium fluorenone ketyl.	95
Figure 15. Formation of <i>E,Z</i> -enynes by head-head coupling of alkynes with Ir(bph) catalyst.	97
Figure 16. Pd catalysed formation of functionalised biphenylene derivatives.	97
Figure 17. Catalytic formation of 9,10-disubstituted phenanthrenes (R = Me, Ph, CO ₂ Me, TMS).	98
Figure 18. Formation of regiospecific poly(phenyl-ruthenacyclopentatriene).	100
Figure 19. Facile, high yield degradation of zirconocene polymers to form macrocycles.	101

Figure 20. Silole (a), phosphole (b) and thiophene (c) structures.....	102
Figure 21. Synthetic route to unsymmetrical 2,5-bis(phenylethynyl)-3,4-diphenyl-siloles.	103
Figure 22. Pd/Cu catalysed synthesis of bis(phenylethynyl)thiophenes.....	104
Figure 23. Regiospecific synthesis of rhodacyclopentadienes.	105
Figure 24. Synthesis of Rh starting materials.	106
Figure 25. Typical <i>in situ</i> $^{31}\text{P}\{^1\text{H}\}$ NMR spectrum for the rhodacyclopentadienes (Compound 1).	107
Figure 26. Example ^1H NMR spectrum for compound 6	108
Figure 27. Removal of TMS groups from compound 10a using F^-	109
Figure 28. Absorption spectra of compounds 1-7 and 9	111
Figure 29. Emission spectra of compounds 1-9	111
Figure 30. Absorption and emission spectra for compounds 10a and 10b	112
Figure 31. Absorption and emission spectra ($\lambda_{\text{ex}} = 379$ and 500 nm) of the reaction mixture from the attempted synthesis of a $\text{CH}=\text{C}(\text{CN})_2$ substituted rhodacycle.....	113
Figure 32. Two step mechanism for <i>mer,trans</i> - $[\text{RhH}(\text{PMe}_3)_3(\text{C}\equiv\text{C}-\text{C}_6\text{H}_4-4-\text{R})_2]$ formation.	114
Figure 33. Formation of rhodacycles bearing a $\text{RhC}\equiv\text{C}-\text{C}_6\text{H}_4-4-\text{NMe}_2$ acetylide moiety.	115
Figure 34. Absorption spectra of compounds 11-15	117
Figure 35. Emission spectra of compounds 11-15	117
Figure 36. One molecule in the asymmetric unit of 4	123
Figure 37. Molecular structure of 5	124
Figure 38. Molecular structure of 7	125
Figure 39. Molecular structure of 11	125
Figure 40. Molecular structure of 12	126
Figure 41. Molecular structure of 13	127
Figure 42. Molecular structure of 14	127
Figure 43. Molecular structure of 15	128
Figure 44. Synthetic route to compound 16	129
Figure 45. Diagram of <i>mer,trans</i> - $[\text{RhH}(\text{PMe}_3)_3(\text{C}\equiv\text{C}-\text{C}\equiv\text{C}-\text{C}_6\text{H}_4-4-\text{NPh}_2)_2]$, 17	129
Figure 46. Absorption and emission spectra for compound 16	130
Figure 47. Unfavourable $\text{CH}\cdots\text{HC}$ interactions between H^* that prevent co-planarity of phenyl rings <i>ii</i> and <i>vi</i>	131

Figure 48. Plots of absorption maxima vs. Hammett constant (σ_{p+}/σ_{p-}) for the rhodacycles 1-3 and 5-9 and the analogous 1,4-bis(4-R-phenylethynyl)benzenes (BPEBs), 2,5-bis(4-R-phenylethynyl)thiophenes (BPETs) and 9,10-bis(4-R-phenylethynyl)anthracenes (BPEAs).	132
Figure 49. Synthesis of Rh-Me Rhodacycles, 18-22	133
Figure 50. One molecule in the asymmetric unit of 22	135
Figure 51. $^{31}\text{P}\{^1\text{H}\}$ NMR spectrum of intermediate Rh π -complexes.....	137
Figure 52. Synthesis of Rh-Cl rhodacyclopentadiene, 23	138
Figure 53. <i>In situ</i> $^{31}\text{P}\{^1\text{H}\}$ NMR spectrum of compound 23	138
Figure 54. Absorption spectra for compounds 18-22	140
Figure 55. Absorption and emission spectra for compound 23	140
Figure 56. 1,2,4-tris(phenylethynyl)-3,5,6-tri(phenyl)benzene and 1,3,5-tris(phenylethynyl)-2,4,6-tri(phenyl)benzene.	142
Figure 57. Regioselective cyclic trimerisation of diphenylbutadiyne using methylidinetricobalt nonacarbonyl catalyst.	143
Figure 58. Dewar benzene intermediate formed thermally during solvent-free synthesis of 1,2,3-tris(R-ethynyl)-4,5,6-tri(R)benzene (R = CH ₃ OCOCH ₂)......	144
Figure 59. 1,3,5-tri(phenylethynyl)-2,4,6-(phenyl)benzene derivatives which exhibit liquid crystal phase behaviour.....	145
Figure 60. Stereospecific cyclotrimerisation of 1,4-bis(4-R-phenyl)buta-1,3-diyne using preformed rhodacycles.....	146
Figure 61. Proposed catalytic cycle for the cyclotrimerisation of butadiynes using rhodacyclopentadiene catalysts.....	147
Figure 62. Molecular structure of 1,2,4-tris(phenylethynyl)-3,5,6-tri(phenyl)benzene.. ..	149
Figure 63. Absorption spectra of compounds 25a , 25b and 25c	151
Figure 64. Emission spectra of compounds 25a , 25b and 25c	151

Chapter 3

Figure 1. Mono-metallic (a) and bi-metallic (b) complexes of buta-1,3-diyne.	180
Figure 2. Example of a four-coordinate, square planar Rh complex containing η^2 -acetylenic, halide and phosphine ligands simultaneously.....	181

Figure 3. Formation of a Pt-diyne π -complex by homocoupling of two acetylide ligands.	182
Figure 4. Synthesis of a Pt σ -2-butadienyl complex <i>via</i> a thermally unstable π -propargyl intermediate.	183
Figure 5. Protonation of $\text{Ru}(\eta^2\text{-PhC}\equiv\text{CC}\equiv\text{CPh})(\text{CO})_2(\text{PPh}_3)_2$ with non-nucleophilic acids.	183
Figure 6. <i>Endo</i> - and <i>exo</i> - isomers of $\text{Nb}(\eta^5\text{-C}_5\text{H}_4\text{SiMe}_3)_2\text{Cl}(\eta^2\text{-(RC}\equiv\text{CC}\equiv\text{CR)}$, (R = Ph, TMS).	184
Figure 7. Molecular structure of $\text{Fe}(\text{CO})_2(\text{PEt}_3)_2(\eta^2\text{-TMSC}\equiv\text{CC}\equiv\text{CTMS})$	185
Figure 8. Formation of a fused bicyclic compound from $\text{Ni}(\text{PPh}_3)_2(\eta^2\text{-PhC}\equiv\text{CC}\equiv\text{CPh})$. .	186
Figure 9. 'Pt(PPh ₃) ₂ ' complex with a novel transition metal complexed diposphine butadiyne.	186
Figure 10. Bi-metallic coordination to butadiyne in <i>exo</i> - and <i>endo</i> -positions.	187
Figure 11. Molecular structure of $[(2,6\text{-dimethylpyridine})\text{Ni}]_2(\text{TMS-C}\equiv\text{CC}\equiv\text{C-TMS})_2$. .	188
Figure 12. Reversible formation of $[\{(\text{dippe})\text{Pd}\}_2(\mu\text{-(1,2-}\eta^2\text{):(3,4-}\eta^2\text{)-HC}\equiv\text{CC}\equiv\text{CH})]$	189
Figure 13. Thermal Si-C bond activation by a donor stabilised Pt(0) complex.	190
Figure 14. Proposed intermediate formed by π -coordination of diyne to $\text{Rh}(\text{PMe}_3)_4\text{Me}$. .	191
Figure 15. General reaction scheme for the formation of compounds 1-3	192
Figure 16. $^{31}\text{P}\{^1\text{H}\}$ NMR spectrum of compound 1	193
Figure 17. ^1H NMR spectrum of compound 1	193
Figure 18. $^{31}\text{P}\{^1\text{H}\}$ NMR spectrum of compound 4	194
Figure 19. Molecular structure of $\text{Rh}(\text{PMe}_3)_3\text{Me}(\eta^2\text{-4-MeO-C}_6\text{H}_4\text{-C}\equiv\text{C-C}_6\text{H}_4\text{-4-CN})$	197
Figure 20. Proposed step-wise reaction mechanism.	198
Figure 21. The doublet of doublet region of the <i>in situ</i> $^{31}\text{P}\{^1\text{H}\}$ NMR spectrum recorded after the addition of one equivalent of 4-MeO-C ₆ H ₄ -C≡C-C≡C-C ₆ H ₄ -4-OMe to compound 2	200
Figure 22. Two regioisomers formed by sequential reaction of $\text{Rh}(\text{PMe}_3)_4\text{Me}$ with 4-MeO-C ₆ H ₄ -C≡C-C≡C-C ₆ H ₄ -4-OMe and 4-F ₃ C-C ₆ H ₄ -C≡C-C≡C-C ₆ H ₄ -4-CF ₃ in either order. .	201
Figure 23. Two isomeric RhCl intermediates with diyne lying in the RhPCL equatorial plane.	202
Figure 24. Incorrectly proposed bi-metallic intermediate, 8	202
Figure 25. $[\text{Rh}(\text{PMe}_3)_3(\text{Cl})]_2(\mu\text{-(1,2-}\eta^2\text{):(3,4-}\eta^2\text{)-4-F}_3\text{C-C}_6\text{H}_4\text{-C}\equiv\text{C-C}\equiv\text{C-C}_6\text{H}_4\text{-4-CF}_3)$. .	203
Figure 26. Molecular structure of 9 •5C ₆ D ₆	205
Figure 27. Diagram showing the two possible isomers of compound 10	207

Figure 28. Molecular structure of $\text{Rh}(\text{PMe}_3)_3\text{Cl}(\eta^2\text{-MeO-C}_6\text{H}_4\text{-C}\equiv\text{C-C}_6\text{H}_4\text{-CN})$, 10	208
Figure 29. $^{19}\text{F}\{^1\text{H}\}$ NMR stack plot showing CF_3 group coalescence between 50-60 °C and an increased level of dissociation of tolan at higher temperature.....	210

Chapter 4

Figure 1. Substituted rhodacycle with favourable $\text{CH}\cdots\text{O}$ interactions.	224
Figure 2. Rhodacycle prepared by reductive coupling of two equivalents of $\text{R-4-C}_6\text{H}_4\text{-C}\equiv\text{C-C}_6\text{H}_4\text{-C}\equiv\text{C-C}\equiv\text{C-C}_6\text{H}_4\text{-C}\equiv\text{C-C}_6\text{H}_4\text{-4-R}$ with $\text{R}(\text{PMe}_3)_4\text{X}$	225
Figure 3. Four possible regioisomers formed by the reductive coupling of two equivalents of an unsymmetrical diyne with $\text{Rh}(\text{PMe}_3)_4\text{X}$	227

List of Tables

Chapter 1

Table 1. Pd/Cu catalysed cross coupling of aryl halides with TMSA.	43
Table 2. Protected alkyne deprotection under basic conditions.	44
Table 3. Catalytic homocoupling of terminal alkynes to form butadiynes.	46
Table 4. Crystallographic data for compounds 1 , 9 , 21 and 29	50
Table 5. Crystallographic data for compounds 32 , 38 and 39	51
Table 6. Summary of the photophysical properties of luminescent diynes.	56
Table 7. Photophysical properties of 1,6-bis(4-trifluoromethylphenyl)hex-3-ene-1,4-diyne in CHCl ₃	58

Chapter 2

Table 1. Summary of the optical properties of compounds 1-10 in toluene.	110
Table 2. Summary of the optical properties of compounds 11-15	116
Table 3. Crystal data for compounds 4 , 5 , 7 , and 11-15	118
Table 4. Selected bond lengths (Å) and bond angles (°) for compounds 1 , 2 , 4 , 5 and 7	120
Table 5. Selected bond lengths (Å) and angles (°) for compounds 11-15	121
Table 6. Summary of the optical properties of compound 16	130
Table 7. Selected bond lengths (Å) and bond angles (°) for 22	135
Table 8. Crystallographic data for compound 22	136
Table 9. Summary of the optical properties of compounds 18-22	139
Table 10. Crystallographic data for compound 25a	148
Table 11. Summary of the optical properties for compounds 25a , 25b and 25c	150
Table 12. Summary of the optical properties for three BPEBs.	152

Chapter 3

Table 1. Selected bond lengths (Å) and angles (°) in compound 4	195
Table 2. Summary of the crystallographic data for compound 4	196
Table 3. Selected bond lengths (Å) and angles (°) in compound 9 •5C ₆ D ₆ and 9 •2THF. π is the midpoint of the C(1)≡C(2) bond.	204
Table 4. Summary of the crystallographic data for compound 9	206
Table 5. Selected bond lengths (Å) and angles (°) in compound 10	207
Table 6. Summary of the crystallographic data for compound 10	209

Preface

The work in this thesis has been carried out to expand and investigate further the work on a novel, luminescent 2,5-bis(4-R-phenylethynyl)rhodacyclopentadiene system, or rhodacycle, that has been reported recently.¹ Luminescent organometallic complexes such as this are of scientific interest due to their possible incorporation into OLED type devices as the light emitting layer material.

Chapter One is primarily concerned with the synthesis of a wide range of 1,4-diarylbuta-1,3-diyne and related compounds which are necessary for the formation of the metallacycles via the reductive coupling of two equivalents of diyne at a $\text{Rh}(\text{PMe}_3)_4\text{X}$ centre. A number of compounds in this chapter have already been published or are included in manuscripts that are in preparation.²

Chapter Two investigates the synthesis and isolation of pure rhodacycles and reports the photophysical properties which they exhibit. A number of these compounds have been characterised by X-ray crystallography and a discussion of the metallacycle structures in the solid state, and how this relates to their optical properties, is also included. The profound effects of the diyne *para*-substituent and of the ligands on the Rh centre on both the structural and optical properties of the system are reported. This chapter also includes an introduction to the cyclotrimerisation of buta-1,3-diyne. A select few examples of 1,2,4-tris(4-R-phenylethynyl)-3,5,6-tri(4-R-phenyl)benzenes have been prepared and the optical properties have been investigated and shown to be significantly different to the properties of the rhodacycles. During the synthesis of the rhodacycles a number of intermediate compounds were observed which provide some insight into the mechanism of formation of the rhodacycles.

Chapter Three describes these observations and a number of intermediates have been isolated, along with some related model compounds, and are discussed. From information gathered in Chapter Two and from the isolated intermediate compounds in this chapter, a step-wise mechanism for rhodacycle formation is proposed.

¹ J. P. Rourke, A. S. Batsanov, J. A. K. Howard, T. B. Marder, *Chem. Commun.*, 2001, 2626.

² See publications list, page 6.

Chapter 1

Synthesis, characterisation, molecular structures and photophysical properties of 1,4-bis(4-R-phenyl)buta-1,3-diyne and related compounds

1.1 Introduction

1.1.1 The Sonogashira Reaction: Catalytic formation of C-C bonds using Pd/Cu catalysis

The catalytic formation of ethynyl arenes from aryl halides and terminal alkynes using Pd and Cu species has been utilised extensively since it was first discovered. Cassar first found that $\text{Pd}(\text{PPh}_3)_4$ would successfully catalyse the reaction in the presence of base,¹ though soon after, Sonogashira *et al.* published the same reaction involving air stable $\text{Pd}(\text{PPh}_3)_2\text{Cl}_2$ with CuI in diethylamine which would proceed under mild conditions² (Figure 1).

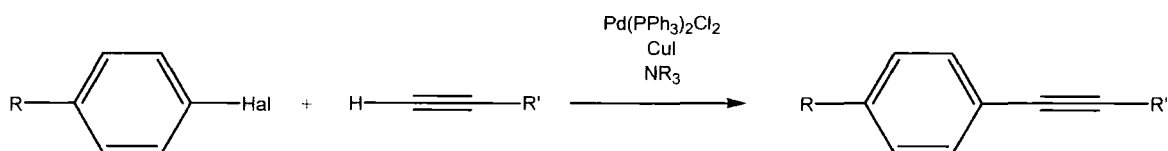


Figure 1. General Sonogashira cross-coupling reaction.

The catalytic cycle proposed by Sonogashira involves an *in situ* catalyst initiation step to form the active Pd(0) catalyst from the air-stable Pd(II) precursor. In this step, a $(\text{PPh}_3)_2\text{Pd}(\text{CCR})_2$ species is formed by the transmetalation of two equivalents of Cu-acetylide, formed by deprotonation of the terminal alkyne by the amine, to the palladium. This intermediate undergoes reductive elimination of one equivalent of oxidatively homocoupled diyne, generating $\text{Pd}(0)(\text{PPh}_3)_2$ *in situ*. The rate of alkyne homocoupling, and indeed re-oxidation of Pd(0) to Pd(II) by O_2 in the presence of Cu, is faster than that of the aryl halide-alkyne cross-coupling and so the reaction must be carried out under rigorously oxygen free conditions and in the absence of any added oxidant. The full cycle is shown in Figure 2.

Oxidative addition of the aryl halide, the first step in the catalytic cycle for cross-coupling, has been reviewed.³ The rate of oxidative addition can be increased by increasing the nucleophilicity of the Pd centre, often through the use of bulky, electron

donating phosphine ligands. Oxidative addition rates can also be increased by making the aryl halide more reactive either by changing the halide, (the reactivity with $\text{Pd}(\text{PPh}_3)_4$ has been shown to be $\text{Ar-I} > \text{Ar-Br} \gg \text{Ar-Cl} \gg \text{Ar-F}$) or by introducing electron withdrawing substituents at the *para* position of the arene ring.⁴

Transmetalation of Cu-acetylide to Pd is the next step in the cycle. An amine, often also used as the solvent for the reaction, deprotonates the alkyne to generate a Cu-acetylide *in situ* which exchanges with the halide to form $\text{Pd}(\text{CCR})$ and the corresponding ammonium salt.

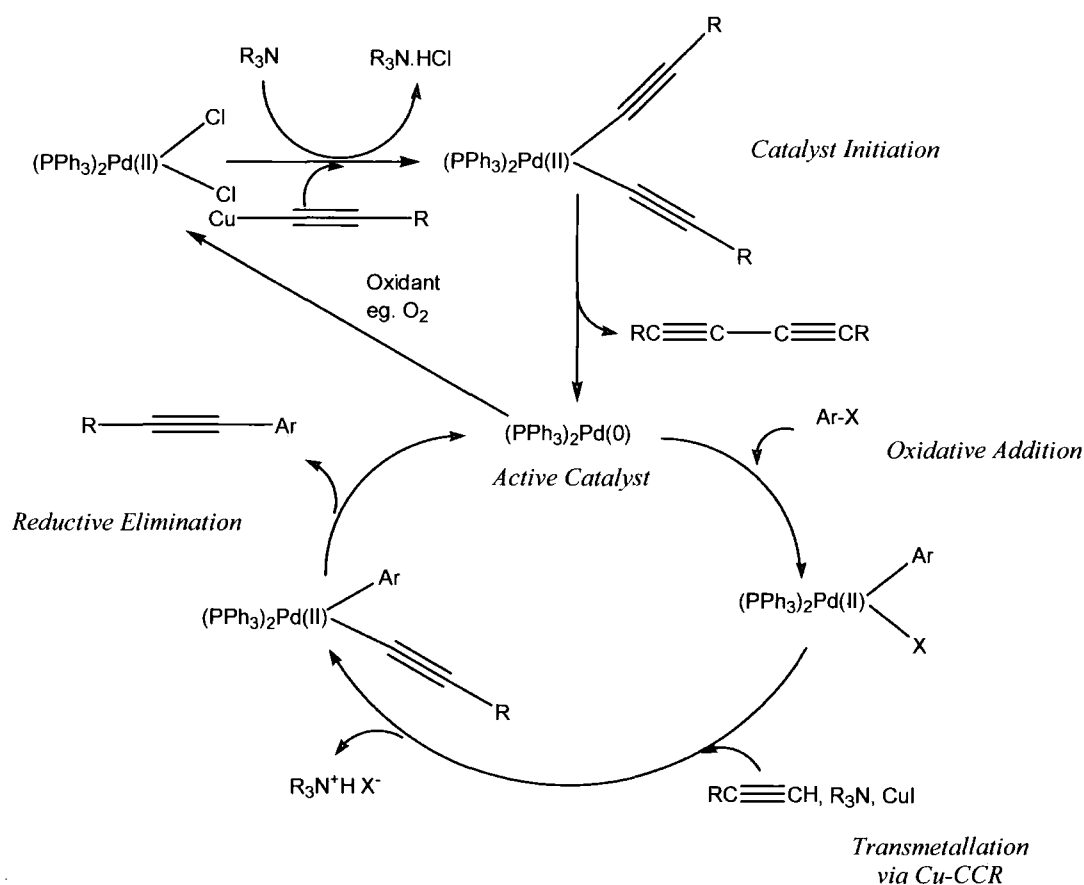


Figure 2. Proposed cycle for the Sonogashira reaction.

For the successful formation of the C-C bond, the Ar and CCR substituents on Pd must isomerise to *cis* positions so that reductive elimination of product and finally regeneration of the $\text{Pd}(0)$ catalyst can occur. It is also possible that a mono-phosphine species or an anionic $[\text{bis}(\text{phosphine})\text{PdX}]^-$ species is important in oxidative addition, and this issue is still the subject of research and debate.

1.2 Homocoupling of terminal alkynes to form buta-1,3-diyne

1.2.1 Examples of copper catalysis

The first example of diyne synthesis directly from terminal alkynes was by Glaser who self coupled terminal alkynes (*via* a Cu acetylide intermediate) with CuCl in air, in the presence of NH₄OH.⁵ This technique has since been modified and used extensively. Eglinton and Galbraith used Cu(II) as a catalyst in the presence of oxygen.⁶ The reaction was carried out in methanol with pyridine as the base. Although the reaction is catalytic in the presence of O₂, it is very slow and so an excess of Cu(OAc)₂ is often used. Hay successfully coupled phenylacetylene, 1-ethynylcyclohexanol and 1-hexyne, three commonly available terminal acetylenes, using catalytic amounts of CuI and TMED in acetone with oxygen as the oxidant.⁷ This method gave high yields and allowed reactions to be carried out in a variety of organic solvents, without high temperatures due to the activity of the catalyst.

Recent advances in Cu(I)/(II) catalysed alkyne homocoupling reactions have improved yields and selectivity whilst also providing additional safety, environmental and economic advantages. Solvent-free reactions using solid state Cu catalysts supported on KF/alumina have been employed for diyne synthesis at room temperature with morpholine as a base⁸ and another similar reaction with enhancement of the reaction rate with microwave irradiation.⁹ To minimise the use of organic solvents and also to allow recycling of the catalyst, green solvent systems have been investigated. Alkyne homocoupling in supercritical CO₂, using NaOAc as the base instead of amines has been presented.¹⁰ Some methanol is required to act as a 'modifier', increasing the solubility of the CuCl₂ and NaOAc, enhancing the reaction. A Glaser type coupling reaction of terminal alkynes under near-critical water in the presence of cupric chloride and without the need for organic solvents and bases has been developed.¹¹ Hydrophobic [bmim]PF₆ ionic liquids with CuCl-TMED catalyst systems under aerobic conditions give good diyne yields.¹² The hydrophobic nature of the ionic liquid allows catalyst recovery.

1.2.2 Examples of palladium catalysis

The initiation step to generate the active Pd catalyst in the Sonogashira catalytic cycle can be exploited to synthesise buta-1,3-diyne catalytically. Using the same Pd/Cu catalyst precursor system as in ethynyl arene synthesis above, the Pd(0) formed during initiation, can be prevented from engaging in aryl halide oxidative addition provided that a stoichiometric amount oxidant is present, as the reoxidation is faster than oxidative addition (*vide supra*). It has been shown that Pd(0) is not an active catalyst in homocoupling and that the reaction cannot proceed without added oxidant to re-oxidise Pd(0) back to Pd(II).¹³ It has been suggested that the copper may play a dual role in the reaction, first, being used to mediate the transfer of alkyne to Pd *via* the transmetallation from a Cu-acetylide species and second, to aid in the reoxidation of Pd(0) as is found in the industrially important Wacker process¹⁴ (Figure 3).

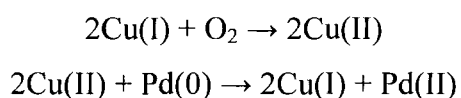


Figure 3. Reoxidation of Pd(0) to Pd(II) with Cu(II).

There are a number of known oxidants that have proved to be successful in the re-oxidation of Pd(0) to Pd(II) necessary for the synthesis of diynes from terminal alkynes. These include chloroacetone¹⁵ (using Pd(PPh₃)₄, CuI and NEt₃ in benzene), bromoacetate¹⁶ (using Pd(PPh₃)₂Cl₂, CuI and NEt₃ or DABCO in THF), molecular iodine¹⁷ (using Pd(PPh₃)₂Cl₂, CuI in ⁱPr₂NH), allyl bromide¹⁸ (using Pd(0)(dba)₂, ⁿBu₄NBr and NaOH in DCM), trimethylamine-N-oxide¹⁹ (amine and phosphine free synthesis from PdCl₂, CuI and NaOAc in MeCN) and also in the presence of air.^{13,20,21}

Ligands around the palladium are not limited to electron donating phosphines. Successful alkyne homocoupling has been achieved using the pyridine-containing catalyst shown in Figure 4.²²

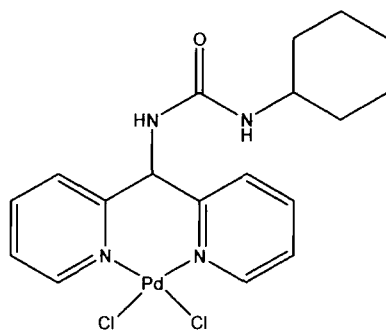
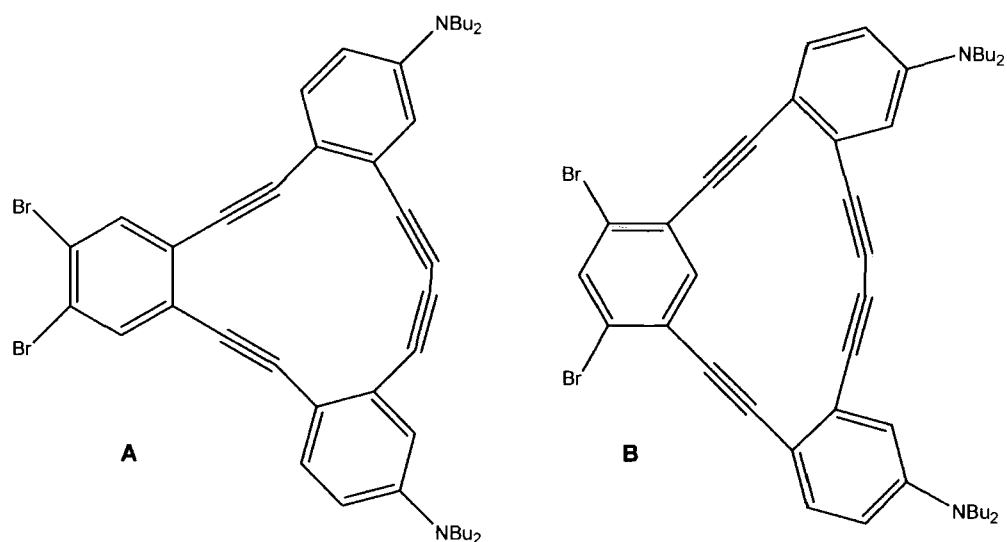


Figure 4. Example of a pyridine-based Pd catalyst used in diyne synthesis.

Recently, Haley *et al.* utilised Pd/Cu (co)catalysed reactions in the synthesis of ring systems that contain a butadiyne link²³ (Figure 5). The catalytic ring closure with Cu(II), Cu(I) and palladium species with mono and chelating phosphine ligands were explored and the yields of each reaction were found to be dependent on the size of the ring formed. In the synthesis of 14 or 15 membered ring containing dehydrobenzoannulenes (DBAs), the group found that the yields of formation for the 14 membered ring DBA (**A**) were higher with palladium catalyst/CuI co-catalyst whereas 15 membered ring DBA (**B**) was formed in higher yield with copper catalysts. The group suggest that this phenomenon is related to the metal containing catalytic intermediates formed *in situ*. Smaller ring sizes lead to strain in the twisted copper intermediate which results in the *cis* geometry of the Pd bis(acetylide) intermediate being more favourable. Larger ring sizes allow the formation of a dimeric Cu(I) acetylide intermediate, this time in a pseudo-*trans* configuration.

1.2.3 Catalysis by other metal systems

Terminal alkyne homocoupling is not limited to the use of Pd/Cu catalysts although other examples are few. The synthesis of diynes has also been achieved with $\text{Co}_2(\text{CO})_8$, (pretreated with phenanthroline in MeCN under a CO atmosphere).²⁴ Silver(I) has recently been used as a triple bond activator for Cu(II) alkyne homocoupling.²⁵ This is the first time silver has been used in this way and is particularly interesting as the reaction occurred with terminal aliphatic alkynes bound to a solid support (Figure 6). Fathi and co-workers suggest that Ag(I) activates the CH bond by forming a π -complex with the triple bond. The group screened 3 silver salts and found the clear activation trend in the order: AgOAc < AgOTf < AgOTs.



A Yield %	Catalyst	B Yield %
24	Cu(OAc) ₂	80
35	CuCl	76
67	PdCl ₂ (PPh ₃) ₂	24
76	PdCl ₂ (dppe)	12

Figure 5. Pd and Cu catalysts and their yield of reaction depending on ring size formed.

The prominent effect of AgOTs may be attributed to the weaker coordination nature of OTs⁻ over OAc⁻ and OTf⁻, which makes the Ag(I) more 'naked', facilitating its association with the C≡C bond and hence the activation of CH.

The dimerisation of alkynyl Grignard reagents with Pd catalysts in the presence of oxidants such as N-substituted isocyanide dichlorides is known,²⁶ although use of alkynyl Grignards limits the scope of this reaction due to the intolerance of functionality. Oxovanadium²⁷ compounds such as VO(OR)Cl₂, have been shown to induce homocoupling of a range of organolithium and organomagnesium compounds under mild conditions. Treatment of 1-alkynyllithiums with VO(OEt)Cl₂ in ether at -78 °C afforded the corresponding 1,3-diynes in high yields.

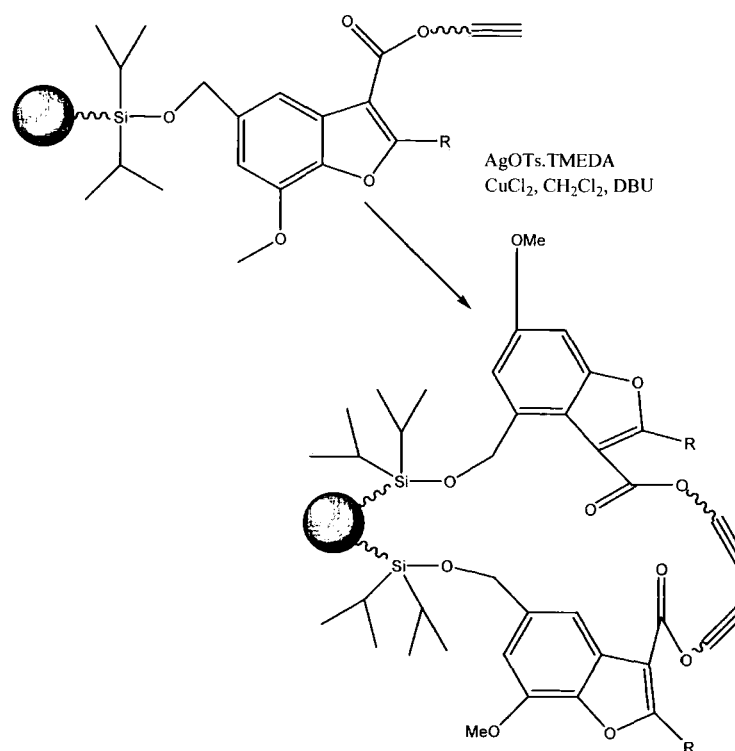


Figure 6. Ag⁺ as a promoter for Cu(II) catalysed homocoupling.

1.2.4 Diyne synthesis from R-C≡C-X systems

The synthesis of butadiynes is also possible using R-C≡C-X species, and several examples are known. Use of these systems enables diyne synthesis without the formation of *E,Z*-enyne byproducts that can occur with Pd/Cu catalysis. Organosilanes^{28,29,30} and organotin^{31,32,33,34} compounds have previously been used, although the latter are toxic and separation of the reaction byproducts is difficult. A range of catalyst systems have been employed for these reactions, including CuI with²⁸ or without³⁰ fluoride activator, activator free Pd-1,3-bis(diphenylphosphino)propane,²⁹ Pd catalysis with allylacetate, air³¹ or (*E*)-diiodoethene³² as the oxidant and CuCl₂/MnBr₂ co-catalysis with a molecular iodine oxidant.³³ Organogermanes in the presence of BF₃·Et₂O and *para*-trifluoromethylphenyl(difluoro)-λ³-bromane have also been used to homocouple alkynes in reasonable yields by uncatalysed Michael additions.³⁴

It is possible to homocouple the lithium salts of a limited range of terminal alkynes with NiCl₂(PPh₃)₂³⁵ in the presence of two equivalents of PPh₃, tetramethylguanidine or substituted amidine bases at low temperature by reductive elimination of butadiyne from a dialkynyl Ni(II) intermediate complex. Ni(CO)₄ is also known to form butadiyne from

lithium acetylides³⁶ although the reaction is not clean, with the ratio of product to side-products dependent on both temperature and solvent. Pd(0) or Pd(II) in the presence of copper can act as catalysts for the homocoupling of lithium alkynyltriisopropoxyborates. The reaction will proceed in a range of solvents with THF proving to be the most effective.³⁷ Alkynyl boronates can be used as versatile starting compounds for diyne preparation.³⁸ Upon exposure to air, and to Cu(I) or Cu(II) salts in aprotic solvents, alkynyl boronates can be coupled to give 1,3-butadiynes in high yields.

Iodoalkynes are a further example of the wide variety of methods used in butadiyne synthesis. Two equivalents of iodoalkyne can be coupled with Pd(PPh₃)₄ catalyst in DMF solution with loss of iodine.³⁹ This facile reaction gives diynes in high yields without any toxic byproducts.

1.2.5 Synthesis of unsymmetrical diynes

Glaser type reactions, and those using Pd/Cu co-catalysts, give poor results regarding the synthesis of unsymmetrical diynes from a mixture of terminal alkynes, a reaction which results in the simultaneous production of similar diyne compounds that are tedious and difficult to separate. Chodkiewicz showed that it was possible to couple alkynyl halides and terminal alkynes with Cu catalysts to synthesise unsymmetrical diynes without symmetrical diyne byproducts.⁴⁰ The reaction later became known as the Chodkiewicz-Cadiot reaction. The reaction has been modified such that at room temperature in the presence of catalytic amounts of Pd(PPh₃)₂Cl₂ and pyrrolidine, successful coupling of R-I, R-Br and R-Cl alkynyl halides with terminal alkynes is possible.⁴¹ A related reaction by Nishihara and co-workers involves the coupling of alkynylsilanes and alkynyl halides with Cu(I) catalysis in DMF which has afforded a range of unsymmetrical diynes in moderate to good yields.^{30,42}

The Chodkiewicz-Cadiot reaction, and modifications thereof, are not the only way in which unsymmetrical diynes can be prepared. The readily available compound TMS-C≡C-C≡C-TMS can be selectively and sequentially desilylated with MeLi, allowing step wise coupling of a butadiyne moiety with appropriate halides⁴³ (Figure 7).

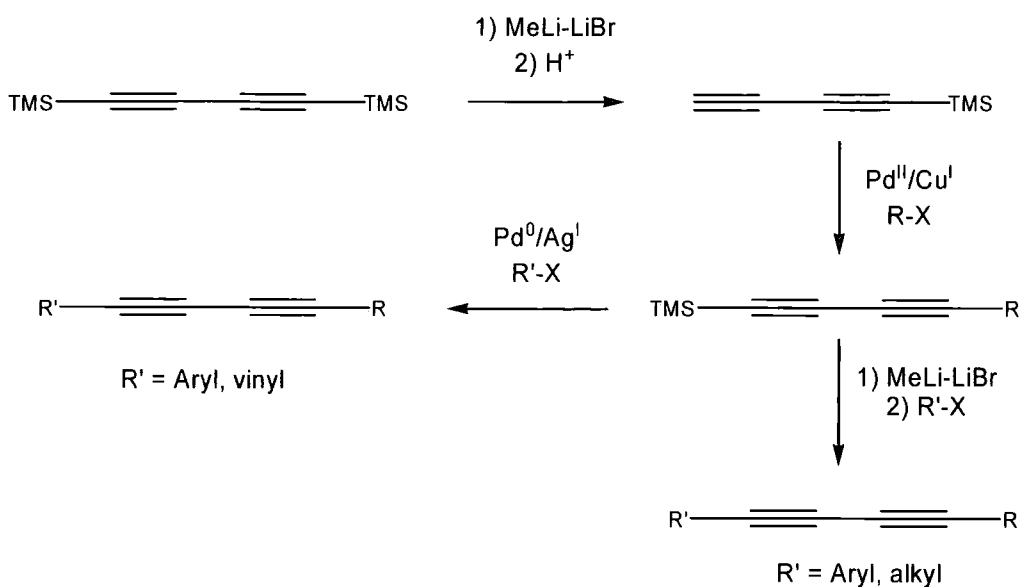


Figure 7. Route to unsymmetrical diyne *via* $\text{TMS-C}\equiv\text{C-C}\equiv\text{C-H}$.

Coupling of aryl halides with the related $\text{H-C}\equiv\text{C-C}\equiv\text{C-C}(\text{Me}_2)\text{OH}$ has also proved useful for synthesis⁴⁴ (Figure 8). The $\text{C}(\text{Me}_2)\text{OH}$ group, often used as a protecting group for terminal alkynes, can be easily removed with NaOH in refluxing toluene, which in certain cases, can result in terminal butadiynes that are stable at ambient conditions for a period of months without any detectable degradation.

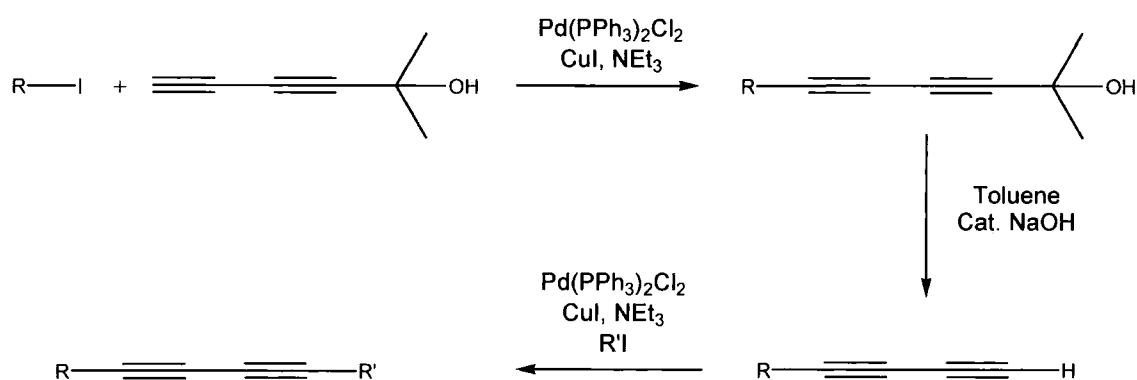


Figure 8. Formation of unsymmetrical butadiyne from terminal butadiynes and aryl iodides.

Treating lithium dialkynyldisiamylborates, $\text{Li}[\text{Sia}_2\text{B}(\text{C}\equiv\text{CR})(\text{C}\equiv\text{CR}')]]$ ($\text{Sia} = \text{CHMe}^i\text{Pr}$), formed from the sequential addition of two different 1-alkynyllithiums to

Sia₂B(OMe), with iodine in THF, gives elimination of unsymmetrical diynes in reasonable yields *via* a convenient synthesis from the commercially available borane-methyl sulfide.⁴⁵

An interesting route to unsymmetrical diynes has been proposed by Tykwinski and co-workers⁴⁶ (Figure 9). The key step in this process involves a Fritsch-Buttenberg-Wiechell rearrangement, in which an alkyldiene carbenoid intermediate subsequently rearranges to the diyne. The reaction proceeds under mild conditions and provides an alternative to Pd/Cu catalysed homocoupling.

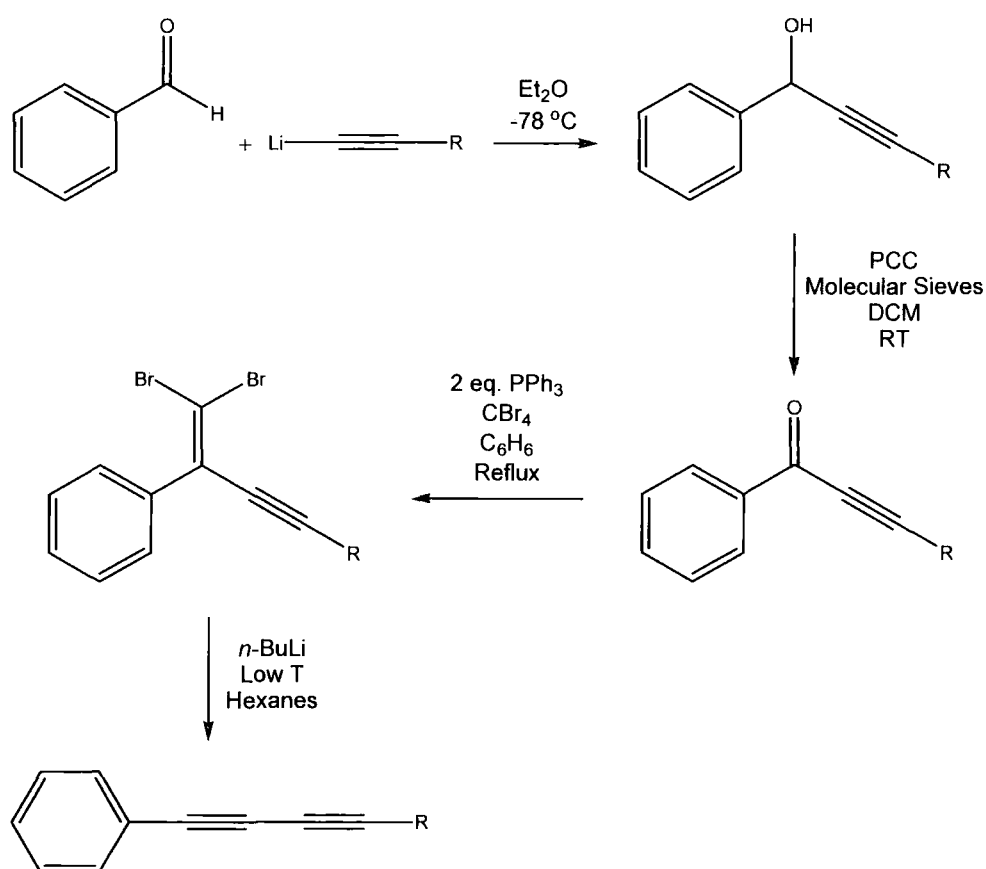


Figure 9. Novel route to unsymmetrical butadiynes without the need for Pd or Cu catalysis.

1.3 Crystal structures containing the buta-1,3-diyne moiety

There are 541 organic buta-1,3-diyne structures in the CSD and of these 85 are based on the 1,4-(4-R-phenyl)buta-1,3-diyne moiety, with a further three structures based

on the di-pyridyl analogue. However, just 7 of these structures contain a terminal butadiyne as these are notoriously unstable, although it has been proposed that packing effects can aid stabilisation.⁴⁴ TMS or TIPS groups, regularly used to protect terminal alkynes, account for 25 structures, with C(Me₂)OH, another widely used alkyne protecting group accounting for 3 structures.

1.4 Optical properties of 1,4-(4-R-phenyl)buta-1,3-diyne and related compounds

There is little information in the literature regarding fully photophysically characterised diynes. Many diynes are not conjugated to a sufficient extent to give strong luminescence in the visible region of the spectrum. The few examples in the literature include butadiyne containing poly-(4-phenylenevinylene) polymers of the type $-(C_6H_4-C\equiv C-C\equiv C-C_6H_4-CH=CH-C_6H_4-CH=CH)-_n$ ⁴⁷ formed by polycondensation reactions (and the structurally similar $-(C_6H_4-C\equiv C-C_6H_4-C\equiv C-C\equiv C-C_6H_4-C\equiv C-C_6H_4-CH=CH-C_6H_4-CH=CH)-_n$ ⁴⁸). Wide polymer dispersity is achieved on polymerization that results in a range of λ_{abs} and quantum yield depending on polymer chain length. There are a number of examples of dehydroannulenes that show interesting optical properties. Komatsu and co-workers have compared the absorption of dehydroannulene fused with three 3,6-dimethoxy-4,5-dimethylbenzene units at the 1,2-positions, a series of 4-benzoquinone-fused dehydroannulenes and some mixed species.⁴⁹ They found that for the mixed species, absorption was bathochromically shifted compared to that of the non-mixed analogues due the presence of electron donating 4-dimethoxybenzene and electron accepting 4-benzoquinone units in the same π -system reducing the HOMO-LUMO gap (Figure 10). This work is related to previous work by Haley co-workers.⁵⁰

Examples of compounds containing a single butadiyne moiety include 1,4-[3,5-bis(2-pyridyl-4-pyridine)]buta-1,3-diyne,⁵¹ used to synthesise blue luminophores (metal species linked by a butadiyne bridge). The first bisbenzocrown ethers linked with polyne bridges have been prepared, and Lagow and co-workers have compared C₄ linkers with C₈ linkers and noted that a red shift in absorption occurs as the level of conjugation increases.⁵² The electronic absorption of Fc-4-C₆H₄-C \equiv C-C \equiv C-C₆H₄-4-Fc has also been studied.⁵³

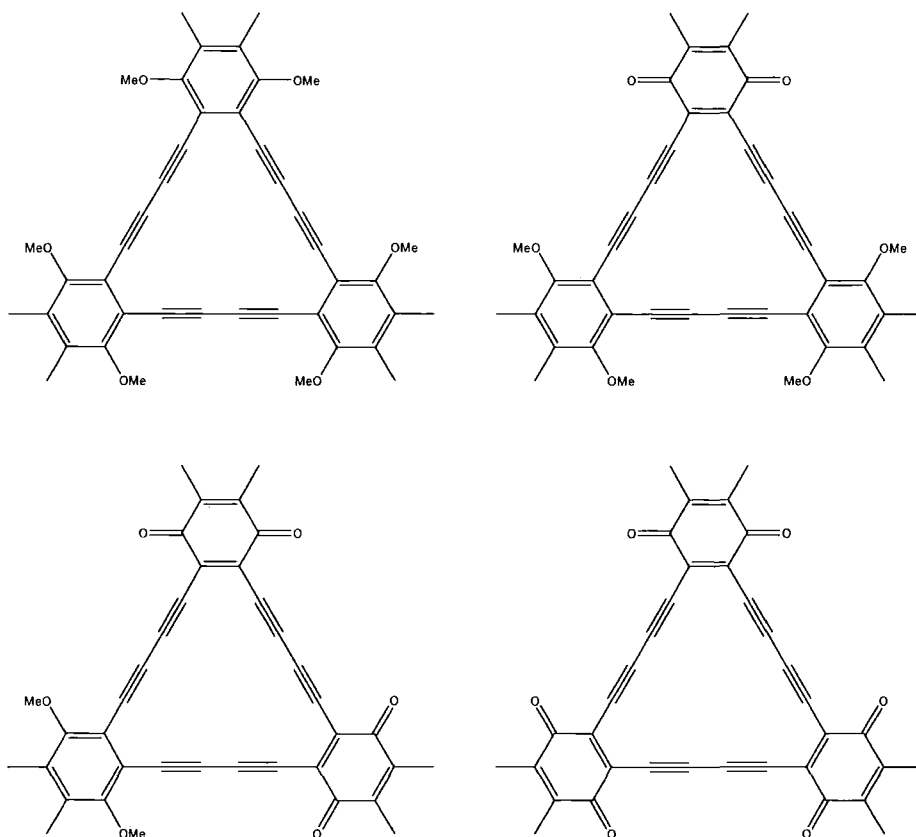


Figure 10. 3,6-dimethoxy-4,5-dimethylbenzene- and 4-benzoquinone-fused dehydroannulenes.

Marder and co-workers have studied the second and third order non-linear optical (NLO) properties of a series of end capped acetylenic oligomers.⁵⁴ The group studied asymmetric end-capped acetylenes and diynes, with a range of donor and acceptor substituents of varying strength, and found that these compounds exhibited moderate powder SHG efficiencies. Perry *et al.* have studied the relationship between the electronic structure of a series of donor-acceptor phenylacetylene and diphenylbuta-1,3-diyne compounds and the second-order non-linear polarizability (β), as determined by EFISH measurements.⁵⁵ The group note that the value of β is dominated by intermolecular charge transfer transitions, with strong donor-acceptor pairs producing large values of β , mainly because they have low energy absorption bands.

1.5 Substituted bis(4-*R*-phenyl)hex-3-ene-1,4-diyne

1.5.1 Synthesis of enediynes

There are a number of routes to synthesise *cis*- and *trans*-bis(phenyl)hexa-3-ene-1,4-diyne. The most straight forward methods involve Pd/Cu Sonogashira catalytic cross-coupling either of terminal alkynes with 1,2-haloalkenes^{56,57,58} or by the reaction of aryl halides with the parent enediyne.⁵⁹ Reactions of this type allow a single product isomer to be prepared as the haloalkene starting materials have a fixed geometry. For example, use of *trans*-1,2-dichloroethene gives the *trans*-enediyne product only (Figure 11).

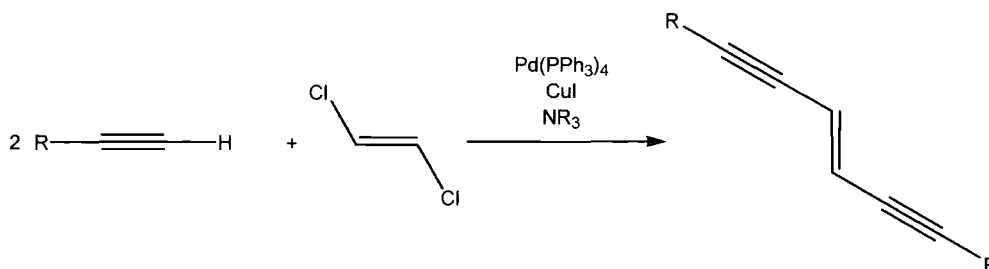


Figure 11. Pd/Cu catalysed formation of a *trans*-enediyne.

A more complex method of preparing enediynes has involved a one pot Ramberg-Bäcklund reaction with the enediyne products being formed as an approximately 1:1 mixture of geometrical *cis/trans* isomers.^{60,61} Dipropargylic sulphones are reacted with dibromodifluoromethane in the presence of alumina-supported KOH resulting in a facile rearrangement affording the corresponding linear enediynes in good yields and the full procedure uses readily available starting materials (Figure 12).

Jones and Huber have filed a U.S. patent on the synthesis of enediynes from propargylic halides in the presence of THF or ether, using non-nucleophilic lithium bases which initiate a carbenoid coupling-elimination sequence.⁶² Product formation occurs through the reaction of propargylic halide with the monohalocarbenoid generated *in situ* to form enediyne. Addition of a carbenoid destabilisation agent was found to enhance reaction yields.

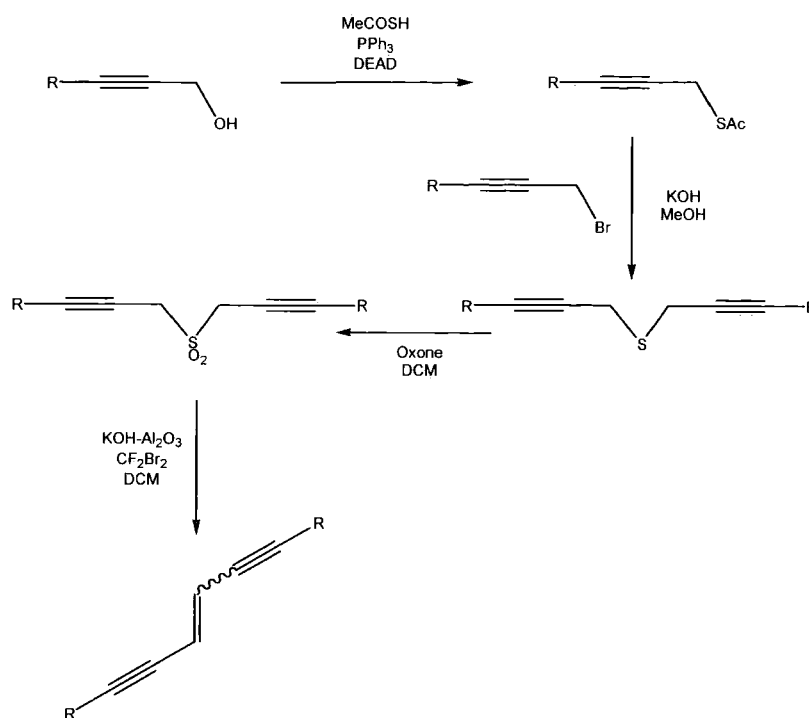


Figure 12. Enediyne synthesis involving a Ramberg-Bäcklund rearrangement.

1.5.2 Photophysical properties of bis(4-R-phenyl)hex-3-ene-1,4-diyne

Arai and co-workers have studied the photophysical properties for the parent enediyne⁶³ Ph-C≡C-CH=CH-C≡C-Ph, and that of a Me₂N-NO₂, donor-acceptor unsymmetrical enediyne.⁵⁶ The group found that *cis-trans* photoisomerisation was possible under UV irradiation around 350 nm with quantum yields of isomerisation of ca. 0.2. For the parent compound, they also observed emission bands around 360-380 nm with emission quantum yields of 0.31 and 0.42 for the *cis* and *trans* isomers respectively, also observing some formation of the triplet. For the donor-acceptor enediyne, the absorption was red-shifted compared to that of the parent enediyne due to charge transfer effects. The optical properties were also found to be solvent dependant. No emission was observed for this compound in polar solvents and quantum yields of fluorescence decreased from 0.33 to 0.25 in cyclohexane to benzene. Absorption bands that showed vibrational progressions in cyclohexane were red-shifted and broadened in benzene. The *cis-trans* photoisomerisation was almost solvent independent. These observations suggest that the introduction of donor or acceptor groups on the phenyl rings significantly changes the nature of the singlet excited state.

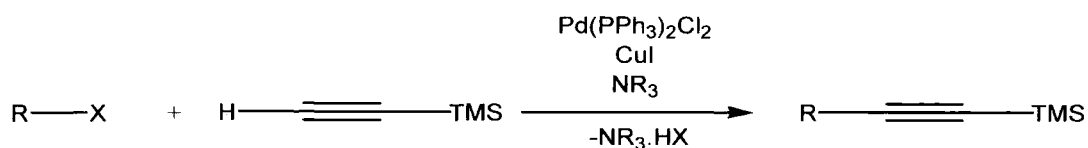
1.6 Results and Discussion

Synthesis and characterisation of 1,4-bis(4-R-phenyl)buta-1,3-diyne and related compounds

A number of substituted 1,4-bis(4-R-phenyl)buta-1,3-diyne and related buta-1,3-diyne compounds have been synthesised *via* catalytic routes previously described. A range of techniques have been utilised in the synthesis, purification and characterisation of each compound and several crystal structures of both diynes and precursor compounds required for the diyne syntheses have been obtained. Photophysical properties of the luminescent diynes have been measured and will be discussed.

1.6.1 Synthesis of terminal alkynes

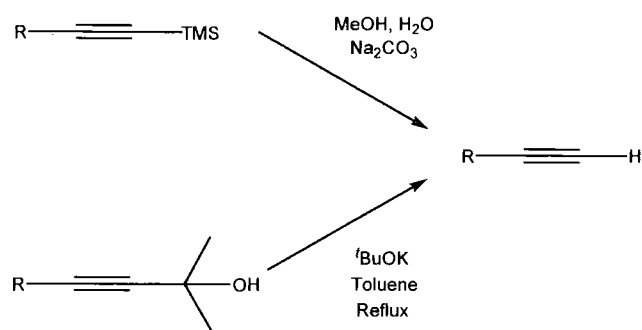
In order to synthesise 1,4-diarylbuta-1,3-diyne, *para*-substituted phenyl acetylenes and other related substituted phenyl acetylenes were first prepared. A convenient synthetic route to these compounds is *via* the formation of protected acetylenes. Two groups have been widely used in the protection of the alkyne moiety, $-\text{TMS}^2$ and $-\text{C}(\text{Me})_2\text{OH}$.⁶⁴ A Pd/Cu catalysed Sonogashira reaction is used to provide a facile and high yielding method for the cross-coupling of a substituted aryl halide ($\text{X} = \text{I}, \text{Br}$) with TMSA or 2-methyl-but-3-yn-2-ol. Aryl bromides are less reactive than aryl iodides and so higher temperatures and longer reaction times were required for these reactions to reach completion. Each reaction was monitored by GC-MS, either by the appearance of the product or by the disappearance of starting materials. The products could be obtained in moderate to good yields after filtration through a short silica gel column to remove ammonium halide byproduct, and subsequent removal of solvent *in vacuo* (Table 1). However, due to the volatility of **5**, removal of the solvent *in vacuo* was not possible and so the product was isolated by distillation of solvent from the sample leading to a low yield. Products that were shown to be pure by GC-MS and NMR spectroscopy were used for further synthesis.



Compound	R Group	X	Yield %
1	4-Me ₂ N-C ₆ H ₄ -	I	92
2	4-Me-C ₆ H ₄ -	I	83
3	4-NC-C ₆ H ₄ -	Br	95
4	4-MeO ₂ C-C ₆ H ₄ -	I	75
5	4-F ₃ C-C ₆ H ₄ -	Br	29
6	4-OHC-C ₆ H ₄ -	Br	97
7	1-naphthalenyl	I	97
8	2-thienyl	Br	65
9	3,5-(CF ₃) ₂ C ₆ H ₃ -C≡C-C ₆ H ₄ -	Br	75
10	2-thienyl-C≡C-4-C ₆ H ₄ -	I	79

Table 1. Pd/Cu catalysed cross coupling of aryl halides with TMSA.

Deprotection of the protected alkynes was easily achieved under basic conditions. The silyl group was removed with Na₂CO₃ in methanol/H₂O⁶⁵ and KO^tBu or powdered NaOH in refluxing toluene was used for the alcohol deprotection. The TMS reactions were complete after stirring overnight, and then the product was extracted into Et₂O or DCM, washed with water to remove any excess carbonate, and then the organic fractions were separated, dried over MgSO₄ and the solvent was removed *in vacuo* to give good yields of most products (Table 2). On isolation, the products were often pure, as indicated by GC-MS and/or NMR, although further purification on silica gel columns was also used in some cases. Removal of the alcohol protecting group required the refluxing of a toluene solution of protected alkyne overnight. Once cooled, the solutions were filtered to remove excess KO^tBu and then the solvent could be removed *in vacuo*. Filtration of the products through short silica gel pads was necessary to obtain compounds of sufficient purity for diyne synthesis and the reaction yields are generally lower than observed for the TMS analogues.



TMS deprotection

Compound	R Group	Yield %
11	4-Me ₂ N-C ₆ H ₄ -	71
12	4-Me-C ₆ H ₄ -	30
13	4-NC-C ₆ H ₄ -	88
14	4-MeO ₂ C-C ₆ H ₄ -	97
15	4-F ₃ C-C ₆ H ₄ -	29
16	4-OHC-C ₆ H ₄ -	96
17	4-H ₂ N-C ₆ H ₄ -	79
18	1-naphthalenyl	93
19	2-thienyl	65
20	3,5-(CF ₃) ₂ -C ₆ H ₃ -C≡C-C ₆ H ₄ -	87
21	2-thienyl-C≡C-C ₆ H ₄ -	97
22	4-Me ₂ N-C ₆ H ₄ -C≡C-C ₆ H ₄ -	86 (K ₂ CO ₃)

Alcohol deprotection

Compound	R Group	Yield %
23	4-MeO-C ₆ H ₄ -	42
24	4-MeS-C ₆ H ₄ -	80
25	4-TMS-C≡C-C ₆ H ₄ -	35

Table 2. Protected alkyne deprotection under basic conditions.

The previously unreported terminal alkyne 4-(phenylethynyl)-4-(methoxybenzylidene)-amine, **26**, was synthesised in moderate yield by an acid (solid *para*-toluenesulphonic acid) catalysed condensation reaction between 4-methoxybenzaldehyde and 4-ethynylaniline (Figure 13). The reversible nature of the reaction results in the imine product being unstable to water and so the reaction mixture was stirred over MgSO₄ to remove liberated water and to drive the reaction to completion. The acid was only added once the substrates had been mixed so as not to inhibit the addition step of the reaction by protonation of the amine. As both aldehyde and amine bear an aromatic substituent, the product is sufficiently stable for isolation, and synthesis can be achieved without the use of a Dean-Stark apparatus.

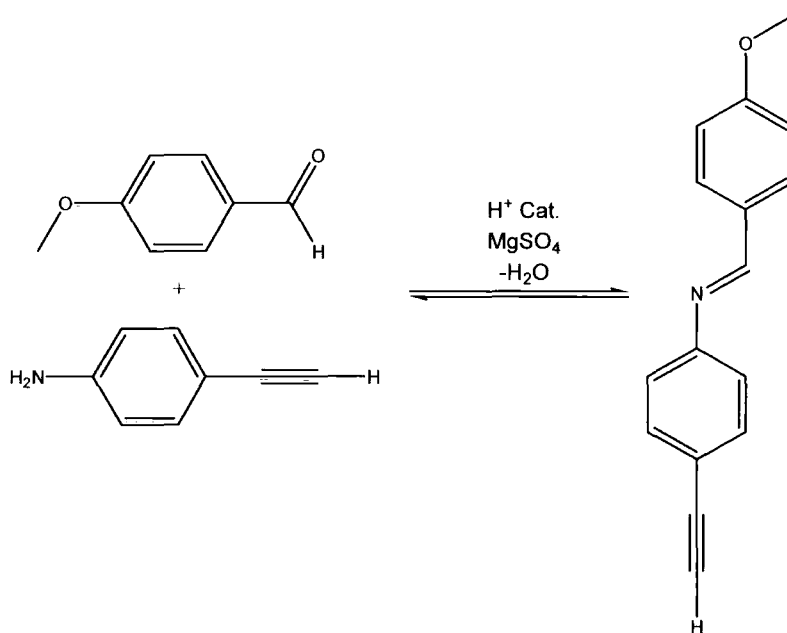
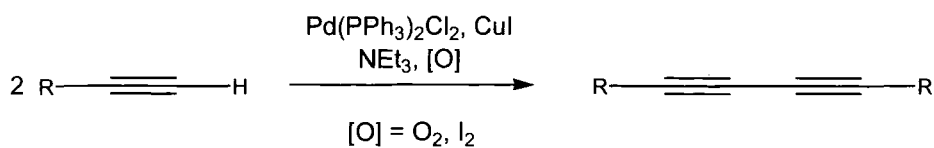


Figure 13. Acid catalysed formation of an unreported terminal alkyne containing imine, **26**.

1.6.2 Synthesis of butadiynes

The synthesis of 17 diynes, each bearing different aromatic substituents, has been achieved by the catalytic homocoupling of terminal alkynes. Pd/Cu co-catalysis has been used for the synthesis of **27** to **41**, utilising either I₂ or O₂ as oxidants, with NEt₃ or *i*Pr₂NH as base (Table 3). The compound 1,4-bis(4-methoxyphenyl)buta-1,3-diyne, **42**, was prepared by Cu catalysis in MeOH with pyridine base. Analytically pure diynes were obtained by recrystallisation, column chromatography or sublimation.



Compound	R Group	Oxidant	Yield %
27	C ₆ H ₅ -	I ₂	81
28	4-Me-C ₆ H ₄ -	I ₂	52
29	4-F ₃ C-C ₆ H ₄ -	I ₂	66
30	4-NC-C ₆ H ₄ -	I ₂	31
31	4-Me ₂ N-C ₆ H ₄ -	I ₂	59
32	4-MeO ₂ C-C ₆ H ₄ -	I ₂	73
33	4-MeS-C ₆ H ₄ -	O ₂	35
34	4-O ₂ N-C ₆ H ₄ -	I ₂	73
35	4-OHC-C ₆ H ₄ -	I ₂	63
36	1-naphthalenyl	O ₂	66
37	4-TMS-C≡C-C ₆ H ₄ -	O ₂	55
38	4-Hex ₂ N-C ₆ H ₄ -C≡C-C ₆ H ₄ -	I ₂	80
39	2-Thienyl	I ₂	40
40	3,5-(CF ₃) ₂ -C ₆ H ₃ -C≡C-C ₆ H ₄ -	I ₂	24
41	C ₆ F ₅ -	I ₂	61

Table 3. Catalytic homocoupling of terminal alkynes to form butadiynes.

Pd/Cu catalysis provides a facile coupling method with both high yields and pure products obtainable. Reactions with O₂ as the oxidant gave products that were easier to isolate, but often resulted in lower yields and sometimes incomplete reactions. I₂ oxidation, in the absence of O₂, proved in some cases to be higher yielding and, with an extra synthetic step involving a sodium thiosulfate wash to remove any unreacted iodine, also resulted in purer product.

Two previously unreported, luminescent diynes have been prepared. The conjugated four aromatic ring compound 1,4-bis[(3,5-bis(trifluoromethyl)phenyl)-4-ethynylphenyl]buta-1,3-diyne, **40**, was prepared by the Pd/Cu catalysed homocoupling of two equivalents of **20** with I₂ as oxidant (Figure 14). A low yield of pure product was

obtained as separation of the diyne compound from a bromide impurity, 3,5-(CF₃)₂C₆H₃-C≡C-4-C₆H₄-Br, present from the synthesis of the terminal acetylene starting material, was difficult to achieve both by chromatographic and sublimation techniques.

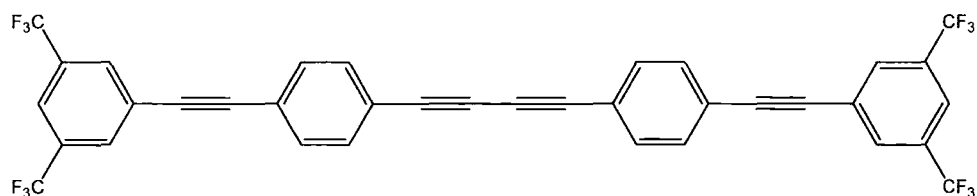


Figure 14. The compound 1,4-bis[(3,5-bis(trifluoromethyl)phenyl)-4-ethynylphenylethynyl]buta-1,3-diyne.

The second unreported diyne, 1,4-bis(4-dicyanovinylphenyl)buta-1,3-diyne, **43**, was synthesised by reaction of **35** with malononitrile in refluxing ⁱPrOH using a small amount of 2,2,6,6-tetramethylpiperidine as a catalyst for the reaction (Figure 15). Upon cooling, the brown product precipitated and was isolated by filtration and washed with hexanes. Pure diyne was obtained as a yellow solid in almost quantitative yield (97 %) by sublimation under high vacuum at 280 °C.

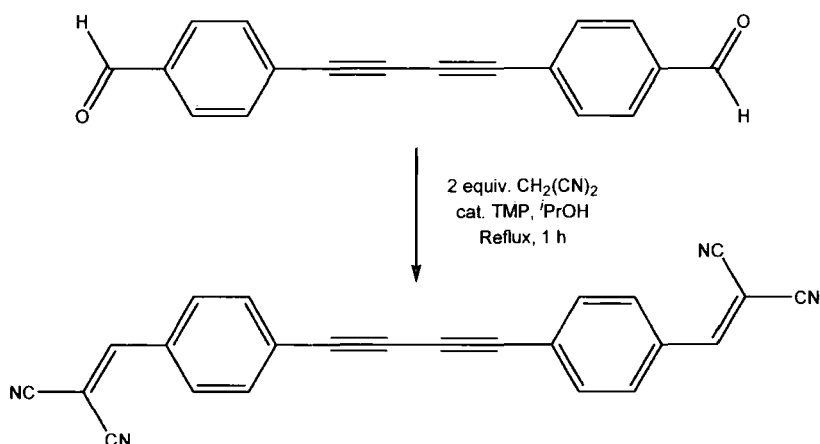


Figure 15. Synthesis of 1,4-bis(4-dicyanovinylphenyl)buta-1,3-diyne, **43**.

Compounds **20**, **21**, **22**, **37**, **38** and **40** have been prepared from the reaction of an aryl halide with **25**. Compound **25** can be synthesised from 1-iodo-4-bromobenzene by sequential Pd/Cu catalysed Sonogashira cross-coupling reactions, first with 2-methylbut-3-

yn-2-ol in NEt_3 at room temperature and then by coupling with TMSA in refluxing NEt_3 . Under rigorously dry conditions, **25** can be obtained in moderate yield by selective removal of the alcohol group with NaOH powder in refluxing toluene, leaving the TMS group intact.⁶⁶ Hydrodesilylation using four equivalents of K_2CO_3 in methanol and water can also be used to selectively cleave the TMS group to give 4-(4-ethynyl-phenyl)-2-methylbut-3-yn-2-ol, demonstrating the orthogonal deprotection of 4-(4-trimethylsilylethynyl-phenyl)-2-methylbut-3-yn-2-ol.

1.7 Crystal structures

A number of diynes and the compounds used in diyne synthesis have been characterised by single crystal X-ray analysis, some of which have since been published.^{13,67,68} The crystallographic data for compounds **1**, **9**, **21** and **29** are presented in Table 4 and the data for compounds **32**, **38** and **39** are presented in Table 5.

1.7.1 Crystal structures of alkyne precursor compounds

Me₂N-C₆H₄-C≡C-TMS, 1

Orthorhombic crystals (space group = $Pnma$) of **1** were grown by slow evaporation of solvent from a concentrated solution in MeOH. $Z' = 1.5$ and there are three independent molecules all possessing crystallographic mirror symmetry (Figure 16).⁶⁷ For two molecules, the mirror plane is perpendicular to arene ring and amino group planes, and passes through the Si(1), N(1), C(2), C(3), C(4), C(5), C(8) and Si(2), N(2), C(11), C(12), C(13), C(14), C(17) atoms respectively. The entire third molecule lies in the mirror plane except for atoms C(20) and its equivalent C(20A). The Si(1), N(1), C(2), C(3), C(4), C(5), C(8) and Si(2), N(2), C(11), C(12), C(13), C(14), C(17) 'rods' are all significantly bent.

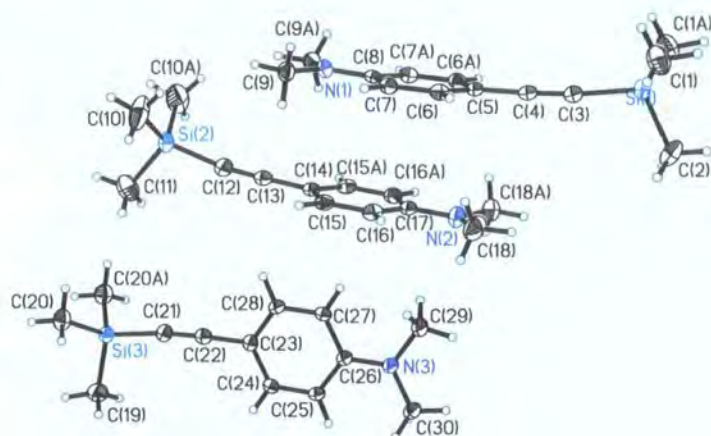


Figure 16. Independent molecules in the asymmetric unit of compound **1**. Thermal ellipsoids are shown at 50 % probability.

1-[3,5-bis(trifluoromethylphenylethynyl)-4-(trimethylsilylethynyl)benzene, 9

Single crystals of **9** were grown by slow evaporation of solvent from a concentrated DCM/hexane solution. Analysis of the colourless, orthorhombic crystals (space group = *Pbca*) reveals a single molecule in the asymmetric unit that is almost planar with a slight angle of 2.5° between the two phenyl rings (Figure 17). There is rotational disorder in each of the CF₃ units, and the C(7)≡C(8) and C(17)≡C(18) bonds measure 1.198(3) Å and 1.205(3) Å respectively.

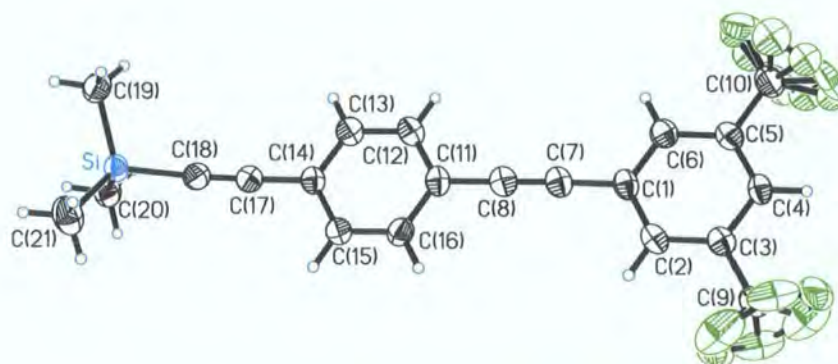


Figure 17. Molecular structure of **9**. Thermal ellipsoids are shown at 50 % probability.

Molecule	1 - 04srv103	9 - 06srv136	21 - 06srv185	29 - 04srv097
Empirical formula	C ₁₃ H ₁₉ NSi	C ₂₁ H ₁₆ F ₆ Si	C ₁₄ H ₈ S	C ₁₈ H ₈ F ₆
Formula Weight	217.38	410.43	208.26	338.24
Temperature (K)	120(2)	120(2)	120(2)	120(2)
Crystal system	Orthorhombic	Orthorhombic	Monoclinic	Monoclinic
Space Group	<i>Pnma</i>	<i>Pbca</i>	<i>Cc</i>	<i>P2₁/c</i>
a (Å)	13.015(2)	13.4135(12)	5.9484(8)	13.258(3)
b (Å)	9.581	8.6033(8)	17.115(2)	6.215(1)
c (Å)	32.611(6)	35.191(3)	10.595(1)	17.517(13)
α (°)	90.00	90.00	90.00	90.00
β (°)	90.00	90.00	100.48(1)	94.70(3)
γ (°)	90.00	90.00	90.00	90.00
Volume (Å ³)	4066.5(16)	4061.1(6)	1060.7(2)	1438.5(11)
Z	12	8	4	4
Density (calculated) Mg/m ³	1.065	1.343	1.304	1.562
Absorption coefficient (mm ⁻¹)	0.145	0.171	0.263	0.145
Crystal size (mm ³)	0.23 x 0.15 x 0.15	0.35 x 0.20 x 0.11	0.48 x 0.17 x 0.13	0.33 x 0.25 x 0.08
Theta range for data collection (°)	2.50 to 30.37	2.30 to 28.30	2.38 to 29.78	2.33 to 27.50
Reflections collected	4949	4661	3080	3298
Independent reflections	3898	3183	2687	2498
Data / Restraints / Parameters	4949 / 0 / 367	4661 / 102 / 292	3080 / 2 / 165	3298 / 0 / 249
Final R indices	R1 = 0.0379 wR2 = 0.0952	R1 = 0.0480 wR2 = 0.1195	R1 = 0.0424 wR2 = 0.0983	R1 = 0.0447 wR2 = 0.1142
R indices (all data)	R1 = 0.0506 wR2 = 0.1005	R1 = 0.0748 wR2 = 0.1293	R1 = 0.0490 wR2 = 0.1088	R1 = 0.0595 wR2 = 0.1205

Table 4. Crystallographic data for compounds **1**, **9**, **21** and **29**.

Molecule	32 - 04srv166	38 - 05srv188	39 - 06srv169
Empirical formula	C ₄₀ H ₂₈ O ₈	C ₅₆ H ₆₈ N ₂	C ₁₂ H ₆ S ₂
Formula Weight	636.62	769.12	214.29
Temperature (K)	120(2)	120(2)	120(2)
Crystal system	Triclinic	Triclinic	Monoclinic
Space Group	<i>P</i> -1	<i>P</i> -1	<i>P</i> 2 ₁ / <i>n</i>
a (Å)	7.0249(5)	11.6701(12)	5.797(2)
b (Å)	10.4613(8)	14.3089(15)	13.840(5)
c (Å)	11.7016(8)	15.3542(15)	13.307(5)
α (°)	75.204(3)	93.22(1)	90.00
β (°)	72.585(3)	111.81(1)	101.05(1)
γ (°)	75.457(3)	101.17(1)	90.00
Volume (Å ³)	778.97(10)	2312.1(4)	1047.8(7)
Z	2	2	4
Density (calculated) Mg/m ³	1.357	1.105	1.358
Absorption coefficient (mm ⁻¹)	0.095	0.063	0.460
Crystal size (mm ³)	0.44 x 0.40 x 0.06	0.23 x 0.07 x 0.04	0.30 x 0.18 x 0.07
Theta range for data collection (°)	1.86 to 30.50	1.91 to 25.00	2.94 to 29.09
Reflections collected	6778	7962	2816
Independent reflections	4305	2809	2356
Data / Restraints / Parameters	4305 / 0 / 273	7962 / 0 / 531	2816 / 0 / 145
Final R indices	R1 = 0.0551 wR2 = 0.1304	R1 = 0.0668 wR2 = 0.1376	R1 = 0.0410 wR2 = 0.0922
R indices (all data)	R1 = 0.0718 wR2 = 0.1401	R1 = 0.1837 wR2 = 0.1738	R1 = 0.0520 wR2 = 0.0985

Table 5. Crystallographic data for compounds **32**, **38** and **39**.

2-(4-ethynylphenylethynyl)thiophene, **21**

Monoclinic crystals of **21** were obtained by slow evaporation of solvent from a hexane/DCM solution (space group Cc , $Z = 4$). The crystals contain one independent molecule in the asymmetric unit which is almost planar with a slight [2.1°] interplanar angle between the thiophene and benzene rings and with both alkyne bonds close to linearity [$C(6)\equiv C(7) = 1.200(2)$ Å and $C(14)\equiv C(15) = 1.162(3)$ Å] (Figure 18). The sulfur atom is disordered between positions S(1) and S(3) in 57:43 ratio. In either position, S and C atoms were refined as a single atom with a mixed scattering factor.

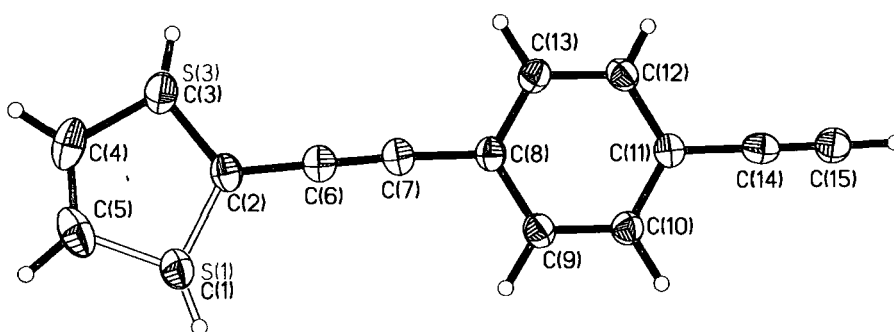


Figure 18. Molecular structure of 2-(4-ethynylphenylethynyl)thiophene, **21**. Thermal ellipsoids are shown at 50 % probability.

1.7.2 Crystal structures of buta-1,3-diyne

1,4-bis(4-trifluoromethylphenyl)buta-1,3-diyne, **29**

Crystals of **29** were grown from a concentrated solution in hexane at low temperature. The compound crystallises in the monoclinic space group $P2_1/c$ with $Z = 4$, and there is one independent molecule in the asymmetric unit (Figure 19).¹³ The $C(7)\equiv C(8)$ and $C(9)\equiv C(10)$ bond lengths are $1.204(2)$ Å and $1.206(2)$ Å respectively. The two phenyl rings form an angle of 10.9° . The $C(7),C(8),C(9),C(10)$ butadiyne bridge is slightly distorted from linearity by up to 3.6° . As expected, due to $sp-sp$ hybridisation, $C(8)-C(9)$ is shorter than a typical C-C single bond [$1.372(2)$ Å].

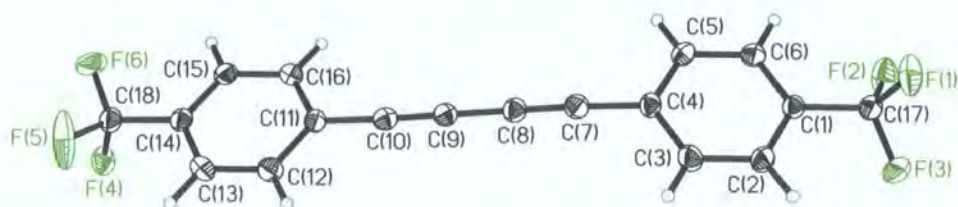


Figure 19. Molecular structure of 1,4-bis(4-trifluoromethylphenyl)buta-1,3-diyne, **29**. Thermal ellipsoids are shown at 50 % probability.

1,4-bis(4-carbomethoxyphenyl)buta-1,3-diyne, 32

Compound **32** was crystallised by slow evaporation of benzene from a concentrated solution as triclinic crystals (space group = $P-1$) with all of the molecules aligned with their long axes parallel.⁶⁸ The molecule possesses no crystallographic symmetry and is substantially non-planar (Figure 20). The two phenyl rings form an angle of 23.9°. Torsional angles between the aromatic rings and their carboxy groups are 10.4° around the C(2)-C(3) bond and 13.2° around the C(18)-C(19) bond. The carboxylate groups are in an anti-parallel arrangement with respect to each other. The C(9)≡C(10) and C(11)≡C(12) bond lengths are 1.2054(19) Å and 1.2041(19) Å respectively and the C(10)-C(11) bond length is 1.3716(19) Å. The C(9),C(10),C(11),C(12) butadiyne bridge is distorted from linearity by a maximum of 3.6°.

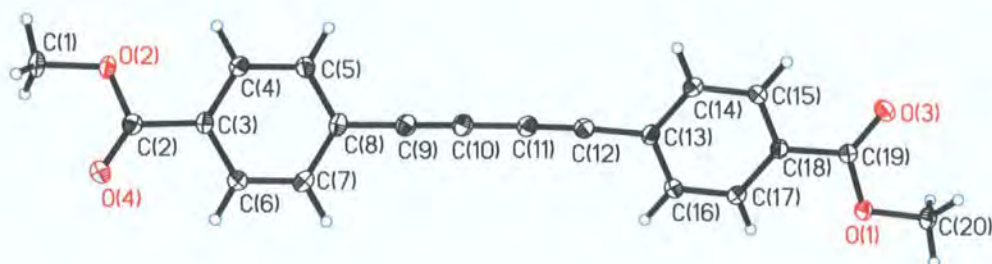


Figure 20. Molecular structure of 1,4-bis(4-carbomethoxyphenyl)buta-1,3-diyne, **32**. Thermal ellipsoids are shown at 50 % probability.

1,4-bis(4-N,N-dihexylaminophenylethynyl-4-phenyl)buta-1,3-diyne, 38

Single crystals of **38** were grown by slow evaporation of solvents from a concentrated solution of compound in a mixture of DCM, EtOH and hexane. Triclinic

crystals in space group $P-1$ ($Z = 2$) show two half molecules in the unit cell related to their other halves by inversion symmetry. Each half molecule is in a ‘special position’ at the edge of the unit cell and so the two half molecules are not directly related to each other (Figure 21). The first molecule is non-planar and shows an interplanar angle of 49.1° between the inner and outer phenyl rings and an angle of 7.4° for the C(34)-C(29)-N(2)-C(45) dihedral angle. The butadiyne bonds C(15) \equiv C(16) and C(43) \equiv C(44) are similar lengths to each other [1.206(5) Å and 1.193(5) Å respectively] and to the tolan alkyne bonds, C(7) \equiv C(8) and C(35) \equiv C(36) [1.194(5) Å and 1.201(5) Å respectively]. The second molecule is much more planar than the first with an interplanar angle of 4.4° between the inner and outer phenyl rings. The C(2),C(1),N(1),C(17) dihedral angle is slightly smaller than for the first molecule [5.4°].

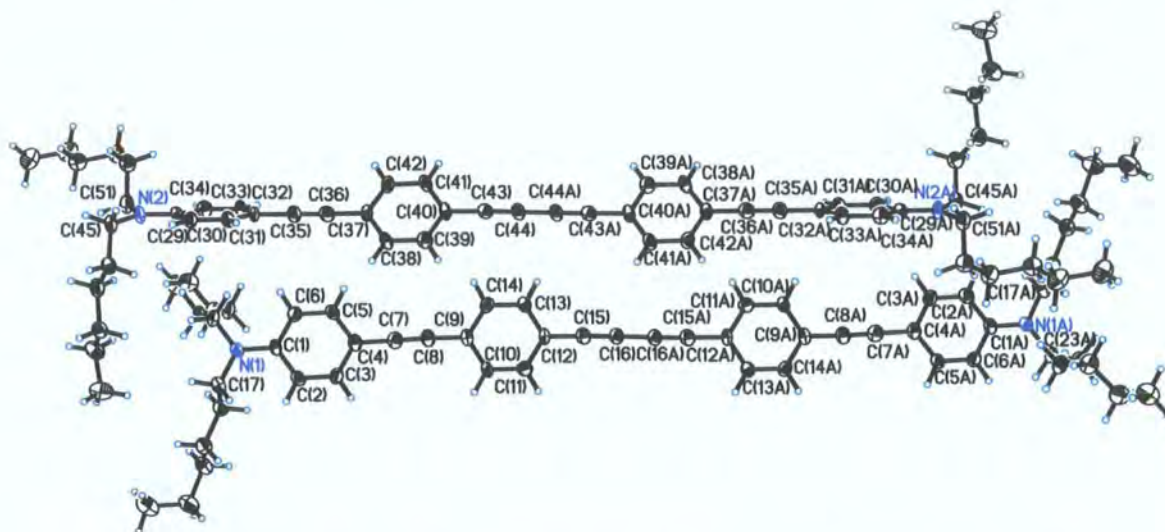


Figure 21. Molecular structure of **38**. Thermal ellipsoids are shown at 50 % probability.

1,4-bis(2-thienyl)buta-1,3-diyne, 39

Monoclinic crystals (space group $P2_1/n$) of **39** were grown at low temperature from a concentrated solution in cyclohexane. The structure shows a single independent molecule in the unit cell and both thiophene rings are disordered by 180° rotations around the diyne axis: S(1) and C(3)H have occupancies of 87.5(2) %, C(1)H and S(3) of 12.5(2) %, S(11) and C(13)H of 63.7(2) %, C(11)H and S(13) of 36.3(2) %. The bonds C(6) \equiv C(7) and C(8) \equiv C(9) measure 1.212(2) Å and 1.208(2) Å respectively and the C(7)-C(8) bond is 1.374(2) Å (Figure 22).

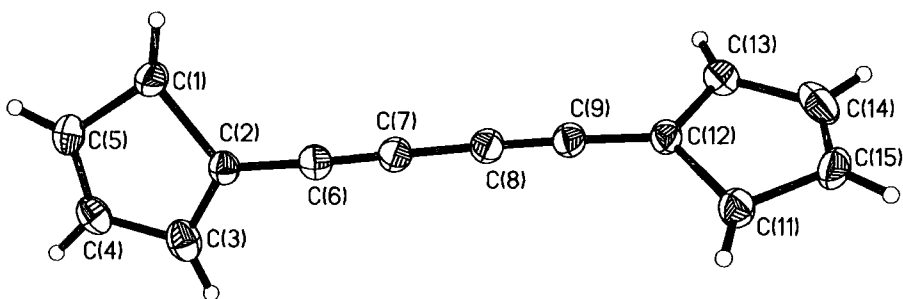


Figure 22. Molecular structure of **39**. Thermal ellipsoids are shown at 50 % probability.

1.8 Synthesis of an enediyne

The previously unreported enediyne compound 1,6-bis(4-trifluoromethylphenyl)hex-3-ene-1,4-diyne, **44**, has been prepared *via* the Pd/Cu catalysed cross-coupling of two equivalents of **15** with *trans*-1,2-dichloroethene (Figure 23). The reaction was carried out in a nitrogen filled glove box using Pd(PPh₃)₄ catalyst rather than Pd(PPh₃)₂Cl₂ in order to prevent the formation of butadiyne byproduct during the initiation step necessary for the Pd(PPh₃)₂Cl₂ catalyst reduction, as separation of enediyne and butadiyne would be difficult due to the similarity between the compounds. Pure compound was obtained as a pale yellow solid after purification on a silica column and was found to emit blue light upon UV irradiation. The photophysical properties have been studied.

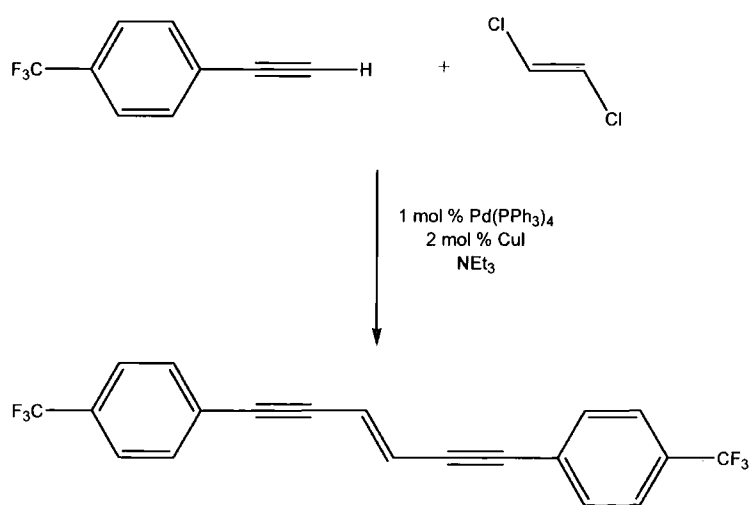


Figure 23. Synthesis of 1,6-bis(4-trifluoromethylphenyl)hex-3-ene-1,4-diyne, **44**.

1.9 Photophysical properties of buta-1,3-diyne and an enediyne

1.9.1 Optical properties of buta-1,3-diyne

The photophysical properties (absorption and fluorescence maxima, quantum yields and lifetimes) of the diynes **36**, **37**, **38**, **40** and **42** are presented Table 6.

Compound	Solvent	λ_{\max} abs (nm)	ϵ ($\text{mol}^{-1} \text{cm}^{-1} \text{dm}^3$)	λ_{\max} em (nm)	Stokes shift (cm^{-1})	Φ (%)	τ (ps)
36	CHCl_3	348	29000	380, 403, 414	2420	14	330
		375	25000				
37	Toluene	297	36000	366, 387, 398	2260	7	-
		313	52000				
		338	60000				
		363	48000				
38	Toluene	398	149000	444	2600	58	-
40	CHCl_3	344	72000	386, 409, 419	3160	32	290
		373	51000				
43	Toluene	380	a	428	2800	3	100
		408					
43	CHCl_3	384 410 sh	a	437	3160	4	-

^a Compound too insoluble for accurate ϵ measurement

Table 6. Summary of the photophysical properties of luminescent diynes.

The absorption spectra for diynes **36**,⁶⁹ **37**, **38**, **40** and **43** are shown in Figure 24. The absorption band for compound **37** shows vibrational fine structure with the absorption maxima separated by approximately 2000 cm^{-1} , corresponding to alkyne vibrational modes. Compound **43** shows solvatochromism with polar CHCl_3 shifting the maximum by 4 nm compared to the absorption maximum in less polar toluene. It was not possible to measure accurate extinction coefficients for **43** due to its very low solubility. Compounds **38** and **40** have large extinction coefficients compared to those for shorter diynes **36**, **37** and **43** with values for the absorption maxima of $72000 \text{ mol}^{-1} \text{cm}^{-1} \text{dm}^3$ and $149000 \text{ mol}^{-1} \text{cm}^{-1} \text{dm}^3$ respectively. Increasing the length of conjugation within the diyne shifts both absorption and emission bands to lower energy and greatly increases ϵ .

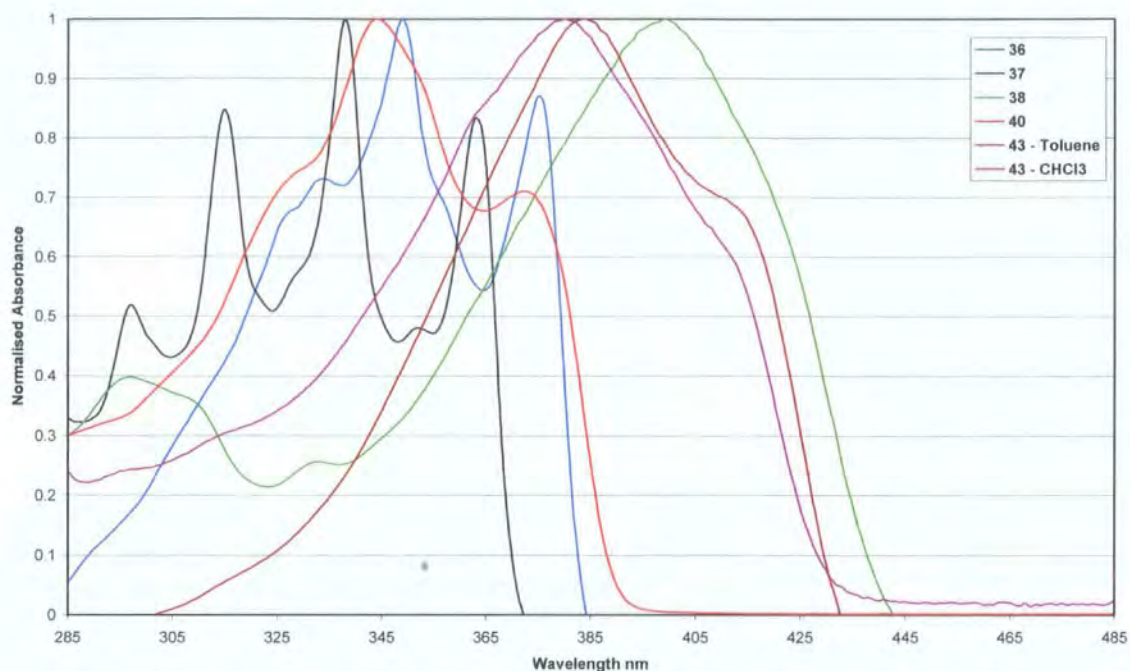


Figure 24. Normalised absorption spectra for luminescent diynes **36**, **37**, **38**, **40** and **43**.

The emission spectra for compounds **36**, **37**, **38**, **40** and **43** are shown in Figure 25. Each compound shows one major emission band with less intense bands (or shoulders) at lower energy. The longer diynes, **38** and **40** have considerably higher quantum yields compared to the 1,4-(4-R-phenyl)buta-1,3-diyne and the naphthalene substituted diyne. The lifetime of compound **43** is very short (100 ps), and those for **36** and **40** are somewhat longer (330 and 290 ps respectively). Attempts to measure the lifetime of compound **38** were not successful as the fluorescence emission consisted of two separate decays in the two different analytically pure samples measured.

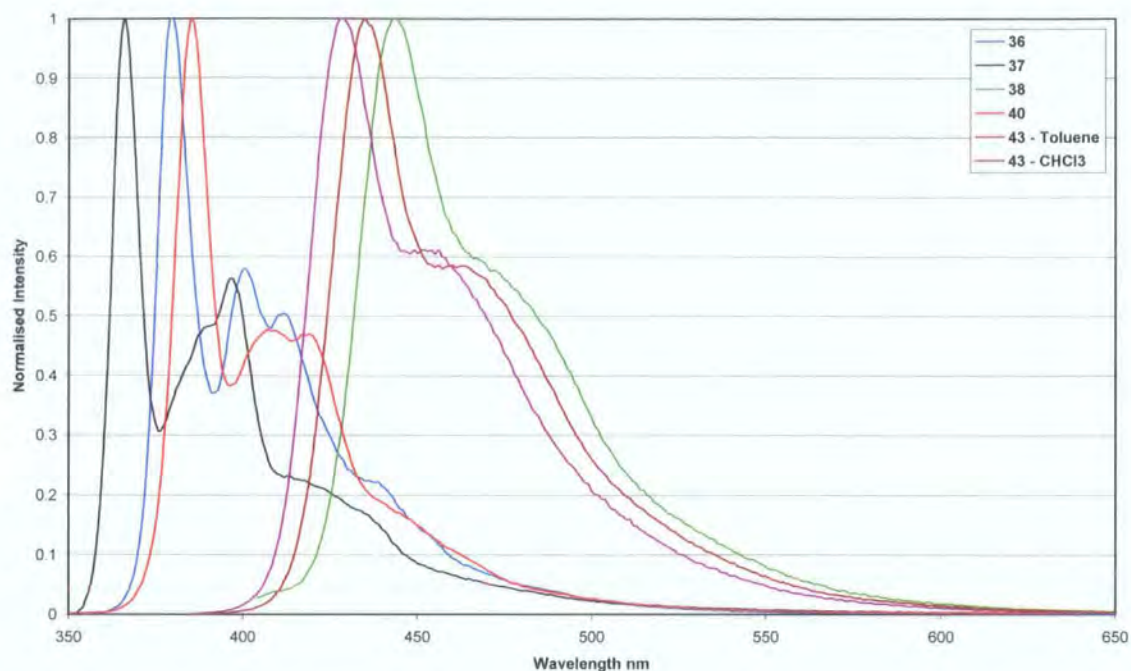


Figure 25. Normalised emission spectra for luminescent diynes **36**, **37**, **38**, **40** and **43**.

1.9.2 Optical properties of 1,5-bis(4-trifluoromethylphenyl)hex-3-ene-1,4-diyne

The photophysical properties of compound **44** (absorption and fluorescence maxima, quantum yield and lifetime) are shown in Table 7 and the absorption and emission spectra are shown in Figure 26.

Compound	Solvent	λ_{\max} abs (nm)	ϵ ($\text{mol}^{-1} \text{cm}^{-1} \text{dm}^3$)	λ_{\max} em (nm)	Stokes shift (cm^{-1})	Φ (%)	τ (ns)
44	CHCl_3	329	39000	359	2540	44	1.05
		353	26000	380	2012		

Table 7. Photophysical properties of 1,6-bis(4-trifluoromethylphenyl)hex-3-ene-1,4-diyne in CHCl_3 .

Compound **44** shows an absorption band with two maxima and an emission band with two maxima and a shoulder at low energy (ca. 405 nm). Stokes shifts of 2540 cm^{-1} and 2012 cm^{-1} for each maxima respectively are observed. The quantum yield is moderately high and the fluorescence lifetime is longer than those for the luminescent diynes **36**, **37**, **38**, **40** and **43**, though still singlet emission.

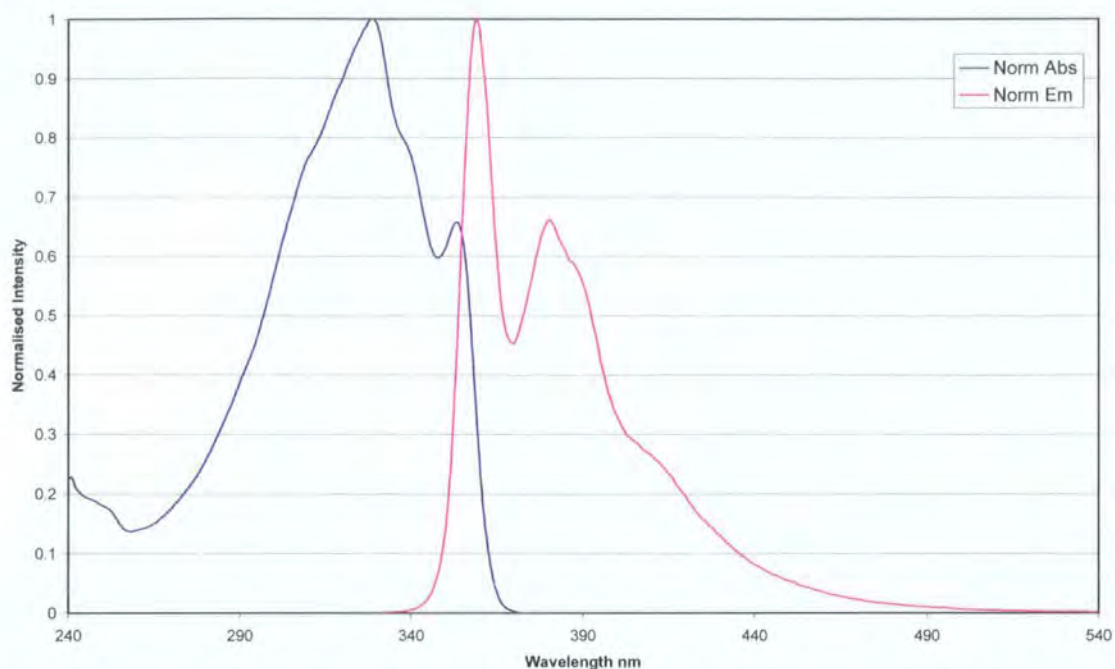


Figure 26. Absorption and emission spectra of *E*-1,6-bis(4-trifluoromethylphenyl)hex-3-ene-1,4-diyne, **44** in CHCl_3 .

1.10 Conclusions

Pd/Cu catalysed Sonogashira cross-coupling methodology to form protected phenylacetylenes, and their subsequent deprotection under basic conditions provides a convenient synthetic route to a series of substituted ethynylbenzenes. Under aerobic conditions or with a stoichiometric amount of added oxidant, Pd/Cu catalysis can be used to homocouple ethynylbenzenes to form substituted buta-1,3-diyne in moderate to high yields. Compounds with *para*-substituents that increase the extent of the conjugation through the molecule are found to emit light in the UV-Vis region with moderate to high quantum yields.

The Pd/Cu catalysed Sonogashira cross-coupling reaction can also be used in the preparation of the regiospecific enediyne *trans*-1,6-bis(4-trifluoromethylphenyl)hex-3-ene-1,4-diyne in moderate yield from 4-ethynylbenzotrifluoride with *trans*-1,2-dichloroethene. The compound shows luminescent properties which have been studied.

1.11 Experimental

1.11.1 General

All reactions were carried out using standard Schlenk techniques or in an Innovative Technology Inc. nitrogen filled glove box. Solvents were dried before use with appropriate drying agents. The reagents used in synthesis were purchased from commercial suppliers and tested for purity by GC-MS before use.

NMR spectroscopy experiments were performed on Varian Mercury-200, Unity-300 and Inova-500 and Bruker Avance-400 spectrometers at the following frequencies: ^1H – 200, 300, 400, 500 MHz, $^{13}\text{C}\{^1\text{H}\}$ – 101, 126 MHz, $^{19}\text{F}\{^1\text{H}\}$ – 188, 282 MHz. NMR experiments were run in CDCl_3 solvent unless otherwise indicated.

GC-MS analyses were performed on a Agilent Technologies 6890 N gas chromatograph equipped with a 5973 inert mass selective detector and a 10 m fused silica capillary column (5 % cross linked phenylmethylsilicone), under the following operating conditions: injector temperature 250 °C, detector temperature 300 °C, the oven temperature was ramped from 70 °C to 280 °C at 20 °C/min. UHP helium was used as the carrier gas.

Sublimations were carried out using a Kugelrohr oven to control temperature, which was attached to a vacuum line with a turbo pump capable of pressures of 10^{-4} Torr.

Mass spectra were obtained using the GC-MS above or on a MicroMass AutoSpec spectrometer operating in EI mode and elemental analyses were performed using an Exeter Analytical E440 machine by departmental services at Durham University.

UV/Vis absorption spectra were recorded on a Hewlett-Packard 8453 diode array spectrophotometer using standard 1 cm width quartz cells. Fluorescence spectra and quantum yield measurements were recorded on a Horiba Jobin-Yvon Fluoromax-3 spectrophotometer. The spectra of dilute solutions with absorbance maxima of less than 0.1 were recorded using conventional 90 degree geometry. The emission spectra were fully corrected using the manufacturers correction curves for the spectral response of the emission optical components.

The quantum yields of compounds **36-38**, **40**, **43** and **44** were estimated by comparing each with standards of known quantum yield. The absorbance of the samples was kept below 0.12 to avoid inner filter effects and all measurements were carried out at room temperature. The fluorescence quantum yields were measured against quinine sulphate in 0.1M H_2SO_4 ($\Phi = 0.54$)⁷⁰ and norharmane in 0.1M H_2SO_4 ($\Phi = 0.58$).⁷¹ The

fluorescent lifetimes of **36**, **40** and **43** were measured using time correlated single photon counting (TCSPC) using either a 396 nm pulsed laser diode or the 3rd harmonic of a cavity dumped, mode locked Ti-sapphire laser (Coherent MIRA), 300 nm. The fluorescence emission was collected at right angles to the excitation source with the emission wavelength selected using a monochromator and detected by a single photon avalanche diode (SPAD). The excitation wavelengths used for fluorescence measurements were the wavelengths at which strongest absorption was observed in the absorption spectra of each compound. The instrument response function was measured using a dilute LUDOX[®] suspension as the scattering sample, setting the monochromator at the emission wavelength of the laser, giving an instrument response function (IRF) of 200 or 100 ps at 396 or 300 nm respectively. The resulting intensity decay is a convolution of the fluorescence decay with the IRF, and iterative reconvolution of the IRF with a decay function and non-linear least squares analysis was used to analyse the convoluted data.⁷⁰⁻⁷³

Raman spectra were recorded on solid samples using a LabRamHR Raman microscope with the laser set at 633 nm. IR spectra were recorded as KBr discs using either a Perkin Elmer 1600 series or Spectrum 100 series FT-IR spectrometer.

Single-crystal diffraction experiments were carried out on Bruker 3-circle diffractometers with CCD area detectors APEX (**1**, **29**, **32**, **38**), SMART 6K (**9**, **21**), or SMART 1K (**39**), using graphite-monochromated Mo- K_{α} radiation ($\lambda = 0.71073 \text{ \AA}$) and Cryostream (Oxford Cryosystems) open-flow N₂ cryostats. The structures were solved by direct methods and refined by full-matrix least squares against F^2 of all data, using SHELXTL software.⁷⁴ Non-H atoms were refined in anisotropic and H atoms in isotropic approximation.

1.11.2 Synthesis of TMS protected ethynylbenzenes

1 - 4-(Trimethylsilylethynyl)-N,N-dimethylaniline *via* 4-iodo-N,N-dimethylaniline

The compounds N,N-dimethylaniline (0.20 mol, 24.22 g) and NaHCO₃ (0.33 mol, 27.72 g) were mixed in 500 ml of distilled H₂O in a 3 L round bottomed flask. Over 30 min, I₂ (0.20 mol, 50.76 g) dissolved in 1.5 L of DCM was added. The mixture was stirred at room temperature overnight. The dark blue solution was washed with copious amounts of a saturated solution of Na₂S₂O₃ and then the organic layer separated, dried over MgSO₄

and the solvent was removed *in vacuo*. The resulting blue solid was dissolved in hexanes and filtered through a 10 cm silica gel column with hexane eluant. Removal of the solvent *in vacuo* yielded 4-iodo-N,N-dimethylaniline as a white solid. Yield: 36.53 g, 74 %. ^1H NMR (300 MHz) δ : 7.47 (m, 2H, CH_{arom}), 6.49 (m, 2H, CH_{arom}), 2.93 (s, 6H, NMe_2). m/z : 246 [M^+].

The compounds 4-iodo-N,N-dimethylaniline (101.2 mmol, 25.00 g), CuI (1.01 mmol, 0.19 g) and $\text{Pd}(\text{PPh}_3)_2\text{Cl}_2$ (1.01 mmol, 0.71 g) were added to a flask that had been evacuated and refilled with N_2 3 times. Diisopropylamine (350 ml) was added *via* cannula and the mixture was stirred. TMSA (110 mmol, 10.80 g) was added under nitrogen and the solution was stirred overnight. The solvent was removed *in vacuo* and the residue was dissolved in Et_2O and filtered through a 5 cm silica gel column. After removal of the ether *in vacuo*, a dark grey solid was obtained which was dissolved in a small amount of hexane and filtered through a 5 cm alumina column and eluted with hexanes. Removal of the solvent *in vacuo* gave 4-(trimethylsilylethynyl)-N,N-dimethylaniline as a white solid. Yield: 20.19 g, 92 %. A small portion of solid was dissolved in methanol with heating. Upon slow evaporation of the solvent, crystals suitable for X-ray analysis were obtained. ^1H NMR (400 MHz) δ : 7.37 (d, $J = 9$ Hz, 2H, CH_{arom}), 6.62 (d, $J = 9$ Hz, 2H, CH_{arom}), 2.97 (s, 6H, NMe_2), 0.23 (s, 9H, SiMe_3). m/z : 217 [M^+].

2 - 4-(trimethylsilylethynyl)toluene

The compounds 4-iodotoluene (91.73 mmol, 20.00 g), CuI (4.6 mmol, 0.87 g) and $\text{Pd}(\text{PPh}_3)_2\text{Cl}_2$ (0.92 mmol, 0.64 g) were added to a flask that had been evacuated and refilled with N_2 3 times, and then were slurried in NEt_3 (350ml). TMSA (100 mmol, 9.82 g) was added under N_2 and the mixture was stirred rapidly overnight, after which it was filtered through a sinter and washed with ether. After removal of the solvents *in vacuo*, the residual oil was dissolved in a small amount of hexane and filtered through a short silica gel column with hexane eluant. Removal of hexane *in vacuo* gave the product **2** as an orange oil. Yield: 14.36 g, 83 %. ^1H NMR (200 MHz) δ : 7.34 (m, 2H, CH_{arom}), 7.07 (m, 2H, CH_{arom}), 2.31 (s, 3H, Me), 0.24 (s, 9H, SiMe_3). m/z : 188 [M^+].

3 - Synthesis of 4-(trimethylsilylethynyl)benzonitrile

The compounds 4-bromobenzonitrile (54.90 mmol, 10.00 g), CuI (1.10 mmol, 0.21 g) and Pd(PPh₃)₂Cl₂ (1.10 mmol, 0.77 g) were added to a flask that had been evacuated and refilled with N₂ 3 times and then NEt₃ (400 ml) added *via* cannula. Under nitrogen and with rapid stirring, TMSA (58.00 mmol, 5.70 g) was added and stirring was continued overnight. The solvent was removed *in vacuo* and the residue was dissolved in Et₂O and filtered through a 10 cm silica gel column, eluting with Et₂O. Removal of the ether *in vacuo* gave the product as a yellow solid. Yield: 10.35 g, 95 %. ¹H NMR (200 MHz) δ: 7.50 (m, 4H, CH_{arom}), 0.19 (s, 9H, SiMe₃). *m/z*: 199 [M⁺].

4 - Synthesis of 4-[(trimethylsilyl)ethynyl]benzoic acid methyl ester

The compounds 4-iodo-benzoic acid methyl ester (35.0 mmol, 9.16 g), CuI (0.70 mmol, 0.13 g) and Pd(PPh₃)₂Cl₂ (0.35 mmol, 0.25 g) were added to a flask which had been evacuated and refilled with N₂ 3 times. NEt₃ (350 ml) was transferred to the flask *via* cannula. TMSA (38.45 mmol, 3.78 g) was added under nitrogen to the rapidly stirred solution. Stirring was continued for 3 h and then the solvent was removed *in vacuo*. The residue was dissolved in hexane and filtered through a 10 cm silica gel column with hexane eluant. After removal of the hexane *in vacuo*, 4-[(trimethylsilyl)ethynyl]benzoic acid methyl ester was obtained as a white solid. Yield: 6.07 g, 75 %. ¹H NMR (400 MHz) δ: 7.98 (m, 2H, CH_{arom}), 7.52 (m, 2H, CH_{arom}), 3.91 (s, 3H, OCH₃), 0.26 (s, 9H, SiMe₃). *m/z*: 232 [M⁺].

5 - 4-(trimethylsilylethynyl)benzotrifluoride

The compounds 4-bromobenzotrifluoride (100.0 mmol, 22.50 g), CuI (2.00 mmol, 0.38 g) and Pd(PPh₃)₂Cl₂ (1.00 mmol, 0.70 g) were added to a flask that had been evacuated and refilled with N₂ 3 times. NEt₃ (350 ml) was transferred to the flask *via* cannula. TMSA (115.0 mmol, 11.30 g) was added and then the resulting mixture was refluxed at 90 °C overnight. The solvent was removed *in vacuo* and the resulting residue was dissolved in hexanes and filtered through a short silica gel column. The hexane was removed *in vacuo* to give the product as a yellow liquid. Yield: 23.30 g, 96 %. ¹H NMR

(400 MHz) δ : 7.56 (s, 4H, CH_{arom}), 0.27 (s, 9H, SiMe₃). ¹⁹F{¹H} NMR (188 MHz) δ : -63.30 (s, 3F, CF₃). *m/z*: 242 [M⁺].

6 - 4-(trimethylsilylethynyl)benzaldehyde

The compound 4-bromobenzaldehyde (25.0 mmol, 5.00 g) was slurried in NEt₃ (200 ml) with PPh₃ (1.25 mmol, 0.33 g), PdCl₂ (0.25 mmol, 45 mg) and Cu(OAc)₂ (0.25 mmol, 50 mg). TMSA (28.0 mmol, 5.50 ml) was added and the mixture heated to 50 °C for 6 h. The solvent was removed *in vacuo* and the crude residue was applied to the top of a 5 cm silica gel column which was eluted using 1:3 DCM:hexanes. The solvents were removed *in vacuo* to give the product as an off-white solid. Yield: 5.28 g, 97 %. ¹H NMR (400 MHz) δ : 9.99 (s, 1H, CHO), 7.90 (d, *J* = 8 Hz, 2H, CH_{arom}), 7.60 (d, *J* = 8 Hz, 2H, CH_{arom}), 0.26 (s, 9H, SiMe₃). *m/z*: 202 [M⁺].

7 - 1-(trimethylsilylethynyl)naphthalene

The compounds 1-iodonaphthalene (13.78 mmol, 3.50 g), CuI (0.28 mmol, 0.052 g) and Pd(PPh₃)₂Cl₂ (0.14 mmol, 0.097 g) were added to a flask that had been evacuated and refilled with N₂ 3 times. NEt₃ (350 ml) was transferred to the flask *via* cannula. TMSA (15.15 mmol, 1.49 g) was added under nitrogen to the rapidly stirred solution and stirring was continued overnight. The solvent was removed *in vacuo* and then the residue was dissolved in hexanes and filtered through a 10 cm silica gel column. Hexane was removed *in vacuo* to give the product as a colourless oil. Yield: 3.01 g, 97 %. ¹H NMR (400 MHz) δ : 8.35 (d, *J* = 8 Hz, 1H, CH_{arom}), 7.84 (d, *J* = 8 Hz, 1H, CH_{arom}), 7.83 (d, *J* = 8 Hz, 1H, CH_{arom}), 7.71 (d, *J* = 8 Hz, 1H, CH_{arom}), 7.39 (t, *J* = 8 Hz, 1H, CH_{arom}), 7.32 (t, *J* = 8 Hz, 1H, CH_{arom}), 7.41 (t, *J* = 8 Hz, 1H, CH_{arom}), 0.15 (s, 9H, SiMe₃). *m/z*: 224 [M⁺].

8 - 2-(trimethylsilylethynyl)thiophene

Copper iodide (0.58 mmol, 0.11 g) and Pd(PPh₃)₂Cl₂ (0.58 mmol, 0.41 g) were added to a flask that had been evacuated and refilled with N₂ 3 times. NEt₃ (300 ml) was transferred to the flask *via* cannula, and 2-bromothiophene (29.1 mmol, 4.74 g) and TMSA (33.4 mmol, 3.28 g) were added under N₂ and then the mixture was heated to 50 °C and stirred overnight. The solvent was removed *in vacuo* and the resulting residue was

dissolved in a small amount of hexane and filtered through a short silica gel column with hexane as eluant. The hexane was removed *in vacuo* to give product as a yellow liquid. Yield: 3.39 g, 65 %. ^1H NMR (400 MHz) δ : 7.23 (m, 2H, 2 x CH), 6.95 (dd, $J = 4, 5$ Hz, 1H, CH), 0.25 (s, 9H, SiMe₃). m/z : 180 [M^+].

9 - 4-[3,5-bis(trifluoromethyl)phenylethynyl]-1-(trimethylsilylethynyl)-benzene

The compounds 1-bromo-3,5-bis-(trifluoromethyl)benzene (3.78 mmol, 1.10 g), CuI (0.076 mmol, 14 mg) and Pd(PPh₃)₂Cl₂ (0.038 mmol, 27 mg) were added to a flask that had been evacuated and refilled with N₂ 3 times. Dried and degassed NEt₃ (100 ml) was transferred to the flask *via* cannula, and 4-(trimethylsilyl)ethynyl-1-ethynylbenzene (3.78 mmol, 0.75 g) was added under a flow of nitrogen and the resulting mixture was refluxed overnight. The solvent was removed *in vacuo* and the residual solid was applied to the top of a short silica gel column which was eluted with 9:1 hexane:DCM. The solvent was removed *in vacuo* to give crude the product as a yellow solid. Recrystallisation from MeOH gave the product as a white solid. Crystals grown by slow evaporation of product from a mixture of DCM and hexanes were suitable for X-ray analysis. Yield: 1.15 g, 75 %. ^1H NMR (400 MHz) δ : 7.95 (s, 2H, CH_{arom}), 7.82 (s, 1H, CH_{arom}), 7.48 (s, 4H, CH_{arom}), 0.26 (s, 9H, SiMe₃). $^{19}\text{F}\{^1\text{H}\}$ NMR (188 MHz) δ : -63.55 (s, 6F, 2 x CF₃). $^{13}\text{C}\{^1\text{H}\}$ NMR (101 MHz) δ : 132.19, 132.01, 131.74, 131.55, 125.56, 124.43, 124.26, 121.93 (C_{arom}), 121.76 (CF₃), 104.40, 97.25, 92.49, 88.12 (C \equiv C), 0.01 (TMS). Anal. Calcd. for C₂₁H₁₆F₆Si: C, 61.91; H, 3.96. Found: C, 61.61; H, 4.24 %. IR (KBr): $\nu_{\text{C}\equiv\text{C}} = 2227, 2160 \text{ cm}^{-1}$. m/z : 407 [M^+].

10 - 4-(trimethylsilylethynyl)-1-(2-thienylethynyl)benzene

The compounds Pd(PPh₃)₂Cl₂ (0.024 mmol, 17 mg) and CuI (0.048 mmol, 9 mg) were added to a flask that had been evacuated and refilled with N₂ 3 times. Dried and degassed NEt₃ (100 ml) was added *via* cannula, and 2-iodothiophene (2.38 mmol, 0.50 g) and 4-(trimethylsilyl)ethynyl-1-ethynylbenzene (2.40 mmol, 0.48 g) were added under a positive flow of nitrogen and then the resulting mixture was stirred for 3 h. The solvent was removed *in vacuo* and then the residue was applied to the top of a silica gel column which was eluted with hexane. The hexane was removed *in vacuo* and the product was isolated as a white solid. Yield: 0.53 g, 79 %. ^1H NMR (400 MHz) δ : 7.48 (s, 4H,

CH_{arom}), 7.82 (m, 2H, CH_{thio}), 6.79 (m, 1H, CH_{thio}), 0.04 (s, 9H, SiMe₃). ¹³C{¹H} NMR (101 MHz) δ: 132.21, 131.98, 131.30, 131.23, 127.67, 127.24, 123.14, 123.12 (C_{arom}), 104.70, 96.49, 92.79, 84.65 (C≡C), 0.01 (SiMe₃). Anal. Calcd. for C₁₇H₁₆SSi: C, 72.80; H, 5.75. Found: C, 72.56; H, 5.73 %. IR (KBr): ν_{C≡C} = 2152, ν_{TMS} = 1252 cm⁻¹. *m/z*: 280 [M⁺].

1.11.3 Synthesis of ethynylbenzenes

11 - 4-ethynyl-N,N-dimethylaniline

The compound N,N-dimethyl-4-[(trimethylsilyl)ethynyl]aniline (39.30 mmol, 8.54 g) was added to a stirred suspension of Na₂CO₃ (150.00 mmol, 15.90 g) in MeOH (300 ml) and H₂O (30 ml). After stirring for 6 h, the reaction mixture was diluted with Et₂O (200 ml). The organic fraction was separated, washed with water (2 x 200 ml), dried over MgSO₄ and then the solvent was removed *in vacuo*. The resulting solid was dissolved in hexane and filtered through a 5 cm alumina column with hexane as eluant. On removal of the solvent *in vacuo*, a white solid was obtained. Yield: 4.05 g, 71 %. ¹H NMR (400 MHz) δ: 7.38 (d, *J* = 9 Hz, 2H, CH_{arom}), 6.62 (d, *J* = 9 Hz, 2H, CH_{arom}), 2.85 (s, 7H, NMe₂ and CH). *m/z*: 145 [M⁺].

12 - 4-ethynyltoluene

The compound 4-[(trimethylsilyl)ethynyl]toluene (76.24 mmol, 14.36 g) was added to a stirred suspension of Na₂CO₃ (220.0 mmol, 23.32 g) in MeOH (300 ml) and H₂O (50 ml). The mixture was stirred overnight before being diluted with Et₂O (200 ml) and then washed with water (2 x 200 ml). The organic fraction was separated, dried over MgSO₄ and the solvent was removed *in vacuo*. The oil obtained was redissolved in hexane and filtered through a 5 cm silica gel column. Removal of the solvent *in vacuo* gave the product as a brown oil. Yield: 2.62 g, 30 %. ¹H NMR (400 MHz) δ: 7.27 (d, *J* = 7 Hz, 2H, CH_{arom}), 6.98 (d, *J* = 7 Hz, 2H, CH_{arom}), 2.90 (s, 1H, CH), 2.20 (s, 3H, Me). *m/z*: 116 [M⁺].

13 - 4-ethynylbenzotrifluoride

The compound 4-(trimethylsilylethynyl)benzotrifluoride (51.92 mmol, 10.35 g) was added to a suspension of Na_2CO_3 (100.00 mmol, 10.60 g) in MeOH (300 ml) and H_2O (100 ml) and the mixture was stirred overnight. Et_2O (250 ml) was added and the organic fraction was separated and then washed with water (2 x 200 ml). After drying the organic fraction over MgSO_4 , the solvent was removed *in vacuo*. The brown solid was applied to the top of a 5 cm silica gel column which was eluted with toluene. Removal of the solvent *in vacuo* gave 4-ethynylbenzotrifluoride as an orange solid. Yield: 5.83 g, 88 %. ^1H NMR (400 MHz) δ : 7.55 (m, 4H, CH_{arom}), 3.35 (s, 1H, CH). m/z : 127 [M^+].

14 - 4-ethynylbenzoic acid methyl ester

The compound 4-(trimethylsilylethynyl)-benzoic acid methyl ester (25.8 mmol, 6.00 g) was added to a suspension of Na_2CO_3 (103.40 mmol, 10.96 g) in MeOH (300 ml) and H_2O (50 ml) then the mixture was stirred for 4 h before DCM (250 ml) was added. The organic fraction was separated, washed with water (3 x 100 ml) and then dried over MgSO_4 . The solvent was removed *in vacuo* and the resulting off-white solid was applied to the top of a 5 cm silica gel column which was eluted with hexane. Removal of the hexane *in vacuo* yielded the product as a white solid. Yield: 4.00 g, 97 %. ^1H NMR (400 MHz) δ : 7.99 (m, 2H, CH_{arom}), 7.55 (m, 2H, CH_{arom}), 3.92 (s, 3H, OCH_3), 3.23 (s, 1H, CH). m/z : 160 [M^+].

15 - 4-ethynylbenzotrifluoride

The compound 4-(trimethylsilylethynyl)benzotrifluoride (41.25 mmol, 10.00 g) was added to a suspension of Na_2CO_3 (113.20 mmol, 12.00 g) in MeOH (250 ml) and water (100 ml). The mixture was stirred for 24 h and then diluted with Et_2O (450 ml) and washed with water (2 x 150 ml). After separation and then drying of the organic fraction over MgSO_4 , the ether was removed by distillation. The remaining liquid was dissolved in DCM and filtered through a sinter. The DCM was then also removed by distillation using a Vigreux column. With rapid stirring, the 4-ethynylbenzotrifluoride was briefly dried *in vacuo*. ^1H NMR spectroscopy showed there to be 1.5 equiv. of DCM remaining. Yield:

2.00 g, 29 %. ^1H NMR (400 MHz) δ : 7.59 (s, 4H, CH_{arom}), 5.20 (s, 3H, DCM), 3.19 (s, 1H, CH). m/z : 170 [M^+].

16 - 4-ethynylbenzaldehyde

The compounds 4-(trimethylsilylethynyl)benzaldehyde (24.7 mmol, 5.00 g) and Na_2CO_3 (30.7 mmol, 3.25 g) were stirred in MeOH (150 ml), DCM (100 ml) and H_2O (10 ml) for 6 h. The reaction mixture was diluted with DCM (200 ml) and then the organic layer was separated, washed with water (3 x 100 ml) and dried over MgSO_4 . Removal of the solvent *in vacuo* gave the product as an off-white solid. Yield: 3.08 g, 96 %. ^1H NMR (400 MHz) δ : 10.00 (s, 1H, CHO), 7.83 (d, $J = 8$ Hz, 2H, CH_{arom}), 7.62 (d, $J = 8$ Hz, 2H, CH_{arom}), 3.29 (s, 1H, CH). m/z : 129 [M^+].

17 - 4-ethynylaniline

The compound 4-(trimethylsilylethynyl)aniline (40.6 mmol, 7.69 g) was added to a stirring suspension of Na_2CO_3 (125.0 mmol, 13.25 g) in MeOH (200 ml) and water (30 ml) and stirred overnight. The product was extracted into DCM (250 ml) and washed with water (3 x 100 ml). The organic fraction was separated, dried over MgSO_4 and the solvent was removed *in vacuo*. The residue was applied to the top of a 5 cm silica gel column which was eluted with 2:1 DCM:hexane. Removal of the solvent *in vacuo* gave the product as a yellow solid. Yield: 3.74 g, 79 %. ^1H NMR (400 MHz) δ : 7.30 (d, $J = 9$ Hz, 2H, CH_{arom}), 6.59 (d, $J = 9$ Hz, 2H, CH_{arom}), 3.81 (s, 2H, NH_2), 2.96 (s, 1H, CH). m/z : 117 [M^+].

18 - 1-ethynynaphthalene

The compound 1-[(trimethylsilylethynyl)]naphthalene (13.4 mmol, 3.01 g) was added to a suspension of Na_2CO_3 (20.0 mmol, 2.12 g) in MeOH (250 ml), water (100 ml) and Et_2O (100 ml). The mixture was stirred for 24 h and then diluted with Et_2O (150 ml). The organic fraction was separated and washed with water (2 x 150 ml). After drying over MgSO_4 , the solvent was removed *in vacuo* to give the product as a yellow oil. Yield: 1.90 g, 93 %. ^1H NMR (400 MHz) δ : 8.38 (d, $J = 8$ Hz, 1H, CH_{arom}), 7.87 (d, $J = 8$ Hz, 2H,

CH_{arom}), 7.75 (d, $J = 8$ Hz, 1H, CH_{arom}), 7.50 (t, $J = 8$ Hz, 1H, CH_{arom}), 7.44 (t, $J = 8$ Hz, 1H, CH_{arom}), 7.47 (t, $J = 8$ Hz, 1H, CH_{arom}), 3.38 (s, 4H, CH_{arom}). m/z : 152 [M⁺].

19 - 2-ethynylthiophene

The compound 2-(trimethylsilylethynyl)thiophene (18.8 mmol, 3.39 g) was added to a stirring suspension of Na₂CO₃ (50.0 mmol, 5.30 g) in MeOH (100 ml), DCM (100 ml) and H₂O (20 ml). The solution was stirred overnight before dilution with DCM (200 ml) and extracted with water (3 x 50 ml). The organic fraction was separated, dried over MgSO₄ and then the solvent was removed *in vacuo* to give the product as a yellow oil. Yield: 1.60 g, 65 %. ¹H NMR (400 MHz) δ : 7.20 (m, 2H, 2 x CH), 6.98 (dd, $J = 5$ and 4 Hz, 1H, CH), 3.35 (s, 1H, CH). m/z : 108 [M⁺].

20 - 4-[3,5-bis(trifluoromethyl)phenylethynyl]-1-ethynylbenzene

The compound 4-[3,5-bis(trifluoromethyl)phenylethynyl]-1-(trimethylsilylethynyl)benzene (1.23 mmol, 0.50 g) was added to a stirring suspension of Na₂CO₃ (2.46 mmol, 0.26 g) in MeOH (50 ml), Et₂O (50 ml) and H₂O (10 ml). The mixture was stirred for 3 h and then the product was extracted into Et₂O (100 ml) and washed with water (3 x 50 ml). The organic fraction was then separated and dried over MgSO₄. The solvent was removed *in vacuo* to give the product as a yellow solid. Yield: 0.36 g, 87 %. ¹H NMR (400 MHz) δ : 7.95 (s, 2H, CH_{arom}), 7.83 (s, 1H, CH_{arom}), 7.50 (s, 4H, CH_{arom}), 3.21 (s, 1H, CH). ¹⁹F{¹H} NMR (282 MHz) δ : -63.55 (s, 6H, 2 x CF₃). ¹³C{¹H} NMR (101 MHz) δ : 130.13, 130.69, 130.59, 130.37, 124.04, 121.78, 120.94, 120.47 (C_{arom}), 120.43 (CF₃), 90.80, 86.74, 81.65, 78.21 (C \equiv C). Anal. Calcd. for C₁₈H₈F₆: C, 63.92; H, 2.38. Found: C, 64.29; H, 2.60 %. IR (KBr): $\nu_{C\equiv C} = 2221$, $\nu_{CH} = 3302$ cm⁻¹. m/z : 338 [M⁺].

21 - 1-ethynyl-[4-(2-thienylethynyl)]benzene

The compounds 4-(trimethylsilylethynyl)-1-(2-thienylethynyl)benzene (0.89 mmol, 0.25 g) and Na₂CO₃ (2.23 mmol, 0.24 g) were stirred in a mixture of Et₂O (50 ml), MeOH (50 ml) and H₂O (5 ml) overnight. The product was extracted into Et₂O (100 ml), then washed with H₂O (3 x 50 ml) and dried over MgSO₄. The solvent was removed *in vacuo* and the residual solid was applied to the top of a 5 cm alumina column which was eluted

with 1:4 DCM:hexane. After removing the solvent *in vacuo*, the product was obtained as a pale yellow solid. Single crystals, suitable for X-ray analysis, were grown by slow evaporation of a solution of product from a mixture of DCM and hexanes. Yield: 0.18 g, 97 %. ¹H NMR (400 MHz) δ : 7.47 (s, 4H, CH_{arom}), 7.31 (m, 2H, CH_{thio}), 7.02 (m, 1H, CH_{thio}), 3.18 (s, 1H, CH). Anal. Calcd. for C₁₄H₈S: C, 80.73; H, 3.87. Found: C, 79.79; H, 4.03 % (Submitted for HRMS). IR (KBr): $\nu_{C\equiv C}$ = 2201, ν_{CH} = 3269 cm⁻¹. *m/z*: 208 [M⁺].

22 - 4-[(4-ethynylphenylethynyl)-phenyl]-N,N-dimethylamine

A mixture of [4-(4-trimethylsilylethynylphenylethynyl)]-N,N-dimethylamine (0.95 mmol, 0.30 g) and K₂CO₃ (3.80 mmol, 0.53 g) were slurried in MeOH (50 ml), Et₂O (50 ml) and H₂O (10 ml) and stirred overnight. The product was extracted into Et₂O (100 ml) and then washed with water (3 x 50 ml). The organic fraction was separated, dried over MgSO₄ and the solvent was removed *in vacuo*. The resulting yellow solid was applied to the top of a 5 cm alumina pad which was eluted with 4:1 hexanes:DCM and then further recrystallised from a DCM/hexanes to give the product as a white solid. Yield: 0.20 g, 86 %. ¹H NMR (200 MHz) δ : 7.37 (s, 4H, CH_{arom}), 7.35 (m, 2H, CH_{arom}), 6.59 (m, 2H, CH_{arom}), 2.93 (s, 7H, NMe₂ and CH). IR (KBr): $\nu_{(\text{arene ring})}$ = 1351, 1523, 1596, 1606, $\nu_{C\equiv C}$ = 2209, ν_{CH} = 3242 cm⁻¹. *m/z*: 244 [M⁺].

23 - 4-ethynylanisole

The compound 4-(4-methoxyphenyl)-2-methyl-3-butyn-2-ol (26.3 mmol, 4.24 g) was stirred in a slurry of KO^tBu (27.3 mmol, 3.06 g) in toluene (300 ml) and the mixture was heated to reflux overnight. After cooling, the reaction mixture was filtered through a 5 cm silica gel column and eluted with toluene. The compound 4-ethynylanisole was obtained as an orange oil on removal of the solvent *in vacuo*. Yield: 1.45 g, 42 %. ¹H NMR (400 MHz) δ : 7.43 (m, 2H, CH_{arom}), 6.85 (m, 2H, CH_{arom}), 3.82 (s, 3H, OCH₃), 3.00 (s, 1H, CH). *m/z*: 132 [M⁺].

24 - 4-ethynylthioanisole

The compound 4-(4-thiomethoxyphenyl)-2-methyl-but-3-yn-2-ol (35.0 mmol, 7.23 g) was slurried in toluene (300 ml) with KO^tBu (38.0 mmol, 4.26 g) and the mixture was

stirred at reflux for 15 h. The mixture was then filtered through a 5 cm silica gel column with toluene as eluant. The resulting solution was reduced in volume *in vacuo*, washed once with water (200 ml) and then the organic layer was separated and dried over MgSO₄. The solvent was removed *in vacuo* to give the product as a brown oil. Yield: 4.17 g, 80 %. ¹H NMR (400 MHz) δ: 7.42 (d, *J* = 8 Hz, 2H, CH_{arom}), 7.20 (d, *J* = 8 Hz, 2H, CH_{arom}), 3.10 (s, 1H, CH), 2.90 (s, 3H, SCH₃). *m/z*: 148 [M⁺].

25 - 1-ethynyl-4-(trimethylsilylethynyl)benzene

The compound 4-(4-trimethylsilylethynylphenyl)-2-methyl-but-3-yn-2-ol (13.38 mmol, 3.43 g) and NaOH (1.34 mmol, 0.054 g) were refluxed in toluene (200 ml) for 4 h. The mixture was then filtered and the solvent removed *in vacuo*. The resulting solid was applied to the top of a short silica gel column which was eluted with hexane. Removal of the hexane *in vacuo* gave an oil which gradually solidified to give the product as a pale yellow solid. Yield: 0.93 g, 35 %. ¹H NMR (400 MHz) δ: 7.21 (s, 4H, CH_{arom}), 2.96 (s, 1H, CH), 0.05 (s, 9H, SiMe₃). *m/z*: 198 [M⁺].

26 - (4-ethynylphenyl)-(4-methoxybenzylidene)-amine

The compounds 4-methoxybenzaldehyde (0.85 mmol, 116 mg) and 4-ethynylaniline (0.85 mmol, 100 mg) were dissolved in toluene and stirred for 1 h. MgSO₄ (41.5 mmol, 5.00 g) was added to the flask and then two crystals of *p*-toluenesulphonic acid were added. The reaction was stirred for a further 4 h. The mixture was filtered through a sinter and the residual MgSO₄ washed thoroughly with DCM (400 ml). The solvents were removed *in vacuo*. GC-MS of the residual solid showed there to be a small amount of starting material present. The solid was added to the top of a 5 cm celite column which was eluted with hexane (250 ml) to remove the hexane soluble starting material impurity. The product was obtained as a yellow solid by eluting the column with DCM followed by removal of the solvent *in vacuo*. Yield: 120 mg, 60 %. ¹H NMR (400 MHz) δ: 8.34 (s, 1H, CH_{imine}), 7.85 (d, *J* = 9 Hz, 2H, CH_{arom}), 7.51 (d, *J* = 7 Hz, 2H, CH_{arom}), 7.14 (d, *J* = 7 Hz, 2H, CH), 6.90 (d, *J* = 9 Hz, 2H, CH_{arom}), 3.88 (s, 3H, OMe), 3.10 (s, 1H, CH). ¹³C{¹H} NMR (126 MHz) δ: 162.73, 160.46, 152.91, 133.35, 130.96, 129.23, 121.22, 119.31, 114.50 (C_{arom} and HC=N), 83.94, 77.47 (C≡C), 55.85 (OMe). Anal. Calcd. for C₁₆H₁₄NO: C, 81.68; H, 5.57; N, 5.95. Found: C, 80.49; H, 5.51; N, 5.91

%. IR (KBr): $\nu_{(\text{arene ring})} = 1510, 1572, 1591, 1604, 1621$, $\nu_{\text{CH}} = 3257 \text{ cm}^{-1}$. HRMS Calcd. for $\text{C}_{16}\text{H}_{14}\text{NO}$: $[\text{MH}] = 236.10699$. Found: 236.10693.

1.11.4 Synthesis of 1,4-bis(4-R-phenyl)buta-1,3-diyne and related compounds

27 - 1,4-diphenylbuta-1,3-diyne

Phenylacetylene (9.79 mmol, 1.00 g), CuI (0.098 mmol, 0.02 g), $\text{Pd}(\text{PPh}_3)_2\text{Cl}_2$ (0.098 mmol, 0.07 g) and I_2 (4.90 mmol, 1.24 g) were added to a flask that had been evacuated and refilled with N_2 3 times and then dry, degassed $^i\text{Pr}_2\text{NH}$ (150 ml) was added *via* cannula. The mixture was stirred for 2 h at room temperature and then the solvent was removed *in vacuo*. The residue was dissolved in hexanes and filtered through a 10 cm silica gel column with hexane as eluant. Removal of the solvent *in vacuo* gave the product as a crystalline white solid. Yield: 0.80 g, 81 %. ^1H NMR (200 MHz) δ : 7.43 (m, 10H, CH_{arom}). Anal. Calcd. for $\text{C}_{16}\text{H}_{10}$: C, 95.02; H, 4.98. Found: C, 94.92; H, 4.94 %. Raman (solid): $\nu_{(\text{arene ring})} = 1596$, $\nu_{(\text{C}\equiv\text{C})} = 2215 \text{ cm}^{-1}$. m/z : 202 $[\text{M}^+]$.

28 - 1,4-bis(4-tolyl)buta-1,3-diyne

The compounds 4-ethynyltoluene (8.61 mmol, 1.00 g), CuI (0.43 mmol, 0.082 g), $\text{Pd}(\text{PPh}_3)_2\text{Cl}_2$ (0.172 mmol, 0.121 g) and I_2 (4.29 mmol, 1.09 g) were added to flask that had been evacuated and refilled with N_2 3 times. Dry, degassed NEt_3 (150 ml) was added *via* cannula and the mixture was stirred overnight. The solvent was removed *in vacuo* and then the resulting solid was applied to the top of a 10 cm silica gel column which was eluted with hexane until no further product was obtained. Removal of the solvent *in vacuo* yielded a white solid, which was washed with methanol to remove any residual starting material and dried *in vacuo*. Yield: 0.52 g, 52 %. ^1H NMR (400 MHz) δ : 7.43 (d, $J = 8$ Hz, 2H, CH_{arom}), 7.15 (d, $J = 8$ Hz, 2H, CH_{arom}), 2.37 (s, 3H, CH_3). Anal. Calcd. for $\text{C}_{18}\text{H}_{14}$: C, 93.87; H, 6.13. Found: C, 93.70; H, 6.12 %. Raman (solid): $\nu_{(\text{arene ring})} = 1605$, $\nu_{(\text{C}\equiv\text{C})} = 2212 \text{ cm}^{-1}$. m/z : 230 $[\text{M}^+]$.

29 - 1,4-bis(4-trifluoromethylphenyl)buta-1,3-diyne

The compounds 4-ethynylbenzotrifluoride (11.8 mmol, 2.00 g), CuI (0.24 mmol, 0.045 g), Pd(PPh₃)₂Cl₂ (0.2 mmol, 0.083 g) and I₂ (5.88 mmol, 1.49 g) were added to dry NEt₃ (150 ml) solvent in a flask that had been evacuated and refilled with N₂ 3 times. The mixture was stirred overnight and then the solvent was removed *in vacuo*. The residual solid was applied to the top of a 10 cm silica gel column which was eluted with hexane. Removal of the solvent *in vacuo* yielded an off-white solid. White 1,4-bis(4-trifluoromethylphenyl)buta-1,3-diyne was obtained by recrystallisation from MeOH. A small amount of the product was dissolved in a minimum amount of hexane solvent and cooling resulted in crystals suitable for X-ray analysis. Yield: 1.32 g, 66 %. ¹H NMR (400 MHz) δ: 7.57 (m, 8H, CH_{arom}). ¹⁹F{¹H} NMR (282 MHz, C₆D₆) δ: -63.26 (s, 6H, CF₃). Anal. Calcd. for C₁₈H₈F₆: C, 63.92; H, 2.38. Found: C, 64.15; H, 2.54 %. Raman (solid): ν_(arene ring) = 1261, 1614, ν_(C≡C) = 2218 cm⁻¹. m/z: 338 [M⁺].

30 - 1,4-bis(4-cyanophenyl)buta-1,3-diyne

The compounds 4-ethynylbenzotrifluoride (15.7 mmol, 2.00 g), CuI (0.79 mmol, 0.15 g), Pd(PPh₃)₂Cl₂ (0.31 mmol, 0.22 g) and I₂ (9.00 mmol, 2.28 g) were slurried in NEt₃ (200 ml) in a flask that had been evacuated and refilled with N₂ 3 times. The mixture was stirred rapidly for 24 h and then filtered through a sinter and washed with Et₂O (150 ml). The solvents were then removed *in vacuo*. The resulting brown solid was dissolved in DCM and washed thoroughly with a saturated solution of Na₂S₂O₃. After separation of the organic fraction and drying over MgSO₄, the DCM was removed *in vacuo*. The residual yellow solid was then applied to the top of a 5 cm silica gel column which was eluted with hot toluene. Sublimation of the crude material at 240 °C under high vacuum gave the product as a yellow solid. Yield: 0.51g, 31 %. ¹H NMR (200 MHz) δ: 7.58 (s, 8H, CH_{arom}). Anal. Calcd. for C₁₈H₈N₂: C, 85.70; H, 3.18; N, 11.10. Found: C, 85.10; H, 3.18; N, 10.91 %. Raman (solid): ν_(arene ring) = 1603, ν_(C≡C) = 2212 cm⁻¹. m/z: 252 [M⁺].

31 - 1,4-bis(4-N,N-dimethylaminophenyl)buta-1,3-diyne

The compounds 4-ethynyl-N,N-dimethylaniline (22.1 mmol, 3.21 g), CuI (1.1 mmol, 0.21 g), Pd(PPh₃)₂Cl₂ (0.44 mmol, 0.31 g) and I₂ (15.0 mmol, 3.81 g) were stirred

for 24 h in $^i\text{Pr}_2\text{NH}$ (200 ml) in a flask that had been evacuated and refilled with N_2 3 times. The solvent was removed *in vacuo* and the residual solid was added to a sinter which was eluted with DCM. The organic fraction was washed thoroughly with a saturated solution of $\text{Na}_2\text{S}_2\text{O}_3$ and then dried over MgSO_4 . The DCM was removed *in vacuo* and the residual solid applied to the top of a 5 cm silica gel column which was eluted with hot toluene. The volume of solvent was reduced and the product was allowed to crystallise in the freezer before isolation on a sinter, washing with a small amount of hexane and drying *in vacuo*. Yield: 1.87 g, 59 %. $^1\text{H NMR}$ (400 MHz) δ : 7.32 (d, $J = 8$ Hz, 4H, CH_{arom}), 6.55 (d, $J = 8$ Hz, 4H, CH_{arom}), 2.92 (s, 12H, NMe_2). Anal. Calcd. for $\text{C}_{20}\text{H}_{20}\text{N}_2$: C, 83.30; H, 6.99; N, 9.71. Found: C, 82.89; H, 6.97; N, 9.60 %. Raman (solid): $\nu_{(\text{arene ring})} = 1603$, $\nu_{(\text{C}\equiv\text{C})} = 2202$ cm^{-1} . m/z : 288 [M^+].

32 - 1,4-bis(4-carbomethoxyphenyl)buta-1,3-diyne

The compounds 4-ethynylbenzoic acid methyl ester (5.2 mmol, 0.83 g), CuI (0.26 mmol, 0.049 g), $\text{Pd}(\text{PPh}_3)_2\text{Cl}_2$ (0.10 mmol, 0.073 g) and I_2 (3.0 mmol, 0.76 g) were slurried in $^i\text{Pr}_2\text{NH}$ (200 ml) and the mixture was stirred for 6 h. The solvent was removed *in vacuo* and the residue dissolved in DCM. The organic fraction was washed thoroughly with a saturated solution of $\text{Na}_2\text{S}_2\text{O}_3$, dried over MgSO_4 , and then the solvent was removed *in vacuo* to give a brown solid. The solid was applied to the top of a 10 cm silica gel column which was eluted with hot toluene. The solvent volume was reduced and the product was crystallised at low temperature, isolated as a white solid on a sinter, and washed with a small amount of cold toluene and then hexane and dried *in vacuo*. A small amount of solid was dissolved in hot benzene which was initially allowed to cool and then the solvent allowed to evaporate slowly over a period of several weeks. The resulting single crystals were used to perform an X-ray diffraction. Yield: 0.60 g, 73 %. $^1\text{H NMR}$ (400 MHz) δ : 7.95 (d, $J = 8$ Hz, 4H, CH_{arom}), 7.52 (d, $J = 8$ Hz, 4H, CH_{arom}), 3.87 (s, 6H, OCH_3). Anal. Calcd. for $\text{C}_{20}\text{H}_{14}\text{O}_4$: C, 75.46; H, 4.43. Found: C, 75.65; H, 4.40 %. Raman (solid): $\nu_{(\text{arene ring})} = 1605$, $\nu_{(\text{C}\equiv\text{C})} = 2216$ cm^{-1} . m/z : 318 [M^+].

33 - 1,4-bis(4-thiomethoxyphenyl)buta-1,3-diyne

The compounds 4-ethynylthioanisole (4.0 mmol, 0.60 g), CuI (0.08 mmol, 0.016 g) and $\text{Pd}(\text{PPh}_3)_2\text{Cl}_2$ (0.041 mmol, 0.029 g) were slurried in NEt_3 (100 ml). The mixture was

stirred overnight with the reaction vessel left open to the air and then the solvent was removed *in vacuo*. The residual solid was dissolved in DCM and filtered through a 5 cm silica gel column with DCM eluant. The solvent was removed *in vacuo* and the solid was purified by sublimation under high vacuum at 230 °C to give the product as an off-white solid. Yield: 0.21 g, 35 %. ¹H NMR (400 MHz) δ: 7.35 (d, *J* = 9 Hz, 4H, CH_{arom}), 7.11 (d, *J* = 9 Hz, 4H, CH_{arom}), 2.42 (s, 6H, SCH₃). Anal. Calcd. for C₂₀H₁₄S₄: C, 73.43; H, 4.79. Found: C, 73.30; H, 4.80 %. Raman (solid): $\nu_{(\text{arene ring})} = 1589$, $\nu_{(\text{C}\equiv\text{C})} = 2211$ cm⁻¹. *m/z*: 294 [M⁺].

34 - 1,4-bis(4-nitrophenyl)buta-1,3-diyne

The compounds 1-nitro-4-ethynylbenzene (3.4 mmol, 0.50 g), CuI (0.034 mmol, 0.010g) and Pd(PPh₃)₂Cl₂ (0.034 mmol, 0.024 g) were slurried in NEt₃ (100 ml) under a nitrogen atmosphere. I₂ (1.70 mmol, 0.43 g) was added and the mixture was stirred for 3 d. The amine solvent was removed *in vacuo* and the residual solid applied to the top of a 5 cm silica gel column which was eluted with hot toluene. Removal of the toluene *in vacuo* gave a dark brown solid. The crude product was purified by sublimation under high vacuum at 250 °C to give a yellow solid. Yield: 0.36 g, 73 %. ¹H NMR (400 MHz) δ: 8.24 (d, *J* = 9 Hz, 4H, CH_{arom}), 7.70 (d, *J* = 9 Hz, 4H, CH_{arom}). Anal. Calcd. for C₁₆H₁₆N₂O₄: C, 65.75; H, 2.76; N, 9.59. Found: C, 65.70; H, 2.76; N, 9.58 %. Raman (solid): $\nu_{(\text{arene ring})} = 1099, 1334, 1597$, $\nu_{(\text{C}\equiv\text{C})} = 2219$ cm⁻¹. *m/z*: 292 [M⁺].

35 - 1,4-bis(4-benzaldehyde)buta-1,3-diyne

The compounds 4-ethynylbenzaldehyde (7.68 mmol, 1.00 g), CuI (0.077 mmol, 0.015 g), Pd(PPh₃)₂Cl₂ (0.077 mmol, 0.054 g) and I₂ (3.84 mmol, 0.97 g) were slurried in a degassed solution of NEt₃ for 2 d. The solvent was removed *in vacuo* and the residual solid dissolved in hot toluene and filtered through a 5 cm silica gel column, eluting with hot toluene. Removal of the solvent *in vacuo* gave the product as a yellow solid. Yield: 0.62 g, 63 %. ¹H NMR (500 MHz) δ: 10.04 (s, 2H, CHO), 7.88 (d, *J* = 8 Hz, 4H, CH_{arom}), 7.69 (d, *J* = 8 Hz, 4H, CH_{arom}). Anal. Calcd. for C₁₈H₁₀O₂: C, 83.71; H, 3.90. Found: C, 83.41; H, 3.84 %. Raman (solid): $\nu_{(\text{arene ring})} = 1165, 1601$, $\nu_{(\text{C}\equiv\text{C})} = 2210$ cm⁻¹. *m/z*: 258 [M⁺].

36 - 1,4-di-(1-naphthyl)buta-1,3-diyne

The compounds 1-ethynyl-naphthalene (0.85 mmol, 0.13 g), CuI (0.066 mmol, 0.013 g) and Pd(PPh₃)₂Cl₂ (0.033 mmol, 0.023 g) were slurried in NEt₃ (100 ml). The mixture was stirred overnight with the reaction vessel left open to the air. The solvent was then removed *in vacuo* and the residual solid was applied to the top of a 5 cm silica gel column which was eluted with DCM. The solvent was removed *in vacuo* and the solid was purified by sublimation under high vacuum at 180 °C to yield pure product as an off white solid. Yield: 0.10 g, 66 %. ¹H NMR (400 MHz) δ: 8.44 (d, *J* = 8 Hz, 1H, CH_{arom}), 7.99 (d, *J* = 8 Hz, 1H, CH_{arom}), 7.89 (d, *J* = 8 Hz, 1H, CH_{arom}), 7.84 (d, *J* = 8 Hz, 1H, CH_{arom}), 7.65 (t, *J* = 8 Hz, 1H, CH_{arom}), 7.57 (t, *J* = 8 Hz, 1H, CH_{arom}), 7.47 (t, *J* = 8 Hz, 1H, CH_{arom}). Anal. Calcd. for C₂₄H₁₄: C, 95.33; H, 4.67. Found: C, 95.55; H, 4.68 %. Raman (solid): ν_(arene rings) = 1253, 1331, 1377, 1410, 1465, 1508, 1574, ν_(C≡C) = 2207 cm⁻¹. *m/z*: 302 [M⁺].

37 - 1,4-bis(4-trimethylsilylethynylphenyl)buta-1,3-diyne

The compounds 1-ethynyl-4-(trimethylsilylethynyl)benzene (5.04 mmol, 1.00 g), CuI (0.20 mmol, 0.039 g) and Pd(PPh₃)₂Cl₂ (0.10 mmol, 0.071 g) were slurried in NEt₃ (100 ml). The mixture was stirred for 2 d with the reaction vessel open to the air. The amine solvent was removed *in vacuo* and the residual solid was applied to the top of a 5 cm silica gel column which was eluted with 4:1 hexane:DCM. The solvents were removed *in vacuo* to give the product as a yellow solid. Yield: 0.55 g, 55 %. ¹H NMR (400 MHz) δ: 7.35 (AB, 8H, CH_{arom}), 0.18 (s, 18H, SiMe₃). Anal. Calcd. for C₂₆H₂₆Si₂: C, 79.13; H, 6.64. Found: C, 79.31; H, 6.80 %. IR (KBr): ν_(CHaryl) = 2956, ν_(C≡C) = 2152, ν_(Si-Me) = 1252 cm⁻¹. Raman (solid): ν_(arene ring) = 1597, ν_(C≡C) = 2153, 2211 cm⁻¹. *m/z*: 394 [M⁺].

38 - 1,4-bis[4-(4-N,N-dihexylaminophenylethynyl)phenyl]buta-1,3-diyne

The compound 4-(4-N,N-dihexylaminophenylethynyl)ethynylbenzene (0.65 mmol, 0.25 g), CuI (0.013 mmol, 0.003 g) and Pd(PPh₃)₂Cl₂ (0.065 mmol, 0.46 g) were slurried in NEt₃ (150 ml). The mixture was stirred for 3 d with the vessel open to air. The solvent was then removed *in vacuo* and the residual solid added to the top of a short silica gel column which was eluted with 3:1 hexane:DCM. The solvent was removed *in vacuo* to

give an orange solid. In a 5 mm diameter test tube, a small amount of product was dissolved in hexane which was then layered with ethanol. Over a period of weeks, single crystals suitable for X-ray analysis formed. Yield: 0.20 g, 80 %. $^1\text{H NMR}$ (400 MHz) δ : 7.37 (AB, 8H, CH_{arom}), 7.38 (d, $J = 9$ Hz, 4H, CH_{arom}), 6.59 (d, $J = 9$ Hz, 4H, CH_{arom}), 3.20 (s, 8H, CH_2), 1.51 (s, 8H, CH_2), 1.24 (s, 24H, 3 x CH_2), 0.83 (s, 12H, 4 x CH_3). Anal. Calcd. for $\text{C}_{20}\text{H}_{20}\text{N}_2$: C, 87.45; H, 8.91; N, 3.64. Found: C, 87.35; H, 8.83; N, 3.42 %. Raman (solid): $\nu_{(\text{arene ring})} = 1135, 1592, \nu_{(\text{C}\equiv\text{C})} = 2197 \text{ cm}^{-1}$. m/z : 769 [M^+].

39 - 1,4-bis(2-thienyl)buta-1,3-diyne

The compounds 2-ethynylthiophene (9.24 mmol, 1.00 g), CuI (0.19 mmol, 0.035 g), $\text{Pd}(\text{PPh}_3)_2\text{Cl}_2$ (0.09 mmol, 0.065 g) and I_2 (4.70 mmol, 1.19 g) were added to a flask that had been evacuated and refilled with N_2 3 times. NEt_3 (200 ml) was added *via* cannula and the mixture was stirred overnight. The amine solvent was removed *in vacuo* and the residual solid was dissolved in hexane and filtered through a 5 cm silica gel column with hexane eluant. The crude product was recrystallised from hexane three times to give an off white, analytically pure, crystalline solid. Slow evaporation of solvent from a solution of product in cyclohexane gave single crystals that were suitable for X-ray analysis. Yield: 0.39 g, 40 %. $^1\text{H NMR}$ (400 MHz) δ : 7.35 (d, $J = 4$ Hz, 1H, CH_{thio}), 7.33 (d, $J = 4$ Hz, 1H, CH_{thio}), 7.00 (t, $J = 4$ Hz, 1H, CH_{thio}). Anal. Calcd. for $\text{C}_{12}\text{H}_6\text{S}_2$: C, 67.26; H, 2.82. Found: C, 67.00; H, 2.76 %. Raman (solid): $\nu_{(\text{thienyl ring})} = 1430, 1524, \nu_{(\text{C}\equiv\text{C})} = 2184, 2205 \text{ cm}^{-1}$. m/z : 214 [M^+].

40 - 1,4-bis[(3,5-bis(trifluoromethyl)phenyl)-4-ethynylphenyl]buta-1,3-diyne

The compounds 4-[3,5-bis(trifluoromethyl)phenylethynyl]-1-ethynylbenzene (3.69 mmol, 1.25 g), CuI (0.074 mmol, 0.015 g), $\text{Pd}(\text{PPh}_3)_2\text{Cl}_2$ (0.037 mmol, 0.026 g) and I_2 (1.85 mmol, 0.47 g) were slurried in dry NEt_3 (200 ml) in a flask open to air for 24 h. The amine solvent was removed *in vacuo* and the residual solid was applied to the top of a 5 cm silica gel column which was eluted with 1:1 hexane:DCM. After removal of the solvents *in vacuo*, the residual solid was sublimed at 200 °C under high vacuum to give a yellow solid. The low yield obtained was due to difficulty in separating the product from 1-(4-bromophenylethynyl)-3,5-bis(trifluoromethyl)benzene, an impurity found in the starting material. Yield: 0.30 g, 24 %. $^1\text{H NMR}$ (400 MHz) δ : 7.96 (s, 2H, CH_{arom}), 7.84 (s, 1H,

CH_{arom}), 7.54 (AB, 4H, CH_{arom}). ¹⁹F{¹H} NMR (282 MHz) δ: -63.52 (s, 12F, 4 x CF₃). ¹³C{¹H} NMR (101 MHz) δ: 132.84, 132.44, 132.11, 132.06, 125.42, 124.49, 123.01, 122.67 (C_{arom}), 121.79 (CF₃), 92.26, 89.02, 82.24, 76.26 (C≡C). Anal. Calcd. for C₃₆H₁₄F₁₂: C, 64.11; H, 2.09. Found: C, 63.95; H, 2.11 %. Raman (solid): ν_(arene ring) = 1602, ν_(C≡C) = 2214 cm⁻¹. *m/z*: 674 [M⁺].

41 - 1,4-bis(pentafluorophenyl)buta-1,3-diyne

Pentafluorophenylacetylene (7.86 mmol, 1.51 g), CuI (0.157 mmol, 0.03 g), Pd(PPh₃)₂Cl₂ (0.079 mmol, 0.06 g) and I₂ (3.93 mmol, 1.00 g) were slurried in NEt₃ (100 ml) and the mixture stirred overnight. The solvent was removed *in vacuo* and the residual solid was applied to the top of a 5 cm silica gel column which was eluted with hexane. Removal of the solvent *in vacuo* gave the product as a yellow solid. Pure product was obtained as a white solid after sublimation under high vacuum at 100 °C. Yield: 0.90 g, 61 %. ¹⁹F{¹H} NMR (188 MHz) δ: -134.26 (m, 4F, CF_{arom}), -148.92 (m, 2F, CF_{arom}), -160.76 (m, 4F, CF_{arom}). Anal. Calcd. for C₁₆F₁₀: C, 50.29. Found: C, 50.04 %. Raman (solid): ν_(arene ring) = 1407, 1460, 1508, ν_(C≡C) = 2102, 2234 cm⁻¹. *m/z*: 382 [M⁺].

42 - 1,4-bis(4-methoxyphenyl)buta-1,3-diyne

The compound Cu(OAc)₂ (12.38 mmol, 2.25 g), slurried in MeOH (20 ml) and pyridine (20 ml) was added dropwise to a solution of 4-ethynylanisole (8.25 mmol, 1.09 g) in MeOH (30 ml). Once the addition was complete, the mixture was heated to reflux for 15 min and allowed to cool slowly. The mixture was diluted with 2.0 M HCl (50 ml) and then extracted into Et₂O (150 ml). The organic fraction was washed with water (2 x 30 ml), separated and then dried over MgSO₄. Removal of solvent *in vacuo* gave a yellow solid. Yield: 0.84 g, 78 %. ¹H NMR (400 MHz) δ: 7.39 (d, *J* = 8 Hz, 4H, CH_{arom}), 6.77 (d, *J* = 8 Hz, 4H, CH_{arom}), 3.74 (s, 6H, OCH₃). Anal. Calcd. for C₁₈H₁₄O₂: C, 82.42; H, 5.38. Found: C, 82.37; H, 5.37 %. Raman (solid): ν_(arene ring) = 1601, ν_(C≡C) = 2214 cm⁻¹. *m/z*: 262 [M⁺].

43 - 1,4-bis(4-dicyanovinylbenzene)buta-1,3-diyne

The compounds 1,4-bis(4-ethynylbenzaldehyde)buta-1,3-diyne (1.74 mmol, 0.45 g) and malononitrile (3.50 mmol, 0.23 g) were stirred in 2-propanol (100 ml). Ten drops of 2,2,6,6-tetramethylpiperidine were added and the mixture was heated to reflux for 1 h. The solution was allowed to cool and the resulting precipitate was filtered, washed with ethanol and hexane and dried *in vacuo*. This residual solid was sublimed under vacuum at 280 °C to give the product as an analytically pure, yellow solid. Yield: 0.60 g, 97 %. ¹H NMR (400 MHz) δ: 7.91 (d, *J* = 9 Hz, 4H, CH_{arom}), 7.75 (s, 2H, =CH), 7.67 (d, *J* = 9 Hz, 4H, CH_{arom}). Anal. Calcd. for C₂₄H₁₀N₄: C, 81.35; H, 2.84; N, 15.81. Found: C, 81.24; H, 2.77; N, 15.90 %. Raman (solid): ν_(arene ring) = 1200, 1581, ν_(C≡C) = 2215 cm⁻¹. *m/z*: 354 [M⁺].

1.11.5 Synthesis of 1,6-bis(4-trifluoromethylphenyl)hex-3-ene-1,4-diyne

44 - 1,6-bis(4-trifluoromethylphenyl)hex-3-ene-1,4-diyne

In a nitrogen filled glove box, the compounds Pd(PPh₃)₄ (0.042 mmol, 50 mg) and CuI (0.084 mmol, 16 mg) were added to a 100 ml round bottomed flask. Dried and degassed NEt₃ (50 ml) was added, the mixture was stirred and then *trans*-dichloroethene (2.10 mmol, 0.20 g) was added. To this, 4-ethynylbenzotrifluoride (4.70 mmol, 0.80 g) was added and the mixture was stirred for 3 d. NEt₃ and excess 4-ethynylbenzotrifluoride were removed *in vacuo*. The residual solid was added to the top of a 5 cm silica gel column which was eluted with hexane. The solvent was removed *in vacuo* and the yellow solid was washed once with MeOH (10 ml) and then recrystallised from a small volume of hexane in the freezer to give the product as a yellow solid. Yield: 0.26 g, 34 %. ¹H NMR (400 MHz) δ: 7.58 (AB, 8H, CH_{arom}), 7.84 (s, 2H, CH_{alkene}). ¹⁹F{¹H} NMR (188 MHz) δ: -63.29 (s, 6F, 2 x CF₃). ¹³C{¹H} NMR (100 MHz) δ: 132.09 (C=C), 130.75, 130.42, 126.68 (C_{arom}), 125.58 (CF₃), 121.50 (C_{arom}), 94.08, 90.12 (C≡C). Anal. Calcd. for C₂₀H₁₀F₆: C, 65.95; H, 2.77. Found: C, 65.54; H, 2.75 %. IR (KBr): ν_(arene ring) = 1612, ν_(C=C) = 1928 cm⁻¹. Raman (solid): ν_(arene ring) = 1507, 1581, 1614, ν_(C≡C) = 2151(w), 2181(s) cm⁻¹. *m/z*: 364 [M⁺].

1.12 References

- 1) L. Cassar, *J. Organomet. Chem.*, 1975, **93**, 253.
- 2) K. Sonogashira, Y. Tohda, N. Hagihara, *Tetrahedron Lett.*, 1975, **50**, 4467.
- 3) C. Amatore, M. Azzambì, A. Jutand, *J. Organomet. Chem.*, 1999, **576**, 254.
- 4) P. Fitton, E. A. Rick, *J. Organomet. Chem.*, 1971, **28**, 287.
- 5) C. Glaser, *Ber. Dtsch. Chem. Ges.*, 1869, **2**, 422.
- 6) G. Eglinton, A. R. Galbraith, *J. Chem. Soc.*, 1959, 889.
- 7) A. Hay, *J. Org. Chem.*, 1963, **27**, 3320.
- 8) A. Sharifi, M. Mirzaei, M. R. Naimi-Jamal, *Monatshefte für Chemie*, 2006, **137**, 213.
- 9) G. W. Kabalka, L. Wang, R. M. Pagni, *Synlett*, 2001, **1**, 108.
- 10) J. Li, H. Jiang, *Chem. Commun.*, 1999, **23**, 2369.
- 11) P. H. Li, J. C. Yan, M. Wang, L. Wang, *Chinese J. Chem.*, 2004, **22**, 219.
- 12) J. S. Yadav, B. V. S. Reddy, K. B. Reddy, K. U. Gayathri, A. R. Prasad, *Tetrahedron Lett.*, 2003, **44**, 6493.
- 13) A. S. Batsanov, J. C. Collings, I. J. S. Fairlamb, J. P. Holland, J. A. K. Howard, Z. Y. Lin, T. B. Marder, A. C. Parsons, R. M. Ward, J. Zhu, *J. Org. Chem.*, 2005, **70**, 703.
- 14) R. H. Crabtree, *The Organometallic Chemistry of the Transition Metals*, 3rd ed.; John Wiley and Sons: New York, 2001, pp 207-209.
- 15) R. Rossi, A. Carpita, C. Bigelli, *Tetrahedron Lett.*, 1985, **26**, 523.
- 16) A. Lei, M. Srivastova, X. Zhang, *J. Org. Chem.*, 2002, **67**, 1969.
- 17) Q. Liu, D. Burton, *Tetrahedron Lett.*, 1997, **38**, 4371.
- 18) M. Vlăssă, I. Ciocan-Tarta, F. Margineanu, I. Oprean, *Tetrahedron*, 1996, **52**, 1337.
- 19) J.-H. Li, Y. Liang, X.-D. Xiang, *Tetrahedron*, 2005, **61**, 1903.
- 20) P. Nguyen, Z. Yuan, L. Agocs, G. Lesley, T. B. Marder, *Inorg. Chim. Acta*, 1994, **220**, 289.
- 21) J.-H. Li, Y. Liang, Y.-X. Xie, *J. Org. Chem.*, 2005, **70**, 4393.
- 22) J. Gil-Molto, C. Najera, *Eur. J. Org. Chem.*, 2005, **19**, 4073.
- 23) J. A. Marsden, J. J. Miller, M. M. Haley, *Angew. Chem. Int. Ed.*, 2004, **43**, 1694.
- 24) M. E. Krafft, C. Hirose, N. Dalal, C. Ramsey, A. Steigman, *Tetrahedron Lett.*, 2001, **42**, 7733.
- 25) Y. Liao, R. Faths, Z. Yang, *Org. Lett.*, 2003, **5**, 909.
- 26) Y. Ito, M. Inouye, M. Murakami, *Tetrahedron Lett.*, 1988, **29**, 5379.

- 27) T. Ishikawa, A. Ogawa, T. Hirao, *Organometallics*, 1998, **17**, 5713.
- 28) S.-K. Kang, T. H. Kim, S. J. Pyun, *J. Chem. Soc., Perkin Trans. 1*, 1997, 797.
- 29) H. Yoshida, Y. Yamaryo, J. Ohshita, A. Kunai, *Chem. Commun.*, 2003, **13**, 1510.
- 30) Y. Nishihara, K. Ikegashira, K. Hirabayashi, J. Ando, A. Mori, T. Hiyama, *J. Org. Chem.*, 2000, **65**, 1780.
- 31) E. Shirakawa, Y. Nakao, Y. Murota, T. Hiyama, *J. Organomet. Chem.*, 2003, **670**, 132.
- 32) M. E. Wright, M. J. Porsch, C. Buckley, B. B. Cochran, *J. Am. Chem. Soc.*, 1997, **119**, 8393.
- 33) S.-K. Kang, T.-G. Baik, X. H. Jiao, Y.-T. Lee, *Tetrahedron Lett.*, 1999, **40**, 2383.
- 34) M. Ochiai, Y. Nishi, S. Goto, H. J. Frohn, *Angew. Chem. Int. Ed.*, 2005, **44**, 406.
- 35) E. H. Smith, J. Whittall, *Organometallics*, 1994, **13**, 5169.
- 36) J. Rhee, M. Ryang, S. Tsutsumi, *Tetrahedron Lett.*, 1969, **10**, 4593.
- 37) C. H. Oh, V. R. Reddy, *Tetrahedron Lett.*, 2004, **45**, 5221.
- 38) Y. Nishihara, M. Okamoto, Y. Inoue, M. Mayazaki, M. Mayasaka, K. Takagi, *Tetrahedron Lett.*, 2005, **46**, 8661.
- 39) S. V. Damle, D. Seomoon, P. H. Lee, *J. Org. Chem.*, 2003, **68**, 7085.
- 40) W. Chodkiewicz, *Ann. Chim., (Paris)*, 1957, **2**, 819.
- 41) M. Alami, F. Ferri, *Tetrahedron Lett.*, 1996, **37**, 2763.
- 42) Y. Nishihara, K. Ikegashira, A. Mori, T. Hiyama, *Tetrahedron Lett.*, 1998, **39**, 4075.
- 43) V. Fiandanese, D. Bottalico, G. Marchese, A. Punzi, *Tetrahedron Lett.*, 2003, **44**, 9087.
- 44) C. Wang, L. O. Pålsson, A. S. Batsanov, M. R. Bryce, *J. Am. Chem. Soc.*, 2006, **128**, 3789.
- 45) J. A. Sinclair, H. C. Brown, *J. Org. Chem.*, 1976, **41**, 1078.
- 46) A. L. K. Shi Shun, E. T. Chernick, S. Eisler, R. Tykwinski, *J. Org. Chem.*, 2003, **68**, 1339.
- 47) D. A. M. Egbe, B. Carbonnier, E. L. Paul, D. Mühlbacher, T. Kietzke, E. Birckner, D. Neher, U.-W. Grummt, T. Pakula, *Macromolecules*, 2005, **38**, 6269.
- 48) D. A. M. Egbe, E. Birckner, E. Klemm, *J. Polymer Sci. A, Polymer Chem.*, 2002, **40**, 2670.
- 49) T. Nishinaga, Y. Miyata, N. Nodera, K. Komatsu, *Tetrahedron*, 2004, **60**, 3375.
- 50) M. L. Bell, R. C. Chiechi, C. A. Johnson, D. B. Kimball, A. J. Matzger, W. B. Wan, T. J. R. Weakley, M. M. Haley, *Tetrahedron*, 2001, **57**, 3507.
- 51) L. H. Lee, V. Lynch, R. J. Lagow, *J. Chem. Soc., Perkin Trans. 1*, 2000, 2805.
- 52) Y. Kang, C. Seward, D. Song, S. Wang, *Inorg. Chem.*, 2003, **42**, 2789.

- 53) W.-Y. Wong, K.-Y. Ho, S.-L. Ho, Z. Lin, *J. Organomet. Chem.*, 2003, **683**, 341.
- 54) J. W. Perry, A. E. Steigman, S. R. Marder, D. R. Coulter, *Organic Materials for Non-Linear Optics*, Royal Society of Chemistry, London, 1989, pp. 189.
- 55) A. E. Steigman, J. W. Perry, L.-P. Cheng, *Organic Materials for Non-Linear Optics II*, Royal Society of Chemistry, London, 1991, pp. 149.
- 56) Y. Miki, A. Momotake, T. Arai, *Org. Biomol. Chem.*, 2003, **1**, 2655.
- 57) A. Carpita, R. Rossi, *Tetrahedron Lett.*, 1986, **27**, 4351.
- 58) K. P. C. Vollhardt, L. S. Winn, *Tetrahedron Lett.*, 1985, **26**, 709.
- 59) B. König, E. Schofield, P. Bubenitschek, *J. Org. Chem.*, 1994, **59**, 7142.
- 60) X.-P. Cao, Y. Yang, X. Wang, *J. Chem. Soc., Perkin Trans. 1*, 2002, **22**, 2485.
- 61) X.-P. Cao, T.-Z. Chan, H.-F. Chow, *Tetrahedron Lett.*, 1996, **37**, 1049.
- 62) G. B. Jones, R. S. Huber, U.S. Patent, 1995, 13.
- 63) H. Sakakibara, M. Ikegami, K. Isagawa, S. Tojo, T. Majima, T. Arai, *Chem. Lett.*, 2001, 1050.
- 64) D. E. Ames, D. Bull, C. Takundwa, *Synthesis*, 1981, 364.
- 65) C. Eaborn, D. R. M. Walton, *J. Organomet. Chem.*, 1965, **4**, 217.
- 66) J. G. Rodríguez, J. L. Tejedor, T. L. Parra, C. Díaz, *Tetrahedron*, 2006, **62**, 3355.
- 67) A. S. Batsanov, J. C. Collings, R. M. Ward, A. E. Goeta, L. Porrès, A. Beeby, J. A. K. Howard, J. W. Steed, T. B. Marder, *CrystEngComm*, 2006, **8**, 622.
- 68) T. M. Fasina, J. C. Collings, J. M. Burke, A. S. Batsanov, R. M. Ward, D. Albesa-Jové, L. Porrès, A. Beeby, J. A. K. Howard, A. J. Scott, W. Clegg, S. W. Watt, C. Viney, T. B. Marder, *J. Mater. Chem.*, 2005, **15**, 690.
- 69) P. Nguyen, S. Todd, D. van den Biggelaar, N. J. Taylor, J. C. Collings, R. M. Ward, R. Ll. Thomas, A. S. Batsanov, D. S. Yufit, A. L. Thompson, J. A. K. Howard, O. F. Koentjoro, D. P. Lydon, P. J. Low, S. R. Rutter, K. S. Findlay, L. Porrès, A. Beeby, A. S. Scott, W. Clegg, S. W. Watt, C. Viney, T. B. Marder, in preparation.
- 70) J. R. Lakowicz, *Principles of Fluorescence Spectroscopy*, 2nd ed., Kluwer, New York, 1999.
- 71) A. Pardo, D. Reyman, J. M. L. Poyato, F. Medina, *J. Lumin.*, 1992, **51**, 269.
- 72) D. V. O'Connor, D. Phillips, *Time Correlated Single Photon Counting*, Academic Press, London, 1984.
- 73) D. V. O'Connor, W. R. Ware, J. C. Andre, *J. Phys. Chem.*, 1979, **83**, 1333.
- 74) G. M. Sheldrick, *SHELXTL*, version 6.14; Bruker-Nonius AXS, Madison, Wisconsin, U.S.A., 2003.

Chapter 2

Synthesis, photophysical properties and molecular and crystal structures of rhodacyclopentadienes

2.1 Introduction

2.1.1 Metallacyclopentadienes: MC_4 metallacycles

For a number of years, there has been considerable interest in the incorporation of metal atoms into cyclopentadiene rings due to the tuneable nature of the metal through the use of a variety of ligands and variable oxidation states. Main group XC_4 analogues are well studied and some interesting luminescent compounds are known; however, their application is limited as the properties they display are not easily manipulated or controlled.

Metal complexes of diimines¹ (a), bipyridines² (b) and 2-phenylpyridines^{3,4} (c) have been comprehensively studied. There are, however, fewer examples of analogous MC_4 metal biphenyl (bph) complexes (d) (Figure 1).

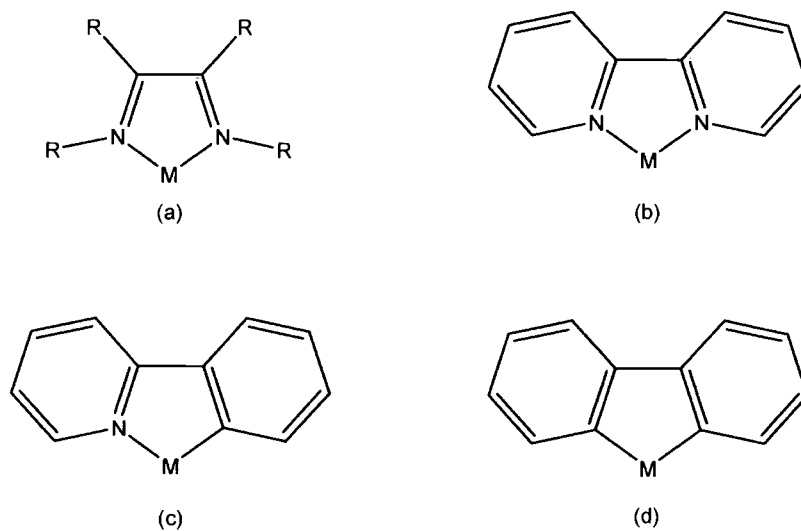


Figure 1. a) Metal diimine complex; b) metal bi-pyridine complex; c) metal 2-phenylpyridine complex; d) metal biphenyl complex.

2.2 Catalytic cyclotrimerisation of alkynes

Research on the mechanism of catalytic alkyne trimerisations first highlighted an MC_4 transient species as an intermediate in the catalytic cycle. These intermediates are formed from the reductive coupling of two equivalents of alkyne with temporary oxidation of the

metal centre (Figure 2). Collman *et al.* used isotopically labelled substrates with Rh(I) and Ir(I) catalysts to elucidate the sequential cyclotrimerisation of alkynes and they proposed a mechanism from these experiments.⁵ The group highlighted the formation of metallacycle (b) as an intermediate and also the intermediate alkynyl π -complex (c). They found that cyclotrimerisation could be suppressed if the reaction proceeded under a 60 psi pressure of CO. By blocking the latent coordination site required for alkyne complexation using CO, the reaction could be stopped. This argues against a Diels-Alder mechanism for benzene formation which should not be inhibited by CO coordination. They also found that even under forcing conditions, maleic anhydride would not react with (b). This also argues against the Diels-Alder mechanism for this system. Formation of a seven membered metallacycloheptatriene (d) is thus suggested, followed by reductive elimination of benzene.

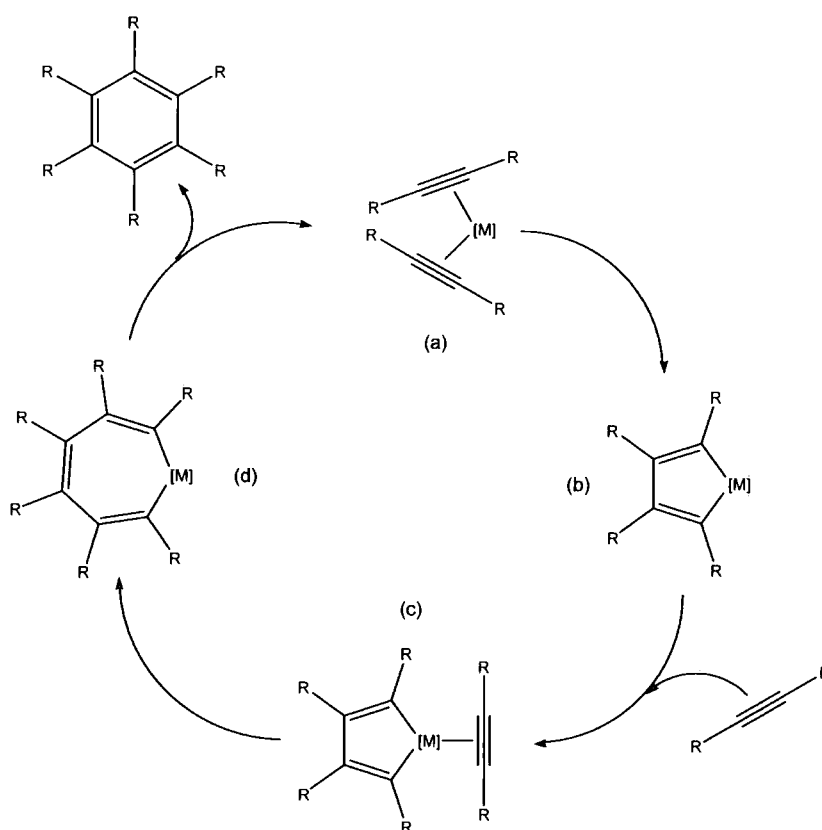


Figure 2. General catalytic cycle for the cyclotrimerisation of internal alkynes.

Catalytic [2+2+2] cyclotrimerisation of alkynes has been extensively investigated, and catalysts based on many early to late transition metals are known.⁶⁻⁹ Recently, research has been concerned with the synthesis and characterisation of metallacycle intermediates which

can be isolated with the use of appropriate metal centres and ligands around the metal and studied as independent species. Metallacycle compounds of this type are known for a wide range of transition metals, including Ti,^{10,11} Zr,¹² Hf,^{13,14} Pt,¹⁵ Pd,¹⁶ Ir,^{5,17} Ru,¹⁸ W,²⁰ Fe,²¹ Au,²² Rh^{5,23} and Co.^{6,24}

2.3 Reductive coupling of buta-1,3-diyne

Reductive coupling of buta-1,3-diyne to form bis-ethynylmetallacyclopentadienes is also known, although examples are limited. Nishihara *et al.* reacted CoCp(PPh₃)₂ with diphenylbutadiynes to form a mixture of diethynylcobaltacyclopentadienes.²⁵ Three regioisomers were found as well as some insoluble polymeric product (Figure 3). The major isomer formed was the asymmetric 2,4-dialkynyl isomer, with the symmetrical 2,5-dialkynyl complex only found when the reaction was undertaken at elevated temperature. Interestingly, the group found that when TMS-C≡C-C≡C-TMS and Me-C≡C-C≡C-Me diynes were used, only single metallacycle isomers were formed. The 2,4-dialkynyl metallacyclopentadiene was formed from the bulkier bis(TMS) butadiyne, whereas the less bulky 2,4-hexadiyne afforded the 2,5-dialkynyl metallacyclopentadiene.

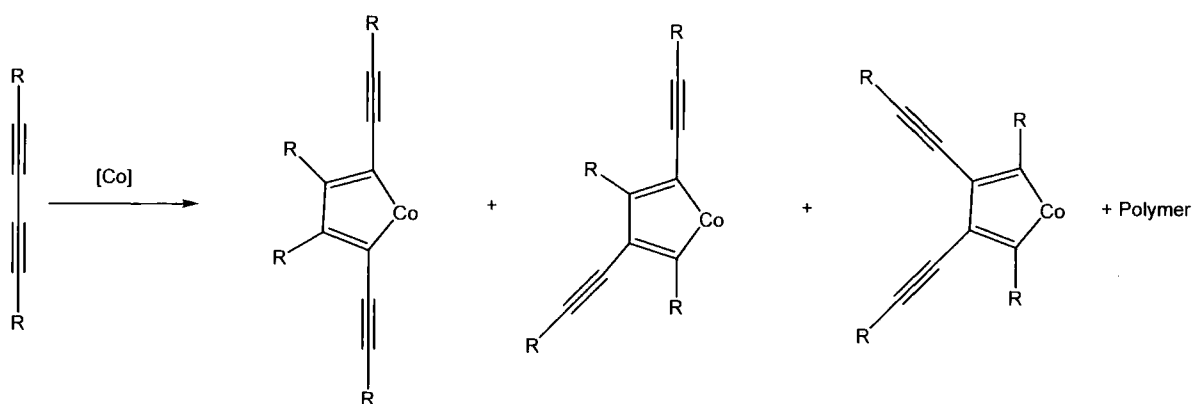


Figure 3. Formation of three stereoisomers by reductive coupling of butadiynes; [Co] = CpCo(PPh₃).

These results fit rules proposed by Wakatsuki *et al.* who previously studied cobalt metallacycle formation with a wide range of alkynes and found that regioselectivity of the cyclisation reaction was determined by the steric factors of the alkynes used rather than their electronic factors.²⁶ Reaction of diphenylbutadiyne with [Ru₃(CO)₁₀(NCMe)₂] in the presence

of Me_3NO also produced a mono-nuclear 2,5-dialkynyl ruthenacyclopentadiene complex, but the yield was low (1.5-4 %).²⁷ Marder and co-workers have developed a high yield, one-pot, regiospecific synthesis of luminescent rhodacyclopentadienes from 1,4-diarylbuta-1,3-diyne and $\text{Rh}(\text{PMe}_3)_4(\text{C}\equiv\text{C-TMS})$.²⁸ The 2,5-isomer is formed exclusively in quantitative yield and has been characterised by X-ray crystallography (Figures 4 and 5).

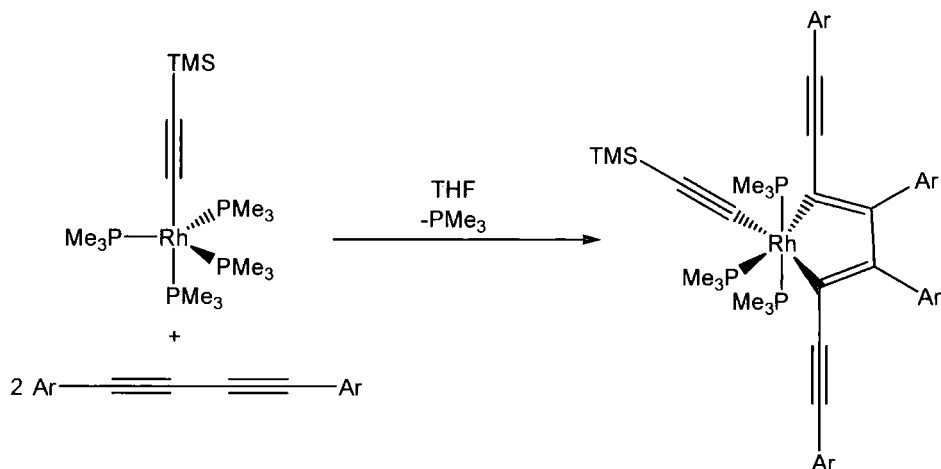


Figure 4. Formation of regiospecific 2,5-bis(arylethynyl)rhodacyclopentadienes.

Hill and co-workers have reported the regioselective synthesis of the ruthenacyclopentadiene compound, $[\text{Ru}\{\kappa^2\text{-(PhC}\equiv\text{C)=CPhCPh=(C}\equiv\text{CPh)}\}(\text{CO})_2(\text{PPh}_3)_2]$ and its structure has been determined by X-ray crystallography.²⁹ They report the exclusive formation of the 2,5-dialkynyl isomer by reaction of $[\text{Ru}(\text{CO})_2(\text{PPh}_3)_3]$ with excess diphenylbutadiyne; however, they did not discuss any optical properties of the ruthenacycle.

Titanium analogues have also been reported.³⁰⁻³² Reaction of TiCl_2Cp_2 with two equivalents of $\text{TMS-C}\equiv\text{C-C}\equiv\text{C-TMS}$ afforded the 2,4-diethynylmetallacycle in 65 % yield, the structure of which has also been determined by X-ray analysis (Figure 6). Zr analogues of Ti metallacycles have been proposed as intermediates in the formation of seven-membered cyclic cumulenes, although they have not been isolated.³³ Buchwald and co-workers attribute the larger size of Zr to Ti as an explanation for the fact that the Ti metallacycle can be isolated without cumulene formation whilst the Zr analogue cannot. The only other example of this type of compound is an osmium compound,³⁴ formed by reaction of $\text{Os}(\text{en})_2(\text{H}_2\text{O})(\text{H}_2)$ with 2,4-hexadiyne, producing the 2,5-diethynylmetallacycle exclusively.

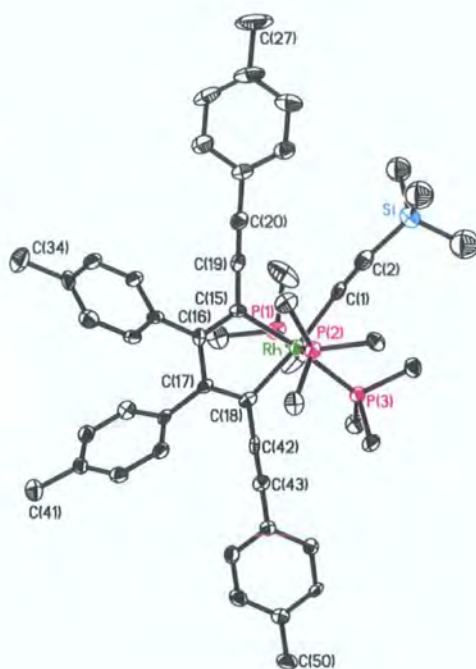


Figure 5. Molecular structure of *mer,cis*-[tris(trimethylphosphine)trimethylsilylethynyl-2,5-bis(4-tolyethynyl)-3,4-bis(4-tolyl)rhodacyclopenta-2,4-diene]. Hydrogen atoms and disorder in the P(1)Me₃ and SiMe₃ ligands have been omitted for clarity and thermal ellipsoids are shown at 50 % probability.²⁸

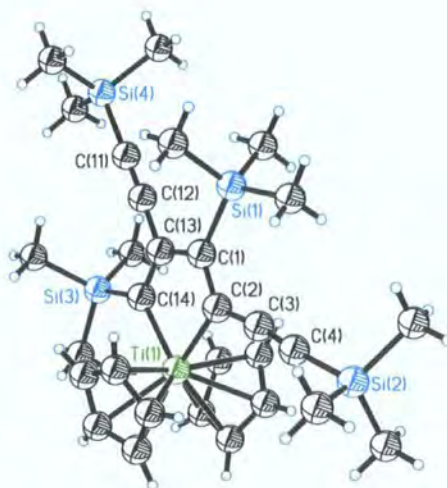


Figure 6. Molecular structure of bis(η^5 -cyclopentadienyl)-2,4-bis(trimethylsilylethynyl)-3,5-bis(trimethylsilyl)titanacyclopenta-2,4-diene. Thermal ellipsoids are shown at 50 % probability.³⁰

2.4 Metal biphenyl (bph) complexes

Metal bph complexes are known for a number of transition metals including Co,³⁵ Ni,³⁶ Pt,³⁷ Pd,³⁸ Ir^{39,40} and Rh.⁴¹ There are few synthetic routes to these complexes, and the methods employed are such that substituted bph complexes are relatively difficult to prepare.

2.4.1 Direct insertion into biphenylene

The main method used for complex formation is direct insertion of a nucleophilic metal centre into the strained, four-membered ring of biphenylene (Figure 7). This approach has been utilised for a range of transition metals.^{35,36,38,42} The thermodynamic driving force for such a reaction is the cleavage of the strained biphenylene C-C bond through oxidative addition to the metal giving two new metal aryl bonds.

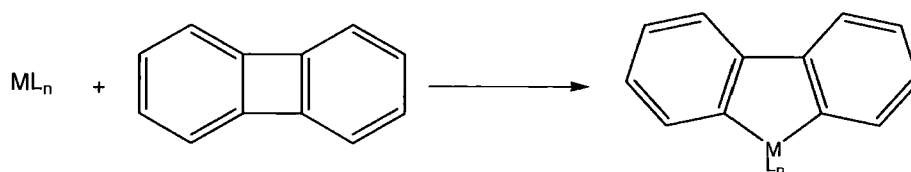


Figure 7. Formation of a metal bph complex from biphenylene.

The reactivity of weakly nucleophilic metal centres with the strained C-C bond of biphenylene is much lower than that of strongly nucleophilic metals, but it has been shown that when the manganese complex $[(\eta^6\text{-biphenylene})\text{Mn}(\text{CO})_3]^+$ is used in place of biphenylene, the reaction with $\text{Pt}(\text{PPh}_3)_2(\text{C}_2\text{H}_4)$ and subsequent formation of $\text{Pt}(\text{bph})(\text{PPh}_3)_2$ occurs in seconds.³⁷ On standing, the product scavenges CO from Mn with loss of phosphine to form $\text{Pt}(\text{bph})(\text{PPh}_3)(\text{CO})$, a transformation which has been speculatively linked to the relief of steric crowding around Pt.

Jones and co-workers found that reaction of $\text{MCp}^*(\eta\text{-C}_2\text{H}_4)_2$ ($M = \text{Co}, \text{Rh}$) with biphenylene, when heated for over two days produced a bimetallic $(\text{Cp}^*)_2\text{M}_2(\text{bph})$ complex.⁴¹ The first Cp^*M unit inserted into the strained C-C biphenylene bond, but the second coordinated to the metallacycle in an η^5 fashion. When the Rh analogue was heated at 120 °C

under a CO atmosphere, a 1:1 mixture of two mono-rhodium species, $\text{Cp}^*\text{Rh}(\text{CO})_2$ and $\text{Cp}^*\text{Rh}(\text{bph})(\text{CO})$ was formed (Figure 8).

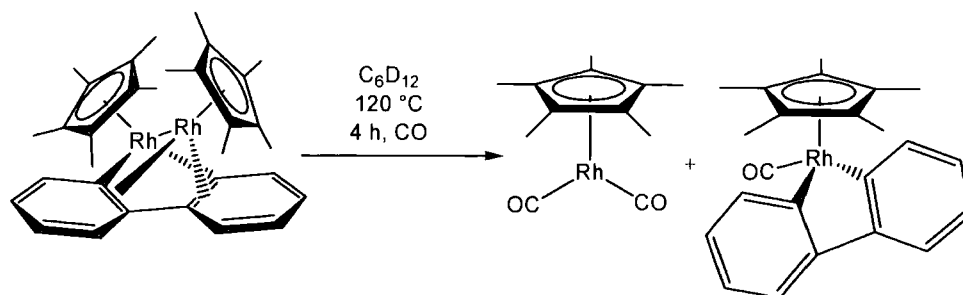


Figure 8. Formation of a Rh bph complex from a bimetallic starting material.

Attempts to form the bph complex directly from $\text{Cp}^*\text{Rh}(\text{CO})_2$ and biphenylene under thermal conditions were unsuccessful, but it was found that if the starting material and biphenylene were photolysed, slow conversion to product occurred, with the reaction reaching completion after three days. The Co analogue reacts similarly under these conditions; however, the insertion product is apparently unstable. Heating of the bimetallic species under a CO atmosphere gave a 2:1 mixture of $\text{Cp}^*\text{Co}(\text{CO})_2$ and fluorenone, with no evidence of any bph complex (Figure 9), although the authors proposed it to be an intermediate.

Both the Rh and Co bimetallic species are fluxional, and low temperature ^1H NMR spectroscopy of the complexes showed two distinct C_5Me_5 peaks (δ 1.73 and 1.16 ppm which coalesce to a singlet at $-25\text{ }^\circ\text{C}$ ($\Delta G^\ddagger = 11.4\text{ kcal/mol}$) for the Co analogue, and at $77\text{ }^\circ\text{C}$ ($\Delta G^\ddagger = 16.8\text{ kcal/mol}$) for the Rh analogue). The structures of both the Rh and Co bimetallic species have been determined by X-ray crystallography and show Rh-Rh and Co-Co bond distances of 2.683 \AA and 2.479 \AA respectively. Although the complexes are described as having a single M-M bond, electron counting suggests that a dative bond from an 18 e^- " $\text{Cp}^*\text{M}(\eta^2\text{-C}_6\text{H}_4)_2$ ", M(I) species to a 16 e^- " $\text{Cp}^*\text{M}(\text{bph})$ " M(III) species would provide a localised, formal description of the bonding.

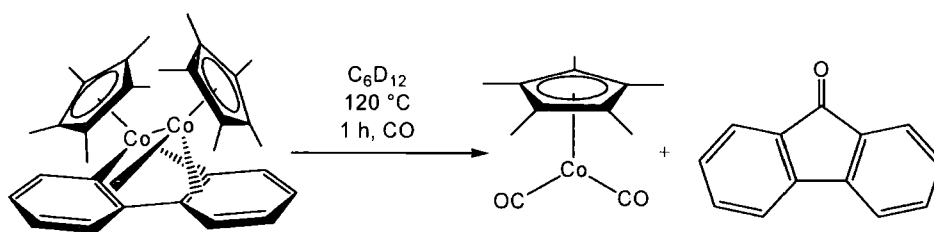


Figure 9. Formation of fluorenone from a bimetallic bph Co complex.

When PMe_3 was used in place of CO , the Co species analogous to the rhodium example was formed, and a 1:1 mixture was obtained from the bimetallic species. Neither the Rh nor Co binuclear complexes react with hydrogen, even at high temperature or H_2 pressure.

Crabtree *et al.* demonstrated the formation of a $16 e^-$ Ir(III) biphenylene adduct, $\text{Ir}(\text{PPh}_3)_2(\text{bph})\text{Cl}$ from an Ir(I) precursor.⁴⁰ The iridacycle reacted with CO , $\text{PhC}\equiv\text{CPh}$, PR_3 or NaBH_4 , but in no case showed disruption of the Ir(bph) metallacycle.

Group 8 transition metals have been successfully inserted into the strained C-C bond of biphenylene and the related compound, benzocyclobutadienoid-[3]-phenylene.^{43,44} Vollhardt and co-workers reported the first example of Fe insertion into benzocyclobutadienoid-[3]-phenylene to give a dibenzoferrole derivative (Figure 10) and a second minor dibenzoferrole- $\text{Fe}(\text{CO})_3$ - π -complex. This example is related to the earlier Rh and Co examples; however, in this instance, the authors depict the M-M bond as a dative interaction.

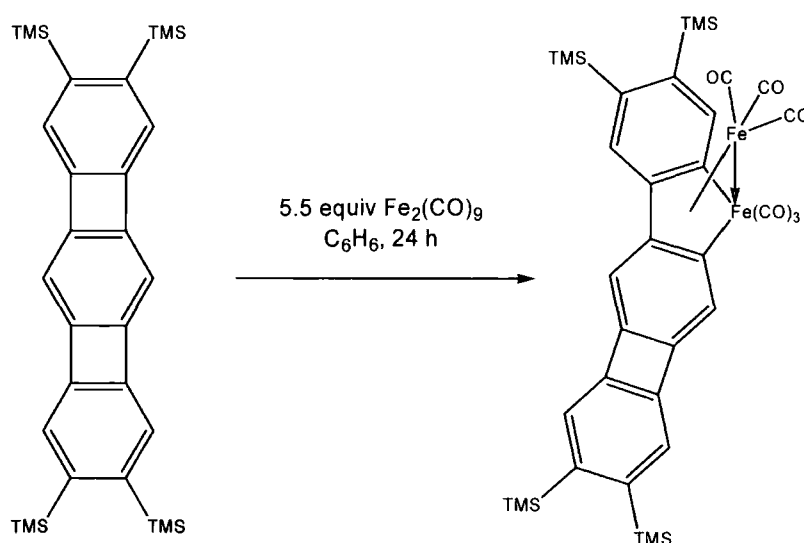


Figure 10. Formation of a dibenzoferrole derivative.

Reaction of $M_3(CO)_{12}$, ($M = Fe, Ru, Os$) directly with biphenylene gives major products of the type $Fe_2(CO)_5(\mu-CO)(\mu-\eta^2-\eta^4-C_6H_4)_2$ (Figure 11), $Ru_2(CO)_5(\mu-CO)(\mu-\eta^2-\eta^4-C_6H_4)_2$ and $Os_2(CO)_6(\mu-\eta^2-\eta^4-C_6H_4)_2$, the Ru and Os analogues of which have been characterised by X-ray crystallography. The reactions for Fe and Ru can be completed within just a few hours at elevated temperatures (3 hours/98 °C and 4 hours/126 °C respectively); however, the Os example is much less reactive, with 33 % of $Os_3(CO)_{12}$ remaining even after heating to 200 °C under nitrogen in a sealed flask for 15 hours. This observation is consistent with stronger M-M and M-CO bonds found in third row transition metals compared to those of first and second row metals.

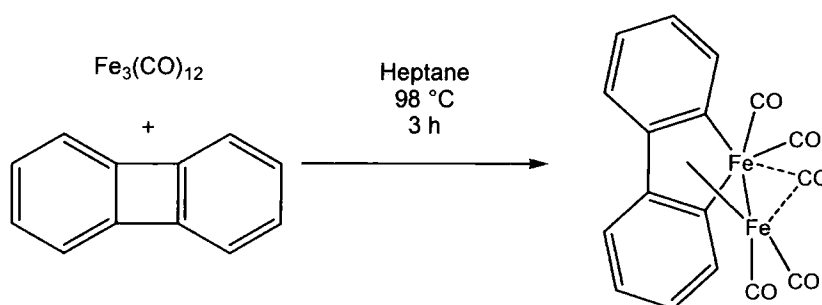


Figure 11. Formation of $Fe_2(CO)_5(\mu-CO)(\mu-\eta^2-\eta^4-C_6H_4)_2$.

Garcia *et al.* have reacted dibenzothiophene with $Ru_3(CO)_{12}$ in refluxing heptane, resulting in C-S bond activation and desulfurisation under mild conditions to give $Ru_2(CO)_5(\mu-CO)(\mu-\eta^2-\eta^4-C_6H_4)_2$ in moderate yields.⁴⁵ The Ru atoms are linked by a Ru-Ru bond (2.697 Å) and a bridging carbonyl, and the structure has been confirmed by X-ray diffraction. The compound is readily cleaved by H_2 to give biphenyl. A similar reaction involving the $[NiH(^iPr_2PCH_2)_2]_2$ dimer has also been used to achieve C-S bond activation, resulting in Ni(bph) complexes in moderate yields, although bph complexes were not the sole reaction products.⁴⁶

2.4.2 Reactions of metal halides with lithiated biphenyls

A second method for the synthesis of bph complexes involves the use of dilithio-biphenyl, although the use of lithium reagents further limits any bph substitution. Reaction occurs between the metal dihalide and 2,2'-dilithiobiphenyl, which can be easily prepared from 2,2'-dibromobiphenyl. Elimination of lithium halide leads to the metallacycle product.

This approach is less common in the literature but was used by Rausch and co-workers in 1973 to synthesise bph complexes of Co, Rh, Ir, Pt and the first example of a Zr biphenyl species.⁴⁷ This method has also been used for the synthesis of Pd^{48,49} and other Pt^{50,51} biphenyl complexes. Romeo *et al.* and Rillema *et al.* have both employed this route to prepare Pt(bph) complexes from PtCl₂(SEt₂)₂ and PtCl₂(CO)₂, the former group having formed a planar Pt₂Et₂S bridged species and the latter group observing mononuclear Pt(bph)(CO)₂ (Figure 12). Romeo and co-workers also noted that the dinuclear Pt(II) complex [Pt₂(μ-SEt₂)₂(Hbph)₄] underwent intramolecular C-H activation to afford the cyclometallated species [Pt₂(μ-SEt₂)₂(bph)₂] and biphenyl.⁵⁰

The strongly donating PEt₃ ligand has been shown to be useful when synthesising Pd and Pt bph complexes directly from C-C insertion into biphenylene. The use of less basic PPh₃, however, results in Pt/Pd complexes which are unreactive to C-C bond cleavage. Analogues can, however, be prepared by reacting Pt(PPh₃)₂Cl₂ with 2,2'-dilithiobiphenyl.⁵²

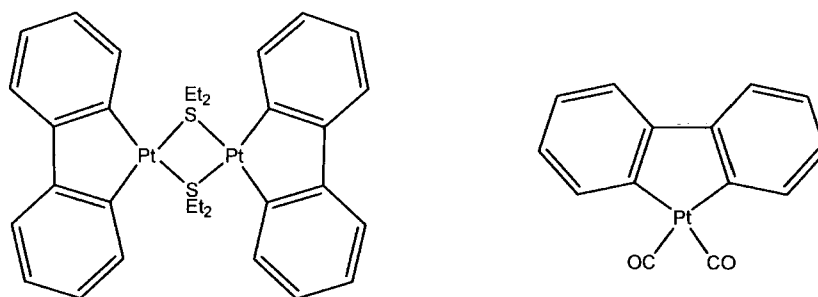


Figure 12. Examples of Pt(bph) complexes formed from Pt chloride salts and 2,2'-dilithiobiphenyl.

Examples of titanium species synthesised *via* this route are known from as early as the 1960s, with Massey and Cohen reporting the synthesis of the (perfluorobiphenyl)TiCp₂ from the 2,2'-octafluorobiphenyl dilithium salt.⁵³ Shortly after, Rausch and Klemann reported the related non-fluorinated analogue, isolated as bright red crystals in 12 % yield.⁵⁴

2.4.3 Other routes

Jones *et al.* have demonstrated the formation of Pt biphenyl complexes directly from CF_3 -substituted biphenyls.⁵⁵ Reaction of 10 equivalents of 4,4'-bis(trifluoromethyl)biphenyl with $[\text{PtH}(\text{dtbpm})\text{CH}_2\text{CMe}_3]$ gives a transient η^2 -arene complex which undergoes C-H activation to form two isomeric $\text{PtH}(\text{Hbph})(\text{dtbpm})$ complexes (C-H activation at the 2 or 3 position in a 5:1 ratio respectively). Upon heating to 85°C , a second C-H activation occurred with loss of H_2 giving $[\text{Pt}(\text{dtbpm})((\text{CF}_3)_2\text{bph})]$ (Figure 13).

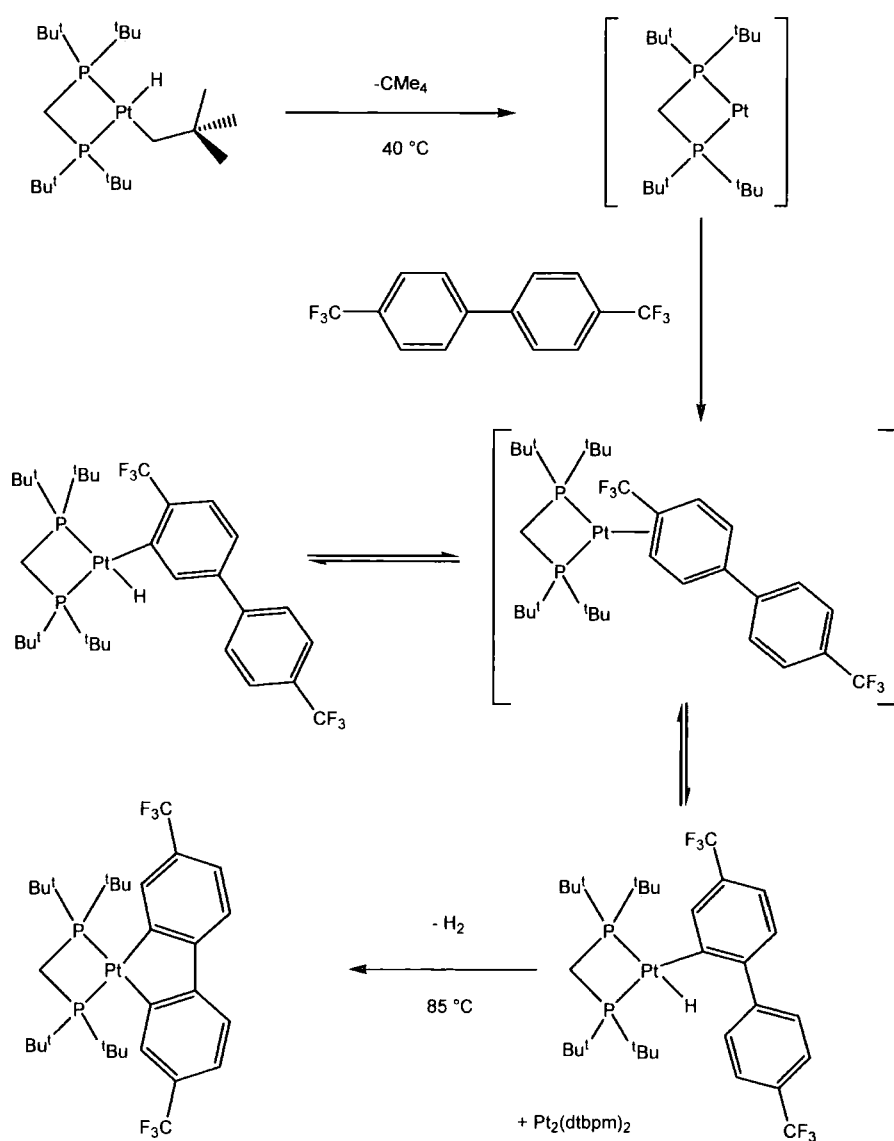


Figure 13. Formation of $\text{Pt}(\text{bph})(\text{dtbpm})$ by C-H activation of 4,4'-bis(trifluoromethyl)biphenyl.

A seemingly unique method of preparing metal bph complexes has been used in the synthesis of Ir metallacycles. Wakatsuki and co-workers³⁹ found that reaction of four equivalents of sodium fluorenone ketyl with $[\text{Cp}^*\text{Ir}(\text{Cl})(\mu\text{-Cl})_2]$ in THF resulted in the formation of the decarbonylation product in 70 % yield along with free fluorenone (Figure 14). Presumably, this involves reduction of the Ir(III) complex to “Cp*Ir” followed by insertion into one of the C-C(O) bonds of fluorenone and subsequent migratory de-insertion of CO.

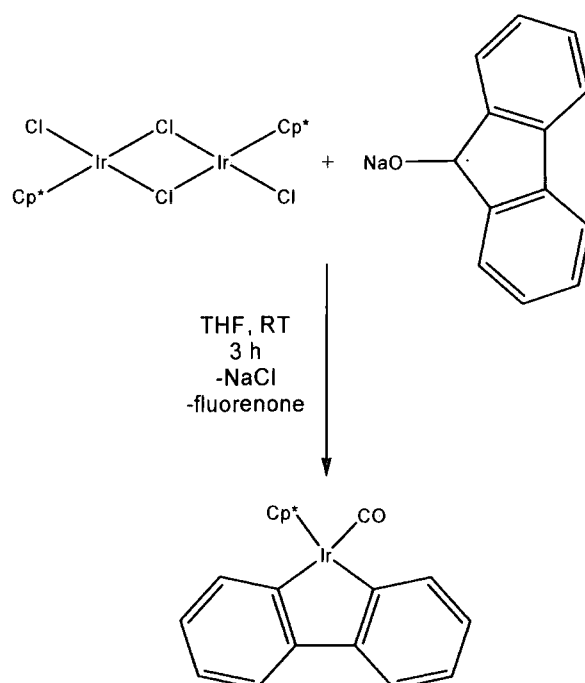


Figure 14. Synthesis of Ir(bph)Cp*(CO) by decarbonylation of sodium fluorenone ketyl.

2.5 Catalysis by metal bph complexes

There are a number of examples whereby metal bph complexes catalyse reactions that form C-C bonds or act as catalysts for the reduction of biphenylene.

Eisch³⁶ and Vollhardt⁵⁶ have both identified Ni(bph) moieties as intermediates in the formation of tetraphenylene from biphenylene. Vollhardt and co-workers found that Ni(cod)(PMe₃)₂ reacted stoichiometrically with biphenylene to form tetraphenylene at 25 °C, and that the reaction proceeded catalytically (10 mol% catalyst) at 100 °C. Jones and co-

workers⁴⁸ have studied the dimerisation of biphenylene to tetraphenylene at 120 °C using Pt and Pd catalysts. The group has studied the mechanistic pathway and proposed that catalysis proceeds first *via* $M(\text{bph})(\text{PEt}_3)_2$ ($M = \text{Pt}, \text{Pd}$), a compound that they have synthesised independently and characterised by X-ray analysis, and then by a transient six coordinate, $M(\text{IV})(\text{bph})_2(\text{PEt}_3)_2$ intermediate. The Pd analogue of $\text{Pt}(\text{IV})(\text{bph})_2(\text{PEt}_3)_2$ was not observed, although this may be due to faster reductive elimination from Pd(IV) than from Pt(IV). The rate of the Pd catalysis was 100 times that for Pt, and decreased as the ratio of free phosphine to biphenylene increased. This observation is consistent with the formation of a $M(\text{bph})(\text{PEt}_3)$ intermediate prior to coordination of the second equivalent of biphenylene. At this point, rearrangement can occur, and $M(2,2''\text{-tetraphenylene})(\text{PEt}_3)_2$ would be formed before tetraphenylene is reductively eliminated again, likely from the monophosphine complex, forming an active, coordinatively unsaturated " $M(\text{PEt}_3)_n$ " species. The group have isolated and characterised $\text{Pt}(2,2''\text{-tetraphenylene})(\text{PEt}_3)_2$, with the molecular structure showing a highly distorted square-planar geometry around the metal. When catalysis was attempted under an atmosphere of H_2 , the formation of tetraphenylene was low as biphenyl was the major product formed, the rate of which was much faster for Pd than Pt.

Jones and co-workers have studied the catalytic hydrogenolysis of biphenylene to biphenyl *via* a $M(\text{bph})$ complex using Ni, Pt and Pd with a range of phosphines.⁵⁷ The metal used had the greatest overall effect on the rate of hydrogenolysis, with $[\text{Ni}(\text{dippe})\text{H}]_2$ proving to be the most active, giving 16 turnovers a day at 50 °C, considerably higher than that for Pd or Pt.

Crabtree *et al.* reported that iridium bph complexes are active catalysts in the dimerisation of terminal alkynes to *E,Z*-enynes⁵⁸ (Figure 15). $\text{Ir}(\text{bph})(\text{PMe}_3)_3\text{Cl}$ in the presence of AgBF_4 , is effective in head to head coupling, the main isomer being the thermodynamically less stable *E*-isomer, unless PMe_3 is present which can block the isomerisation of the intermediate vinyl complex.

AgBF_4 is necessary to remove PMe_3 and Cl^- to generate the active catalyst from the initial Ir complex. The group attribute the preference for head to head dimerisation to the exceptionally low steric bulk of the catalyst in the plane of the insertion reaction.

In the presence of stoichiometric, or in some cases, catalytic amounts of *p*-cresol, $\text{Pd}(\text{PPh}_3)_4$ was found to be a catalyst for the formation of functionalised biphenyl compounds.⁵⁹ The vinylic C-H bond of alkenes can be added across the strained biphenylene C-C bond, a reaction promoted by weak acids. Under similar conditions, arylboronic acids, and ketones and nitriles that possess α -hydrogens can also add across the biphenylene bond to

form biaryl derivatives (Figure 16). Although $\text{Pd}(\text{PPh}_3)_2(2,2'\text{-biphenyl})$ was not observed in these reactions, its presence was inferred from the products formed.

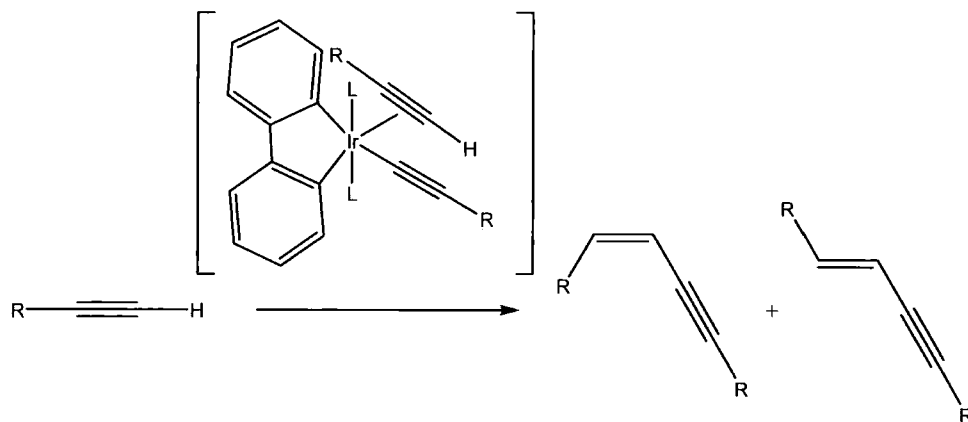


Figure 15. Formation of *E,Z*-enynes by head-head coupling of alkynes with Ir(bph) catalyst.

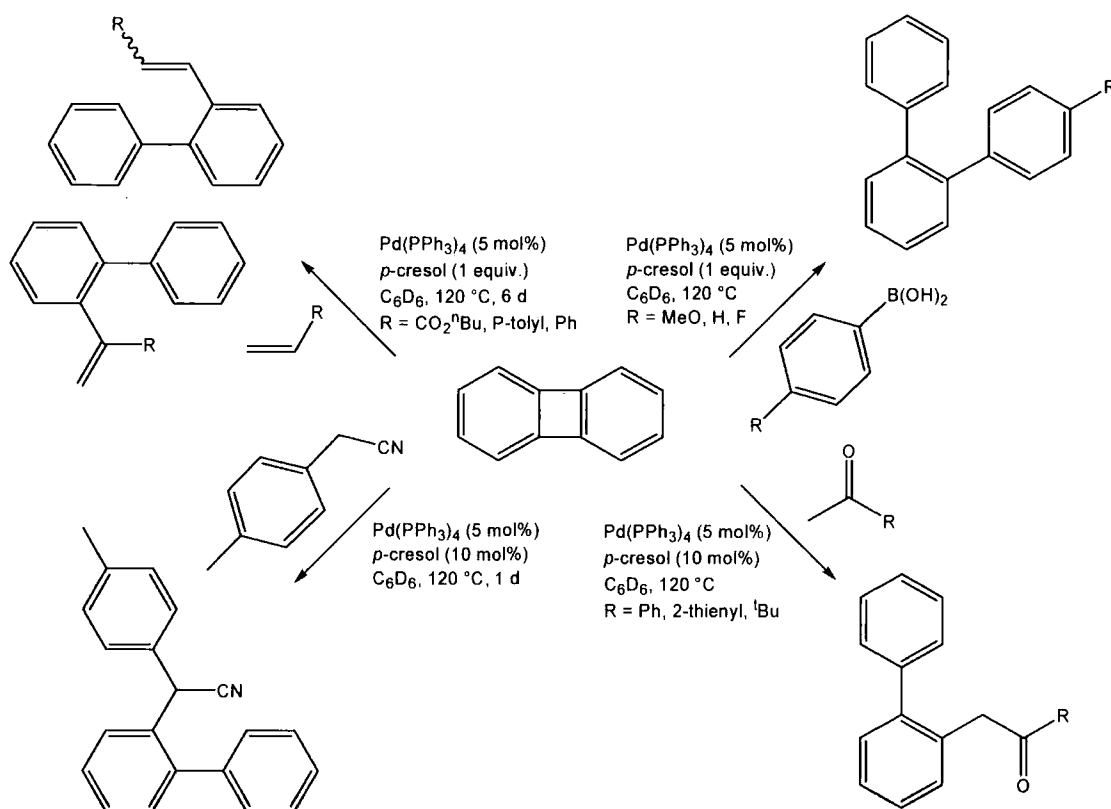


Figure 16. Pd catalysed formation of functionalised biphenylene derivatives.

A number of examples whereby Ni complexes catalyse the formation of 9,10-disubstituted phenanthrenes are known. Jones *et al.*^{60,61} used Ni(dippe)(RC≡CR) (R = Ph, Me) complexes with biphenylene to form disubstituted phenanthrenes catalytically in moderate yields. Under nitrogen, the reaction proceeded slowly, even at 120 °C. Addition of 6 mol% of oxygen to the reaction vessel led to an acceleration of the rate at lower temperatures (70-80 °C) (Figure 17). The oxygen is not involved in oxidation of the metal, but oxidises the phosphine ligand, generating a more active, coordinatively unsaturated Ni species. N-heterocyclic carbene Ni complexes have also been used in this way.⁶² Two mol% of catalyst at 80 °C gave quantitative conversion of biphenylene and diphenylacetylene to 9,10-diphenylphenanthrene in 30 minutes.

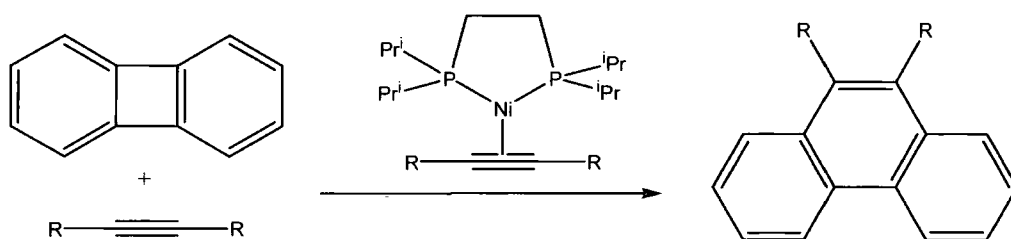


Figure 17. Catalytic formation of 9,10-disubstituted phenanthrenes (R = Me, Ph, CO₂Me, TMS).

Rh(dtbbp)(2,2'-diphenyl)Cl (dtbbp = ^tBu₂PCH₂P^tBu₂) has been used to form substituted phenanthrenes catalytically and in good yields.⁶³ The complex is also reactive towards Lewis bases at room temperature, and has been used in the synthesis of 9-fluorenone and 9-(*t*-butylimino)fluorene, although this was not catalytic.

2.6 Luminescent transition metal biphenyl complexes

Photophysical properties of several Pt^{49,51,64,65} and Pd^{49,66} biphenyl complexes have been reported. Rillema and co-workers have extensively studied the absorption and emission properties of a number of Pt(bph) complexes with the mono- and bidentate ligands, pyridine, acetonitrile, ethylenediamine,⁵³ CO,^{51,65} dpmm,^{67,68} and the bridging ligand SET₂.⁶⁴ Absorption spectra of mono-metallic [Pt(bph)(py)₂], [Pt(bph)(NCMe)₂], [Pt(bph)(en)] and bimetallic [Pt(bph)(SET₃)₂] complexes showed HOMO-LUMO $d\pi_{(Pt)} \rightarrow \pi^*_{(bph)}$ transitions around 300-400 nm and intra-ligand $\pi \rightarrow \pi^*$ transitions at higher energy. The compounds show strong

luminescence in solution, attributable to emission from π^* energy levels centred on biphenyl. Vibrational fine structure was present, consistent with ligand centred emission. The spectra of all of the compounds were remarkable similar, and lower energy bands between 490-620 nm were observed with little change in the profile at 77 K. Triplet lifetimes of 3-14 μ s were recorded. Quantum yields for the mono-metallic complexes were ca. 0.16, and 0.08 for the bimetallic species. The complex Pt(bph)(CO)₂ was found to be a weak emitter in solution, with emission at 562 and 594 nm. Triplet lifetimes between 2 and 3 μ s in CH₂Cl₂ and 4:1 EtOH:MeOH, and less than 1 μ s in 4:1 2-MeTHF:CH₂Cl₂ were reported. Except in very dilute solution, the complex readily self-associated leading to a number of emitting species such as dimers and higher aggregates in solution, and there was also emission from stacked Pt(II) crystals in the solid state. Thus, the solid showed a non-structured emission band at 726 nm, with a shortened lifetime of 0.84 μ s.⁶⁹ They also reported a time-dependent density functional theory (TD-DFT) study of the spectroscopic properties related to aggregation in the Pt(II) bph dicarbonyl complex⁶⁶ to examine singlet and triplet excited states, and to compare calculated geometries with those from the X-ray crystallographic data previously obtained.⁶⁵

The heterobimetallic complex Fe(η^5 -C₅H₄PPh₂)₂Pt(bph) has been synthesised and characterised by X-ray crystallography, and the photophysical properties of the compound have been studied.⁷⁰ Upon coordination to the metal, the Fe(η^5 -C₅H₄PPh₂)₂ $d\pi_{(Fe)} \rightarrow \pi^*_{(Cp)}$ MLCT transition was blue shifted from 442 to 425 nm, and a $d\pi_{(Pt)} \rightarrow \pi^*_{(bph)}$ MLCT transition was observed at 337 nm, with a lifetime of 6.7 μ s (at 77 K). At room temperature, the emission lifetime was too short to be recorded using a nanosecond laser, and the work suggests quenching of the triplet emission by the ferrocenyl moiety *via* an electron transfer mechanism.⁷⁰

2.7 Metallacyclopentadiene containing polymers

π -conjugated polymers containing MC₄ units are currently under investigation. These heteroaromatic polymers are structurally analogous to organic polymers such as poly(pyrrole) and poly(thiophene). Examples are known from reactions of “non-conjugated” diynes of the type R-C \equiv C-Ar-C \equiv C-R’ (where Ar = a range of aromatic units, R/R’ = H, Me, TMS) with transition metal compounds such as [Ru(COD)(hexCp)Br],⁷¹ CoCp(PPh₃)₃,⁷² [Co(hexCp)(PPh₃)₂]^{73,74} and “ZrCp₂”.⁷⁵

Nishihara and co workers⁷⁴ were the first group to prepare and characterise polymers of this type, successfully isolating a number of poly(arylene cobaltacyclopentadienylene)s. They found that use of Cp as a ligand on Co resulted in insoluble polymers. The highest molecular weights were achieved when the ratio of diyne to metal complex was close to unity. Cyclisation at the metal was regiospecific, with the 2,5-isomer forming exclusively to give linear polymers. However, reaction of 1,4-diethynylbenzene with hexyl substituted (hexCp)Co(PPh₃)₂ gave an isomeric mixture of soluble polymers, the ratio of 2,5- vs. 2,4 being 0.6. Reaction between (hexCp)Co(PPh₃)₂ and 1,4-(MeC≡C)₂C₆H₄ at higher temperature (40 °C) gave the reaction a greater degree of regiospecificity in favour of the 2,5-isomer, while also dramatically increasing M_w and M_n values.

The same group has also prepared the first examples of polymers containing unusual ruthenium metallacyclopentatrienes, capable of reversible reduction of the Ru, leading to ferromagnetic interaction between the Ru sites in the reduced state.⁷¹ The polymer can be formed by reductive coupling of non-conjugated diynes at the Ru centre, with maximum M_w being obtained when the diyne:Ru ratio is 1:1. NMR studies on the polymers showed the presence of only one geometrical isomer from which it was concluded that only a 2,5-aryly derivative of ruthenacyclopentatriene exists, indicating a fully π -conjugated main chain structure (Figure 18).

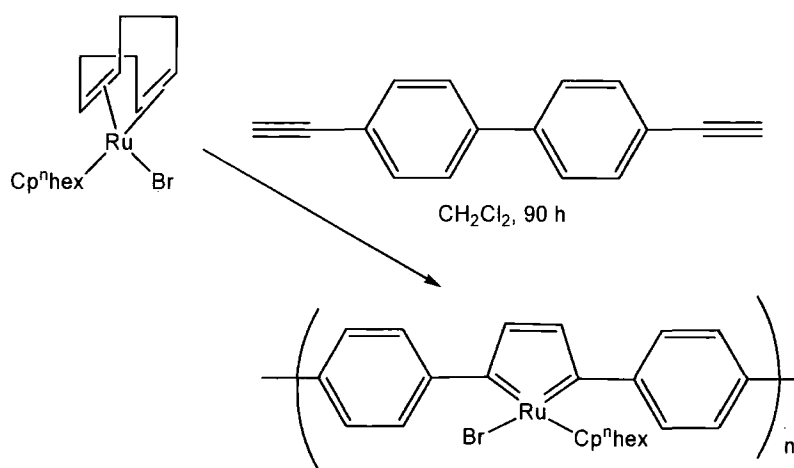


Figure 18. Formation of regiospecific poly(phenyl-ruthenacyclopentatriene).

Zirconocene examples can be synthesised from reaction of diynes with internal silicon substituents with “ZrCp₂” (formed *in situ* by reaction of ZrCp₂Cl₂ with two equivalents of BuLi at -78 °C) and isolated in 50-90 % yields.⁷⁵ The polymers are easily hydrolysed to give the corresponding butadienediyl polymers and also react with iodine to give iodine-containing polymers. Polymer degradation in refluxing THF solution provides a mild and high yielding route to macrocycles, the structures of which depend on the spacer groups incorporated into the polymer backbone (Figure 19).

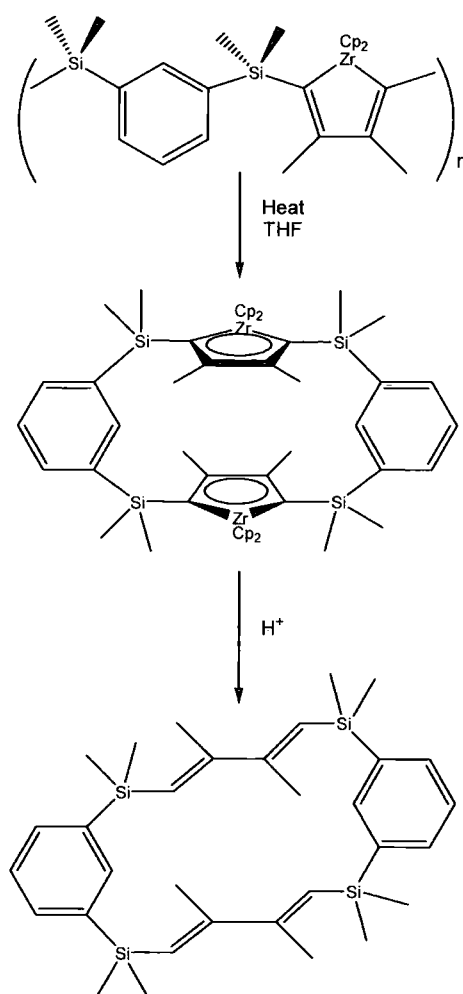


Figure 19. Facile, high yield degradation of zirconocene polymers to form macrocycles.

Matsubara and co-workers have prepared polymer bound photoluminescent iridium complexes bearing 2,2'-biphenyl ligands. Reaction of an [Ir(cod)(bph)Cl]₂ (cod = 1,5-cyclooctadiene) metal precursor with a copolymer, built by the radical copolymerisation of 4-styryldiphenylphosphine and methyl methacrylate gave polymers that were cross-linked by



P-Ir-P bonds (0.06-0.6 mmol/g Ir). Solid state luminescence was observed at 597 nm, the intensity of which was dependent on the molecular weight of the copolymer ligands and on the polymer Ir content.⁷⁶

2.8 Siloles: SiC_4 main group analogues

Although these groups of compounds are outside the central metallacycle topic of this review, main group heterocycles, including siloles and many others, e.g. phospholes and thiophenes (Figure 20), have been well studied and will be briefly introduced.

Siloles are interesting main group analogues of metallacycles which show unique photophysical properties due to the unusual electron deficient nature of the silole ring; these compounds have been reviewed.^{77,78} Siloles have an extremely low lying LUMO due to $\sigma^*-\pi^*$ conjugation in the ring. Synthesis is straight forward and allows a wide range of substituents to be incorporated.

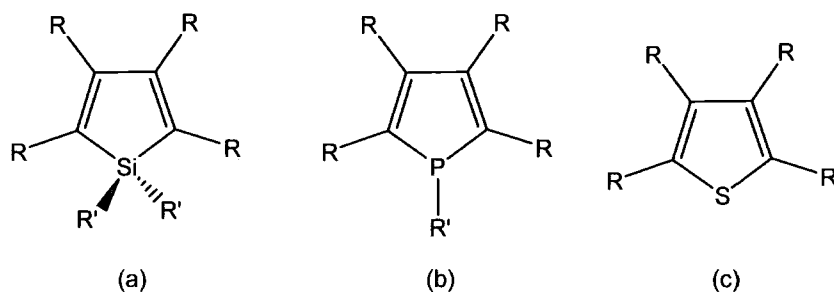


Figure 20. Silole (a), phosphole (b) and thiophene (c) structures.

Tamao and co-workers⁷⁹ reported a route from bis(phenylethynyl)silane which is treated with an excess of lithium dihydronaphthylide to form 2,5-dilithiosilole. Rearrangement *via* an intramolecular reductive cyclisation forms a bis(anion). This species is the key synthetic building block, allowing a wide range of derivatives to be prepared. If appropriate silane starting materials are used, then substitution directly at the Si heteroatom is possible. The nature of synthesis can give a highly tuneable series of emissive materials suitable for use in optical applications. For example, 2,5-di(2-pyridyl)silole has been used as an electron transporting layer in organic electroluminescent devices, demonstrating the utility of the electron deficient nature of the siloles.⁷⁷

Pagenkopf has used the above method in the preparation of luminescent 2,5-bis(phenylethynyl)siloles⁸⁰ related to metallacycles previously discussed.²⁸ By exploiting the versatility of, and adapting Tamao's synthetic route, donor-acceptor siloles were prepared (yields of 50 % and above were obtained) and the luminescent properties studied (Figure 21). All of the compounds that were prepared absorbed and emitted in the visible region, with the maxima strongly dependent on the push-pull substituents of the chromophore. A red shift in both absorption and emission occurred as the polarity of the molecule increased.

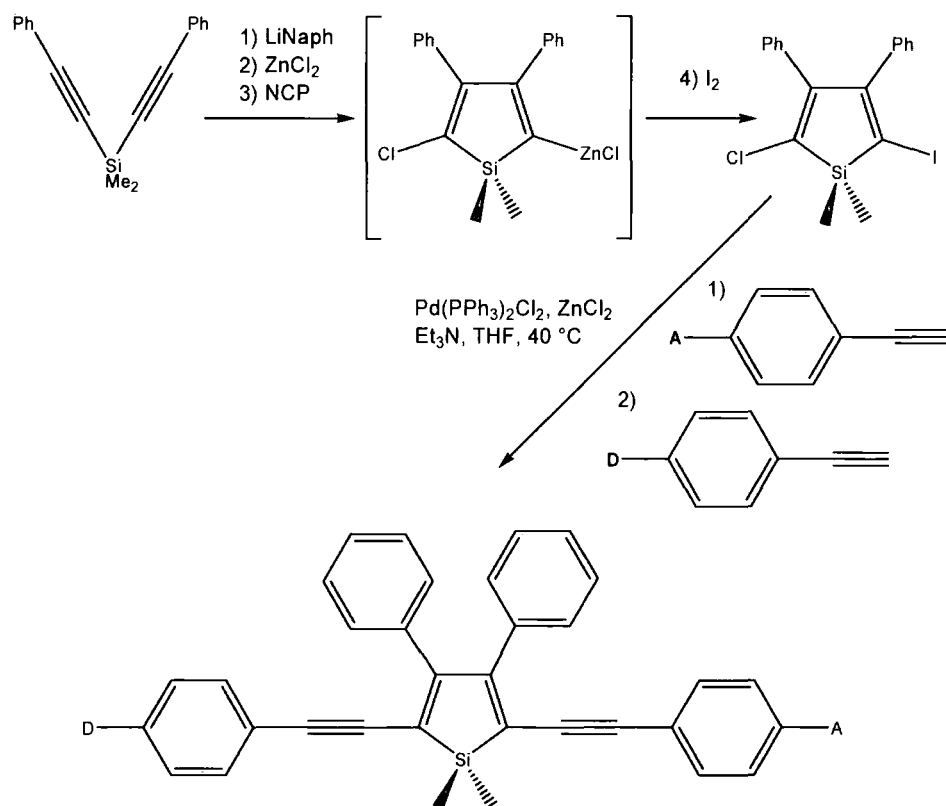


Figure 21. Synthetic route to unsymmetrical 2,5-bis(phenylethynyl)-3,4-diphenyl-siloles.

A number of bis(phenylethynyl)thiophenes (BPETs) have been reported and are of interest due to their luminescence⁸¹⁻⁸⁶ and non-linear optical⁸⁷⁻⁸⁹ properties and also, due to the bent nature of the thiophene moiety, their liquid crystal phase behaviour.⁹⁰⁻⁹³

There are a number of routes for the synthesis of BPETs. The most straightforward methods utilise catalytic cross-coupling of terminal alkynes⁸¹⁻⁸⁴ or alkynyl Grignard

reagents⁹⁴ with dihalothiophenes under Sonogashira reaction conditions to give BPETs in good yields (Figure 22). Pd catalysed cross-coupling has also been used to produce BPETs in good yields from triorganoindium compounds and 2,5-dibromothiophene.⁹⁵

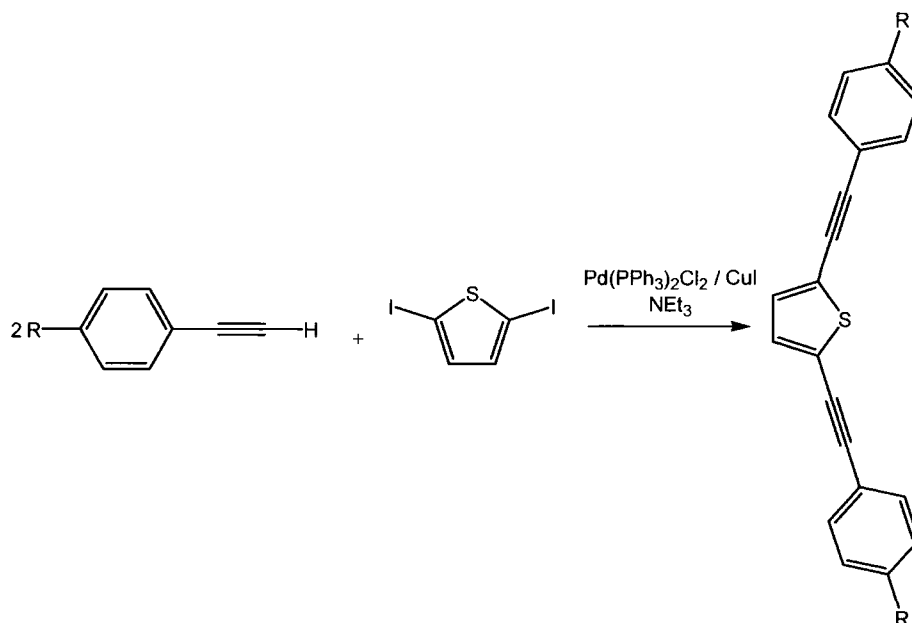


Figure 22. Pd/Cu catalysed synthesis of bis(phenylethynyl)thiophenes.

Other methods have involved longer reaction sequences involving elimination reactions to give BPETs. A one-pot synthesis using benzyl sulfone derivatives and 2-formyl-5-phenylethynylthiophene incorporating two sequential eliminations from the reaction intermediates has been developed, forming symmetrical or unsymmetrical BPETs in good yields.⁹⁶ The compound 1,8-diphenyl-1,7-octadiyne-3,6-dione, synthesised in nine steps from 1,4-butanediol, can also be converted to BPET by reaction with bis(triphenyl)tin sulphide in the presence of BCl_3 .⁹⁷

2.9 Results and Discussion

2.9.1 Synthesis of TMSA rhodacyclopentadienes

A number of regiospecific, luminescent rhodacyclopentadienes have been synthesised in high yields by reaction of two equivalents of substituted 1,4-bis(4-R-phenyl)buta-1,3-diyne with one equivalent of $\text{Rh}(\text{PMe}_3)_4\text{C}\equiv\text{C-TMS}$ in THF solution (Figure 23).

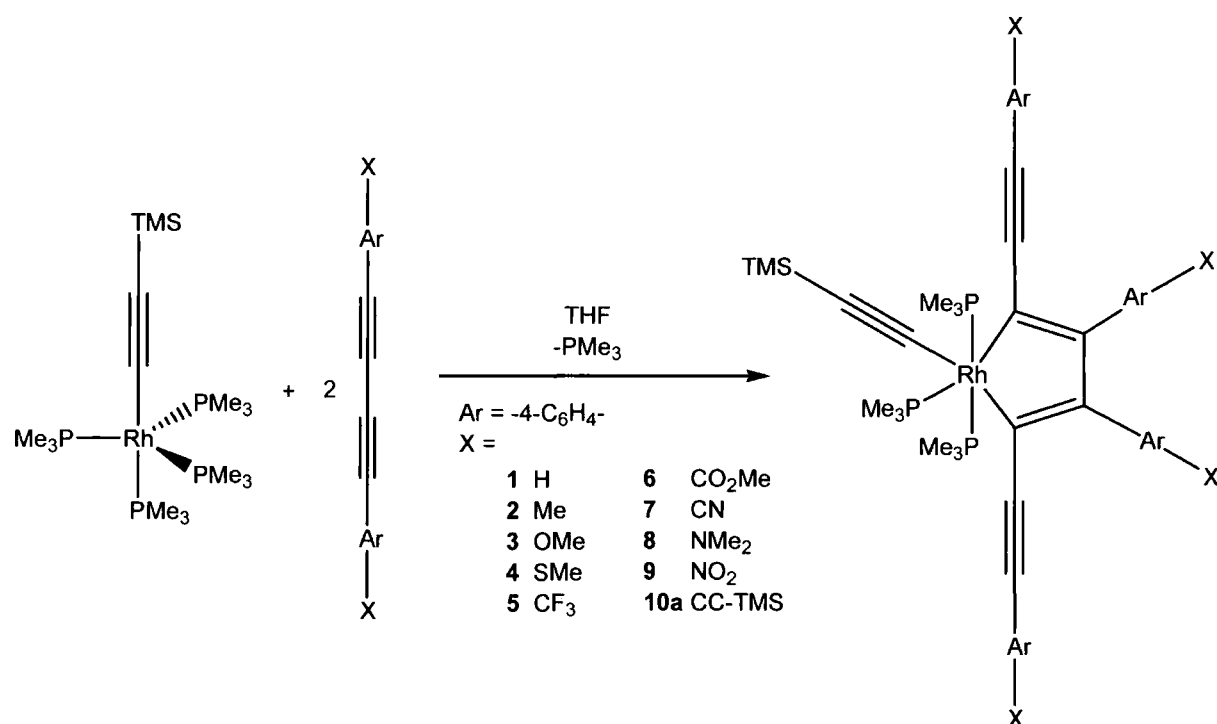


Figure 23. Regiospecific synthesis of rhodacyclopentadienes.

$\text{Rh}(\text{PMe}_3)_4\text{C}\equiv\text{C-TMS}$ was synthesised in quantitative yield by reaction of one equivalent of TMSA with $\text{Rh}(\text{PMe}_3)_4\text{Me}$ with elimination of CH_4 . Thus, dropwise addition of TMSA to a solution of $\text{Rh}(\text{PMe}_3)_4\text{Me}$ in THF gave the 1:1 product exclusively and no further purification was necessary.⁹⁸ $\text{Rh}(\text{PMe}_3)_4\text{Me}$ was synthesised by known methods from $\text{RhCl}_3 \cdot 3\text{H}_2\text{O}$ via $[\text{Rh}(\text{COE})_2\text{Cl}]_2$ and $[\text{Rh}(\text{PMe}_3)_4]\text{Cl}$ precursors (Figure 24).⁹⁹

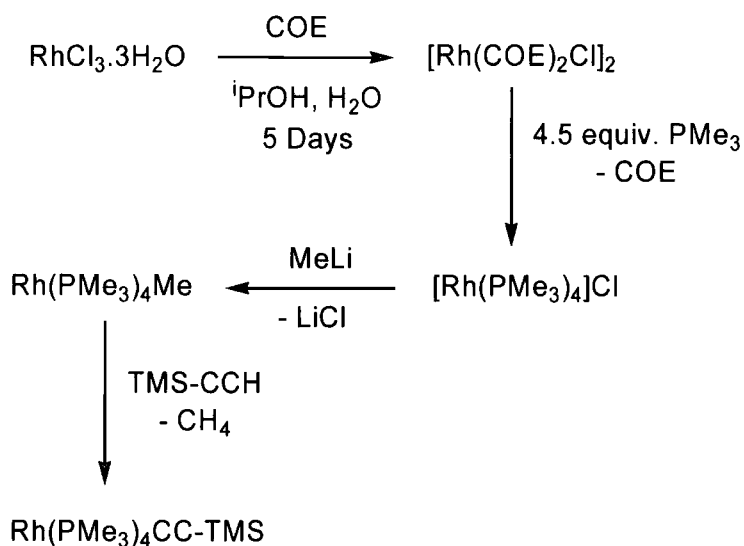


Figure 24. Synthesis of Rh starting materials.

A THF solution of two equivalents of diyne was added to a solution of $\text{Rh}(\text{PMe}_3)_4\text{C}\equiv\text{CTMS}$ and the mixture was stirred for 5 minutes. The solvent was removed *in vacuo* and the reaction mixture was taken to dryness to remove PMe_3 which was liberated during the reaction. The residue was then redissolved in a further portion of THF and the mixture was stirred for an additional 5 minutes and the solvent was again removed *in vacuo*. This cycle was repeated once more and the products were obtained in high yield as air-stable solids, after recrystallisation from THF/hexane or toluene/hexane. At room temperature, it was necessary for the solvent to be cycled a number of times for the reactions to reach completion. For compound **8**, it was necessary to heat the reaction mixture to 45 °C for 96 hours to give conversion to rhodacyclopentadiene; however, so far we have not managed to isolate analytically pure material. Heating the reaction mixture to 80 °C for 8 hours was not successful in forming metallacycle. Solutions of **1** to **10a** in d_6 -benzene or THF were found to emit light when exposed to UV irradiation or ordinary fluorescent room lighting.

In situ NMR spectroscopy was used to monitor the reactions and the results showed that three solvent cycles were sufficient to allow complete, regiospecific conversion to the rhodacyclopentadienes **1-7**, **9** and **10a**. Dienes with strong *para* electron-withdrawing phenyl substituents were found to react significantly faster than diynes with strong *para* electron-donating phenyl substituents, which were slow to react or required heating. Donating substituents increase the electron density at the conjugated alkynyl bonds and so inhibit the reductive coupling reaction on Rh. The reaction is regiospecific for all of the diynes used, with the 2,5-bis(4-R-phenylethynyl) isomer formed exclusively in all cases.

For each of the reactions, the *in situ* $^{31}\text{P}\{^1\text{H}\}$ NMR spectra showed the same pattern of a doublet of doublets with associated doublet of triplets in a 2:1 ratio, indicating two PMe_3 ligands in a mutually *trans* orientation with the third PMe_3 ligand being *trans* to a rhodacycle carbon (Figure 25). Rh-P coupling constants of ca. 98 Hz for the doublet of doublets and 82 Hz for the doublet of triplets, clearly indicate PMe_3 coupling to Rh(III) and that the rhodacycle α -carbon exerts a stronger *trans*-influence than a PMe_3 ligand (*vide infra*). For compounds **2-10a**, the ^1H NMR spectra show 8 sets of doublets corresponding to the phenyl *ortho* and *meta* protons and a doublet and a virtual triplet corresponding to the PMe_3 ligands. For compounds **2, 3, 4, 6** and **8**, peaks associated with the *para*-substituent methyl groups were also observed (Figure 26). The $^{19}\text{F}\{^1\text{H}\}$ NMR spectrum of compound **5** indicates 4 CF_3 environments.

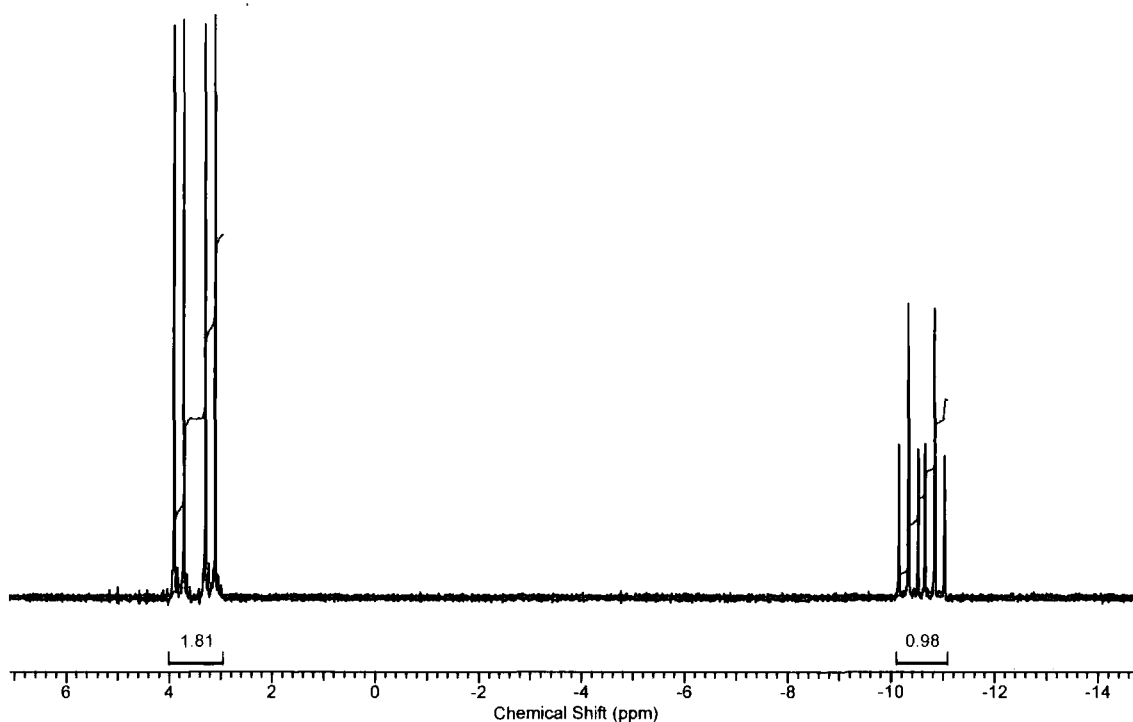


Figure 25. Typical *in situ* $^{31}\text{P}\{^1\text{H}\}$ NMR spectrum for the rhodacyclopentadienes (Compound **1**).

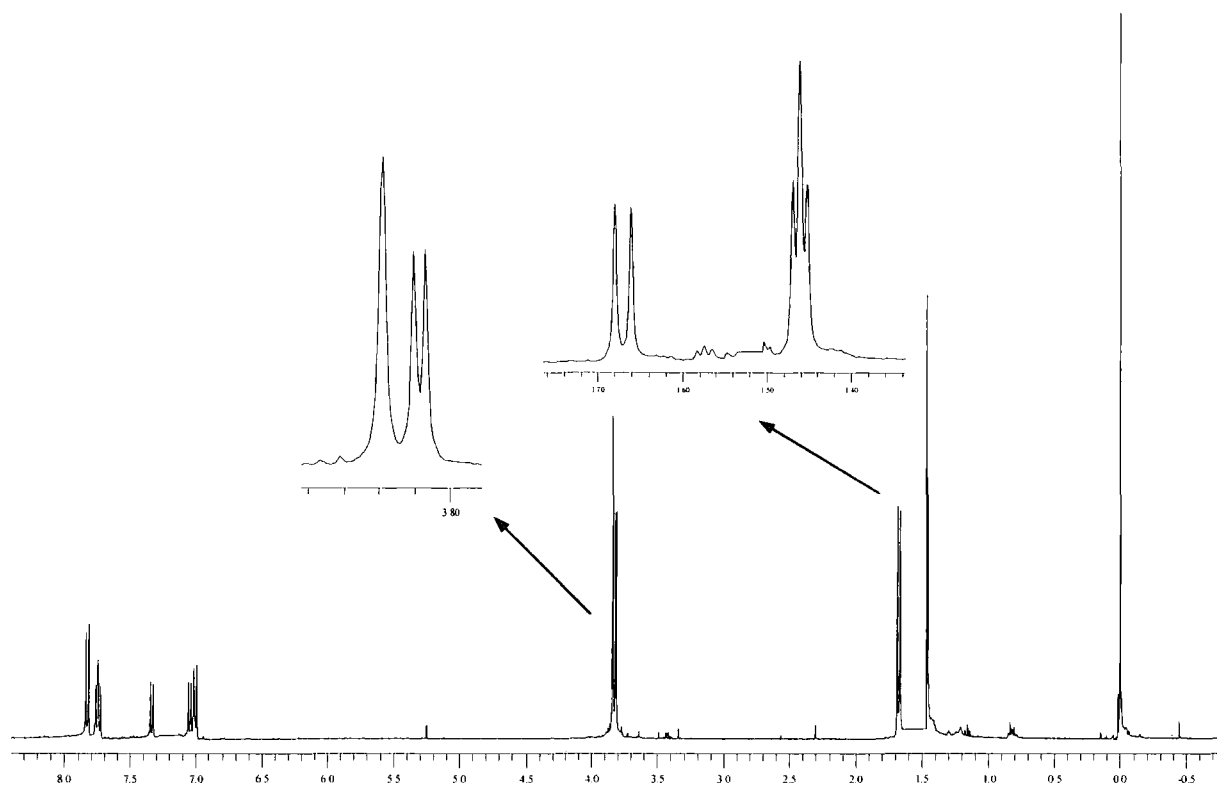


Figure 26. Example ^1H NMR spectrum for compound **6**.

The IR spectra of the compounds show 3 bands between 2000 and 2250 cm^{-1} corresponding to 3 $\text{C}\equiv\text{C}$ stretching modes. For compounds **6** and **10a**, fewer bands are seen due to overlapping peaks. Strong bands are also observed around 1600 cm^{-1} for the aromatic ring modes.

The yield of each reaction was shown to be quantitative by NMR spectroscopy and after recrystallisation, the products were obtained in good to excellent yields. Compounds **1-5** and **8** were isolated as yellow or orange solids, compounds **6**, **7** and **10a** as red solids and compound **9** as a deep purple solid.

From compound **10a**, it was possible to remove selectively the four TMS groups around the metallacycle, leaving the TMS group on the acetylide ligand in place, by treatment with four equivalents of $t\text{Bu}_4\text{NF}$ in THF to give compound **10b** (Figure 27). The product was extracted into CHCl_3 as it was considerably less soluble than the hexane soluble **10a**. Treating the rhodacycle with F^- and washing with water did not lead to any noticeable decomposition of the metallacycle, and compound **10b** was found to emit light under UV irradiation. ^1H NMR spectroscopy shows signals for four terminal alkyne protons and a single TMS group. Removal of the TMS groups may allow for the rhodacycle to undergo

Sonogashira cross-coupling reactions with 4 equivalents of aryl halide with the possibility of greatly increasing conjugation length in the system.

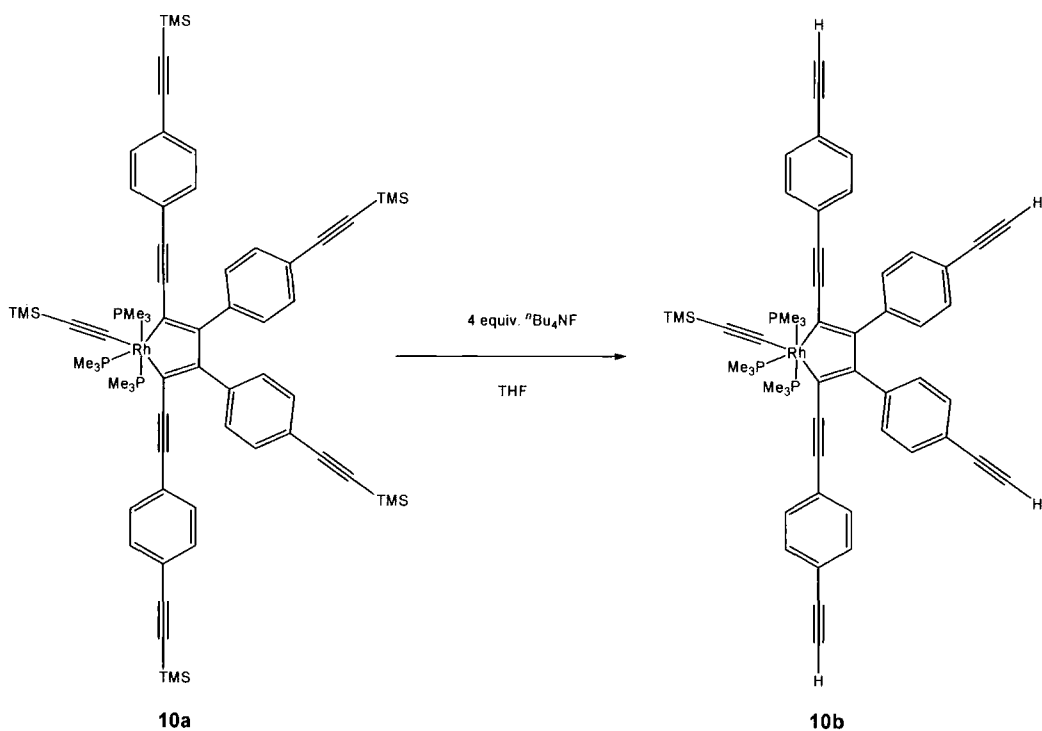


Figure 27. Removal of TMS groups from compound **10a** using F⁻.

2.9.2 Optical properties

The optical properties (absorption and fluorescence maxima, fluorescence quantum yields, Stokes shifts and fluorescence lifetimes) for compounds **1-10** are presented in Table 1.

All of the compounds show intense absorption bands in the UV-visible region (Figure 28). The rhodacycles are all fluorescent in solution at room temperature in the visible region (Figure 29), with modest quantum yields (3-18 %).

X Group	λ_{\max} Abs (nm)	ϵ ($\text{mol}^{-1} \text{cm}^{-1} \text{dm}^3$)	λ_{\max} Em (nm)	Φ (%)	Stokes Shift (cm^{-1})	λ_{\max} R Group Shift (cm^{-1})	Lifetime (ps)
NO₂ (9)	517 544	22000 19000	590 631	18	2390	2730	1210
CO₂Me (6)	485 516	21000 18000	536 576	16	1960	1460	980
CN (7)	482 512	30000 26000	533 572	8	1990	1330	540
CF₃ (5)	464 492	23000 19000	510 547	8	1940	520	560
H (1)	453 481	26000 22000	496 531	15	1910	0	870
Me (2)	454 482	25000 21000	496 532	12	1870	50	660
OMe (3)	454 483	23000 19000	497 531	9	1910	50	450
SMe (4)	468 499	35000 30000	515 553	10	1950	710	550
NMe₂ (8)	466 501	-	516 554	-	2080	620	-
C≡C-TMS (10a)	484 515	33000 29000	534 574	3	1930	1410	-
C≡C-H (10b)	478 507		526 564	-	1910	1160	-

Table 1. Summary of the optical properties of compounds **1-10** in toluene solvent.

It is apparent that the presence of both electron-donating and electron-withdrawing phenyl *para*-substituents shift the wavelength of both the absorption and the emission maxima bathochromically from 453 nm in **1** to 466 nm and 517 nm for compounds **8** and **9** respectively in absorption and from 496 nm in **1** to 516 nm and 590 nm for compounds **8** and **9** respectively in emission. This is the result of the fact that electron donors raise the HOMO more than the LUMO while electron acceptors lower the LUMO more than the HOMO. It is also evident that strong electron-withdrawing phenyl substituents have a greater effect on stabilising the LUMO than electron-donating phenyl substituents have on raising the HOMO energy.

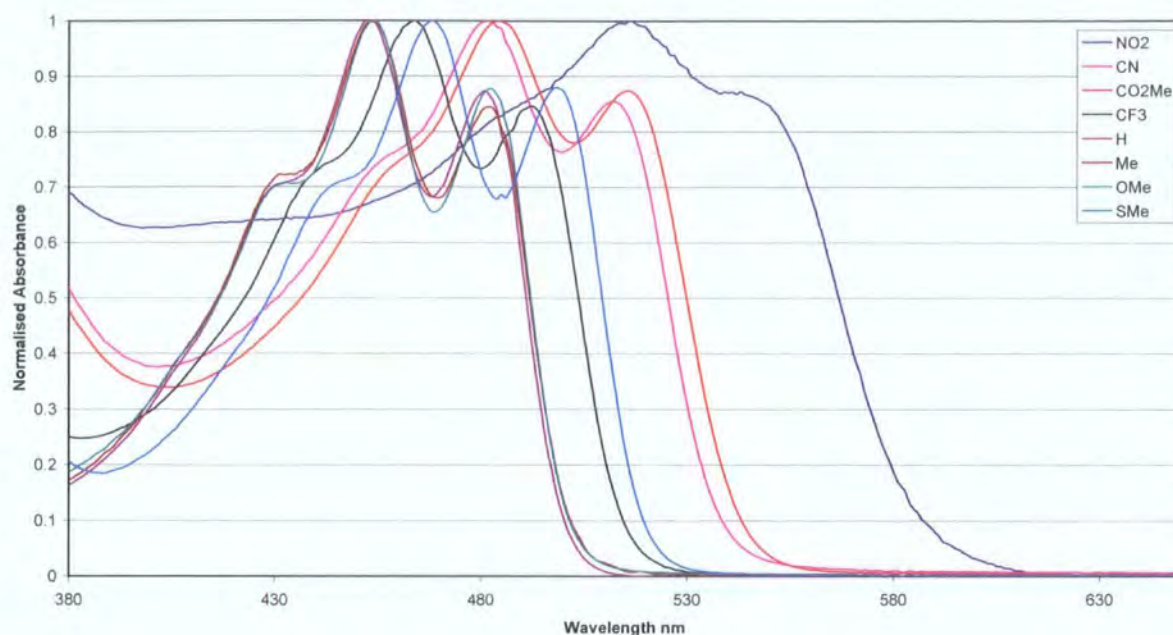


Figure 28. Absorption spectra of compounds 1-7 and 9.

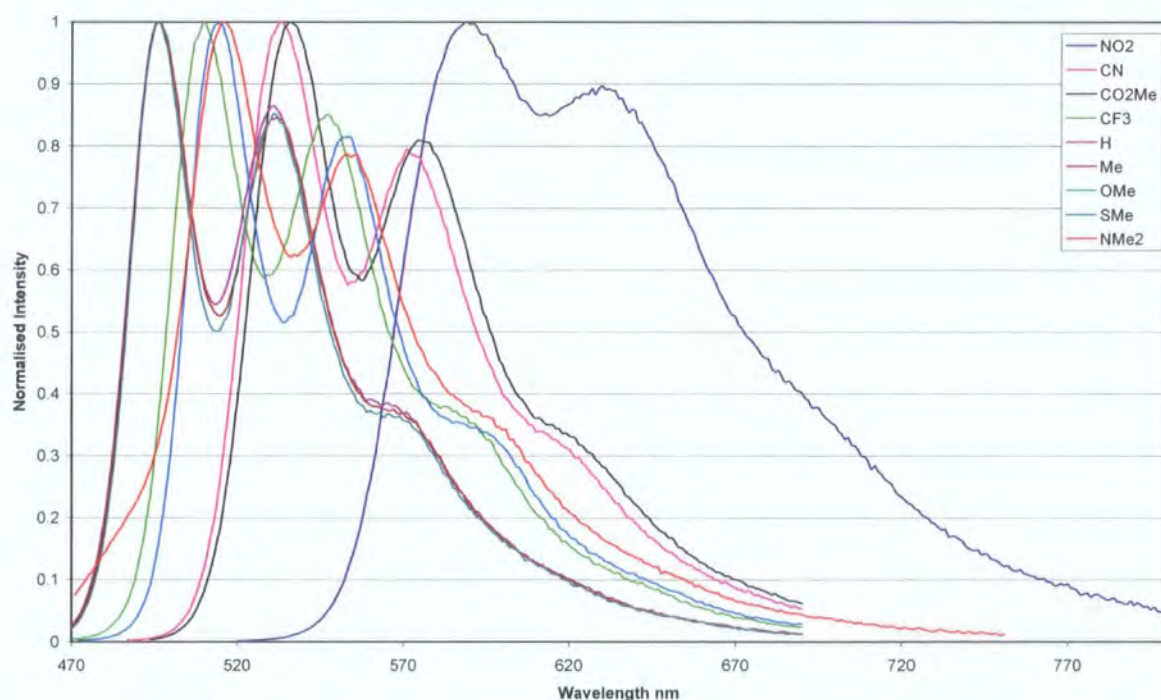


Figure 29. Emission spectra of compounds 1-9.

Compound **10a** demonstrates that the absorption and emission bands are also shifted to lower energy as the length of conjugation within the system is increased. Compound **10b** indicates that the TMS groups are involved in the conjugation within the system as removal of these groups with F^- results in 6-8 nm blue-shifts in the absorption maxima and 8-10 nm shifts in the emission maxima from compound **10a** (Figure 30). As electron-withdrawing

substituents have such a dramatic influence on the wavelength of absorption and emission, we attempted to synthesise a rhodacycle using the strongly electron-withdrawing 1,4-bis(4-dicyanovinylphenyl)buta-1,3-diyne. Acceptor diynes react much faster than donor diynes; however, even with heating of the reaction mixture, we have no observed clear evidence by NMR for rhodacycle formation. Further work is needed to establish the nature of the products of this reaction. We did, however, observe luminescence from the reaction mixture that corresponds to the diyne, and also from a second species which absorbs light at lower energy (500 nm) than that of the diyne (380 nm) (Figure 31).

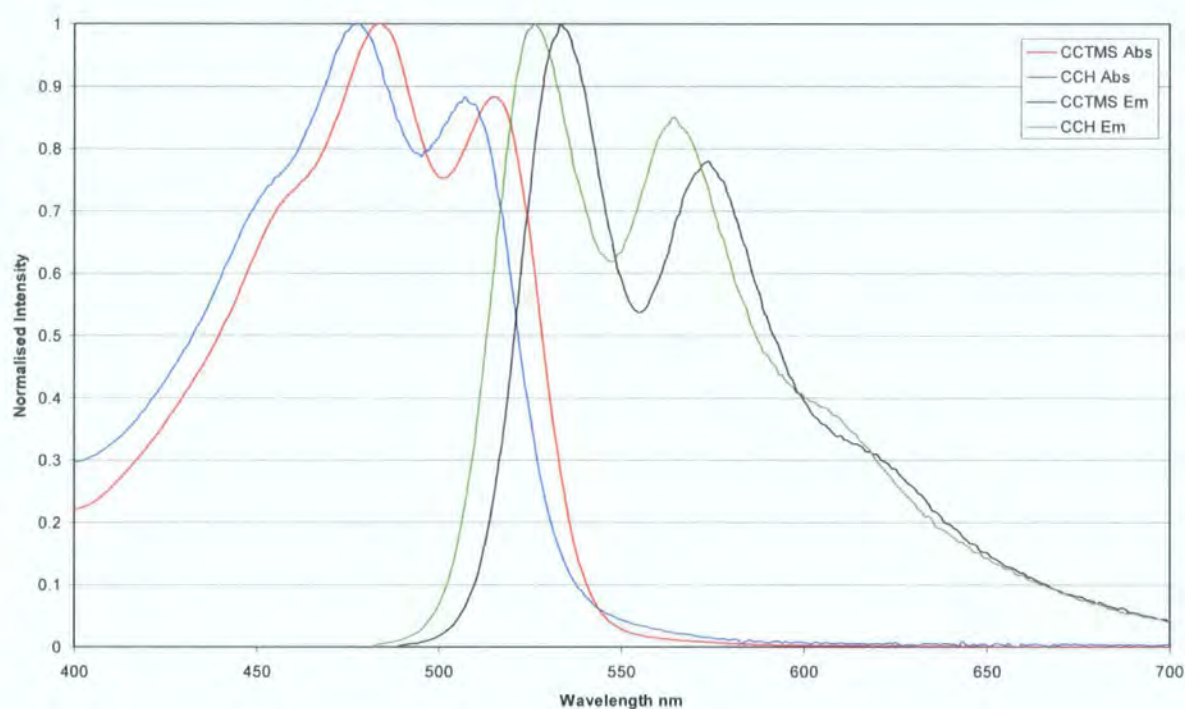


Figure 30. Absorption and emission spectra for compounds **10a** and **10b**.

Figure 31 shows that the absorption spectrum for the reaction mixture is made up of two components, the first being 1,4-bis(4-dicyanovinylphenyl)buta-1,3-diyne, as studied in Chapter 1, and a second broad band due to a new species formed by reaction of diyne with $\text{Rh}(\text{PMe}_3)_4\text{CCTMS}$, that is possibly the rhodacyclopentadiene. Excitation of the sample at 379 nm gave emission at 428 nm which is attributed to the butadiyne as observed previously (See Chapter 1). Excitation at 500 nm gave a broad band with an absorption maxima at 599 nm, which tails out to beyond 800 nm. The emission maximum is red-shifted to a greater extent than that for compound **9** (599 nm), supporting the fact that we do make some

rhodacycle, as $\text{CH}=\text{C}(\text{CN})_2$ is a stronger electron-acceptor than NO_2 and would be expected to further reduce the HOMO-LUMO gap.

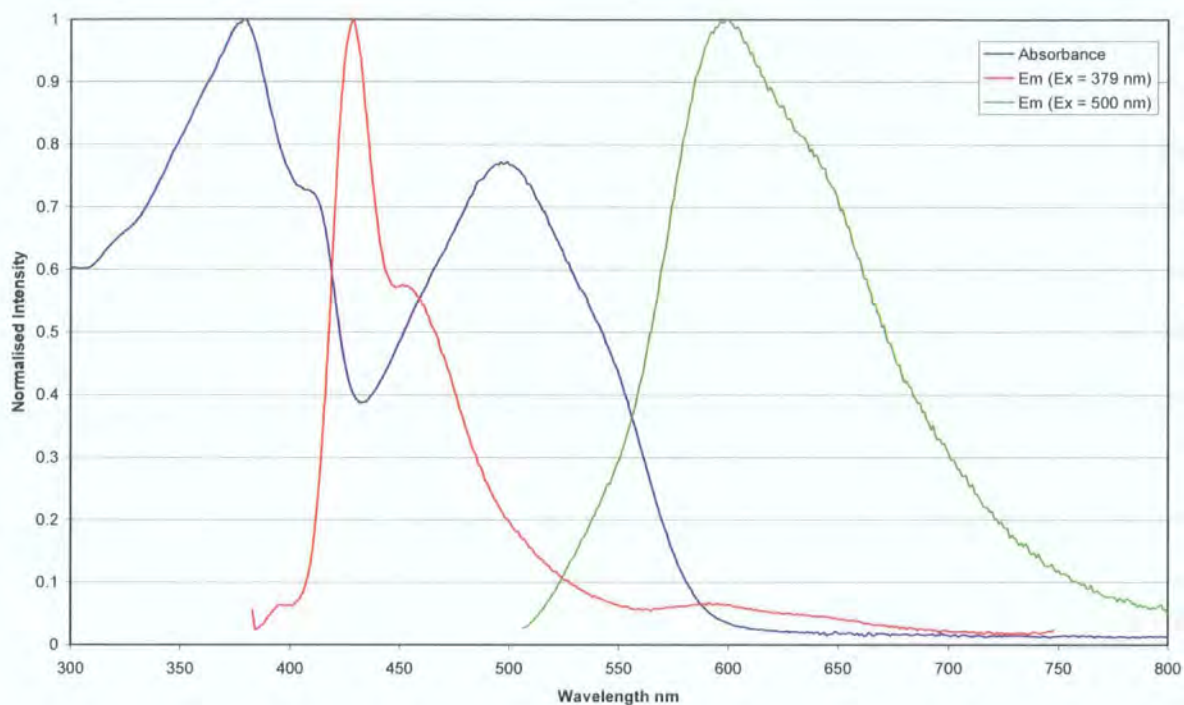


Figure 31. Absorption and emission spectra ($\lambda_{\text{ex}} = 379$ and 500 nm) of the reaction mixture from the attempted synthesis of a $\text{CH}=\text{C}(\text{CN})_2$ substituted rhodacycle.

The fluorescence lifetime measurements of compounds **1-9** indicate emission from a singlet state; however, the modest quantum yields suggest that a significant amount of energy is lost by other means, including the possibility of intersystem crossing to the triplet T_1 state from which we did not observe emission at room temperature in solution.

2.9.3 Synthesis of Rh- $\text{C}\equiv\text{C}-\text{C}_6\text{H}_4-4-\text{NMe}_2$ -based rhodacyclopentadienes

To investigate the role of the acetylide ligand in the optical properties of the rhodacyclopentadienes, it was necessary to prepare a different Rh-acetylide compound that was free of any $[\text{Rh}(\text{PMe}_3)_3(\text{CCR})_2\text{H}]$ impurity (*vide infra*). The compound 4-N,N-dimethylaminophenylacetylene was used for this purpose as the presence of an electron-donating NMe_2 substituent at the *para*-position strengthens the acetylenic CH bond, reducing the reactivity of the acetylene, such that the mono-acetylide is formed cleanly. Dropwise

addition of one equivalent of alkyne to a rapidly stirred solution of $\text{Rh}(\text{PMe}_3)_4\text{Me}$ in THF resulted in the 1:1 reaction only, in quantitative yield, which gave product that was used *in situ* for rhodacycle synthesis. Reaction of two equivalents of 4-N,N-dimethylaminophenylacetylene with $\text{Rh}(\text{PMe}_3)_4\text{Me}$ forms *mer,trans*- $[\text{RhH}(\text{PMe}_3)_3(\text{C}\equiv\text{C}-\text{C}_6\text{H}_4-4-\text{NMe}_2)_2]$ in quantitative yield, the structure of which has been reported.¹⁰⁰ Clearly, the second C-H oxidative addition step, giving the bis(acetylide) hydride complex, must be significantly slower than the initial reaction of $\text{R}-\text{C}\equiv\text{CH}$ with $\text{Rh}(\text{PMe}_3)_4\text{Me}$, when R is a donating group (Figure 32).

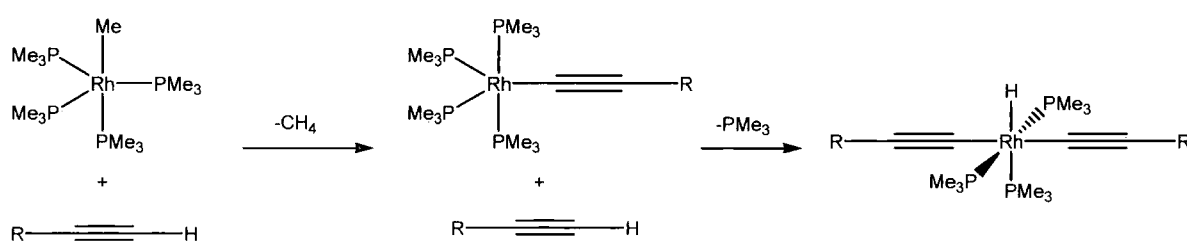


Figure 32. Two step mechanism for *mer,trans*- $[\text{RhH}(\text{PMe}_3)_3(\text{C}\equiv\text{C}-\text{C}_6\text{H}_4-4-\text{R})_2]$ formation.

A THF solution of two equivalents of diyne was added to a solution of $\text{Rh}(\text{PMe}_3)_4\text{C}\equiv\text{C}-\text{C}_6\text{H}_4-4-\text{NMe}_2$ in THF and the reaction was stirred for 5 minutes. The solvent was cycled as for the Rh-TMSA analogues and the reactions were monitored by *in situ* $^{31}\text{P}\{^1\text{H}\}$ NMR spectroscopy. Three cycles were sufficient to give complete regioselective formation of **11-15** (Figure 33). As for the $\text{RhC}\equiv\text{CTMS}$ analogues, diynes with electron-withdrawing *para*-substituents on the phenyl rings, reacted faster than diynes with electron-donating *para*-substituents. In all cases, the *in situ* $^{31}\text{P}\{^1\text{H}\}$ NMR spectra reveal a doublet of doublets ($^1J_{\text{Rh-P}}$ ca. 98 Hz) with associated doublet of triplets ($^1J_{\text{Rh-P}}$ ca. 82 Hz) for PMe_3 *trans* PMe_3 and PMe_3 *trans* rhodacycle respectively and peaks in the ^1H and $^{19}\text{F}\{^1\text{H}\}$ NMR spectra corresponding to the aromatic and substituent groups are observed. The IR spectra of compounds **11-14** show 3 bands between 2000 and 2250 cm^{-1} corresponding to the 3 $\text{C}\equiv\text{C}$ stretching modes.

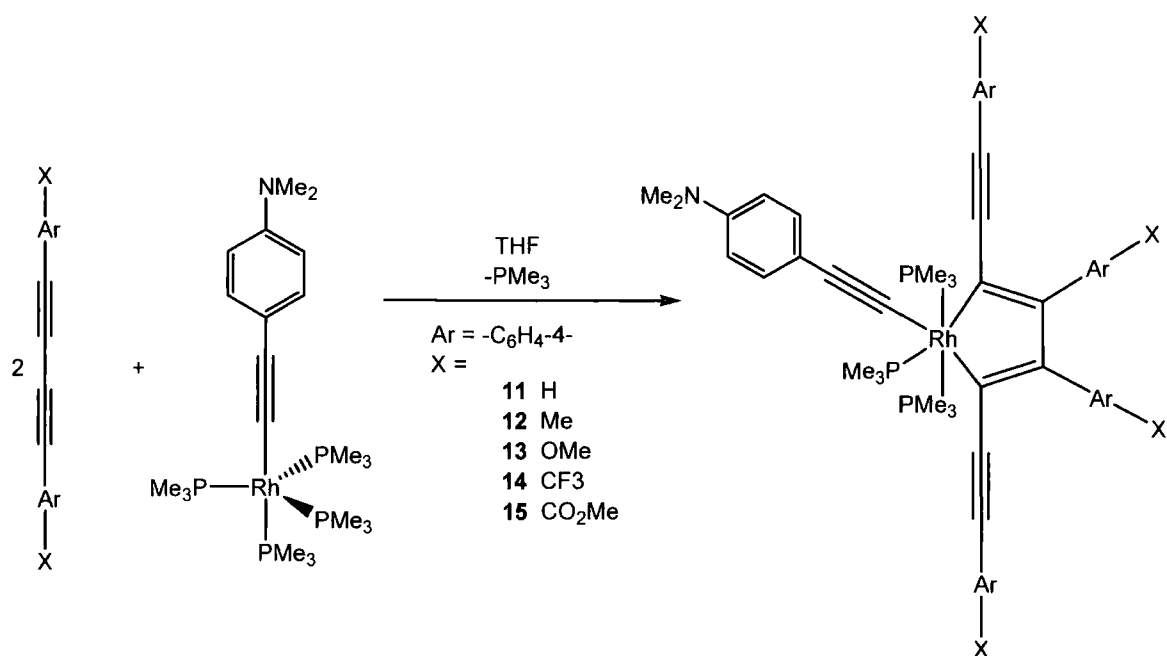


Figure 33. Formation of rhodacycles bearing a RhC≡C-C₆H₄-4-NMe₂ acetylide moiety.

The products were isolated as air-stable solids, in high yields, by recrystallisation from THF/hexane or toluene/hexane. Compounds **11-14** were isolated as yellow/orange solids, while the CO₂Me substituted compound **15** was isolated as a red solid. Compounds **11-15** were found to emit green or yellow light under UV irradiation.

2.9.4 Optical properties of Me₂N-4-C₆H₄-substituted rhodacyclopentadienes

The optical properties (absorption and fluorescence maxima, Stokes shift and fluorescence quantum yield) for compounds **11-15** are presented in Table 2. The compounds show intense absorption bands in the UV-Vis region and these chromophores are also fluorescent in the visible region with comparable Stokes shifts for each example.

Comparison of the data for **11-15** with that obtained for compounds **1-3**, **5** and **6** reveals that replacement of the TMS group with 4-Me₂NC₆H₄- on the acetylide ligand results in very little shift in either the absorption and emission maxima. The lack of effect may be attributed to unfavourable CH \cdots HC interactions between phenyl ring *ii* (see schematic for Table 5 for ring numbering) and acetylide phenyl ring *vi*, which prevent the phenylethynyl unit at the rhodacyclopentadiene 2 position and the phenyl acetylide from simultaneously lying in the metallacycle plane, as shown by X-ray diffraction analysis of single crystals of

11-15 (*vide infra*). The absorption and emission spectra for compounds **11-15** are shown in Figures 34 and 35 respectively.

R Group	λ_{\max} Abs (nm)	ϵ ($\text{mol}^{-1} \text{cm}^{-1} \text{dm}^3$)	λ_{\max} Em (nm)	Φ (%)	Stokes Shift (cm^{-1})	λ_{\max} R Group Shift (cm^{-1})
CO₂Me (15)	487	33000	542	4	2080	1440
	519	29000	579			
CF₃ (14)	466	24000	513	3	1970	620
	496	20000	546			
H (11)	455	27000	500	7	1980	0
	485	24000	535			
Me (12)	456	28000	500	10	1930	50
	485	25000	536			
OMe (13)	456	27000	499	8	1890	50
	485	24000	534			

Table 2. Summary of the optical properties of compounds **11-15**.

A series of related compounds in which the $-\text{C}\equiv\text{C}-\text{C}_6\text{H}_4-4-\text{NMe}_2$ ligand has been replaced by the longer acetylene $-\text{C}\equiv\text{C}-\text{C}_6\text{H}_4-\text{C}\equiv\text{C}-\text{C}_6\text{H}_4-4-\text{NHex}_2$ have also been prepared.¹⁰¹ The increased conjugation length within this ligand surprisingly had very little effect on the absorption and emission properties of the rhodacycles. As for the $-\text{C}_6\text{H}_4-4-\text{NMe}_2$ compounds, X-ray diffraction studies on the CF_3 substituted derivative showed there to be a significant rotation of the aryl ring attached to the Rh-acetylide moiety out of co-planarity with the metallacycle and thus conjugation is not increased, as most of the acetylide ligand π -system is decoupled from that of the rhodacycle.

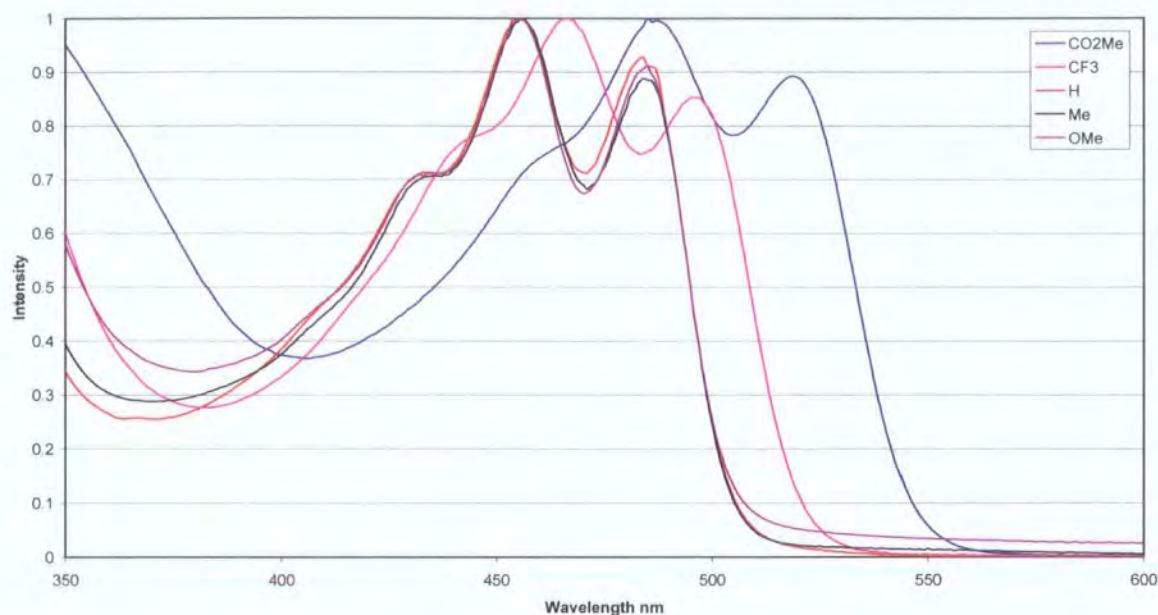


Figure 34. Absorption spectra of compounds 11-15.

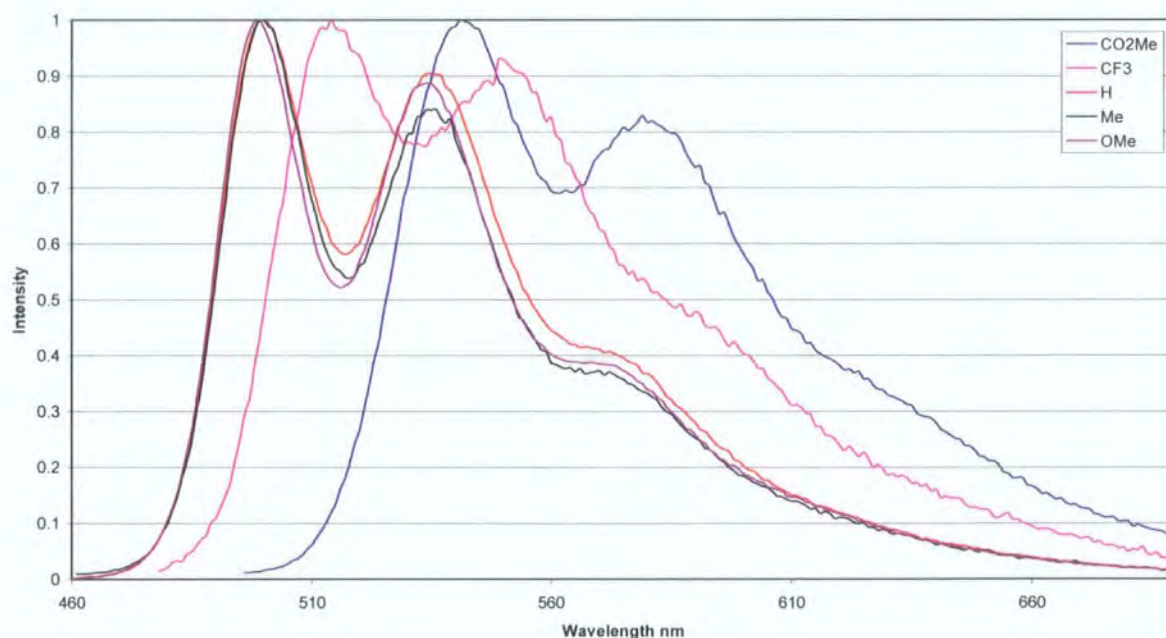


Figure 35. Emission spectra of compounds 11-15.

2.9.5 Crystal structures of acetylide substituted rhodacyclopentadienes

Compounds **1**¹⁰² and **2**²⁸ have previously been characterised by X-ray crystallography and the data is presented, along with data for compounds **4**, **5** and **7**, in Tables 3 and 4. Compounds **11-15** have also been crystallised and the data is presented in Tables 3 and 5.

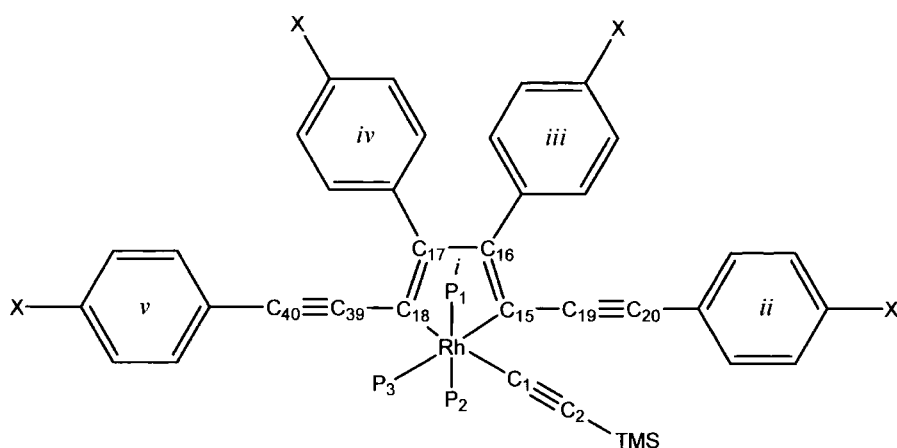
Molecule	4 - 05srv306	5 - 04srv236	7 - 05srv223	11 - 04srv251
Empirical formula	C ₅₀ H ₆₄ P ₃ RhS ₄ Si	C ₅₀ H ₅₂ F ₁₂ P ₃ RhSi	C ₅₂ H ₆₄ N ₄ P ₃ RhSi 2.75(C ₄ H ₈ O)	C ₅₁ H ₅₇ NP ₃ Rh
Formula Weight	1017.16	1104.83	1167.27	879.80
Temperature (K)	120(2) K	120(2) K	120(2) K	120(2)
Crystal system	Monoclinic	Monoclinic	Monoclinic	Monoclinic
Space Group	Cc	P2 ₁ /n	I2/a	P2 ₁ /n
a (Å)	50.938(5)	8.9710(6)	18.261(2)	12.8519(19)
b (Å)	42.820(4)	22.9570(19)	15.104(2)	21.653(3)
c (Å)	19.277(2)	25.0100(18)	43.802(5)	18.049(3)
α (°)	90.00	90.0	90.0	90.00
β (°)	90.01(1)	92.511(4)	93.23(1)	110.605(4)
γ (°)	90.00	90.0	90.0	90.00
Volume (Å ³)	42046(7)	5145.8(7)	12062(2)	4701.2(12)
Z	32	4	8	4
Density (calculated) (Mg/m ³)	1.285	1.426	1.286	1.243
Absorption Coefficient (mm ⁻¹)	0.630	0.525	0.430	0.499
Crystal size (mm ³)	0.44 x 0.20 x 0.08	0.47 x 0.30 x 0.16	0.35 x 0.11 x 0.11	0.22 x 0.22 x 0.10
Theta range for data collection (°)	2.49 to 29.89	2.38 to 30.03	1.43 to 27.50	1.53 to 30.54
Reflections collected	96229	15051	13848	14358
Independent reflections	81607	13038	10634	10412
Data / Restraints / Parameters	96229 / 17 / 4224	15051 / 12 / 637	13848 / 2 / 686	14358 / 0 / 464
Final R indices	R1 = 0.0376 wR2 = 0.0729	R1 = 0.0311 wR2 = 0.0798	R1 = 0.0398 wR2 = 0.1030	R1 = 0.0476 wR2 = 0.0729
R indices (all data)	R1 = 0.0526 wR2 = 0.0794	R1 = 0.0373 wR2 = 0.0824	R1 = 0.0585 wR2 = 0.1173	R1 = 0.0749 wR2 = 0.1096

Table 3. Crystal data for compounds **4**, **5**, **7**, and **11-15**.

Molecule	12 - 04srv338	13 - 04srv283	14 - 04srv297	15 - 04srv311
Empirical formula	C ₅₅ H ₆₅ NP ₃ Rh	C ₅₅ H ₆₅ NO ₄ P ₃ Rh	C ₅₅ H ₅₃ F ₁₂ NP ₃ Rh	C ₅₉ H ₆₅ NO ₈ P ₃ Rh
Formula Weight	935.90	999.90	1151.80	1111.94
Temperature (K)	120(2)	120(2) K	120(2) K	120(2) K
Crystal system	Orthorhombic	Triclinic	Monoclinic	Monoclinic
Space Group	<i>Pbca</i>	<i>P</i> -1	<i>P</i> ₂ ₁ / <i>c</i>	<i>P</i> ₂ ₁ / <i>c</i>
a (Å)	24.738(4)	9.116(4)	19.140(5)	10.5103(17)
b (Å)	8.689(2)	11.045(5)	19.297(5)	30.259(5)
c (Å)	47.068(9)	25.755(12)	18.396(5)	19.592(3)
α (°)	90.00	99.540(9)	90.0	90.0
β (°)	90.00	92.766(9)	116.743(5)	111.470(7)
γ (°)	90.00	98.889(9)	90.0	90.0
Volume (Å ³)	10117(3)	2519(2)	6068(3)	5798.5(16)
Z	8	2	4	4
Density (calculated)	1.229	1.318	1.261	1.274
Absorption Coefficient (mm ⁻¹)	0.468	0.480	0.430	0.429
Crystal size (mm)	0.24 x 0.20 x 0.02	0.22 x 0.20 x 0.08	0.40 x 0.34 x 0.24	0.40 x 0.14 x 0.02
Theta range for data collection (°)	1.65 to 25.00	0.80 to 30.35	1.19 to 30.60	1.75 to 30.50
Reflections collected	8918	25842	48994	41546
Independent reflections	5985	13415	18407	15917
Data / Restraints / Parameters	8918 / 0 / 567	13415 / 4 / 596	18407 / 34 / 578	15917 / 4 / 577
Final R indices	R1 = 0.0529 wR2 = 0.1224	R1 = 0.0946 wR2 = 0.1695	R1 = 0.0578 wR2 = 0.1685	R1 = 0.1345 wR2 = 0.2561
R indices (all data)	R1 = 0.0872 wR2 = 0.1371	R1 = 0.1603 wR2 = 0.1918	R1 = 0.0806 wR2 = 0.1820	R1 = 0.3063 wR2 = 0.3244

Table 3 (continued). Crystal data for compounds 4, 5, 7, and 11-15.

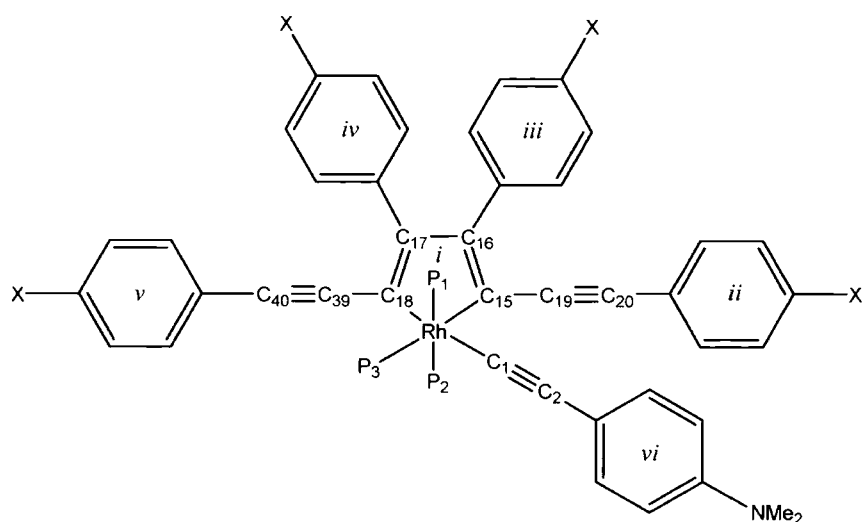
For both Tables 4 and 5, there are schematic diagrams indicating the atom and ring plane numbering system used.



<i>p</i> -X Group	H	Me	SMe	CF ₃	CN
	1	2	4	5	7
Rh-P ₁	2.3180(5)	2.3215(15)	2.3137(18)	2.3223(4)	2.3249(8)
Rh-P ₂	2.3230(5)	2.3248(14)	2.331(2)	2.3248(4)	2.3199(7)
Rh-P ₃	2.3763(6)	2.3721(14)	2.3668(19)	2.3729(4)	2.3660(7)
Rh-C ₁	2.0411(17)	2.068(6)	2.051(4)	2.0372(16)	2.036(2)
Rh-C ₁₅	2.1003(16)	2.087(5)	2.084(4)	2.0828(15)	2.098(2)
Rh-C ₁₈	2.0950(16)	2.110(5)	2.095(4)	2.0933(15)	2.072(3)
C ₁ ≡C ₂	1.221(2)	1.167(7)	1.201(6)	1.216(2)	1.224(3)
C ₁₉ ≡C ₂₀	1.210(2)	1.211(7)	1.206(6)	1.208(2)	1.201(4)
C ₃₉ ≡C ₄₀	1.209(2)	1.217(7)	1.218(5)	1.209(2)	1.204(3)
C ₁₅ =C ₁₆	1.374(2)	1.389(6)	1.394(6)	1.372(2)	1.371(3)
C ₁₇ =C ₁₈	1.377(2)	1.382(6)	1.350(6)	1.380(2)	1.380(3)
C ₁₆ -C ₁₇	1.463(2)	1.465(8)	1.462(6)	1.462(2)	1.455(3)
P ₁ -Rh-P ₂	169.269(17)	168.39(5)	169.50(7)	169.638(15)	167.47(3)
C ₁ -Rh-C ₁₈	173.76(6)	173.51(18)	174.64(16)	173.27(6)	173.95(10)
C ₁₅ -Rh-P ₃	172.25(4)	173.91(14)	174.14(13)	174.08(4)	172.60(7)
Rh-C ₁ -C ₂	177.61(16)	175.1(5)	173.9(4)	175.00(14)	176.6(2)
<i>ii</i> - <i>i</i> *	58.3	19.4	7.63	58.97	1.49
<i>iii</i> - <i>i</i> *	58.6	64.9	45.97	45.05	54.54
<i>iv</i> - <i>i</i> *	64.0	51.2	60.40	47.80	48.91
<i>v</i> - <i>i</i> *	11.0	8.1	8.33	19.25	4.70

* Interplanar angles vs. plane *i* (rhodacycle)

Table 4. Selected bond lengths (Å) and bond angles (°) for compounds 1, 2, 4, 5 and 7.



<i>p</i> -X Group	H	Me	OMe	CF ₃	CO ₂ Me
	11	12	13	14	15
Rh-P ₁	2.3043(7)	2.3113(12)	2.3146(17)	2.3173(9)	2.304(3)
Rh-P ₂	2.3150(8)	2.3136(13)	2.3352(17)	2.3175(9)	2.331(2)
Rh-P ₃	2.3632(7)	2.3490(12)	2.3758(19)	2.3706(10)	2.378(3)
Rh-C ₁	2.042(3)	2.042(4)	2.086(6)	2.042(3)	2.057(9)
Rh-C ₁₅	2.090(2)	2.072(4)	2.081(6)	2.068(3)	2.087(10)
Rh-C ₁₈	2.085(3)	2.091(4)	2.076(5)	2.083(3)	2.114(11)
C ₁ ≡C ₂	1.201(4)	1.213(6)	1.184(8)	1.209(4)	1.072(10)
C ₁₉ ≡C ₂₀	1.205(3)	1.202(6)	1.217(7)	1.199(4)	1.207(14)
C ₃₉ ≡C ₄₀	1.211(4)	1.204(5)	1.207(8)	1.205(4)	1.189(13)
C ₁₅ =C ₁₆	1.369(4)	1.363(6)	1.376(7)	1.375(4)	1.356(14)
C ₁₇ =C ₁₈	1.381(3)	1.373(5)	1.363(8)	1.362(4)	1.398(13)
C ₁₆ -C ₁₇	1.461(4)	1.462(6)	1.468(7)	1.461(4)	1.437(13)
P ₁ -Rh-P ₂	168.73(3)	169.61(5)	171.09(6)	170.02(3)	170.68(10)
C ₁ -Rh-C ₁₈	173.49(10)	175.06(16)	172.9(2)	172.17(11)	173.7(4)
C ₁₅ -Rh-P ₃	173.27(7)	173.40(11)	175.02(15)	174.56(8)	172.6(3)
Rh-C ₁ -C ₂	177.3(2)	174.9(4)	172.2(5)	177.0(3)	170.9(10)
<i>ii</i> - <i>i</i> [*]	Disorder	69.0	48.16	8.47	4.11
<i>iii</i> - <i>i</i> [*]	53.3	59.80	51.49	45.22	52.83
<i>iv</i> - <i>i</i> [*]	50.5	67.2	55.57	51.62	49.19
<i>v</i> - <i>i</i> [*]	12.1	58.0	7.89	Disorder	6.68
<i>vi</i> - <i>i</i> [*]	96.3	49.3	44.6	96.9	73.5

* Interplanar angles vs. plane *i* (rhodacycle)

Table 5. Selected bond lengths (Å) and angles (°) for compounds 11-15.

There are a number of similarities in each of the structures that have been analysed. The structural studies confirm the formation of the 2,5-bis(arylethynyl) isomer in all cases,

with the Rh in a distorted octahedral environment having a meridonal disposition of the three PMe_3 ligands.

The Rh-P(1) and Rh-P(2) bond lengths are all similar [2.304(3) Å to 2.3352(17) Å] and the Rh-P(3) bond length is slightly longer [2.3490(12) Å to 2.378(3) Å]. This confirms the stronger *trans*-influence of C_α of the rhodacycle compared with that of PMe_3 , in agreement with the $^{31}\text{P}\{^1\text{H}\}$ NMR coupling constants (*vide supra*). The Rh-C(15) and Rh-C(18) bond lengths are all similar, indicating that the PMe_3 ligand and the acetylide ligand have a similar *trans*-influence. The Rh-C(1) bond lengths are generally slightly shorter than those of C(15) and C(18), consistent with the sp vs. sp^2 hybridisation at carbon. All of the $\text{C}\equiv\text{C}$ bond lengths are similar in length being ca. 1.20 Å, indicating that the *para*-substituent does not have a significant effect on the geometry. The C(15)-C(16) and C(17)-C(18) bonds are all longer than in cyclopentadiene, and the C(16)-C(17) bond length is shorter, indicating that there is delocalisation within the RhC_4 metallacycle.¹⁰³ The C(1)-Rh-C(18) and C(15)-Rh-P(3) bond angles are all similar [172.17(11)° to 175.06(16)° and 172.25(4)° to 175.02(15)° respectively] and the *trans* P(1)-Rh-P(2) bond angle is smaller than 180° [167.47(3)° to 171.09(6)°] resulting from steric repulsions with Me substituents on P(3). Due to steric crowding around the C(16)-C(17) bond, phenyl rings *iii* and *iv* are inclined from planarity by up to 67.20°. It is worth noting that in each of the molecular structures, the three PMe_3 ligands are oriented in a similar fashion. P(1) Me_3 is oriented with one Me group directed away from the metallacycle and the other two Me groups directed along the two Rh-C metallacycle bonds. P(2) Me_3 is inclined such that one Me group points along the Rh-C(18) metallacycle bond with the other two directed to each side of the acetylide ligand. Two Me groups in P(3) Me_3 point either side of the alkyne directly bonded to phenyl ring *v*. In all of the examples, the solid state structure is entirely consistent with the solution state data.

It is interesting to note that for compounds **11**, **14** and **15**, aryl ring *ii* is almost planar with the metallacycle while aryl ring *vi* is nearly orthogonal to the metallacycle [96.3°, 96.9° and 73.5° respectively]. In compounds **12** and **13**, however, aryl ring *ii* is considerably inclined [69.0° and 48.16° respectively] whereas aryl ring *vi* is now less rotated with respect to the metallacycle [49.3° and 44.6° respectively], suggesting that unfavourable arene-arene steric interactions in compounds **11-15** prevent a co-planar arrangement of aryl rings *ii* and *vi*. Indeed, these two rings are approximately orthogonal in most cases, effectively decoupling the two π -systems. As a result, extending the

acetylide π -system using $-\text{C}\equiv\text{C}-\text{C}_6\text{H}_4-\text{C}\equiv\text{C}-\text{C}_6\text{H}_4-4-\text{NHex}_2$ has little effect on the optical properties of the compounds (*vide supra*).

Compound **4** was crystallised in a 5 mm diameter glass tube by slow diffusion of a layer of hexane into a THF solution (Figure 36). Monoclinic crystals (space group = Cc) were found to have eight independent molecules in the asymmetric unit. Chemically related thiomethoxy groups, $\text{S}(14)\text{C}(50)\text{H}_3$, $\text{S}(64)\text{C}(300)\text{H}_3$ and $\text{S}(74)\text{C}(350)\text{H}_3$ in separate independent molecules, are disordered between two positions each, in the ratios 55:45, 67:33 and 80:20, respectively.

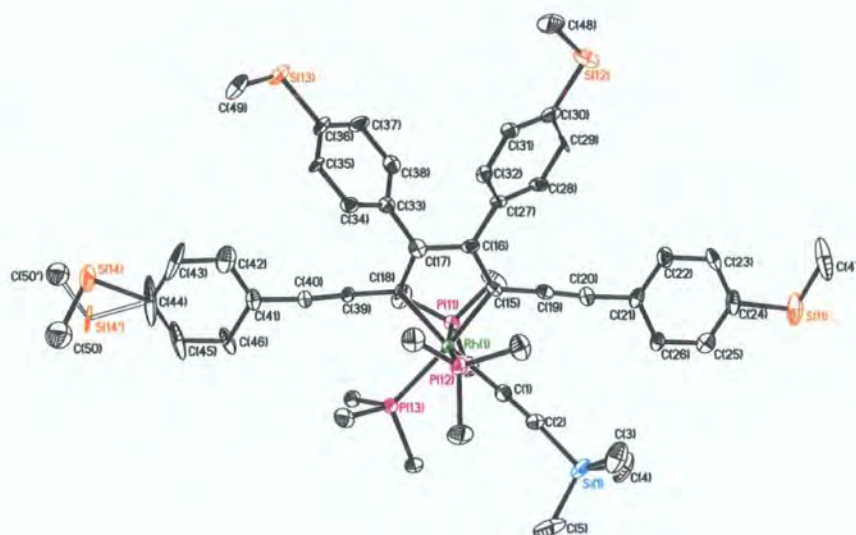


Figure 36. One molecule in the asymmetric unit of **4**. Hydrogen atoms are omitted for clarity and thermal ellipsoids are shown at 50 % probability.

Compound **5** was crystallised as yellow, monoclinic crystals (space group = $P2_1/n$) which were grown in a 5 mm diameter glass tube by slow diffusion of a layer of hexane into a THF/toluene solution. The metallacycle is almost planar; however, there is considerable twist from planarity of phenyl rings *ii* and *v* with an angle of 47.59° between the two rings and angles of 58.97° and 19.25° between *ii* and *v* and the metallacycle respectively (Figure 37). The $\text{C}(50)\text{F}_3$ group is rotationally disordered and the F(10), F(11) and F(12) atoms are distributed between positions A (70%) and B (30%), which were refined with anisotropic ADP, equal for each pair (i.e. F(10A) and F(10B), etc.), and constrained threefold symmetry for each orientation.

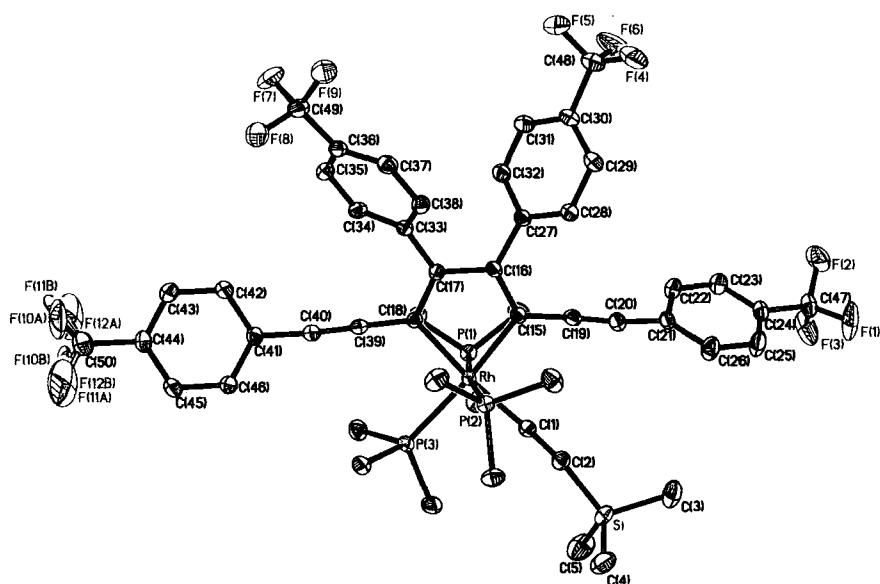


Figure 37. Molecular structure of **5**. Hydrogen atoms are omitted for clarity and thermal ellipsoids are shown at 50 % probability.

Compound **7** was crystallised in a 5 mm diameter glass tube as a THF solvate by slow diffusion of a layer of hexane into a THF solution. Phenyl rings *ii* and *v* are both close to planarity with respect to the metallacycle, each with only slight inclination [1.49° and 4.70° respectively] (Figure 38). The C(21), C(22), C(23) and C(24) atoms with attached hydrogens are disordered between positions A (40%), B (40%) and C (20%). The structure contains four non-equivalent THF molecules of crystallisation, all of which are disordered. In molecule O(1)C(51)C(52)C(53)C(54), atoms O(1), C(52) and C(53) are disordered between positions A (70%) and B (30%). In molecule O(2)C(55)C(56)C(57)C(58), atom O(2) is disordered between positions A (85%) and C (15%), atoms C(55) and C(56) between positions A (47%), B (33%) and C (20%), and atoms C(57) and C(58) between positions A (67%) and B (33%). The molecule O(3)C(59)C(60)C(61)C(62) is disordered between two positions with 50% occupancies, related *via* a twofold axis (transformation $3/2-x, y, 1-z$). The molecule O(4)C(63)C(64)C(65)C(66) is disordered between two overlapping positions of 25% occupancy each, related *via* an inversion centre (transformation $2-x, -y, 1-z$). Both positions are compatible with only one position of the preceding molecule, hence the non-stoichiometric occupancy.

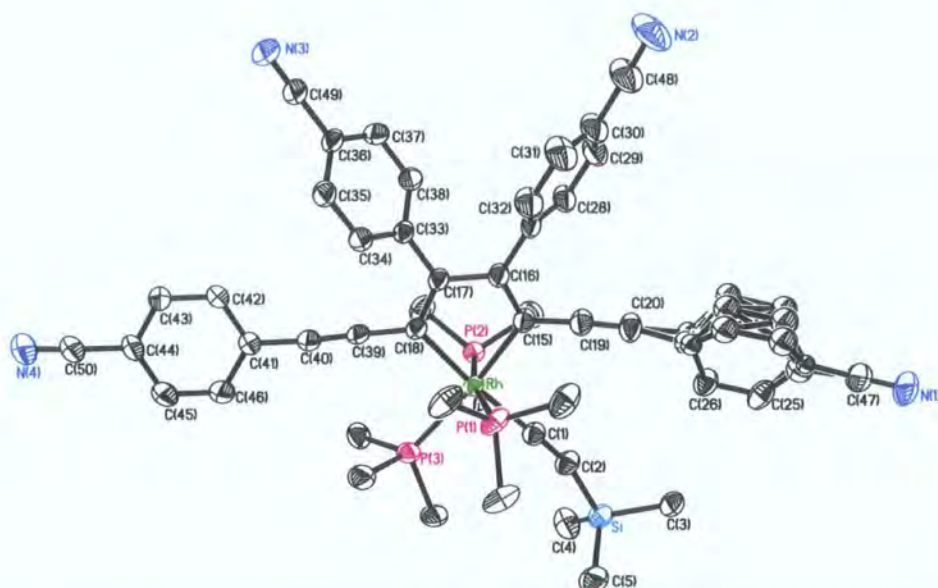


Figure 38. Molecular structure of **7**. Hydrogen atoms and solvent molecules are omitted for clarity and thermal ellipsoids are shown at 50 % probability.

Monoclinic crystals (space group = $P2_1/n$) of **11** were grown in a 5 mm diameter glass tube by slow diffusion of a layer of hexane into a THF solution. Phenyl ring *v* is almost planar with the rhodacycle [12.1°] and there is disorder in phenyl ring *ii* between two orientations [16.6° and 14.7° for *ii_a* and *ii_b* respectively] (Figure 39). Ring *vi* is nearly orthogonal to the metallacycle plane [96.3°].

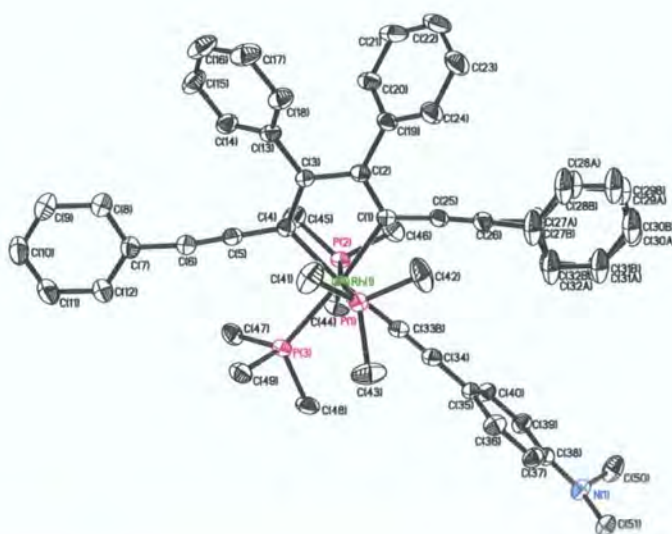


Figure 39. Molecular structure of **11**. Hydrogen atoms are omitted for clarity and thermal ellipsoids are shown at 50 % probability.

Single crystals of **12** were grown in a 5 mm diameter glass tube by slow diffusion of a layer of hexane into a toluene solution. Phenyl ring *vi* is rotated out of the metallacycle plane by 49.3° causing the inclination of phenyl ring *ii* from planarity with respect to the metallacycle by 69.0° (Figure 40). Phenyl ring *v* is also inclined by 58.0° , reducing conjugation along the ‘rod’.

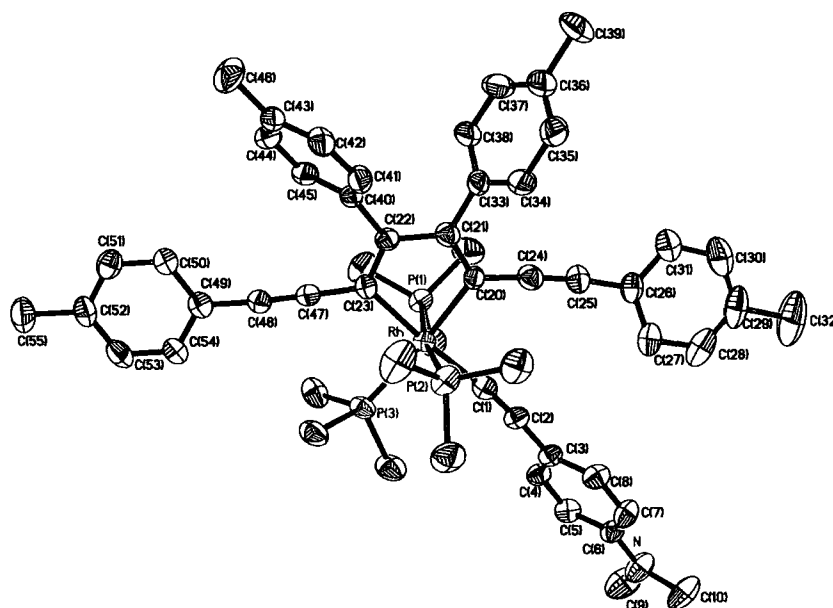


Figure 40. Molecular structure of **12**. Hydrogen atoms are omitted for clarity and thermal ellipsoids are shown at 50 % probability.

Single crystals of **13** were grown in a 5 mm diameter glass tube by slow diffusion of a layer of hexane into a THF solution. Phenyl ring *ii* is considerably rotated [45.16°] with respect to the metallacycle, reducing steric interactions resulting from the inclination of phenyl ring *vi* [44.6°] (Figure 41). Phenyl ring *v*, however, has only a slight inclination [7.89°] from co-planarity with the metallacycle. There is disorder about the O(4)-C(53) bond and also in the NMe₂ fragment of the acetylide ligand.

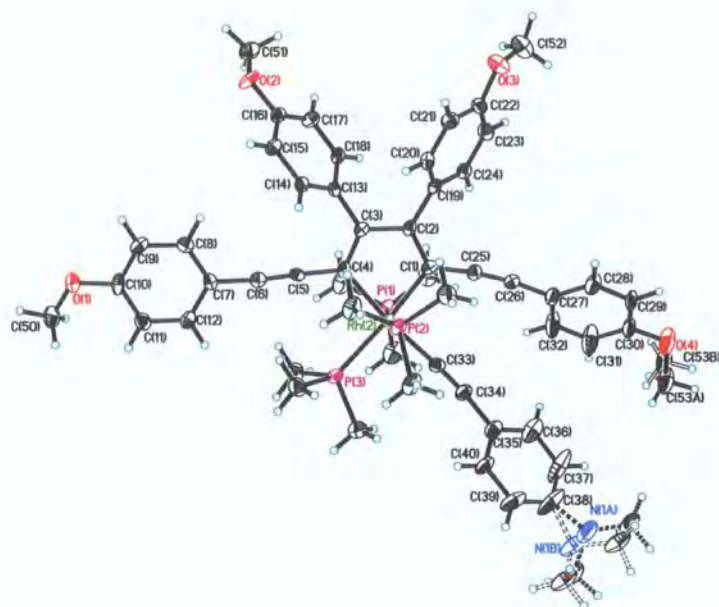


Figure 41. Molecular structure of **13**. Thermal ellipsoids are shown at 50 % probability.

Single crystals of **14** were grown in a 5 mm diameter glass tube by slow diffusion of a layer of hexane into a THF solution. Phenyl ring *ii* is almost planar with the metallacycle [8.47°]; however, there is a significant degree of disorder between two positions for phenyl ring *v*, with inclinations of 74.1° and 13.8° for *v* and *v_a* respectively (Figure 42). There is disorder in the CF_3 groups and also in the NMe_2 group of the acetylide ligand.

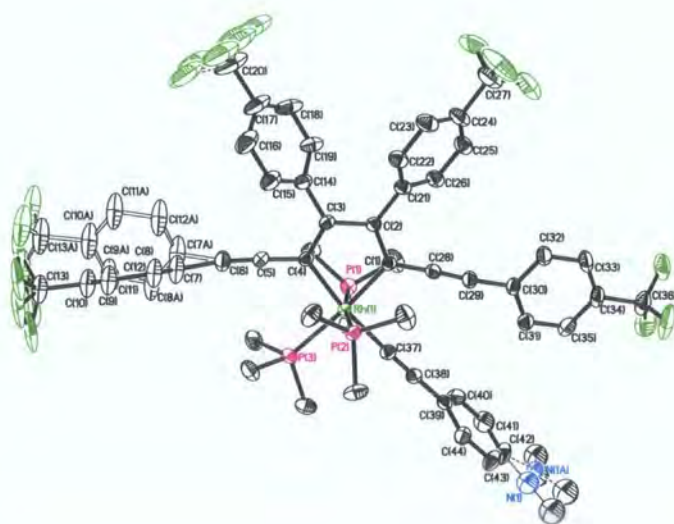


Figure 42. Molecular structure of **14**. Hydrogen atoms are omitted for clarity and thermal ellipsoids are shown at 50 % probability.

Monoclinic (space group = $P2_1/c$) single crystals of **15** were grown in a 5 mm diameter glass tube by slow diffusion of a layer of hexane into a THF solution. Both phenyl rings *ii* and *v* are close to linearity with respect to the metallacycle [4.11° and 6.68° respectively] (Figure 43). There is disorder about the O(7)-C(40) bond and the Ph-NMe₂ fragment of the acetylide ligand is also disordered.

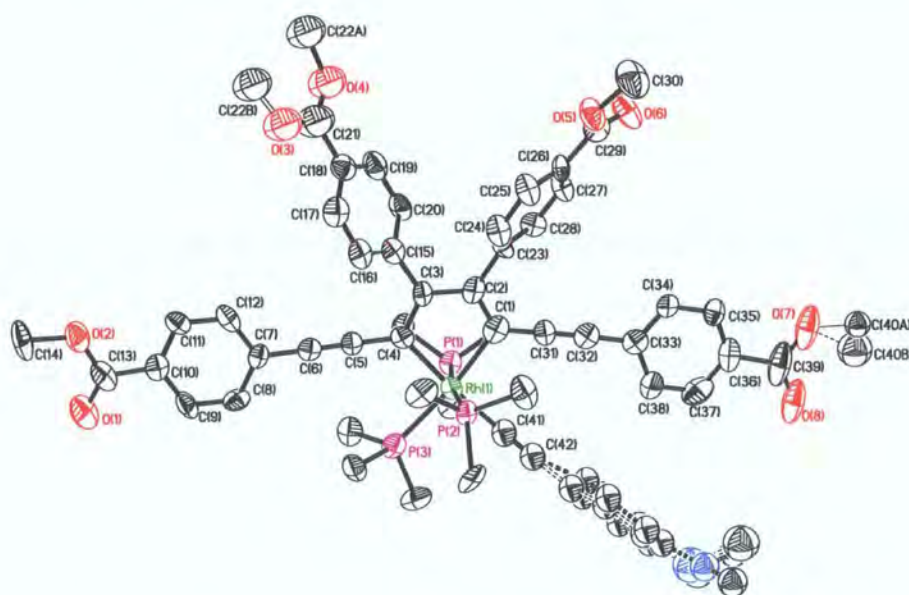


Figure 43. Molecular structure of **15**. Hydrogen atoms are omitted for clarity and thermal ellipsoids are shown at 50 % probability.

2.9.6 Synthesis of a Rh-C≡C-C≡C-NPh₂-based rhodacyclopentadiene

In an attempt to synthesise an acetylide-substituted rhodacyclopentadiene in which both phenyl rings *ii* and *vi* might lie in the metallacycle plane, and to study the influence of this on the absorption and emission spectra (and hence study any increased level of delocalisation through the molecule), Rh(PMe₃)₄Me was reacted with one equivalent of the terminal butadiyne 4-Ph₂N-C₆H₄-C≡C-C≡C-H to give [Rh(PMe₃)₄C≡C-C≡C-C₆H₄-4-NPh₂]. The mono-diyne compound [Rh(PMe₃)₄C≡C-C≡C-C₆H₄-4-NPh₂] was formed cleanly, as shown by ³¹P{¹H} NMR spectroscopy, and was used without further purification. A solution of the Rh-acetylide was then treated with 2 equivalents of 1,4-bis(4-tolyl)buta-1,3-diyne to give **16** (Figure 44). Complete conversion to rhodacycle was achieved at room temperature after allowing the sample to stand for 48 hours. The

$^{31}\text{P}\{^1\text{H}\}$ NMR spectra showed a doublet of doublets with associated doublet of triplets as observed for the $\text{Rh-C}\equiv\text{CTMS}$ and $\text{Rh-C}\equiv\text{C-C}_6\text{H}_4\text{-4-NMe}_2$ analogues. Compound **16** was found to emit green light under UV irradiation.

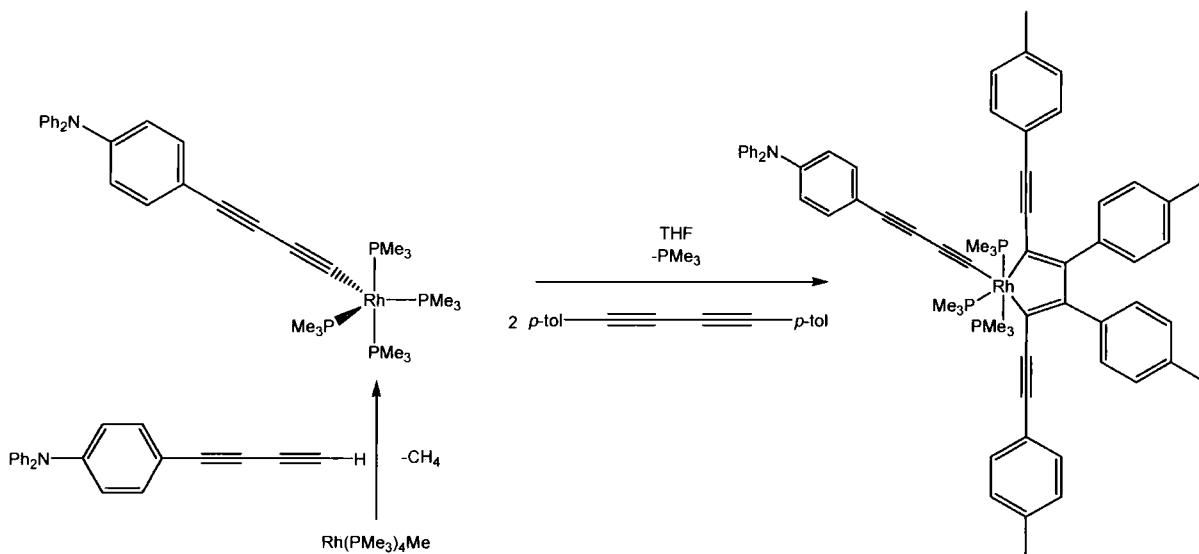


Figure 44. Synthetic route to compound **16**.

Treating $\text{Rh}(\text{PMe}_3)_4\text{Me}$ with two equivalents of the terminal butadiyne gave *mer,trans*- $[\text{RhH}(\text{PMe}_3)_3(\text{C}\equiv\text{C-C}\equiv\text{C-C}_6\text{H}_4\text{-4-NPh}_2)_2]$, **17**, cleanly and in quantitative yield (Figure 45).

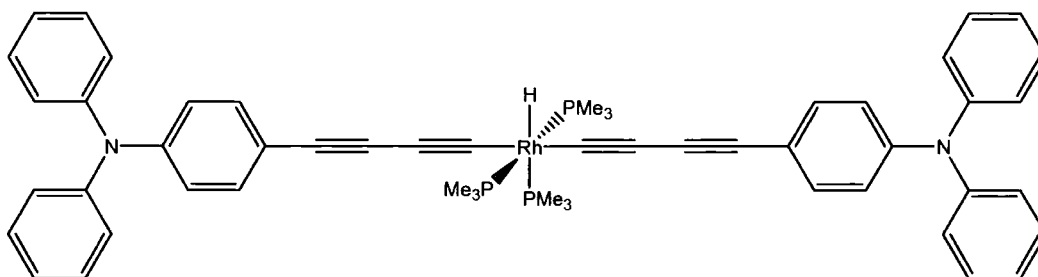


Figure 45. Diagram of *mer,trans*- $[\text{RhH}(\text{PMe}_3)_3(\text{C}\equiv\text{C-C}\equiv\text{C-C}_6\text{H}_4\text{-4-NPh}_2)_2]$, **17**.

2.9.7 Optical properties

The optical properties (absorption and emission maxima, extinction coefficients and Stokes shift) of compound **16** are presented in Table 6. The absorption and emission spectra are shown in Figure 46.

	λ_{\max} Abs (nm)	ϵ (mol^{-1} $\text{cm}^{-1} \text{dm}^3$)	λ_{\max} Em (nm)	Stokes Shift (cm^{-1})
16	454	25000	496	1870
	483	22000	531	

Table 6. Summary of the optical properties of compound **16**.

The data shows that changing the acetylide ligand from $-\text{C}\equiv\text{C}-\text{C}_6\text{H}_4-4-\text{NMe}_2$ to $-\text{C}\equiv\text{C}-\text{C}\equiv\text{C}-\text{C}_6\text{H}_4-4-\text{NPh}_2$ has little effect on the absorption and emission maxima as the values for compound **16** are very close to those for compounds **2** and **12**. This is possibly due to the fact that even with the $-\text{C}\equiv\text{C}-\text{C}\equiv\text{C}-\text{C}_6\text{H}_4-4-\text{NPh}_2$ aryl ring being further away from the metal, it is still not coplanar with both the metallacycle ring and phenyl ring *ii* and so conjugation is not extended as could be expected (Figure 47). It may also be attributed to the fact that the ' $\text{Rh}(\text{PMe}_3)_3(\text{CCR})$ ' fragment does not contribute a large amount to the overall photophysical properties for these compounds.

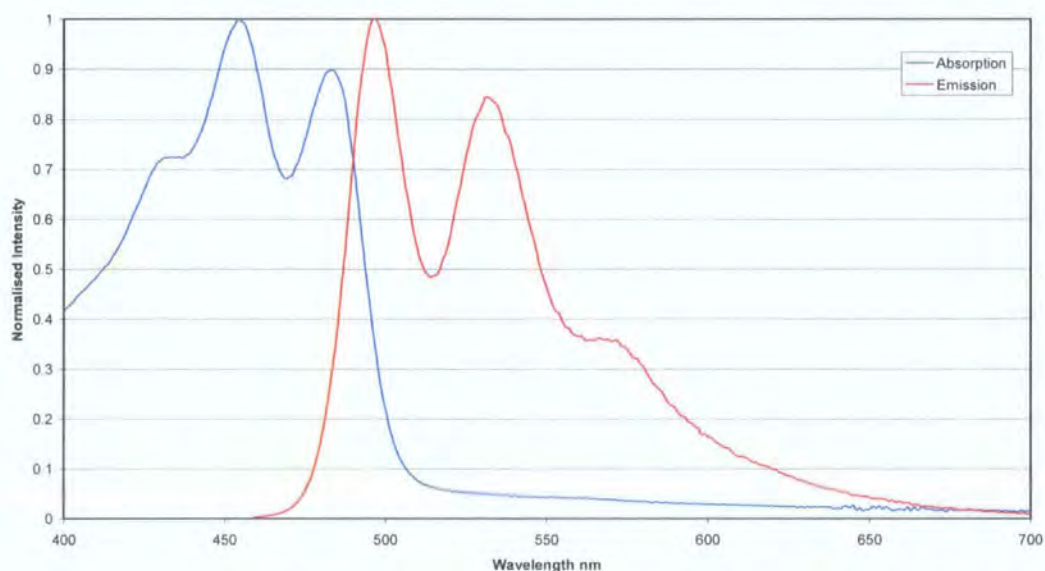


Figure 46. Absorption and emission spectra for compound **16**.

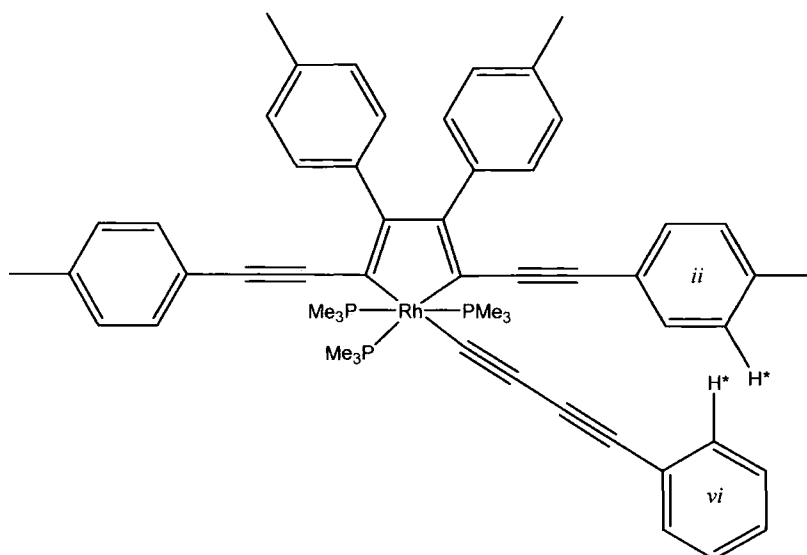


Figure 47. Unfavourable CH...HC interactions between H* that prevent co-planarity of phenyl rings *ii* and *vi*.

2.9.8 Comparison of rhodacycle optical properties with organic analogues

Due to the structure of the rhodacycles, it is worth comparing their photophysical properties with those of several analogous organic compounds, namely 1,4-bis(4-*R*-phenylethynyl)benzenes (BPEBs),¹⁰⁴ 2,5-bis(4-*R*-phenylethynyl)thiophenes (BPETs)^{85,86} and 9,10-bis(4-*R*-phenylethynyl)-anthracenes (BPEAs).^{105,106} Figure 48 shows a plot of absorption maxima against Hammett values (σ_{p+} for electron-donating *para*-substituents and σ_{p-} for electron-withdrawing *para*-substituents)¹⁰⁷ for a series of substituted rhodacycles, BPEBs, BPETs and BPEAs. Rhodacycles bearing electron-withdrawing *para*-substituents are red shifted more than any of the organic analogues, whereas rhodacycles bearing electron-donating *para*-substituents are red-shifted more than BPEBs and BPETs but less than the BPEAs. For all compound types, the graph shows a shift of absorbance maxima to lower energy with both stronger electron-withdrawing and electron-donating *para*-substituents on the phenyl ring, signifying a reduced energy gap between the S_0 ground state and S_1 excited state in either case. This is the result of the fact that electron donors raise the HOMO more than the LUMO while electron acceptors lower the LUMO more than the HOMO. However, in each of the series, the effect of withdrawing substituents is greater than that of donor substituents, as can be seen from the gradients of each line. The slope for the rhodacycles containing donor substituents is smaller than that

for the other three classes of compound showing that for the rhodacycles, donors have a less profound effect on the HOMO-LUMO gap than in the BPEB, BPET and BPEA analogues. The fit of the slopes for all of the acceptors is poor, with CN and CO₂Me for rhodacycles, BPEBs and BPETs shifting the absorption maxima to higher and lower energy respectively than what could be expected from the corresponding Hammett values. The fit is also poor if the absorption values are plotted against σ_p , indicating that neither inductive nor π -delocalisation effects satisfactorily explain the optical properties of the acceptor substituted compounds.

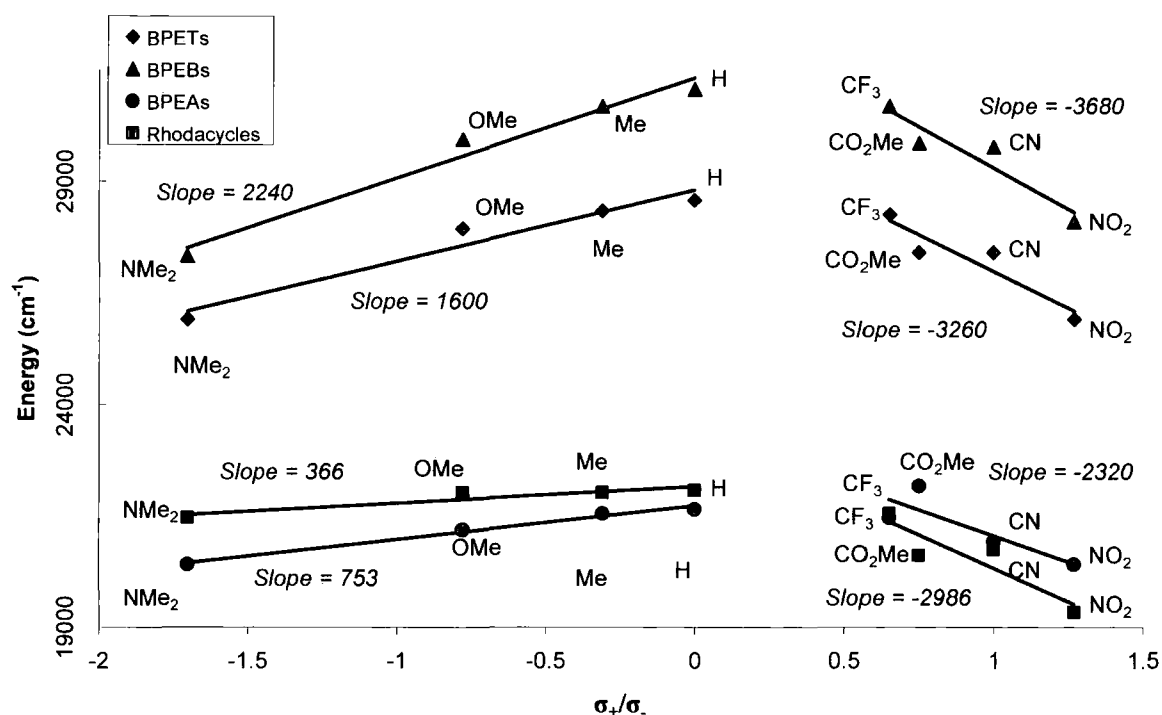


Figure 48. Plots of absorption maxima vs. Hammett constant (σ_{p+}/σ_{p-}) for the rhodacycles **1-3** and **5-9** and the analogous 1,4-bis(4-R-phenylethynyl)benzenes (BPEBs), 2,5-bis(4-R-phenylethynyl)thiophenes (BPETs) and 9,10-bis(4-R-phenylethynyl)anthracenes (BPEAs).^{95,104,105}

2.9.9 Synthesis of Rh-Me-based analogues

To investigate the importance of the acetylide ligands on the optical properties of the rhodacycles, and to examine the regioselectivity and scope of the reaction, examples of analogous compounds, **18-22**, synthesised directly by reaction of 1,4-bis(4-R-

phenyl)butadiynes with $\text{Rh}(\text{PMe}_3)_4\text{Me}$, were prepared. A THF solution of two equivalents of diyne was added to a rapidly stirred solution of $\text{Rh}(\text{PMe}_3)_4\text{Me}$ in THF and the solvent was cycled 3 times. The reactions were followed by *in situ* $^{31}\text{P}\{^1\text{H}\}$ NMR spectroscopy which, after solvent cycling, showed three sets of peaks (doublet of doublets of doublets, a doublet of triplets and a doublet of doublets of doublets) in a 1:1:1 ratio, which are assigned to intermediate diyne π -complexes (see Chapter 3). It was possible to convert these intermediates and the free diyne remaining in solution, to rhodacycles **18** to **22** by heating at 80°C for 1-12 hours (Figure 49).

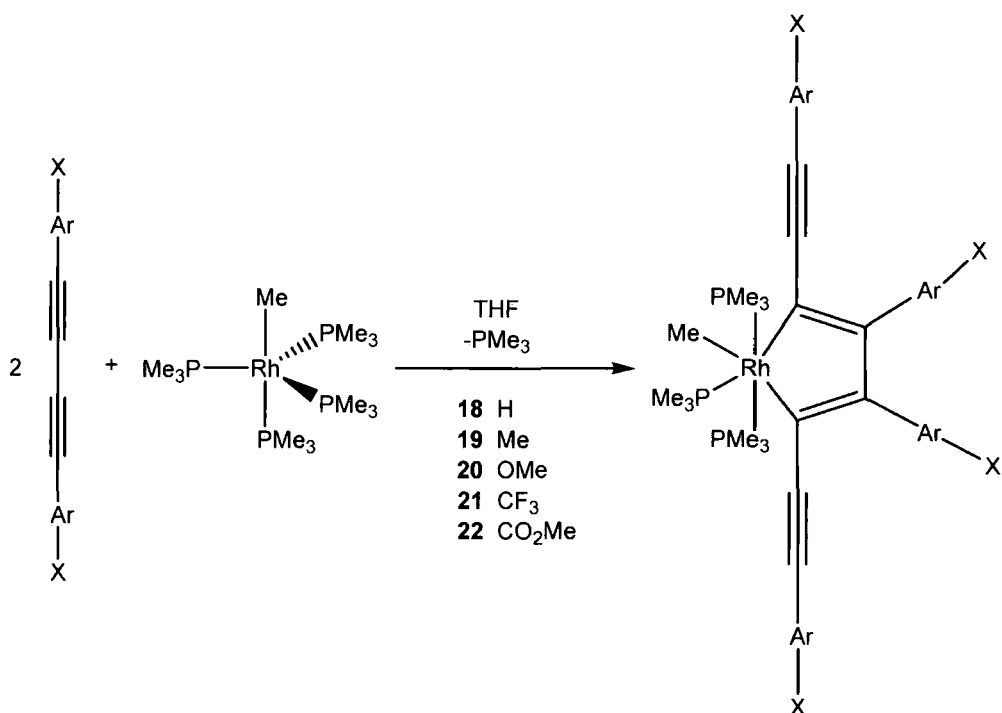


Figure 49. Synthesis of Rh-Me Rhodacycles, **18-22**.

When complete conversion to product had been achieved, the $^{31}\text{P}\{^1\text{H}\}$ NMR spectrum for each compound showed a doublet of doublets with associated doublet of triplets in a 2:1 ratio, indicating the same geometry around the Rh centre as for the acetylide-substituted rhodacycle analogues, with the methyl ligand *trans* to a Rh-C bond in the rhodacycle RhC_4 plane. The $^1J_{\text{Rh-P}}$ coupling constants are slightly larger (ca. 105 Hz and 88 Hz for the dd and dt respectively) than those of the acetylide analogues, indicating an increased electron density at Rh, though still indicative of PMe_3 coupled to Rh(III). IR spectra of the samples showed two peaks (or one peak due to overlap) at ca. 2100 cm^{-1} , corresponding to the alkyne vibrational modes. The compounds were isolated after

recrystallisation from THF/hexane. Unlike compounds **1** to **16**, solutions of **18** to **22** in d^6 -benzene or THF did not emit light under UV irradiation.

2.9.10 Crystal structure of **22**

Single crystals of **22** were grown in a 5 mm diameter glass tube as THF solvates by slow diffusion of a layer of hexanes into a THF solution. Once mixed, the solvents were allowed to evaporate slowly. X-ray analysis revealed triclinic crystals (space group = $P-1$) with two molecules in the asymmetric unit related by a pseudo-inversion centre ($1/2\ 1/4\ 1/4$) (Figure 50). Selected bond lengths (Å) and bond angles (°) for compound **22** are shown in Table 7 and 8. The structure of **22** is very similar to those obtained for rhodacycles based on RhCCR (*vide supra*). The coordination around Rh is a distorted octahedron, with a meridional disposition of the three phosphine ligands, [Rh-P(1) = 2.3109(8) Å, Rh-P(2) = 2.3138(9) Å, Rh-P(3) = 2.3403(9) Å]. It is worth noting from the structure that the three PMe_3 ligands are oriented in a similar fashion to that in the $\text{Rh}(\text{C}\equiv\text{CR})$ analogues. P(1) Me_3 is oriented with one Me group directed away from the metallacycle and the other two Me groups are directed along the two Rh-C metallacycle bonds. P(2) Me_3 is inclined such that one Me group points along one Rh-C metallacycle bond with the other two directed to each side of the methyl ligand. Two Me groups in P(3) Me_3 point to either side of the alkyne bonded to phenyl ring *v*.

Rh-C(1) is slightly longer than Rh-C(15,18), consistent with increased C(1) p-character in the σ -bond. The phenyl rings directly attached to the metallacycle, *iii* and *iv*, are inclined by 50.71° and 40.84° to relieve steric crowding. The 'rod' of the molecule is substantially non-planar with phenyl ring *ii* inclined by 36.84° with respect to the metallacycle and phenyl ring *v* inclined to an even greater extent [77.91°]. The alkynyl bonds C(19) \equiv C(20) [1.208(4) Å] and C(39) \equiv C(40) [1.214(4) Å] and the formal double bonds C(15)=C(16) [1.371(4) Å] and C(17)=C(18) [1.368(4) Å] are typical of the rhodacycle structures. The methyl ligand lies almost in the metallacycle plane, *trans* to the Rh-C(18) bond which is longer [2.126(3) Å] than Rh-C(15) [2.079(3) Å] due to the strong *trans*-influence of the methyl ligand. One of the four carbomethoxy groups, O(8)C(50)O(7)C(5) is disordered between two orientations, A and B, in a 2:1 ratio. The ADPs of all four THF molecules of crystallisation suggest disorder, which was not resolved except for the atoms O(12) and C(64) (positions A and B in 3:2 ratio).

	CO ₂ Me	CO ₂ Me
	22 – molecule a	22 – molecule b
Rh-P ₁	2.3109(8)	2.3081(3)
Rh-P ₂	2.3138(9)	2.3101(8)
Rh-P ₃	2.3403(9)	2.3543(9)
Rh-C ₁	2.159(3)	2.170(3)
Rh-C ₁₅	2.079(3)	2.076(3)
Rh-C ₁₈	2.126(3)	2.129(3)
C ₁₉ ≡C ₂₀	1.208(4)	1.197(4)
C ₃₉ ≡C ₄₀	1.214(4)	1.206(4)
C ₁₅ =C ₁₆	1.371(4)	1.369(4)
C ₁₇ =C ₁₈	1.368(4)	1.380(4)
C ₁₆ -C ₁₇	1.469(4)	1.469(4)
P ₁ -Rh-P ₂	169.68(3)	169.68(3)
C ₁ -Rh-C ₁₈	170.20(11)	170.20(11)
C ₁₅ -Rh-P ₃	174.39(8)	174.39(8)
<i>ii</i> - <i>i</i> *	39.6	21.9
<i>iii</i> - <i>i</i> *	54.7	55.9
<i>iv</i> - <i>i</i> *	45.1	44.3
<i>v</i> - <i>i</i> *	72.1	71.6

* Interplanar angles vs. plane *i* (rhodacycle)

Table 7. Selected bond lengths (Å) and bond angles (°) for **22**.

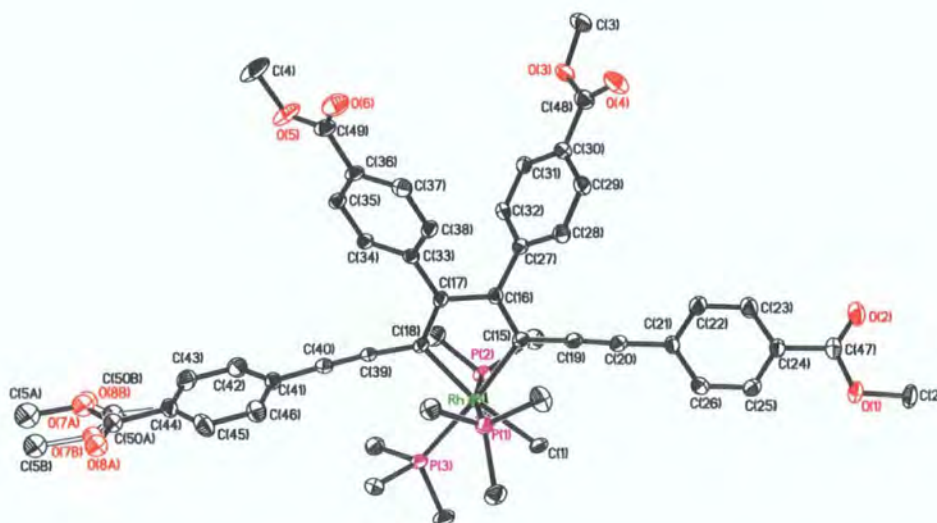


Figure 50. One molecule in the asymmetric unit of **22**. Hydrogen atoms and solvent molecules are omitted for clarity and thermal ellipsoids are shown at 50 % probability.

Molecule	22 - 05srv319
Empirical formula	C ₅₈ H ₇₄ O ₁₀ P ₃ Rh
Formula Weight	1126.99
Temperature (K)	120(2)
Crystal system	Triclinic
Space Group	<i>P</i> -1
a (Å)	18.0185(14)
b (Å)	18.0793(13)
c (Å)	21.1275(17)
α (°)	95.59(1)
β (°)	111.98(1)
γ (°)	113.82(1)
Volume (Å ³)	5582.4(7)
Z	4
Density (calculated)	1.341
Absorption Coefficient (mm ⁻¹)	0.448
Crystal size (mm)	0.42 x 0.24 x 0.06
Theta range for data collection (°)	1.39 to 28.99
Reflections collected	29339
Independent reflections	18989
Data / Restraints / Parameters	18989 / 8 / 1346
Final R indices	R1 = 0.0491 wR2 = 0.1105
R indices (all data)	R1 = 0.0927 wR2 = 0.1267

Table 8. Crystallographic data for compound **22**.

2.9.11 Rh-Cl-based rhodacycles

To develop a better understanding of the selectivity and to explore the scope of the reaction further, attempts were made to replace the acetylide or methyl ligands with a Cl ligand, by preparing rhodacycles directly from the salt [Rh(PMe₃)₄]Cl, a precursor in the synthesis of Rh(PMe₃)₄Me and thus Rh(PMe₃)₄(C≡CR).

Although rhodacycle formation with previous Rh starting compounds was easily achieved under mild reaction conditions, attempts to synthesise Rh-Cl rhodacycles proved

to be significantly less facile. Reactions using diynes bearing H, Me and CF₃ *para*-substituents were attempted; however, reactions under the conditions as used in previous syntheses failed to form rhodacycles. Two intermediate Rh π -complexes, formed in an ca. 2:1 ratio, by coordination of one equivalent of butadiyne to Rh were the only products observed (*vide infra*), even after long periods of heating (Figure 51). This is also supported by ¹⁹F{¹H} NMR spectroscopy which showed 4 CF₃ environments, with two pairs of peaks indicating the unsymmetrical binding of the diyne to Rh (See Chapter 3).

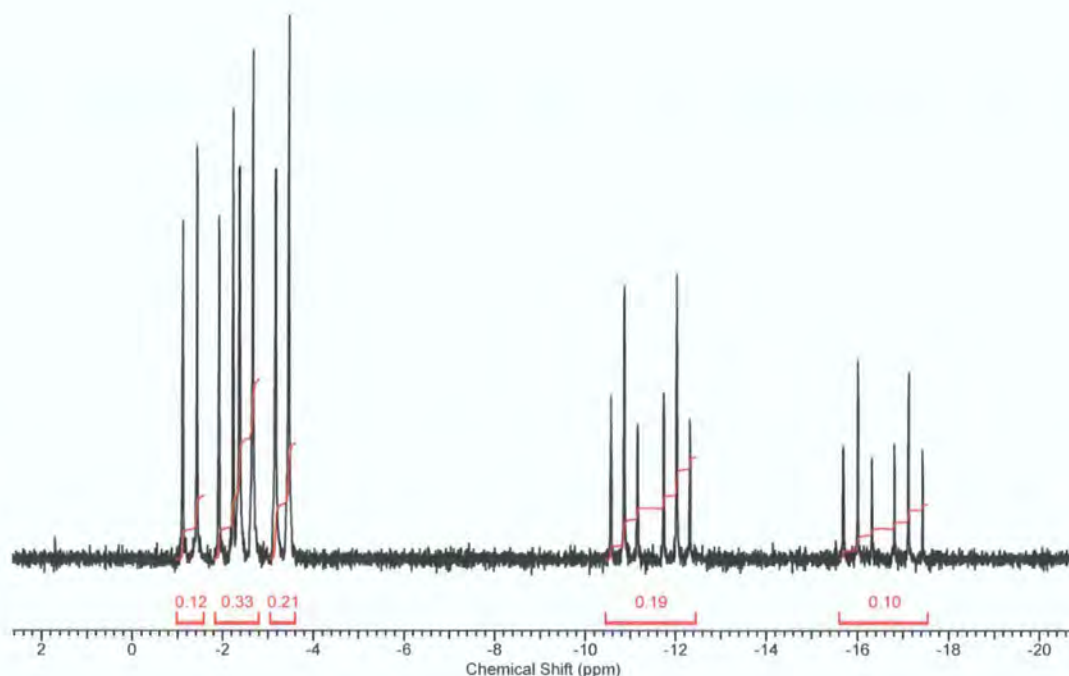


Figure 51. ³¹P{¹H} NMR spectrum of intermediate Rh π -complexes.

The successful synthesis of **23**, was achieved by reaction of [Rh(PMe₃)₄]Cl with an excess (four equivalents) of 1,4-bis(4-trifluoromethylphenyl)buta-1,3-diyne with [Rh(PMe₃)₄]Cl with prolonged heating (four days) at 80 °C (Figure 52). Using *in situ* ³¹P{¹H} NMR spectroscopy to follow the progress of the reaction, the slow appearance of a characteristic doublet of doublets (¹J_{RhP} = 100 Hz) and doublet of triplets (¹J_{RhP} = 86 Hz) associated with rhodacyclopentadiene product was observed, as was the disappearance of the peaks associated with the Rh(I) π -complex intermediates (Figure 53). It was necessary to add the [Rh(PMe₃)₄]Cl to the diyne as this prevented the formation of [Rh(PMe₃)₃(Cl)]₂(μ -(1,2- η^2):(3,4- η^2))-4-F₃C-C₆H₄-C \equiv C-C \equiv C-C₆H₄-4-CF₃). This complex

was found to be very insoluble, and the $\text{Rh}(\text{PMe}_3)_3\text{Cl}$ unit does not dissociate easily, both factors inhibiting the desired cyclisation.

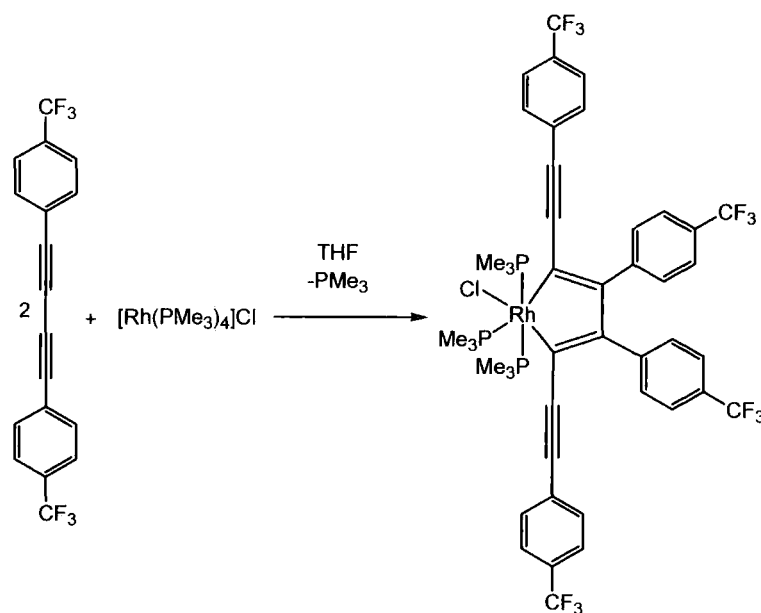


Figure 52. Synthesis of Rh-Cl rhodacyclopentadiene, **23**.

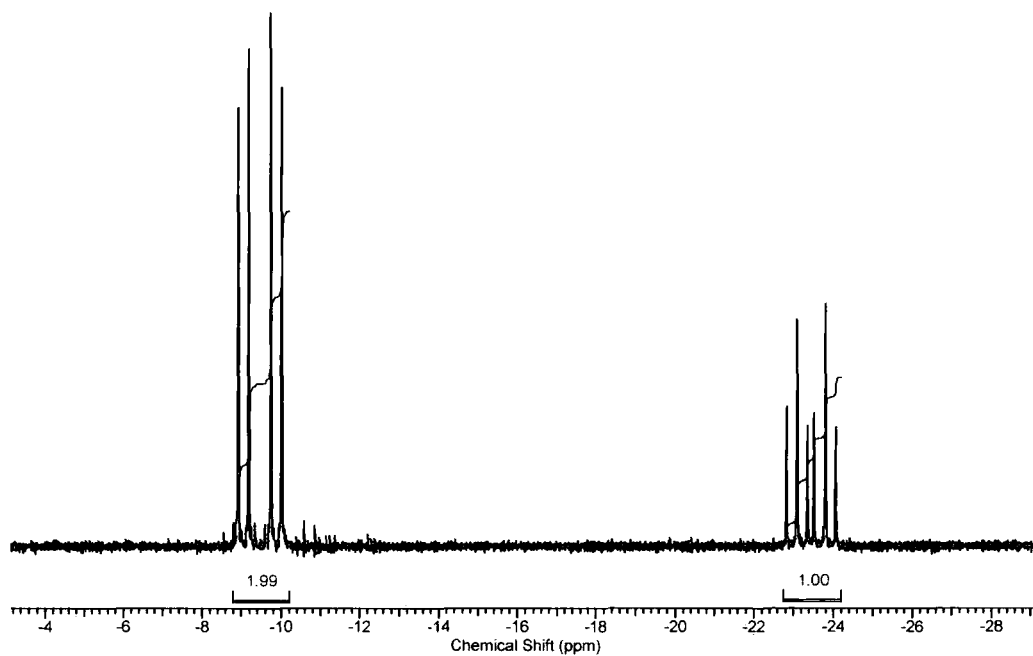


Figure 53. *In situ* $^{31}\text{P}\{^1\text{H}\}$ NMR spectrum of compound **23**.

Compound **23** was isolated as a dark brown solid in moderate yield and was found to emit green light under UV irradiation.

2.9.12 Optical properties of Rh-Me and Rh-Cl-based rhodacyclopentadienes

The absorption maxima and associated Stokes shifts for compounds **18-22** are presented in Table 9, with the absorption spectra shown in Figure 54. Comparing the data for compounds **18-22** with the analogous compounds **1-3**, **5**, **6** and **11-15**, reveals that there is a red-shift in the absorption maxima by 5-8 nm for the Rh-Me compounds, supporting the fact that the Me ligand is a better donor than the acetylide ligands, as is shown by the $^1J_{\text{Rh-P}}$ coupling constants in the $^{31}\text{P}\{^1\text{H}\}$ NMR spectra (*vide supra*). The extinction coefficients for **18-22** are lower than for **11-15**, by ca. 10-30 %. Unlike the acetylide analogues, there is no observed emission.

	$\lambda_{\text{max Abs}}$ (nm)	ϵ (mol ⁻¹ cm ⁻¹ dm ³)
CO₂Me (22)	492	22000
	524	19000
CF₃ (21)	470	20000
	499	16000
H (18)	460	24000
	488	21000
Me (19)	460	25000
	488	21000
OMe (20)	458	17000
	487	16000

Table 9. Summary of the optical properties of compounds **18-22**.

Like the acetylide rhodacyclopentadienes, the Rh-Cl analogue also shows emission under UV-irradiation. The absorption and emission maxima for compound **23** (Figure 55) are red-shifted by 3-9 nm compared to analogous compounds **5** and **14** (471/499 nm vs. 464/492 nm and 466/496 nm respectively in absorption and 518/555 nm vs. 510/547 nm and 513/546 nm respectively in emission), suggesting that similarly to the methyl ligand in

the Rh-Me compounds, the Cl ligand is rather surprisingly also a better donor than the acetylide ligands, as is supported by the observed $^1J_{\text{Rh-P}}$ NMR coupling constants.

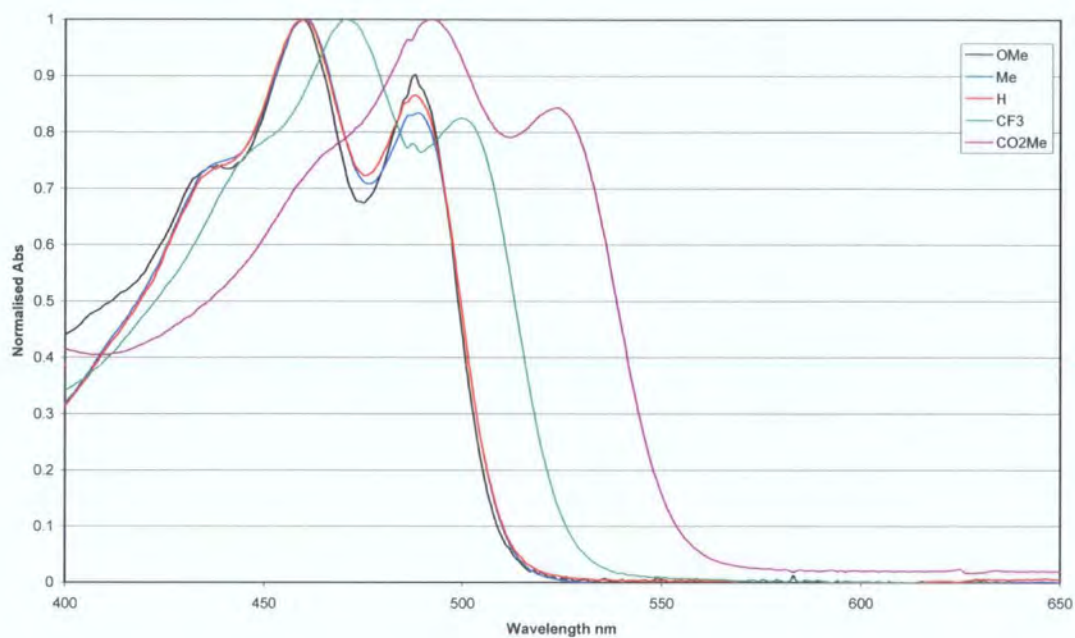


Figure 54. Absorption spectra for compounds **18-22**.

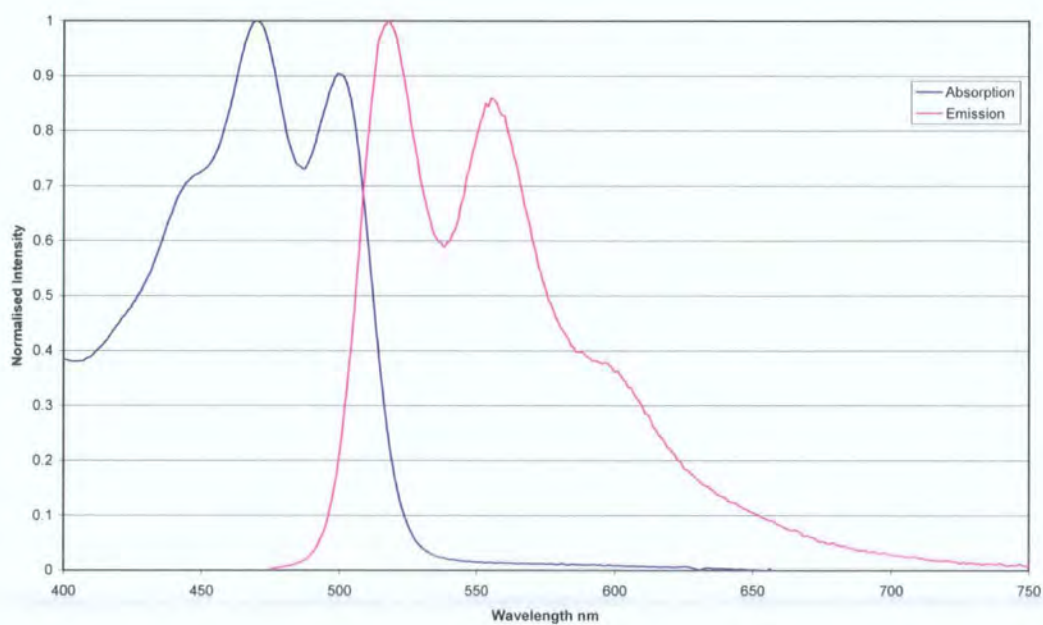


Figure 55. Absorption and emission spectra for compound **23**.

2.10 Cyclotrimerisation of buta-1,3-diyne

It is known that some transition metals can catalyse the cyclotrimerisation of butadiynes (*vide infra*), and due to the conjugation within these cyclotrimers, the compounds would be expected to be highly luminescent. To ensure that we did not accidentally synthesise cyclotrimers during rhodacycle synthesis, and to confirm that the optical properties that we have observed for the rhodacyclopentadienes were not arising from cyclotrimer impurities, we have investigated the synthesis and the optical properties of a select few cyclotrimers, and have studied the absorption and luminescence properties of these compounds. We found that formation of the cyclotrimers only occurs under forcing conditions. The high temperatures and long reaction times necessary for rhodacycle catalysed butadiyne cyclotrimerisation were not necessary for rhodacycle synthesis, and so we are able to prepare rhodacycles without the issue of cyclotrimer impurities. The results also clearly show that the two systems have significantly different optical properties.

2.10.1 Introduction to transition metal catalysed cyclotrimerisation of buta-1,3-diyne

The cyclotrimerisation of alkynes to form substituted benzenes using transition metal catalysts has been extensively studied. There are many examples of a wide range of active transition metal catalysts for this process and these systems have been reviewed (*vide supra*). A number of metallacyclopentadiene compounds formed from the reductive coupling of two equivalents of conjugated butadiynes have also been reported;²⁵⁻³⁴ however, there are few examples of transition metal catalysed cyclotrimerisation of 1,4-diphenylbuta-1,3-diyne to form tris(phenylethynyl)-tri(phenyl)benzenes (Figure 56). Of the limited examples in the literature, the compounds prepared have often been synthesised in low yields, as isomeric mixtures or as side products to other reactions.

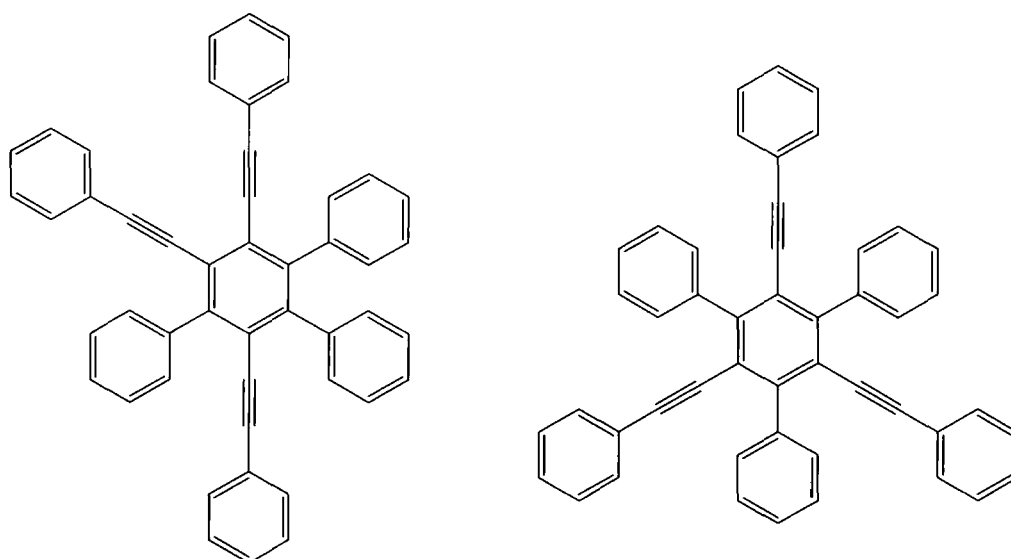


Figure 56. 1,2,4-tris(phenylethynyl)-3,5,6-tri(phenyl)benzene and 1,3,5-tris(phenylethynyl)-2,4,6-tri(phenyl)benzene.

The first report of successful buta-1,3-diyne trimerisation was by Hübel and co-workers who used transition metal carbonyl compounds, including $\text{Co}_2(\text{CO})_8$, $[\text{Co}(\text{CO})_4]_2$ and $[\text{Co}(\text{CO})_4]_2\text{Hg}$, to trimerise $\text{TMS-C}\equiv\text{C-C}\equiv\text{C-TMS}$ to the corresponding mixture of the two cyclotrimer regioisomers, however, the yields were low (21-25 %).¹⁰⁸ It was possible to separate and purify the isomers on alumina columns and also to remove the silyl groups from the products with base to form the deprotected alkyne derivatives. Under H_2 pressure (50 atm) and elevated temperatures (60-100 °C), it was found that the products could be catalytically hydrogenated to give ethyl substituted benzenes. The group obtained slightly better yields for the trimerisation of 1,4-diphenylbuta-1,3-diyne using $\text{Hg}[\text{Co}(\text{CO})_4]_2$ under similar reaction conditions.

Jerussi *et al.* used $[\text{Ni}(\text{PPh}_3)_2(\text{CO})_2]$ to synthesise selectively the unsymmetrical 1,2,4-tris(R-ethynyl)-3,5,6-tri(R)benzenes (R = Me or Ph) in good yields (77 % and 83 % respectively) by reflux under nitrogen in benzene for 10 hours using 10 wt% catalyst.¹⁰⁹ This implies the regioselective formation of the 2,5-dialkynylnickelacyclopentadiene intermediate and so under appropriate conditions, we should be able to prepare nickelacycles with the same 2,5-regioselectivity as our rhodacycles. They also noted that a similar reaction produced a mixture of isomers if $\text{CoCp}(\text{CO})_2$ catalyst was used instead of $[\text{Ni}(\text{PPh}_3)_2(\text{CO})_2]$. Dickson and Michel have also used $\text{CoCp}(\text{CO})_2$ for the cyclotrimerisation of $\text{Me-C}\equiv\text{C-C}\equiv\text{C-Me}$ and 1,4-diphenylbutadiyne and similarly found the product to be a mixture of regioisomers.¹¹⁰ They observed that in both cases, the yield of

the unsymmetrical isomer was greater than that of the symmetrical isomer, consistent with other studies on diphenylbutadiyne,^{108,109} but in contrast with reported results for Me-C≡C-C≡C-Me in the presence of Hg[Co(CO)₄]₂.¹⁰⁸ The reaction yields were affected by changes in reaction conditions and were improved with extended reaction times and by the presence of excess diyne; however, an increase of temperature from 120 °C to 160 °C decreased the overall yield. Catalysis by RhCp(CO)₂ gave similar results. The group also proposed the formation of tris(phenylethynyl)-triphenylcycloheptatrieneone as a side product although this species was not completely characterised. The presence of this species suggests that the formation of benzenes occurs *via* insertion reactions rather than the alternative Diels-Alder mechanism.

In their studies of the formation of diethynylcyclobutadiene ligands on Co from TMS-C≡C-C≡C-TMS and CoCp(CO)₂ and rearrangement thereof, Volhardt and Fritch noted small amounts of two isomeric substituted benzenes as side products.¹¹¹ These were isolated in low yields by column chromatography, with a greater yield of the symmetrical isomer compared to the unsymmetrical isomer.

Methyldinetricobalt nonacarbonyl is another example of a transition metal carbonyl catalyst for butadiyne cyclotrimerisation. Sugihara and co-workers used 2 mol% of Co₃(CO)₉(μ³-CH) to catalyse the exclusive formation of 1,3,5-tris(phenylethynyl)-2,4,6-(phenyl)benzene from diphenylbutadiyne in 87 % yield in just 30 minutes (Figure 57).¹¹²

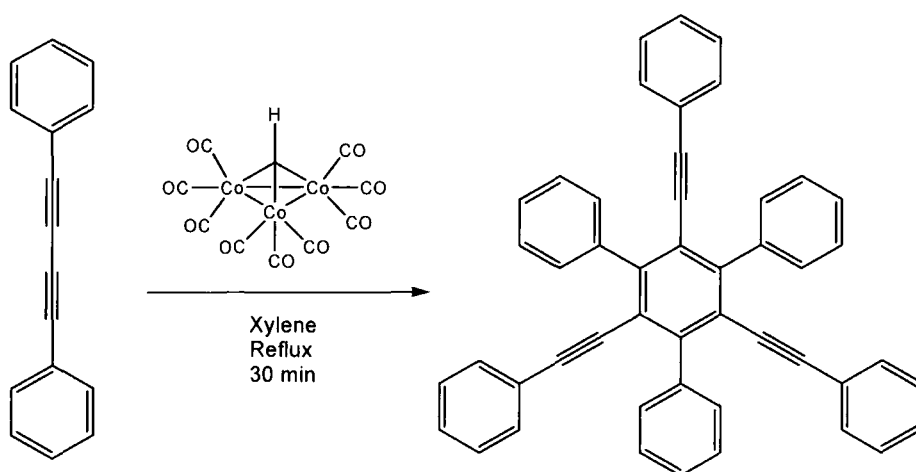


Figure 57. Regioselective cyclic trimerisation of diphenylbutadiyne using methyldinetricobalt nonacarbonyl catalyst.

With the aim of synthesising precursors for constructing sub-units of ‘cubic graphite’, Müllen *et al.* have used 1,3,5-tris(phenylethynyl)-2,4,6-tri(phenyl)benzene under forcing Diels-Alder conditions to prepare oligophenylenes with a relatively large number of densely packed benzene rings.¹¹³

Groups investigating the polymerisation of diacetylenes have reported the formation of the cyclic trimers as minor products by non-catalytic, solvent-free coupling reactions at high temperature¹¹⁴ and by annealing under high pressures (0.03-0.13 GPa) and temperature (250 °C).¹¹⁵ Sugawara *et al.* reported the synthesis of 1,2,3-tris(R-ethynyl)-4,5,6-tri(R)benzene (R = CH₃OCOCH₂-), a regioisomer which has not previously been synthesised by other methods and is characteristic of liquid phase oligomerisation.¹¹⁴ The isomer was observed, along with the 1,2,4-tris(R-ethynyl)-3,5,6-tri(R)benzene and 1,3,5-tris(R-ethynyl)-2,4,6-tri(R)benzene isomers in small yields, formed as byproducts during the catalyst free, melt-state (120 °C) oligomerisation of CH₃OCOCH₂-C≡C-C≡C-CH₂OCOCH₃. The synthesis of this particular isomer provides an insight into the liquid phase trimerisation mechanism which can be rationalised by the intermediacy of Dewar benzene formation, and the subsequent thermally allowed ring opening reaction (Figure 58).

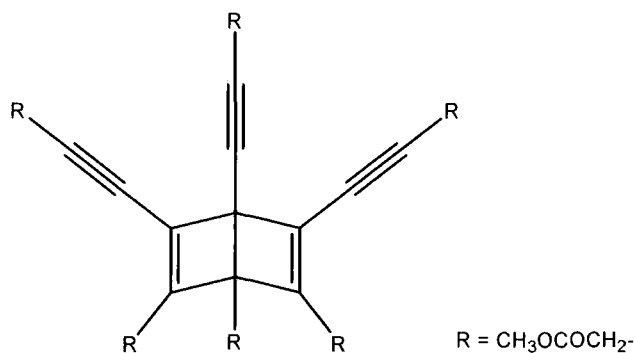


Figure 58. Dewar benzene intermediate formed thermally during solvent-free synthesis of 1,2,3-tris(R-ethynyl)-4,5,6-tri(R)benzene (R = CH₃OCOCH₂).

Hsu and co-workers have utilised the trimerisation activity of Co₂(CO)₈ to prepare alkoxy substituted 1,3,5-tri(phenylethynyl)-2,4,6-(phenyl)benzene derivatives from 1,4-(3,4-dialkyloxyphenyl)buta-1,3-diyne (Figure 59), which have been studied for their

liquid crystal phase behaviour.¹¹⁶ The group found that the compounds exhibited hexagonal columnar mesophases as indicated by their polarised optical microscopy and X-ray diffraction investigations. The reaction yields were comparable to or better than those reported previously for cyclotrimerisation reactions (20-26 %).

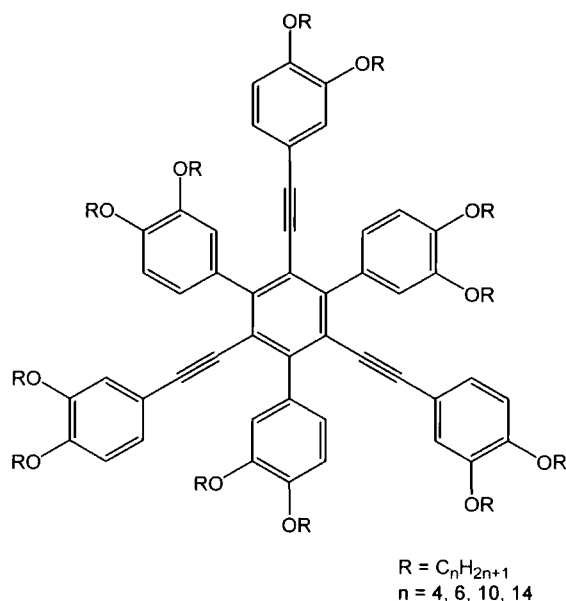


Figure 59. 1,3,5-tri(phenylethynyl)-2,4,6-(phenyl)benzene derivatives which exhibit liquid crystal phase behaviour.

2.11 Cyclotrimerisation results and discussion

2.11.1 Cyclotrimer synthesis

The compounds **1**, **5** and **15**, are shown to cyclotrimerise 1,4-bis(4-R-phenyl)buta-1,3-diyne, **24a-c**, regiospecifically to the hexasubstituted benzenes, **25a-c** (Figure 60). Reactions were carried out such that 21 equivalents of butadiyne to one equivalent of rhodacycle were refluxed in toluene for 3 weeks. 21 equivalents of diyne were used insofar as this was sufficient diyne for the formation of a whole number of benzenes and for the regeneration of the rhodacycle (assuming that the reaction proceeded *via* a catalytic process).

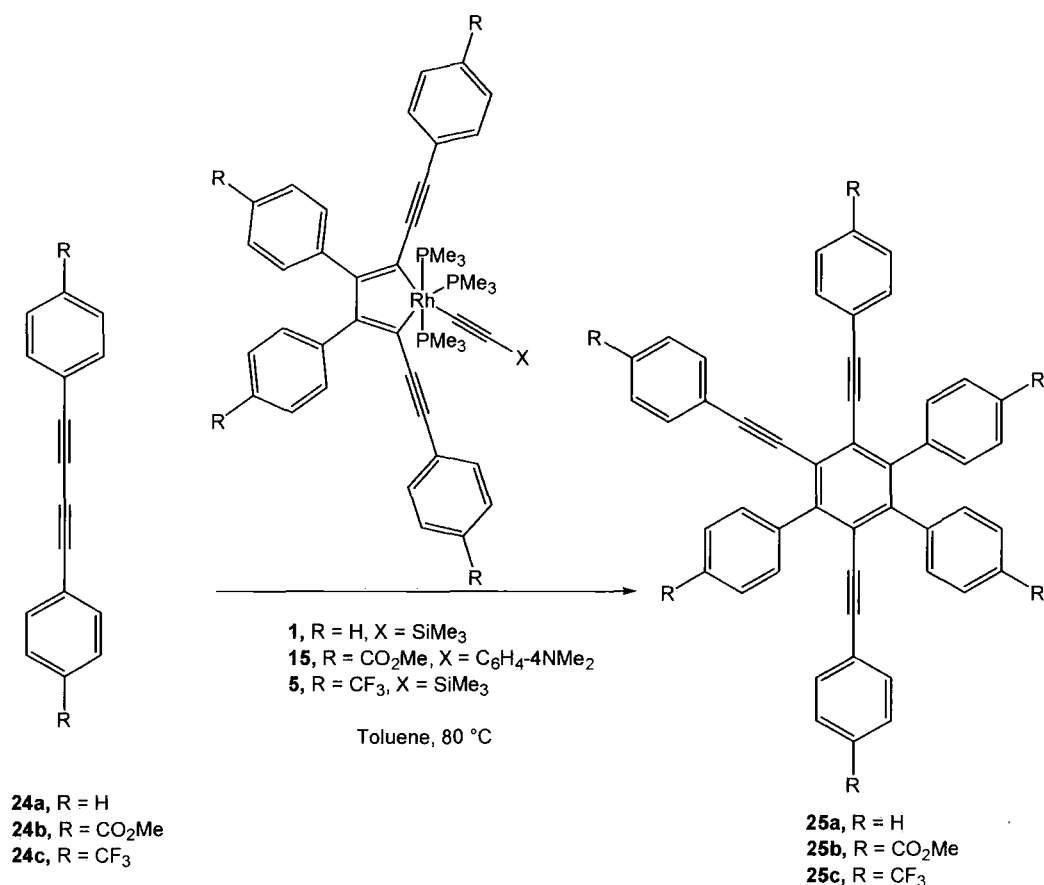


Figure 60. Stereospecific cyclotrimerisation of 1,4-bis(4-R-phenyl)buta-1,3-diyne using preformed rhodacycles.

Immediately after the mixing of **1**, **5** and **15** and **24a-c** in toluene, the solutions were found to emit in the region characteristic of the rhodacycle used. After heating for several days, the same solutions showed emission in the blue region. After 3 weeks at reflux, the products were purified by column chromatography which allowed for easy separation of unreacted diyne.

The spectroscopic evidence clearly indicates that a single regioisomer is the sole product formed during the reaction, demonstrating excellent selectivity for the 1,2,4-tris(4-R-phenylethynyl)-3,5,6-tris(4-R-phenyl)benzene isomer over the 1,3,5-tris(4-R-phenylethynyl)-2,4,6-tris(4-R-phenyl)benzene isomer. The low to moderate yields for the reactions indicate that although butadiyne cyclotrimerisation does occur catalytically, the activity of the rhodacycle catalyst is low. After purification, the products were all found to emit in the blue region when irradiated with UV light. The IR spectra for each of the compounds show a single C≡C stretch at ca. 2200 cm⁻¹ and there is a strong C=O band at 1724 cm⁻¹ for **25b**, and a strong CF₃ peak at 1327 cm⁻¹ for **25c**.

2.11.2 Proposed catalytic cycle

The proposed catalytic cycle for the cyclotrimerisation of 1,4-bis(4-R-phenyl)buta-1,3-diyne using preformed rhodacyclopentadienes is shown in Figure 61.

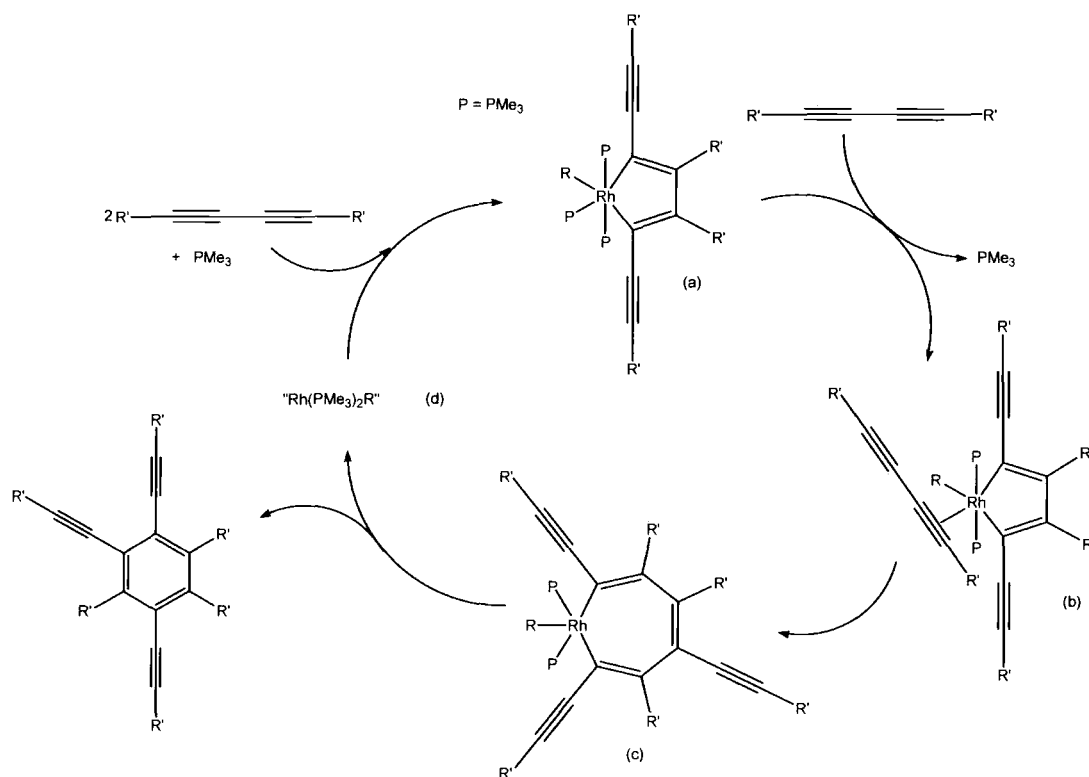


Figure 61. Proposed catalytic cycle for the cyclotrimerisation of butadiynes using rhodacyclopentadiene catalysts.

The first step in the cycle is the dissociation of PMe_3 from (a), and the subsequent π -coordination of free diene to the vacant site on Rh to give intermediate (b). This step is expected to be slow as dissociation of PMe_3 from Rh(III) is unfavourable. Intermediate (b) can then undergo rearrangement, with insertion of the π -coordinated $\text{C}\equiv\text{C}$ bond of the bound diene into the rhodacyclopentadiene, temporarily forming a rhodacycloheptatriene, (c). The slow rate of benzene formation argues against a Diels-Alder type [4+2] mechanism, as the overall rate of reaction *via* this route would not be limited by the rate of ligand dissociation. Intermediate (c) can then reductively eliminate the regioselective cyclotrimer to generate the reactive intermediate " $\text{Rh}(\text{PMe}_3)_2(\text{CCR})$ ", (d), which can coordinate to the free PMe_3 and react with two equivalents of butadiyne to regenerate the

rhodacycle catalyst, (a). As regeneration of the rhodacycle catalyst is regiospecific, a single cyclotrimer isomer is formed exclusively.

2.11.3 Crystal structure of 25a

Single crystals of cyclotrimer **25a** were grown by slow evaporation of a solution in DCM/hexane. The crystallographic data for **25a** is presented in Table 10.

Molecule	25a - 05srv173
Empirical formula	C ₄₈ H ₃₀
Formula Weight	606.72
Temperature (K)	120(2)
Crystal system	Monoclinic
Space Group	<i>I</i> 2/a
a (Å)	18.977(3)
b (Å)	13.7307(18)
c (Å)	27.064(4)
α (°)	90.00
β (°)	105.52(1)
γ (°)	90.00
Volume (Å ³)	6794.7(16)
Z	8
Density (calculated)	1.186
Absorption coefficient (mm ⁻¹)	0.067
Crystal size (mm ³)	0.90 x 0.08 x 0.07
Theta range for data collection (°)	2.61 to 27.51
Reflections collected	7817
Independent reflections	5849
Data / Restraints / Parameters	7817 / 0 / 433
Final R indices	R1 = 0.0489 wR2 = 0.1132
R indices (all data)	R1 = 0.0713 wR2 = 0.1248

Table 10. Crystallographic data for compound **25a**.

Monoclinic crystals (space group = *I*2/a) have a single molecule in the asymmetric unit and the 1,2,4-tris(phenylethynyl)-3,5,6-tri(phenyl)benzene structure (Figure 62) is

confirmed. The hexasubstituted phenyl ring, *i* is almost planar, with the C(1)-C(17) [1.437(19) Å], C(2)-C(27) [1.435(19) Å] and C(5)-C(57) [1.436(19) Å] bonds from *i* to sp hybridised carbons all being shorter than those between *i* and sp² carbons, C(3)-C(31) [1.492(19) Å], C(4)-C(41) [1.494(19) Å] and C(6)-C(61) [1.492(19) Å]. The phenyl substituents are far from co-planar with the central arene ring, and apart from phenyl ring *v* [6.14°], each of the phenyl rings *ii* [63.32°], *iii* [67.57°], *iv* [61.32°], *vi* [72.98°] and *vii* [60.95°] are all rotated simultaneously to reduce crowding around the central ring.

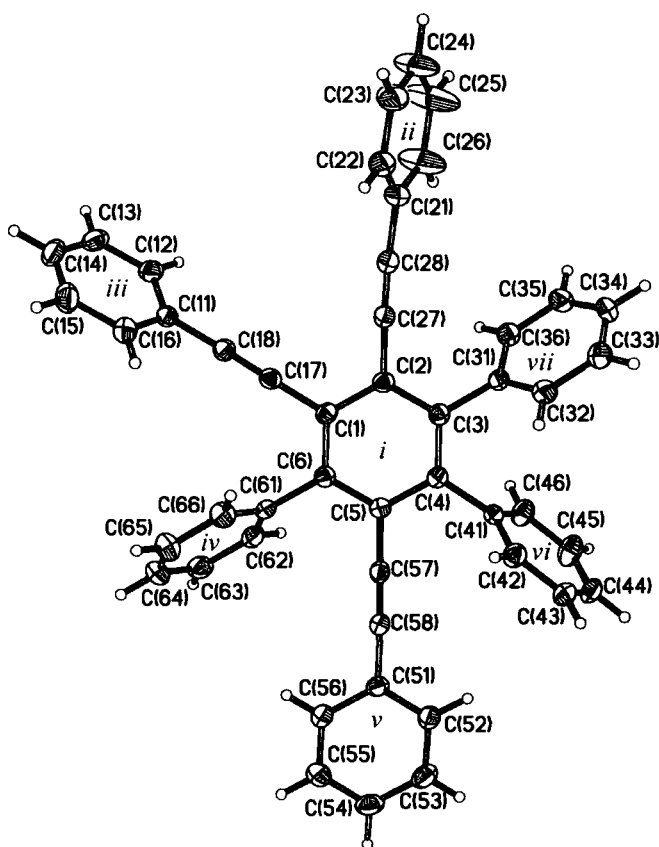


Figure 62. Molecular structure of 1,2,4-tris(phenylethynyl)-3,5,6-tri(phenyl)benzene, **25a**. Thermal ellipsoids are shown at 50 % probability.

2.11.4 Optical properties of 25a-c

The optical properties (absorption and emission maxima, fluorescence quantum yield and Stokes shift) are presented in Table 11. The absorption spectra (Figure 63) for each of the compounds show three absorption bands, each separated by 2000-2500 cm^{-1} , corresponding to the vibrational energies of the alkynyl bonds. The emission spectra (Figure 64) for compounds **25a** and **25c** show a single broad emission band and unusually, **25c** is blue-shifted compared to **25a**. As the CF_3 is a weakly electron-accepting group in the *para*-position, it is expected that in **25c**, the LUMO would be stabilised more than the HOMO, reducing the energy gap between the S_0 ground state and the S_1 excited state, thus shifting the emission wavelength to lower energy, as is the case for **25b**. Unlike **25a** and **25c**, compound **25b** has two emission bands separated by ca. 1000 cm^{-1} .

R group	λ_{max} Abs (nm)	λ_{max} Em (nm)	Φ (%)	Stokes Shift (cm^{-1})
H (25a)	314	393	37	6400
	342			
	366			
CF₃ (25c)	315	384	50	5700
	342			
	366			
CO₂Me (25b)	330	395	61	4990
	354	414		
	381			

Table 11. Summary of the optical properties for compounds **25a**, **25b** and **25c**.

The quantum yields are reasonably high and are dependent on the *para*-substituent. Compound **25b**, with strongly electron-withdrawing CO_2Me groups has a much higher quantum yield than the parent compound **25a**. Compound **25c**, with weakly electron-withdrawing CF_3 groups also has a higher quantum yield, intermediate between that of **25a** and **25b**. Comparing the optical properties of the cyclotrimers **25a-c** with that for the

rhodacycles (*vide supra*) shows that the two compounds have significantly different absorption and emission spectra.

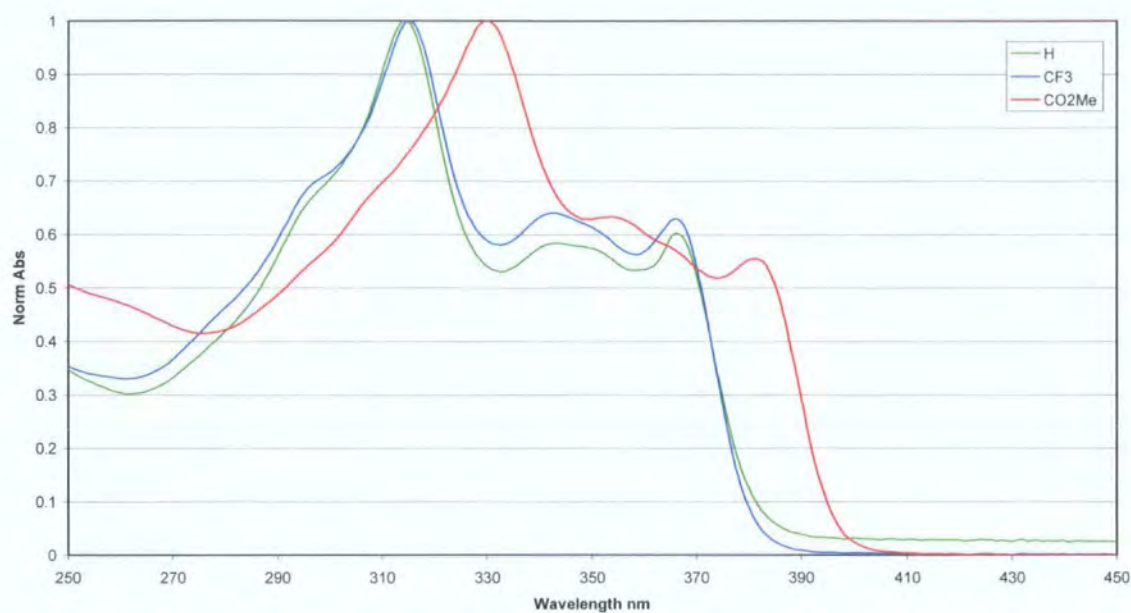


Figure 63. Absorption spectra of compounds **25a**, **25b** and **25c**.

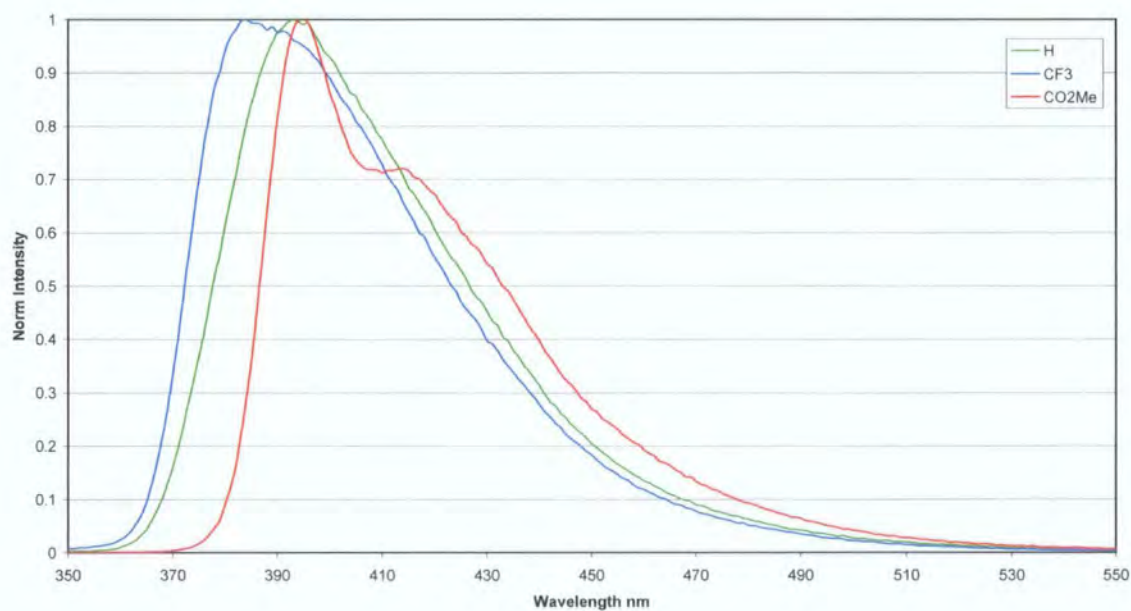


Figure 64. Emission spectra of compounds **25a**, **25b** and **25c**.

Due to the regiospecific nature of cyclotrimer formation, the 1,2,4-tris(4-R-phenylethynyl)-3,5,6-tri(4-R-phenyl)benzenes have very similar structures to 1,4-bis(4-R-

phenylethynyl)benzenes (BPEBs), though **25a-c** have additional substituents at the central arene ring. It is interesting to compare the absorption and emission for compounds **25a-c** with those of the related BPEBs (R = H (**26a**), CO₂Me (**26b**), CF₃ (**26c**)), to examine the effect of the presence of the three phenyl rings and one phenylethynyl substituent on the central benzene ring.^{104,117} A summary of the optical properties (absorption and emission maxima, fluorescence quantum yield (for **26a** and **26b**) and Stokes shifts for the corresponding BPEBs are presented in Table 12.

R group	λ_{\max} Abs (nm)	λ_{\max} Em (nm)	Φ (%)	Stokes Shift (cm ⁻¹)
H (26a)	322	351	79*	2570
	342	365		
CF ₃ (26c)	326	356	-	2590
	346	370		
CO ₂ Me (26b)	335	367	91*	2600

* In DCM

Table 12. Summary of the optical properties for three BPEBs.

Comparison of the data reveals that the two compound types have very different optical properties. Cyclotrimers **25a-c**, each show three absorption bands, with the absorption maxima shifted to higher energy compared to the BPEBs, **26a-c**. This may be due to rotation of, and hence a reduced level of delocalisation between, phenyl rings *i*, *ii* and *v*, resulting from steric crowding, arising from the substitution on the central ring. It is well known that the energy barrier to rotation around the C≡C bonds in BPEB is very low in the ground state.¹¹⁸ Unlike the absorption maxima, the emission maxima for **25a-c** are shifted bathochromically compared to **26a-c** and have much larger Stokes shifts associated with this. The Stokes shifts of **26a-c** increase slightly with the increasing electron-withdrawing ability of R; however, the opposite is the case for **25a-c**, and a substantial decrease is observed from **25a** to **25b**. The quantum yields of **26a** and **26b** is significantly higher than that of **25a** and **25b**.

Although there are no reports on the luminescent properties of hexa(phenylethynyl)benzene (HPEB),^{119,120} comparison of the absorption bands with those for **25a**, shows that the bands for HPEB are red-shifted from those of **25a**, indicating a greater degree of π -conjugation through the molecule. The CO₂Et substituted analogue has also been studied and has absorption and emission maxima at 360 nm and 458 nm respectively with a large Stokes shift (5850 cm⁻¹).¹²¹ These values are also red-shifted compared to that of **25b**. Such large Stokes shifts for **25a-c** and the CO₂Et substituted HPEB suggest that in the excited state, the lowest energy conformation is probably planar.

2.12 Experimental

2.12.1 General

All reactions were carried out using standard Schlenk techniques or in an Innovative Technology Inc. N₂ filled glove box. Solvents were dried before use with appropriate drying agents. The reagents used in synthesis were purchased from commercial suppliers and tested for purity by GC-MS before use.

NMR spectroscopy experiments were performed on Varian Mercury-200, Unity-300 and Inova-500 and Bruker Avance-400 spectrometers at the following frequencies: ¹H – 200, 300, 400, 500 MHz, ¹³C{¹H} – 100 MHz, ³¹P{¹H} – 80, 121, 202 MHz, ¹⁹F{¹H} – 188, 282 MHz in C₆D₆ solvent unless otherwise stated.

Elemental analyses were performed using an Exeter Analytical E440 machine by departmental services at Durham University.

UV-Vis, fluorescence emission spectra, lifetime and quantum yield measurements were recorded in toluene. UV-Vis absorption spectra and extinction coefficients were obtained on a Hewlett-Packard 8453 diode array spectrophotometer using standard 1 cm width quartz cells. Fluorescence spectra and quantum yield measurements were recorded on a Horiba Jobin-Yvon Fluoromax-3 spectrophotometer. The spectra of dilute solutions with absorbance maxima of less than 0.1 were recorded using conventional 90 degree geometry. Excitation wavelengths used for fluorescence measurements were the wavelengths at which strongest absorption was observed in the absorption spectra. The emission spectra were fully corrected using the manufacturers correction curves for the spectral response of the emission optical components.

Mass spectra of compounds **25a-c** were obtained on a MALDI ToF Applied Biosystems Voyager-DE STR mass spectrometer. Raman spectra were recorded on solid samples using a Horiba Jobin-Yvon LabRamHR Raman microscope with the laser set at 785 nm.

The quantum yield of each compound was estimated by comparing it with standards of known quantum yield. The absorbance of the samples was kept below 0.12 to avoid inner filter effects and all measurements were carried out at room temperature. The fluorescence quantum yields of compounds **1-3** and **11-13** were measured against 9,10-bis(phenylethynyl)anthracene (BPEA) in CHCl₃ ($\Phi = 0.95$)¹⁰⁵ and fluorescein in 0.1 M

NaOH ($\Phi = 0.79$),¹²² those of **4-7** and **10a** were measured against acridine orange in EtOH ($\Phi = 0.46$)¹²³ and fluorescein in 0.1 M NaOH ($\Phi = 0.79$), that of **9** was measured against cresyl violet in methanol ($\Phi = 0.54$)¹²⁴ and rhodamine 101 in ethanol ($\Phi = 1.00$)¹²⁵ and that of compounds **25a-c** were measured against quinine sulphate in 0.1 M H₂SO₄ ($\Phi = 0.54$)^{126,127} and anthracene in EtOH ($\Phi = 0.27$).¹²⁶

The fluorescent lifetimes of **1-7** and **9** were measured using time correlated single photon counting (TCSPC) using either a 396 nm pulsed laser diode or the 3rd harmonic of a cavity dumped, mode locked Ti-sapphire laser (Coherent MIRA), 300 nm. The fluorescence emission was collected at right angles to the excitation source with the emission wavelength selected using a monochromator and detected by a single photon avalanche diode (SPAD). The instrument response function was measured using a dilute LUDOX[®] suspension as the scattering sample, setting the monochromator at the emission wavelength of the laser, giving an instrument response function (IRF) of 200 or 100 ps at 396 or 300 nm respectively. The resulting intensity decay is a convolution of the fluorescence decay with the IRF and iterative reconvolution of the IRF with a decay function and non-linear least squares analysis was used to analyse the convoluted data.^{126,128,129}

IR spectra were recorded as KBr discs using either a Perkin Elmer 1600 series or Spectrum 100 series FT-IR spectrometer.

Single-crystal diffraction experiments were carried out on Bruker 3-circle diffractometers with CCD area detectors, APEX (**5**, **14**, **25a**), SMART 1K (**13**, **15**, **22**) or SMART 6K (**4**, **7**, **11**, **12**) using graphite-monochromated Mo- K_{α} radiation ($\lambda = 0.71073$ Å) and Cryostream (Oxford Cryosystems) open-flow N₂ cryostats. The structures were solved by direct methods and refined by full-matrix least squares against F^2 of all data, using SHELXTL software.¹³⁰ Non-H atoms were refined in anisotropic and H atoms in isotropic approximation.

2.12.2 Synthesis of Rh-C≡C-TMS-based rhodacyclopentadienes

1 - *mer,cis*-[tris(trimethylphosphine)trimethylsilylethynyl-2,5-bis(phenylethynyl)-3,4-bis(phenyl)rhodacyclopenta-2,4-diene]

Trimethylsilylacetylene (0.047 mmol, 7 μ l) in THF (1 ml) was added dropwise with stirring to a solution of Rh(PMe₃)₄Me (0.047 mmol, 20 mg) in THF (1 ml) and the resulting solution was stirred for a further 5 min. Then 1,4-biphenylbuta-1,3-diyne (0.094 mmol, 19 mg) in THF (1 ml) was added and the solution stirred for an additional min, before the solvent was removed *in vacuo*. A second volume of THF (2 ml) was added and the solution stirred for 5 min. Again, the solvent was removed *in vacuo*. This process was repeated once more. The product was recrystallised from THF and hexane to give an orange solid. Yield: 33 mg, 85 %. ¹H NMR (400 MHz) δ : 7.72 (d, (AB)', J = 8 Hz, 2H CH_{arom}), 7.40 (d, (AB)', J = 7 Hz, 2H, CH_{arom}), 7.31 (d, (AB)', J = 8 Hz, 2H, CH_{arom}), 7.23 (d, (AB)', J = 8 Hz, 2H, CH_{arom}), 7.06 (m, 12H, CH_{arom}), 1.38 (d, J = 8 Hz, 9H, PMe₃ *trans* to C), 1.35 (vt, J = 3 Hz, 18H, PMe₃ *trans* to PMe₃), 0.37 ppm (s, 9H, SiMe₃). ³¹P{¹H} NMR (121 MHz) δ : -9.32 (dd, ¹ J_{RhP} = 98 Hz, ² J_{PP} = 31 Hz, 2P), -23.10 ppm (dt, ¹ J_{RhP} = 82 Hz, ² J_{PP} = 31 Hz, 1P). Anal. Calcd. for C₄₆H₅₆RhP₃Si: C, 66.34; H, 6.78. Found: C, 66.36; H, 6.94 %. IR (KBr): $\nu_{(C\equiv C)}$ = 2024, 2126, 2156 cm⁻¹. Raman (solid): $\nu_{(arene\ rings)}$ = 1418, 1444, 1594, $\nu_{(C\equiv C)}$ = 2141 cm⁻¹.

2 - *mer,cis*-[tris(trimethylphosphine)trimethylsilylethynyl-2,5-bis(4-tolylethynyl)-3,4-bis(4-tolyl)rhodacyclopenta-2,4-diene]

Trimethylsilylacetylene (0.047 mmol, 7 μ l) in THF (1 ml) was added dropwise with stirring to a solution of Rh(PMe₃)₄Me (0.047 mmol, 20 mg) in THF (1 ml) and the resulting solution was stirred for an additional 5 min. Then 1,4-bis(4-tolyl)buta-1,3-diyne (0.094 mmol, 22 mg) in THF (1 ml) was added dropwise and the solution stirred for 5 min and the solvent was removed *in vacuo*. A second volume of THF (2 ml) was added and the resulting solution was stirred for 5 min. Again, the solvent was removed *in vacuo*. This cycle was repeated once more. The product was recrystallised from THF and hexane to give an orange solid. Yield: 39 mg, 94 %. ¹H NMR (400 MHz) δ : 7.62 (d, (AB)', J = 8 Hz, 2H, CH_{arom}), 7.42 (d, (AB)', J = 8 Hz, 2H, CH_{arom}), 7.35 (d, (AB)', J = 8 Hz, 2H,

CH_{arom}), 7.28 (d, (AB)', $J = 8$ Hz, 2H, CH_{arom}), 6.96 (d, (AB)', $J = 8$ Hz, 2H, CH_{arom}), 7.07 (d, (AB)', $J = 8$ Hz, 2H, CH_{arom}), 7.01 (d, (AB)', $J = 8$ Hz, 2H, CH_{arom}), 6.92 (d, (AB)', $J = 8$ Hz, 2H, CH_{arom}), 2.09 (s, 3H, Me), 2.08 (s, 3H, Me), 2.04 (s, 3H, Me), 2.02 (s, 3H, Me), 1.48 (d, $J = 8$ Hz, 9H, PMe₃ *trans* to C), 1.39 (vt, $J = 3$ Hz, 18H, PMe₃ *trans* to PMe₃), 0.41 ppm (s, 9H, SiMe₃). ³¹P{¹H} NMR (121 MHz) δ : -8.84 (dd, ¹ $J_{RhP} = 99$ Hz, ² $J_{PP} = 31$ Hz, 2P), -23.20 ppm (dt, ¹ $J_{RhP} = 82$ Hz, ² $J_{PP} = 31$ Hz, 1P). Anal. Calcd. for C₅₀H₆₄RhP₃Si: C, 67.56; H, 7.26. Found: C, 67.74; H, 7.28 %. IR (KBr): $\nu_{(C\equiv C)} = 2022, 2129, 2159$ cm⁻¹.

3 - *mer,cis*-[tris(trimethylphosphine)trimethylsilylethynyl-2,5-bis(4-methoxyphenylethynyl)-3,4-bis(4-methoxyphenyl)rhodacyclopenta-2,4-diene]

Trimethylsilylacetylene (0.047 mmol, 7 μ l) in THF (1 ml) was added dropwise with stirring to a solution of Rh(PMe₃)₄Me (0.047 mmol, 20 mg) in THF (1 ml) and the resulting solution stirred for 5 min. Then 1,4-bis(4-methoxyphenyl)buta-1,3-diyne (0.094 mmol, 25 mg) in THF (1 ml) was added and the solution was stirred for an additional 5 min and then the solvent was removed *in vacuo*. A second volume of THF (2 ml) was added and the solution was stirred for 5 min. The solvent was removed *in vacuo*. This cycle was repeated once more. The resulting solid was dissolved in d⁶-benzene and heated for 4 h at 80 °C to give complete conversion to product, which was recrystallised from THF and hexane to give an orange solid. Yield: 36 mg, 91 %. ¹H NMR (400 MHz) δ : 7.63 (d, (AB)', $J = 9$ Hz, 2H, CH_{arom}), 7.30 (d, (AB)', $J = 9$ Hz, 2H, CH_{arom}), 7.21 (d, (AB)', $J = 9$ Hz, 2H, CH_{arom}), 7.12 (d, (AB)', $J = 9$ Hz, 2H, CH_{arom}), 6.73 (d, (AB)', $J = 9$ Hz, 2H, CH_{arom}), 6.70 (d, (AB)', $J = 9$ Hz, 2H, CH_{arom}), 6.90 (d, (AB)', $J = 9$ Hz, 2H, CH_{arom}), 6.56 (d, (AB)', $J = 9$ Hz, 2H, CH_{arom}), 3.15 (s, 3H, Me), 3.13 (s, 3H, Me), 3.08 (s, 3H, Me), 3.06 (s, 3H, Me), 1.37 (d, $J = 7$ Hz, 9H, PMe₃ *trans* to C), 1.28 (vt, $J = 3$ Hz, 18H, PMe₃ *trans* to PMe₃), 0.43 ppm (s, 9H, SiMe₃). ³¹P{¹H} NMR (121 MHz) δ : -8.68 (dd, ¹ $J_{RhP} = 99$ Hz, ² $J_{PP} = 31$ Hz, 2P), -23.22 ppm (dt, ¹ $J_{RhP} = 82$ Hz, ² $J_{PP} = 31$ Hz, 1P). Anal. Calcd. for C₄₈H₆₄RhP₃O₄Si: C, 63.02; H, 7.25. Found: C, 62.68; H, 6.68 %. IR (KBr): $\nu_{(C\equiv C)} = 2018, 2133, 2156$ cm⁻¹.

4 - *mer,cis*-[tris(trimethylphosphine)trimethylsilylethynyl-2,5-bis(4-thiomethoxyphenylethynyl)-3,4-bis(4-thiomethoxyphenyl)rhodacyclopenta-2,4-diene]

Trimethylsilylacetylene (0.047 mmol, 7 μ l) in THF (1 ml) was added dropwise with stirring to a solution of Rh(PMe₃)₄Me (0.047 mmol, 20 mg) in THF (1 ml) and the resulting solution was stirred for 5 min. Then 1,4-bis(4-thiomethoxyphenyl)buta-1,3-diyne (0.094 mmol, 28 mg) in THF (1 ml) was added and the solution was stirred for an additional 5 min and then solvent was removed *in vacuo*. A second volume of THF (2 ml) was added and the solution was stirred for 5 min and then the solvent was removed *in vacuo*. This cycle was repeated once more. The resulting solid was dissolved in d⁶-benzene and heated at 80 °C overnight to give complete conversion to product, which was recrystallised from THF and hexane to give a dark orange solid. Crystals suitable for X-ray analysis were grown from a solution in THF layered with hexanes. Yield: 31 mg, 64 %. ¹H NMR (300 MHz) δ : 7.66 (d, (AB)`, $J = 8$ Hz, 2H, CH_{arom}), 7.37 (d, (AB)`, $J = 8$ Hz, 2H, CH_{arom}), 7.19 (m, 6H, CH_{arom}), 7.02 (d, $J = 8$ Hz, (AB)`, 2H, CH_{arom}), 6.75 (d, (AB)`, $J = 8$ Hz, 4H, CH_{arom}), 1.95 (s, 3H, Me), 1.93 (s, 3H, Me), 1.91 (s, 3H, Me), 1.90 (s, 3H, Me), 1.45 (d, $J = 8$ Hz, 9H, PMe₃ *trans* to C), 1.37 (vt, $J = 3$ Hz, 18H, PMe₃ *trans* to PMe₃), 0.23 ppm (s, 9H, SiMe₃). ³¹P{¹H} NMR (121 MHz) δ : -8.91 (dd, ¹ $J_{RhP} = 98$ Hz, ² $J_{PP} = 31$ Hz, 2P), -23.32 ppm (dt, ¹ $J_{RhP} = 82$ Hz, ² $J_{PP} = 31$ Hz, 1P). Anal. Calcd. for C₅₀H₆₄RhP₃SiS₄: C, 59.04; H, 6.34. Found: C, 59.04; H, 6.35 %. IR (KBr): $\nu_{(C\equiv C)} = 2024, 2124, 2156$ cm⁻¹.

5 - *mer,cis*-[tris(trimethylphosphine)trimethylsilylethynyl-2,5-bis(4-trifluoromethylphenylethynyl)-3,4-bis(4-trifluoromethylphenyl)rhodacyclopenta-2,4-diene]

Trimethylsilylacetylene (0.047 mmol, 7 μ l) in THF (1 ml) was added dropwise with stirring to a solution of Rh(PMe₃)₄Me (0.047 mmol, 20 mg) in THF (1 ml) and the resulting solution was stirred for a further 5 min. Then 1,4-bis(4-trifluoromethylphenyl)buta-1,3-diyne (0.094 mmol, 32 mg) in THF (1 ml) was added and the solution was stirred for 5 min and then the solvent was removed *in vacuo*. A second volume of THF (2 ml) was added and the solution was again stirred for 5 min. Again, the solvent was removed *in vacuo*. This cycle was repeated once more and resulted in an orange solid, which was recrystallised from THF and hexane. Crystals suitable for X-ray

analysis were grown from a solution of THF layered with hexanes. Yield: 42 mg, 81 %. ^1H NMR (400 MHz) δ : 7.54 (d, (AB)', $J = 8$ Hz, 2H, CH_{arom}), 7.42 (d, (AB)', $J = 8$ Hz, 2H, CH_{arom}), 7.36 (d, (AB)', $J = 8$ Hz, 2H, CH_{arom}), 7.35 (d, (AB)', $J = 8$ Hz, 2H, CH_{arom}), 7.27 (d, (AB)', $J = 8$ Hz, 2H, CH_{arom}), 7.21 (d, (AB)', $J = 8$ Hz, 2H, CH_{arom}), 7.11 (d, (AB)', $J = 8$ Hz, 2H, CH_{arom}), 6.95 (d, (AB)', $J = 8$ Hz, 2H, CH_{arom}), 1.35 (d, $J = 8$ Hz, 9H, PMe_3 *trans* to C), 1.29 (vt, $J = 3$ Hz, 18H, PMe_3 *trans* to PMe_3), 0.41 ppm (s, 9H, SiMe_3). $^{31}\text{P}\{^1\text{H}\}$ NMR (121 MHz) δ : -11.95 (dd, $^1J_{\text{RhP}} = 96$ Hz, $^2J_{\text{PP}} = 31$ Hz, 2P), -25.31 ppm (dt, $^1J_{\text{RhP}} = 82$ Hz, $^2J_{\text{PP}} = 31$ Hz, 1P). $^{19}\text{F}\{^1\text{H}\}$ (188 MHz) δ : -62.33 (s, 3F), -62.35 (s, 3F), -62.66 (s, 3F), -62.72 (s, 3F). Anal. Calcd. for $\text{C}_{50}\text{H}_{52}\text{RhP}_3\text{SiF}_{12}$: C, 54.35; H, 4.74. Found: C, 54.37; H, 4.72 %. IR (KBr): $\nu_{(\text{C}=\text{C})} = 2027, 2134, 2156$ cm^{-1} . Raman (solid): $\nu_{(\text{arene rings})} = 1435, 1607, \nu_{(\text{C}=\text{C})} = 2137$ cm^{-1} .

6 - *mer,cis*-[tris(trimethylphosphine)trimethylsilylethynyl-2,5-bis(4-carbomethoxyphenylethynyl)-3,4-bis(4-carbomethoxyphenyl)rhodacyclopenta-2,4-diene]

Trimethylsilylacetylene (0.047 mmol, 7 μl) in THF (1 ml) was added dropwise with stirring to a solution of $\text{Rh}(\text{PMe}_3)_4\text{Me}$ (0.047 mmol, 20 mg) in THF (1 ml) and the resulting solution stirred for a further 5 min. Then 1,4-bis(4-carbomethoxyphenyl)buta-1,3-diyne (0.094 mmol, 30 mg) in THF (1 ml) was added and the solution stirred for 5 min and then the solvent was removed *in vacuo*. A second volume of THF (2 ml) was added and the solution was again stirred for 5 min and the THF was removed *in vacuo*. This process was repeated once more resulting in a red solid which was recrystallised from THF and hexane. Yield: 48 mg, 96 %. ^1H NMR (400 MHz) δ : 8.19 (d, (AB)', $J = 9$ Hz, 2H, CH_{arom}), 8.16 (d, (AB)', $J = 9$ Hz, 2H, CH_{arom}), 8.11 (d, (AB)', $J = 9$ Hz, 2H, CH_{arom}), 8.02 (d, (AB)', $J = 9$ Hz, 2H, CH_{arom}), 7.70 (d, (AB)', $J = 9$ Hz, 2H, CH_{arom}), 7.35 (d, (AB)', $J = 9$ Hz, 2H, CH_{arom}), 7.27 (d, (AB)', $J = 9$ Hz, 2H, CH_{arom}), 7.17 (d, (AB)', $J = 9$ Hz, 2H, CH_{arom}), 3.46 (s, 3H, CO_2Me), 3.44 (s, 3H, CO_2Me), 3.42 (s, 3H, CO_2Me), 3.41 (s, 3H, CO_2Me), 1.36 (d, $J = 8$ Hz, 9H, PMe_3 *trans* to C), 1.28 (vt, $J = 3$ Hz, 18H, PMe_3 *trans* to PMe_3), 0.31 ppm (s, 9H, SiMe_3). $^{31}\text{P}\{^1\text{H}\}$ NMR (121 MHz) δ : -9.35 (dd, $^1J_{\text{RhP}} = 96$ Hz, $^2J_{\text{PP}} = 31$ Hz, 2P), -22.81 ppm (dt, $^1J_{\text{RhP}} = 82$ Hz, $^2J_{\text{PP}} = 31$ Hz, 1P). Anal. Calcd. for $\text{C}_{54}\text{H}_{64}\text{RhP}_3\text{SiO}_8$: C, 60.90; H, 6.06. Found: C, 60.84; H, 6.09 %. IR (KBr): $\nu_{(\text{C}=\text{O})} = 1719, \nu_{(\text{C}=\text{C})} = 2031, 2129$ cm^{-1} .

7 - *mer,cis*-[tris(trimethylphosphine)trimethylsilylethynyl-2,5-bis(4-cyanophenyl-ethynyl)-3,4-bis(4-cyanophenyl)rhodacyclopenta-2,4-diene]

Trimethylsilylacetylene (0.047 mmol, 7 μ l) in THF (1 ml) was added dropwise with stirring to a solution of Rh(PMe₃)₄Me (0.047 mmol, 20 mg) in THF (1 ml) and the resulting solution was stirred for a further 5 min. The 1,4-bis(4-cyanophenyl)buta-1,3-diyne (0.094 mmol, 24 mg) in THF (1 ml) was added and the solution was stirred for 5 min and then the solvent was removed *in vacuo*. A second volume of THF (2 ml) was added and the solution was stirred for 5 min. Again, the solvent was removed *in vacuo*. This cycle was repeated once more. The product was recrystallised from THF and hexane to give a red solid. Crystals suitable for X-ray analysis were grown by slow evaporation from a THF/hexane solution. Yield: 34 mg, 77 %. ¹H NMR (400 MHz) δ : 7.62 (d, (AB)', J = 9 Hz, 2H, CH_{arom}), 7.10 (d, (AB)', J = 8 Hz, 2H, CH_{arom}), 7.08 (d, (AB)', J = 9 Hz, 2H, CH_{arom}), 7.05 (d, (AB)', J = 8 Hz, 2H, CH_{arom}), 6.93 (d, (AB)', J = 8 Hz, 2H, CH_{arom}), 6.91 (d, (AB)', J = 8 Hz, 2H, CH_{arom}), 6.82 (d, (AB)', J = 8 Hz, 2H, CH_{arom}), 6.73 (d, (AB)', J = 9 Hz, 2H, CH_{arom}), 1.26 (d, J = 8 Hz, 9H, PMe₃ *trans* to C), 1.18 (vt, J = 3 Hz, 18H, PMe₃ *trans* to PMe₃), 0.26 ppm (s, 9H, SiMe₃). ³¹P{¹H} NMR (121 MHz) δ : -9.65 (dd, ¹ J_{RhP} = 96 Hz, ² J_{PP} = 31 Hz, 2P), -22.78 ppm (dt, ¹ J_{RhP} = 82 Hz, ² J_{PP} = 31 Hz, 1P). Anal. Calcd. for C₅₀H₆₄RhP₃SiO₄: C, 64.37; H, 5.62; N, 6.00. Found: C, 64.03; H, 5.98; N, 5.86 %. IR (KBr): $\nu_{(C=C)}$ = 2027, 2131, $\nu_{(C=N)}$ = 2224 cm⁻¹.

9 - *mer,cis*-[tris(trimethylphosphine)trimethylsilylethynyl-2,5-bis(4-nitrophenylethynyl)-3,4-bis(4-nitrophenyl)rhodacyclopenta-2,4-diene]

Trimethylsilylacetylene (0.047 mmol, 7 μ l) in THF (1 ml) was added dropwise with stirring to a solution of Rh(PMe₃)₄Me (0.047 mmol, 20 mg) in THF (1 ml) and the resulting solution was stirred for 5 min. Then 1,4-bis(4-nitrophenyl)buta-1,3-diyne (0.094 mmol, 28 mg) in THF (1 ml) was added and the solution was stirred for an additional 5 min and then the solvent was removed *in vacuo*. Further THF (2 ml) was added and the solution was stirred for 5 min and the solvent was removed *in vacuo*. This cycle was repeated once more. Yield: 40 mg, 83 %. ¹H NMR (400 MHz) δ : 7.98 (d, (AB)', J = 9 Hz, 2H, CH_{arom}), 7.96 (d, (AB)', J = 9 Hz, 2H, CH_{arom}), 7.92 (d, (AB)', J = 9 Hz, 2H, CH_{arom}), 7.80 (d, (AB)', J = 9 Hz, 2H, CH_{arom}), 7.39 (d, (AB)', J = 9 Hz, 2H, CH_{arom}), 7.04

(d, (AB)`, $J = 9$ Hz, 2H, CH_{arom}), 6.96 (d, (AB)`, $J = 9$ Hz, 2H, CH_{arom}), 6.82 (d, (AB)`, $J = 9$ Hz, 2H, CH_{arom}), 1.33 (d, $J = 8$ Hz, 9H, PMe₃ *trans* to C), 1.27 (vt, $J = 3$ Hz, 18H, PMe₃ *trans* to PMe₃), 0.28 ppm (s, 9H, SiMe₃). ³¹P{¹H} NMR (121 MHz) δ : -10.27 (dd, ¹ $J_{RhP} = 95$ Hz, ² $J_{PP} = 31$ Hz, 2P), -23.04 ppm (dt, ¹ $J_{RhP} = 82$ Hz, ² $J_{PP} = 31$ Hz, 1P). Anal. Calcd. for C₄₆H₅₂RhP₃N₄O₈Si: C, 54.55; H, 5.17; N, 5.53. Found: C, 55.05; H, 5.47; N, 4.90 %. IR (KBr): $\nu_{(NO_2)} = 1335, 1511$, $\nu_{(arene\ ring)} = 1587$, $\nu_{(C\equiv C)} = 2026, 2132$ cm⁻¹.

10a - *mer,cis*-[tris(trimethylphosphine)trimethylsilylethynyl-2,5-bis(4-trimethylsilylethynylphenylethynyl)-3,4-bis(4-trimethylsilylethynylphenyl)rhodacyclopenta-2,4-diene]

Trimethylsilylacetylene (0.047 mmol, 7 μ l) in THF (1 ml) was added dropwise with stirring to a solution of Rh(PMe₃)₄Me (0.047 mmol, 20 mg) in THF (1 ml) and the resulting solution stirred for an additional 5 min. Then 1,4-bis(4-trimethylsilylethynylphenyl)buta-1,3-diyne (0.094 mmol, 37 mg) in THF (1 ml) was added and the solution was stirred for 5 min and then the solvent was removed *in vacuo*. A second volume of THF (2 ml) was added and the solution stirred for 5 min. Again, the solvent was removed *in vacuo*. This process was repeated once more and resulted in an orange solid. Yield: 50 mg, 87 %. ¹H NMR (400 MHz) δ : 7.55 (d, (AB)`, $J = 8$ Hz, 2H, CH_{arom}), 7.49 (d, (AB)`, $J = 8$ Hz, 2H, CH_{arom}), 7.46 (d, (AB)`, $J = 8$ Hz, 2H, CH_{arom}), 7.39 (d, (AB)`, $J = 8$ Hz, 2H, CH_{arom}), 7.27 (d, (AB)`, $J = 9$ Hz, 2H, CH_{arom}), 7.19 (d, (AB)`, $J = 8$ Hz, 2H, CH_{arom}), 7.08 (d, (AB)`, $J = 8$ Hz, 2H, CH_{arom}), 7.01 (d, (AB)`, $J = 8$ Hz, 2H, CH_{arom}), 1.30 (d, $J = 8$ Hz, 9H, PMe₃ *trans* to C), 1.21 (vt, $J = 4$ Hz, 18H, PMe₃ *trans* to PMe₃), 0.28 ppm (s, 9H, SiMe₃), 0.24 ppm (s, 9H, SiMe₃), 0.22 ppm (s, 9H, SiMe₃), 0.21 ppm (s, 18H, 2 x SiMe₃). ³¹P{¹H} NMR (121 MHz) δ : -8.31 (dd, ¹ $J_{RhP} = 97$ Hz, ² $J_{PP} = 31$ Hz, 2P), -22.13 ppm (dt, ¹ $J_{RhP} = 82$ Hz, ² $J_{PP} = 31$ Hz, 1P). Anal. Calcd. for C₆₆H₈₈RhP₃Si: C, 65.10; H, 7.28. Found: C, 66.88; H, 6.36 %. IR (KBr): $\nu_{(C-TMS)} = 840, 864, 949$, $\nu_{(Si-CH_3)} = 1249$, $\nu_{(arene\ ring)} = 1505, 1597$, $\nu_{(C\equiv C)} = 2027, 2125, 2153$, $\nu_{(CH_3)} = 2909, 2956$ cm⁻¹.

10b - *mer,cis*-[tris(trimethylphosphine)trimethylsilylethynyl-2,5-bis(4-ethynylphenylethynyl)-3,4-bis(4-ethynylphenyl)rhodacyclopenta-2,4-diene]

A 1.0 M THF solution of ⁿBu₄NF (0.27 mmol, 0.27 ml) was added to a rapidly stirred solution of compound **10a** (0.045 mmol, 50 mg) in THF (5 ml). The solution was

stirred overnight and then the solvent was removed *in vacuo*. The residual solid was redissolved in CHCl₃ (20 ml) and then the solution was washed with water (3 x 10 ml), separated and then dried over MgSO₄. The solvent was removed *in vacuo* to give the product as a red solid. Yield: 31 mg, 74 %. ¹H NMR (400 MHz, CDCl₃) δ: 7.36 (m, 4H, CH_{arom}), 7.28 (m, 6H, CH_{arom}), 7.01 (m, 4H, CH_{arom}), 6.96 (d, *J* = 8 Hz, 2H, CH_{arom}), 3.14 (s, 1H, CH), 3.12 (s, 1H, CH), 3.05 (s, 1H, CH), 3.03 (s, 1H, CH), 1.72 (d, *J* = 8 Hz, 9H, PMe₃ *trans* C), 1.49 (vt, *J* = 3 Hz, 18H, PMe₃ *trans* PMe₃), 0.01 (s, 9H, TMS). ³¹P{¹H} NMR (162 MHz, CDCl₃) δ: -8.42 (dd, ¹*J*_{RhP} = 97 Hz, ²*J*_{PP} = 31 Hz, 2P), -21.87 ppm (dt, ¹*J*_{RhP} = 83 Hz, ²*J*_{PP} = 31 Hz, 1P). ²⁹Si (99 MHz, CDCl₃) δ: -28.01 (s, 1Si, TMS). IR (KBr): ν_(C-TMS) = 837, 947, ν_(arene ring) = 1505, 1598, ν_(C=C) = 2023, 2103, 2130, ν_(CH₃) = 2908, 2952, ν_(CH) = 3288 cm⁻¹.

2.12.3 Synthesis of Rh-C≡C-C₆H₄-NMe₂-based rhodacyclopentadienes

11 - *mer,cis*-[tris(trimethylphosphine)N,N-dimethylaminophenylethynyl-2,5-bis(phenylethynyl)-3,4-bis(phenyl)rhodacyclopenta-2,4-diene]

The compound N,N-dimethyl-4-ethynylaniline (0.047 mmol, 7 mg) in THF (1 ml) was added dropwise to a rapidly stirred solution of Rh(PMe₃)₄Me (0.047 mmol, 20 mg) in THF (1 ml) and the resulting solution was stirred for 5 min. Two equiv. of 1,4-diphenylbuta-1,3-diyne (0.094 mmol, 19 mg) in THF (1 ml) were added and stirring was continued for an additional 5 min and the solvent was then removed *in vacuo*. THF (2 ml) was added and the solution was again stirred for 5 min before removal of the THF *in vacuo*. This process was repeated once more to yield an orange solid. The product was recrystallised from toluene and hexane to give an orange solid. Crystals that were suitable for X-ray analysis were obtained by layering a concentrated toluene solution with hexane. Yield: 37 mg, 89 %. ¹H NMR (400 MHz) δ: 7.65 (d, (AB)`, *J* = 8 Hz, 2H, CH_{arom}), 7.48 (d, (AB)`, *J* = 9 Hz, CH_{arom}), 7.48 (d, (AB)`, *J* = 8 Hz, 2H, CH_{arom}), 7.37 (d, (AB)`, *J* = 8 Hz, CH_{arom}), 7.07 (m, 14H, CH_{arom}), 6.67 (d, *J* = 9 Hz, 2H, CH_{arom}), 2.42 (s, 6H, NMe₂), 1.41 (d, *J* = 8 Hz, 9H, PMe₃ *trans* to C), 1.33 (vt, *J* = 4 Hz, 18H, PMe₃ *trans* to PMe₃). ³¹P{¹H} NMR (161 MHz) δ: -8.43 (dd, ¹*J*_{RhP} = 98 Hz, ²*J*_{PP} = 31 Hz, 2P), -21.30 ppm (dt,

$^1J_{RhP} = 82$ Hz, $^2J_{PP} = 31$ Hz, 1P). Anal. Calcd. for $C_{51}H_{57}RhNP_3$: C, 69.62; H, 6.53; N, 1.59. Found: C, 69.35; H, 6.52; N, 1.57 %. IR (KBr): $\nu_{(C\equiv C)} = 2098, 2134, 2156$ cm^{-1} .

12 - *mer,cis*-[tris(trimethylphosphine)N,N-dimethylaminophenylethynyl-2,5-bis(4-tolylolethynyl)-3,4-bis(4-tolyl)rhodacyclopenta-2,4-diene]

The compound N,N-dimethyl-4-ethynylaniline (0.047 mmol, 7 mg) in THF (1 ml) was added dropwise to a rapidly stirred solution of $Rh(PMe_3)_4Me$ (0.047 mmol, 20 mg) in THF (1 ml). The resulting solution was stirred for 5 min. Two equiv. of 1,4-bis(4-tolyl)buta-1,3-diyne (0.094 mmol, 22 mg) in THF (1 ml) were added and stirring was continued for 5 min. The solvent was then removed *in vacuo*. THF (2 ml) was added, the solution was stirred for an additional 5 min and again the solvent removed *in vacuo*. This process was repeated once more to yield an orange solid, which was recrystallised from toluene and hexane. Crystals suitable for X-ray analysis were obtained by layering a concentrated toluene solution with hexane. Yield: 41 mg, 44 %. 1H NMR (300 MHz) δ : 7.65 (d, (AB)', $J = 8$ Hz, 2H, CH_{arom}), 7.59 (d, (AB)', $J = 8$ Hz, 2H, CH_{arom}), 7.48 (d, (AB)', $J = 8$ Hz, 2H, CH_{arom}), 7.38 (d, (AB)', $J = 8$ Hz, 2H, CH_{arom}), 7.25 (d, (AB)', $J = 8$ Hz, 2H, CH_{arom}), 7.08 (d, (AB)', $J = 8$ Hz, 2H, CH_{arom}), 7.05 (d, (AB)', $J = 8$ Hz, 2H, CH_{arom}), 6.93 (d, (AB)', $J = 8$ Hz, CH_{arom}), 6.70 (m, 4H, CH_{arom}), 2.56 (s, 6H, NMe_2), 2.10 (s, 6H, Me), 1.94 (s, 3H, Me), 1.91 (s, 3H, Me), 1.51 (d, $J = 8$ Hz, 9H, PMe_3 *trans* to C), 1.43 (s, 18H, PMe_3 *trans* to PMe_3). $^{31}P\{^1H\}$ NMR (121 MHz) δ : -8.16 (dd, $^1J_{RhP} = 98$ Hz, $^2J_{PP} = 31$ Hz, 2P), -21.31 ppm (dt, $^1J_{RhP} = 82$ Hz, $^2J_{PP} = 31$ Hz, 1P). Anal. Calcd. for $C_{55}H_{61}RhNP_3$: C, 70.89; H, 6.60; N, 1.50. Found: C, 70.88; H, 6.88; N, 1.35 %. IR (KBr): $\nu_{(C\equiv C)} = 2091, 2124, 2160$ cm^{-1} .

13 - *mer,cis*-[tris(trimethylphosphine)N,N-dimethylaminophenylethynyl-2,5-bis(4-methoxyphenylethynyl)-3,4-bis(4-methoxyphenyl)rhodacyclopenta-2,4-diene]

N,N-dimethyl-4-ethynylaniline (0.047 mmol, 7 mg) in THF (1 ml) was added dropwise to a rapidly stirred solution of $Rh(PMe_3)_4Me$ (0.047 mmol, 20 mg) in THF (1 ml) and the resulting solution was stirred for 5 min. Two equiv. of 1,4-bis(4-methoxyphenyl)buta-1,3-diyne (0.094 mmol, 25 mg) in THF (1 ml) were added and stirring was continued for an additional 5 min and the solvent was then removed *in vacuo*. THF (2 ml) was added, the solution was again stirred 5 min and the solvent removed. This

process was repeated once more to yield an orange solid, which was recrystallised from THF and hexane. Crystals suitable for X-ray analysis were grown by slow evaporation of a THF/hexane solution. Yield: 38 mg, 81 %. ^1H NMR (400 MHz) δ : 7.65 (d, (AB)', $J = 8$ Hz, 2H, CH_{arom}), 7.60 (d, (AB)', $J = 9$ Hz, 2H, CH_{arom}), 7.49 (d, (AB)', $J = 9$ Hz, 2H, CH_{arom}), 7.39 (d, (AB)', $J = 9$ Hz, 2H, CH_{arom}), 7.28 (d, (AB)', $J = 9$ Hz, 2H, CH_{arom}), 6.89 (d, (AB)', $J = 9$ Hz, 2H, CH_{arom}), 6.86 (d, (AB)', $J = 8$ Hz, 2H, CH_{arom}), 6.70 (d, (AB)', $J = 9$ Hz, 2H, CH_{arom}), 6.68 (d, (AB)', $J = 9$ Hz, 2H, CH_{arom}), 6.62 (d, (AB)', $J = 9$ Hz, 2H, CH_{arom}), 3.21 (s, 3H, OMe), 3.29 (s, 3H, OMe), 3.23 (s, 3H, OMe), 3.15 (s, 3H, OMe), 2.54 (s, 6H, NMe_2), 1.55 (d, $J = 8$ Hz, 9H, PMe_3 *trans* to C), 1.47 (vt, $J = 4$ Hz, 18H, PMe_3 *trans* to PMe_3). $^{31}\text{P}\{^1\text{H}\}$ NMR (121 MHz) δ : -8.07 (dd, $^1J_{\text{RhP}} = 99$ Hz, $^2J_{\text{PP}} = 31$ Hz, 2P), -21.40 ppm (dt, $^1J_{\text{RhP}} = 82$ Hz, $^2J_{\text{PP}} = 31$ Hz, 1P). Anal. Calcd. for $\text{C}_{55}\text{H}_{65}\text{RhNO}_4\text{P}_3$: C, 66.06; H, 6.55; N, 1.40. Found: C, 65.86; H, 6.57; N, 1.25 %. IR (KBr): $\nu_{(\text{C}=\text{C})} = 2087, 2138, 2152, \text{cm}^{-1}$.

14 - *mer,cis*-[tris(trimethylphosphine)*N,N*-dimethylaminophenylethynyl-2,5-bis(4-trifluoromethylphenylethynyl)-3,4-bis(4-trifluoromethylphenyl)rhodacyclopenta-2,4-diene]

N,N-dimethyl-4-ethynylaniline (0.047 mmol, 7 mg) in THF (1 ml) was added dropwise to a rapidly stirred solution of $\text{Rh}(\text{PMe}_3)_4\text{Me}$ (0.047 mmol, 20 mg) in THF (1 ml) and the resulting solution was stirred for 5 min. Two equiv. of 1,4-bis(4-trifluoromethylphenyl)buta-1,3-diyne (0.094 mmol, 32 mg) in THF (1 ml) were added and stirring was continued for a further 5 min. The solvent was then removed *in vacuo*. THF (2 ml) was added, the solution was again stirred for 5 min and then solvent removed. This process was repeated once more to yield an orange/red solid, which was recrystallised from THF and hexane. Crystals suitable for X-ray analysis were grown by layering a THF solution with hexane. Yield: 44 mg, 81 %. ^1H NMR (400 MHz) δ : 7.40 (m, 8H, CH_{arom}), 7.26 (d, (AB)', $J = 8$ Hz, 4H, CH_{arom}), 7.16 (m, 4H, CH_{arom}), 6.97 (d, $J = 8$ Hz, 2H, CH_{arom}), 6.62 (d, $J = 9$ Hz, 2H, CH_{arom}), 2.54 (s, 6H, NMe_2), 1.40 (d, $J = 8$ Hz, 9H, PMe_3 *trans* to C), 1.35 (vt, $J = 3$ Hz, 18H, PMe_3 *trans* to PMe_3). $^{31}\text{P}\{^1\text{H}\}$ NMR (161 MHz) δ : -8.87 (dd, $^1J_{\text{RhP}} = 98$ Hz, $^2J_{\text{PP}} = 31$ Hz, 2P), -21.13 ppm (dt, $^1J_{\text{RhP}} = 82$ Hz, $^2J_{\text{PP}} = 31$ Hz, 1P). $^{19}\text{F}\{^1\text{H}\}$ (282 Hz) δ : -62.24 (s, 3F), -62.26 (s, 3F), -62.65 (s, 6F). Anal. Calcd. for $\text{C}_{55}\text{H}_{53}\text{RhF}_{12}\text{NP}_3$: C, 57.50; H, 4.65; N, 1.22. Found: C, 57.43; H, 4.64; N, 1.22 %. IR (KBr): $\nu_{(\text{C}=\text{C})} = 2094, 2133, 2156 \text{cm}^{-1}$.

15 - *mer,cis*-[tris(trimethylphosphine)N,N-dimethylaminophenylethynyl-2,5-bis(4-carbomethoxyphenylethynyl)-3,4-bis(4-carbomethoxyphenyl)rhodacyclopenta-2,4-diene]

The compound N,N-dimethyl-4-ethynylaniline (0.047 mmol, 7 mg) in THF (1 ml) was added dropwise to a stirred solution of Rh(PMe₃)₄Me (0.047 mmol, 20 mg) in THF (1 ml) and the resulting solution stirred for a further 5 min. A solution of 1,4-bis(4-carbomethoxyphenyl)buta-1,3-diyne (0.094 mmol, 30 mg) in THF (1 ml) was added and the solution was stirred for 5 min and then the solvent was removed *in vacuo*. A second volume of THF (2 ml) was added and the solution was again stirred for 5 min. THF was removed *in vacuo*. This process was repeated once more resulting in a red solid which was recrystallised from THF and hexane. Crystals that were suitable for X-ray analysis were obtained by layering a concentrated THF solution with hexane. Yield: 47 mg, 89 %. ¹H NMR (400 MHz) δ: 8.19 (d, (AB)', *J* = 8 Hz, 2H, CH_{arom}), 8.16 (d, (AB)', *J* = 8 Hz, 2H, CH_{arom}), 8.02 (d, (AB)', *J* = 8 Hz, 2H, CH_{arom}), 7.91 (d, (AB)', *J* = 8 Hz, 2H, CH_{arom}), 7.57 (d, (AB)', *J* = 8 Hz, 2H, CH_{arom}), 7.49 (d, (AB)', *J* = 8 Hz, 2H, CH_{arom}), 7.40 (d, (AB)', *J* = 8 Hz, 2H, CH_{arom}), 7.31 (d, (AB)', *J* = 8 Hz, 2H, CH_{arom}), 7.20 (d, (AB)', *J* = 8 Hz, 2H, CH_{arom}), 6.65 (d, (AB)', *J* = 9 Hz, 2H, CH_{arom}), 3.47 (s, 3H, CO₂Me), 3.46 (s, 3H, CO₂Me), 3.46 (s, 3H, CO₂Me), 3.44 (s, 3H, CO₂Me), 2.55 (s, 6H, NMe₂), 1.41 (d, *J* = 8 Hz, 9H, PMe₃ *trans* to C), 1.34 (vt, *J* = 3 Hz, 18H, PMe₃ *trans* to PMe₃). ³¹P{¹H} NMR (121 MHz) δ: -8.77 (dd, ¹*J*_{RhP} = 97 Hz, ²*J*_{PP} = 31 Hz, 2P), -21.06 ppm (dt, ¹*J*_{RhP} = 82 Hz, ²*J*_{PP} = 31 Hz, 1P). Anal. Calcd. for C₆₀H₆₅RhNO₈P₃: C, 64.12; H, 5.83; N, 1.25. Found: C, 63.58; H, 5.87; N, 1.18 %. IR (KBr): ν_(C=O) = 1718, ν_(C≡C) = 2098, 2128 cm⁻¹.

2.12.4 Synthesis of Rh-C≡C-C≡C-C₆H₄-NPh₂-based rhodacyclopentadienes and the related compound [RhH(PMe₃)₃(C≡C-C≡C-Ph-NPh₂)₂]

16 - *mer,cis*-[tris(trimethylphosphine)N,N-diphenylaminophenylbutadiynyl-2,5-bis(4-tolyethynyl)-3,4-bis(4-tolyl)rhodacyclopenta-2,4-diene]

The compound 4-(N,N-diphenylamino)phenylbutadiyne (0.047 mmol, 15 mg) in THF (1 ml) was added dropwise to a stirred solution of Rh(PMe₃)₄Me (0.047 mmol, 20 mg) in THF (1 ml) and the resulting solution was stirred for a further 5 min. Then 1,4-

bis(4-tolyl)buta-1,3-diyne (0.096 mmol, 23 mg) in THF (1 ml) was added and the solution was stirred for 5 min and then the solvent was removed *in vacuo*. A second volume of THF (2 ml) was added and the solution was stirred for 5 min. Again, the solvent was removed *in vacuo*. This process was repeated once more. NMR spectroscopy showed the reaction had not reached completion and so the C₆D₆ solution was allowed to stand at room temperature for 48 h with the sample monitored by ³¹P{¹H} NMR spectroscopy until the reaction was complete. Yield: 40 mg, 77 %. ¹H NMR (400 MHz) δ: 8.20 (d, *J* = 8 Hz, 2H, CH_{arom}), 7.64 (d, *J* = 9 Hz, 2H, CH_{arom}), 7.63 (d, *J* = 7 Hz, 2H, CH_{arom}), 7.49 (d, *J* = 8 Hz, 2H, CH_{arom}), 7.38 (d, *J* = 8 Hz, 2H, CH_{arom}), 7.35 (s, 2H, CH_{arom}), 7.27 (d, *J* = 8 Hz, 2H, CH_{arom}), 7.18 (m, 8H, CH_{arom}), 7.09 (d, *J* = 8 Hz, 2H, CH_{arom}), 7.01 (m, 6H, CH_{arom}), 2.30 (s, 3H, Me), 2.27 (s, 3H, Me), 2.22 (s, 3H, Me), 2.15 (s, 3H, Me), 1.62 (d, ¹*J* = 7 Hz, 9H, PMe₃ *trans* to C), 1.53 (t, ¹*J* = 4 Hz, 18H, PMe₃ *trans* to PMe₃). ³¹P{¹H} NMR (81 MHz) δ: -8.70 (dd, ¹*J*_{RhP} = 98 Hz, ²*J*_{PP} = 31 Hz, 2P), -23.14 ppm (dt, ¹*J*_{RhP} = 82 Hz, ²*J*_{PP} = 31 Hz, 1P). Anal. Calcd. for C₆₇H₆₉RhNP₃: C, 74.23; H, 6.42; N, 1.29. Found: C, 73.64; H, 6.55; N, 1.53 %. IR (KBr): ν_(arene ring) = 1282, 1491, 1504, 1590, ν_(C≡C) = 2041, 2132, 2167 cm⁻¹.

17 - *mer,trans*-[RhH(PMe₃)₃(C≡C-C≡C-Ph-NPh₂)₂]

The compound 4-(N,N-diphenylamino)phenylbutadiyne (0.048 mmol, 15 mg) in THF (1 ml) was added to a stirring solution of Rh(PMe₃)₄Me (0.024 mmol, 10 mg) in THF (1 ml) and the resulting solution stirred for 1 h. Solvent and dissociated PMe₃ were removed *in vacuo* and the resulting solid was recrystallised from hexane. The product was isolated as an off-white solid. Yield: 20 mg, 91 %. ¹H NMR (500 MHz) δ: 7.36 (d, *J* = 9 Hz, 4H, CH_{arom}), 6.95 (m, 14H, CH_{arom}), 6.78 (m, 10H, CH_{arom}), 1.29 (t, *J*_{P_{trans}P} = 3 Hz, 18H, PMe₃), 1.03 (d, *J*_{P_{trans}H} = 8 Hz, 9H, PMe₃), -9.11 (dq, ¹*J*_{Rh-H} = ²*J*_{P_{cis}-H} = 17, ²*J*_{P_{trans}-H} = 191 Hz). ³¹P{¹H} NMR (202 MHz) δ: -7.32 (dd, ¹*J*_{Rh-P} = 92 Hz, ²*J*_{P-P} = 25 Hz, 2P, P *trans* to P), -25.20 (dt, ¹*J*_{Rh-P} = 76 Hz, ²*J*_{P-P} = 25 Hz, 1P, P *trans* to H). Anal. Calcd. for C₅₃H₅₆P₃N₂Rh: C, 69.43; H, 6.16; N, 3.06. Found: C, 70.37; H, 6.22; N, 3.08 %. IR (KBr): ν_(arene ring) = 1273, 1489, 1504, 1590 ν_(Rh-H) = 1954, ν_(C≡C) = 2042, 2171 cm⁻¹.

2.12.5 Synthesis of Rh-Me-based rhodacyclopentadienes

18 - *mer,cis*-[tris(trimethylphosphine)methyl-2,5-bis(phenylethynyl)-3,4-bis(phenyl)-rhodacyclopentadiene]

Rh(PMe₃)₄Me (0.118 mmol, 50 mg) and 1,4-diphenylbuta-1,3-diyne (0.237 mmol, 48 mg) were added to THF (5 ml) and the resulting solution was stirred for 5 min. The solvent was removed *in vacuo* and then THF (2 ml) was added and the solution was stirred for an additional 5 min before the solvent was again removed *in vacuo*. THF (2 ml) was added and the solution was heated to 80 °C for 3 h. The solvent was removed *in vacuo* to give the product as a brown solid. Yield: 71 mg, 81 %. ¹H NMR (500 MHz) δ: 7.61 (d, *J* = 8 Hz, 2H, CH_{arom}), 7.48 (d, *J* = 8 Hz, 2H, CH_{arom}), 7.41 (d, *J* = 8 Hz, 2H, CH_{arom}), 7.31 (d, *J* = 8 Hz, 2H, CH_{arom}), 7.21 (m, 4H, CH_{arom}), 7.08 (t, *J* = 8 Hz, 2H, CH_{arom}), 7.03 (t, *J* = 8 Hz, 4H, CH_{arom}), 6.93 (m, 2H, CH_{arom}), 1.32 (d, *J* = 7 Hz, 9H, PMe₃ *trans* to C), 1.16 (s, 18H, PMe₃ *trans* to PMe₃), 0.09 ppm (q, *J* = 7 Hz, 3H, Me). ³¹P{¹H} NMR (121 MHz) δ: -6.35 (dd, ¹*J*_{RhP} = 105 Hz, ²*J*_{PP} = 34 Hz, 2P), -18.47 (dt, ¹*J*_{RhP} = 89 Hz, ²*J*_{PP} = 34 Hz, 1P). Anal. Calcd. for C₄₂H₅₀RhP₃: C, 67.20; H, 6.71. Found: C, 67.58; H, 6.95 %. IR (KBr): ν(C≡C) = 2125 cm⁻¹.

19 - *mer,cis*-[tris(trimethylphosphine)methyl-2,5-bis(4-tolyethynyl)-3,4-bis(4-tolyl)rhodacyclopentadiene]

Rh(PMe₃)₄Me (0.118 mmol, 50 mg) and 1,4-bis(4-tolyl)buta-1,3-diyne (0.237 mmol, 55 mg) were added to THF (5 ml) and the solution refluxed for 12 h in a sealed Young's tube. The solvent was removed *in vacuo* and then THF (2 ml) was added and the solution was stirred for 5 min. The removal of the solvent and addition of further THF (2 ml) was repeated two more times. The crude product was recrystallised from THF and hexane. Yield: 79 mg, 83 %. ¹H NMR (400 MHz): δ: 7.59 (d, (AB)', *J* = 8 Hz, 2H, CH_{arom}), 7.48 (d, (AB)', *J* = 8 Hz, 2H, CH_{arom}), 7.40 (d, (AB)', *J* = 8 Hz, 2H, CH_{arom}), 7.28 (d, (AB)', *J* = 8 Hz, 2H, CH_{arom}), 7.08 (d, (AB)', *J* = 8 Hz, 2H, CH_{arom}), 7.04 (d, (AB)', *J* = 8 Hz, 2H, CH_{arom}), 6.93 (d, (AB)', *J* = 8 Hz, 2H, CH_{arom}), 6.89 (d, (AB)', *J* = 8 Hz, 2H, CH_{arom}), 2.11 (s, 3H, Me), 2.10 (s, 3H, Me), 2.05 (s, 3H, Me), 2.00 (s, 3H, Me), 1.35 (d, *J* = 7 Hz, 9H, PMe₃ *trans* to C), 1.20 (vt, *J* = 3 Hz, 18H, PMe₃ *trans* to PMe₃), 0.10 ppm (q,

$J = 7$ Hz, 3H, Me). $^{31}\text{P}\{^1\text{H}\}$ NMR (121 MHz) δ : -5.78 (dd, $^1J_{\text{RhP}} = 105$ Hz, $^2J_{\text{PP}} = 34$ Hz, 2P), -18.38 (dt, $^1J_{\text{RhP}} = 89$ Hz, $^2J_{\text{PP}} = 34$ Hz, 1P). Anal. Calcd. for $\text{C}_{20}\text{H}_{14}\text{RhP}_3$: C, 68.48; H, 7.25. Found: C, 68.48; H, 7.45 %. IR (KBr): $\nu_{(\text{C}\equiv\text{C})} = 2124$ cm^{-1} .

20 - *mer,cis*-[tris(trimethylphosphine)methyl-2,5-bis(4-methoxyphenylethynyl)-3,4-bis(4-methoxyphenyl)rhodacyclopentadiene]

The compound 1,4-bis(4-methoxyphenyl)buta-1,3-diyne (0.095 mmol, 25 mg) in THF (2 ml) was added to a rapidly stirred solution of $\text{Rh}(\text{PMe}_3)_4\text{Me}$ (0.047 mmol, 20 mg) in THF (2 ml) and the resulting solution was stirred for 5 min. The solvent was removed *in vacuo* and then THF (2 ml) was added and the solution was stirred for 5 min and this cycle repeated two times. The residual solid was then dissolved in C_6D_6 and the resulting solution was heated to 80 °C for 6 h. The crude product was recrystallised from THF and hexane. Yield: 36 mg, 86 %. ^1H NMR (400 MHz) δ : 7.59 (d, (AB)', $J = 9$ Hz, 2H, CH_{arom}), 7.48 (d, (AB)', $J = 8$ Hz, 2H, CH_{arom}), 7.42 (d, (AB)', $J = 9$ Hz, 2H, CH_{arom}), 7.31 (d, (AB)', $J = 9$ Hz, 2H, CH_{arom}), 6.88 (d, (AB)', $J = 9$ Hz, 2H, CH_{arom}), 6.86 (d, (AB)', $J = 8$ Hz, 2H, CH_{arom}), 6.71 (d, (AB)', $J = 9$ Hz, 2H, CH_{arom}), 6.66 (d, (AB)', $J = 9$ Hz, 2H, CH_{arom}), 3.31 (s, 3H, Me), 3.29 (s, 3H, Me), 3.24 (s, 3H, Me), 3.19 (s, 3H, Me), 1.39 (d, $J = 7$ Hz, 9H, PMe_3 *trans* to C), 1.23 (vt, $J = 3$ Hz, 18H, PMe_3 *trans* to PMe_3), 0.12 ppm (q, $J = 7$ Hz, 3H, Me). $^{31}\text{P}\{^1\text{H}\}$ NMR (121 MHz) δ : -6.00 (dd, $^1J_{\text{RhP}} = 105$ Hz, $^2J_{\text{PP}} = 33$ Hz, 2P), -18.45 (dt, $^1J_{\text{RhP}} = 88$ Hz, $^2J_{\text{PP}} = 33$ Hz, 1P). Anal. Calcd. for $\text{C}_{46}\text{H}_{58}\text{RhO}_4\text{P}_3$: C, 63.45; H, 6.71. Found: C, 63.78; H, 6.81 %. IR (KBr): $\nu_{(\text{C}\equiv\text{C})} = 2128$ cm^{-1} .

21 - *mer,cis*-[tris(trimethylphosphine)methyl-2,5-bis(4-trifluoromethylphenylethynyl)-3,4-bis(4-trifluoromethylphenyl)rhodacyclopentadiene]

$\text{Rh}(\text{PMe}_3)_4\text{Me}$ (0.118 mmol, 50 mg) and 1,4-bis(4-trifluoromethylphenyl)buta-1,3-diyne (0.237 mmol, 80 mg) were added to THF (3 ml) and the solution stirred for 5 min and then the solvent was removed *in vacuo*. THF (2 ml) was then added and the solution was heated to 80 °C for 1h. The solvent was again removed *in vacuo* to give the product as an orange, sticky solid which was washed with hexane and dried *in vacuo*. Yield: 83 mg, 69 %. ^1H NMR (400 MHz) δ : 7.39 (m, 4H, CH_{arom}), 7.28 (m, 8H, CH_{arom}), 7.20 (m, 4H, CH_{arom}), 7.02 (d, (AB)', $J = 8$ Hz, CH_{arom}), 1.26 (d, $J = 7$ Hz, 9H, PMe_3 *trans* to C), 1.11

(vt, $J = 3$ Hz, 18H, PMe_3 *trans* to PMe_3), 0.00 ppm (q, $J = 8$ Hz, 3H, Me). $^{31}\text{P}\{^1\text{H}\}$ NMR (121 MHz) δ : -6.93 (dd, $^1J_{\text{RhP}} = 103$ Hz, $^2J_{\text{PP}} = 34$ Hz, 2P), -18.54 (dt, $^1J_{\text{RhP}} = 88$ Hz, $^2J_{\text{PP}} = 34$ Hz, 1P). $^{19}\text{F}\{^1\text{H}\}$ NMR (282) δ : -62.23 (s, 6F), -62.24 (s, 3F), -62.64 (s, 3F), -62.69 (s, 3F). Anal. Calcd. for $\text{C}_{46}\text{H}_{46}\text{RhF}_{12}\text{P}_3 \cdot 0.5\text{C}_6\text{H}_{14}$: C, 55.17; H, 5.10. Found: C, 55.30; H, 4.78 %. IR (KBr): $\nu_{(\text{C}=\text{C})} = 2099, 2134 \text{ cm}^{-1}$.

22 - *mer,cis*-[tris(trimethylphosphine)methyl-2,5-bis(4-carbomethoxyphenyl)-3,4-bis(4-carbomethoxyphenyl)rhodacyclopentadiene]

The compound 1,4-bis(4-carbomethoxyphenyl)buta-1,3-diyne (0.237 mmol, 75 mg) in THF (2 ml) was added to a rapidly stirred solution of $\text{Rh}(\text{PMe}_3)_4\text{Me}$ (0.118 mmol, 50 mg) in THF (2 ml) and the resulting solution was stirred for 5 min. The solvent was removed *in vacuo* and a further 2 ml of THF was added and the solution was stirred for 5 min. The solvent was removed *in vacuo* and this cycle was repeated two more times to remove the liberated PMe_3 . The resulting solution was dissolved in C_6D_6 and heated to 80 °C for 1 h to give complete conversion to a red product which was recrystallised from THF and hexane. Crystals suitable for X-ray analysis were grown over a period of days from a solution of THF layered with hexanes. Yield: 87 mg, 75 %. ^1H NMR (400 MHz) δ : 8.21 (d, (AB)', $J = 8$ Hz, 2H, CH_{arom}), 8.18 (d, (AB)', $J = 9$ Hz, 2H, CH_{arom}), 8.04 (d, (AB)', $J = 8$ Hz, 2H, CH_{arom}), 7.99 (d, (AB)', $J = 9$ Hz, 2H, CH_{arom}), 7.53 (d, (AB)', $J = 8$ Hz, 2H, CH_{arom}), 7.41 (d, (AB)', $J = 8$ Hz, 2H, CH_{arom}), 7.35 (d, (AB)', $J = 9$ Hz, 2H, CH_{arom}), 7.22 (d, (AB)', $J = 8$ Hz, 2H, CH_{arom}), 3.46 (s, 3H, Me), 3.45 (s, 3H, Me), 3.44 (s, 3H, Me), 3.41 (s, 3H, Me), 1.22 (d, $J = 7$ Hz, 9H, PMe_3 *trans* to C), 1.07 (vt, $J = 3$ Hz, 18H, PMe_3 *trans* to PMe_3), 0.03 ppm (q, $J = 8$ Hz, 3H, Me). $^{31}\text{P}\{^1\text{H}\}$ NMR (121 MHz) δ : -6.51 (dd, $^1J_{\text{RhP}} = 103$ Hz, $^2J_{\text{PP}} = 34$ Hz, 2P), -18.47 (dt, $^1J_{\text{RhP}} = 88$ Hz, $^2J_{\text{PP}} = 34$ Hz, 1P). Anal. Calcd. for $\text{C}_{20}\text{H}_{14}\text{RhP}_3 \cdot 0.5\text{C}_6\text{H}_{14}$: C, 61.99; H, 6.48. Found: C, 62.03; H, 6.57 %. IR (KBr): $\nu_{(\text{C}=\text{O})} = 1724$, $\nu_{(\text{C}=\text{C})} = 2120, 2142 \text{ cm}^{-1}$. Raman (solid): $\nu_{(\text{arene rings})} = 1435, 1607$, $\nu_{(\text{C}=\text{C})} = 2137 \text{ cm}^{-1}$.

2.12.6 Synthesis of a Rh-Cl-based rhodacyclopentadiene

23 - *mer,cis*-[tris(trimethylphosphine)chloro-2,5-bis(4-trifluoromethylphenylethynyl)-3,4-bis(4-trifluoromethylphenyl)rhodacyclopentadiene]

Rh(PMe₃)₄Cl (0.045 mmol, 20 mg) in THF (2 ml) was added to a rapidly stirred solution of 1,4-bis(4-trifluoromethylphenyl)buta-1,3-diyne (0.180 mmol, 61 mg) in THF (2 ml) and the mixture was stirred for 5 min. The solvent was removed *in vacuo* and then the residue redissolved in THF (3 ml) and the solution heated to 80 °C for 4 d with the reaction monitored by *in situ* ³¹P{¹H} NMR spectroscopy. The solvent was removed *in vacuo* and the residual solid was washed with hexane to remove excess 1,4-bis(4-trifluoromethylphenyl)buta-1,3-diyne and then dried *in vacuo*. Yield: 83 mg, 69 %. ¹H NMR (400 MHz) δ: 7.64 (d, (AB)', *J* = 8 Hz, 2H, CH_{arom}), 7.43 (d, (AB)', *J* = 8 Hz, 2H, CH_{arom}), 7.33 (d, (AB)', *J* = 8 Hz, 2H, CH_{arom}), 7.27 (d, (AB)', *J* = 8 Hz, 2H, CH_{arom}), 7.26 (d, (AB)', *J* = 8 Hz, 2H, CH_{arom}), 7.17 (d, (AB)', *J* = 8 Hz, 2H, CH_{arom}), 7.09 (d, (AB)', *J* = 8 Hz, 2H, CH_{arom}), 6.90 (d, (AB)', *J* = 8 Hz, 2H, CH_{arom}), 1.37 (d, *J* = 7 Hz, 9H, PMe₃ *trans* to C), 1.27 (vt, *J* = 3 Hz, 18H, PMe₃ *trans* to PMe₃). ³¹P{¹H} NMR (121 MHz) δ: -9.67 (dd, ¹*J*_{RhP} = 100 Hz, ²*J*_{PP} = 32 Hz, 2P), -23.65 (dt, ¹*J*_{RhP} = 85 Hz, ²*J*_{PP} = 32 Hz, 1P). ¹⁹F{¹H} NMR (282) δ: -62.30 (s, 6F), -62.44 (s, 3F), -62.76 (s, 3F), -62.84 (s, 3F). Anal. Calcd. for 3C₄₅H₄₃RhF₁₂P₃Cl.C₁₈H₈F₆: C, 53.10; H, 4.08. Found: C, 53.11; H, 4.08 %. Several analyses indicated the presence of varying amounts of free diyne which is difficult to remove completely from the sample. NMR confirmed the presence of diyne impurity in the samples, with no other visible impurities. The presence of diyne does not affect the photophysical data for the rhodacycle. IR (KBr): ν_(C≡C) = 2099, 2134 cm⁻¹.

2.12.7 Synthesis of cyclotrimers

25a - 1,2,4-tris(phenylethynyl)-3,5,6-(phenyl)benzene

The compound **1** (0.027 mmol, 20 mg) was dissolved in toluene (2 ml) and added to a solution of 1,4-diphenylbuta-1,3-diyne (0.559 mmol, 114 mg) in toluene (2 ml). The resulting solution was refluxed under N₂ for 3 wks. The toluene solvent was removed *in vacuo*. The residual solid was applied to the top of a silica gel column which was first

eluted with hexanes to remove unreacted diyne starting material and then with 50:50 DCM:hexane eluant. The solvent was removed *in vacuo* and the product obtained as a light brown solid which was purified by sublimation under high vacuum. Slow evaporation of a DCM/hexane solution of product gave white crystals that were suitable for X-ray analysis. Yield: 37 mg, 33 %. ¹H NMR (400 MHz) δ: 7.72 (m, 4H, CH_{arom}), 7.54 (m, 8H, CH_{arom}), 7.20 (m, 14H, CH_{arom}), 6.74 (m, 4H, CH_{arom}). Anal. Calcd. for C₄₈H₃₀: C, 95.02; H, 4.98. Found: C, 94.12; H, 4.85 %. IR (KBr): ν_(arene ring) = 1442, 1491, 1596, ν_(C≡C) = 2210 cm⁻¹. Raman (solid): ν_(arene rings) = 1359, 1488, 1539, 1596, ν_(C≡C) = 2203 cm⁻¹. HRMS MALDI Calc. for C₄₈H₃₁ *m/z* = 607.24203; Found, 607.23400 [M⁺].

25b - 1,2,4-tris(4-carbomethoxyphenylethynyl)-3,5,6-tris(4-carbomethoxyphenyl)-benzene

The compound **15** (0.018 mmol, 20 mg) in toluene (2 ml) was added to a stirred solution of 1,4-bis(4-carbomethoxyphenyl)buta-1,3-diyne (0.374 mmol, 119 mg) in toluene (2 ml). The resulting solution was refluxed under N₂ for 3 wks. The toluene was removed *in vacuo* and the residual solid was added to a silica gel column and hot toluene eluant used to remove any starting materials. The product was removed from the column with ethyl acetate, dried *in vacuo* and recrystallisation from hot toluene gave the product as an off-white solid. Yield: 27 mg, 23 %. ¹H NMR (500 MHz) δ: 8.24 (d, *J* = 8 Hz, 2H, CH_{arom}), 7.95 (d, *J* = 8 Hz, 4H, CH_{arom}), 7.92 (d, *J* = 9 Hz, 2H, CH_{arom}), 7.91 (d, *J* = 8 Hz, 2H, CH_{arom}), 7.79 (d, *J* = 9 Hz, 2H, CH_{arom}), 7.77 (d, *J* = 9 Hz, 2H, CH_{arom}), 7.32 (d, *J* = 9 Hz, 2H, CH_{arom}), 7.30 (d, *J* = 9 Hz, 2H, CH_{arom}), 7.26 (d, *J* = 9 Hz, 2H, CH_{arom}), 7.18 (d, *J* = 9 Hz, 2H, CH_{arom}), 6.72 (d, *J* = 8 Hz, 2H, CH_{arom}), 4.02 (s, 3H, Me), 3.92 (s, 3H, Me), 3.92 (s, 6H, Me), 3.90 (s, 3H, Me), 3.87 (s, 3H, Me). Anal. Calcd. for C₆₀H₄₂: C, 75.46; H, 4.43. Found: C, 74.93; H, 4.26 %. IR (KBr): ν_(arene ring) = 1276, 1436, 1604, ν_(C=O) = 1724, ν_(C≡C) = 2203 cm⁻¹. Raman (solid): ν_(arene rings) = 1358, 1502, 1536, 1602, 1721, ν_(C=O) = 1721, ν_(C≡C) = 2207 cm⁻¹. MALDI *m/z*: 955 [M⁺].

25c - 1,2,4-tris(4-trifluoromethylphenylethynyl)-3,5,6-tris(4-trifluoromethylphenyl)-benzene

The compound **5** (0.018 mmol, 21 mg) was dissolved in toluene (2 ml) and added to a solution of 1,4-bis(4-trifluoromethylphenyl)buta-1,3-diyne (0.387 mmol, 131 mg) in toluene (2 ml). The resulting solution was refluxed under nitrogen for 3 wks. The toluene

was removed *in vacuo* and the residual solid was applied to the top of a short silica gel column which was initially eluted with hexane to remove unreacted diyne, then with 1:10 acetone:hexane to remove the rhodacycle catalyst and then with DCM to elute the cyclotrimer. The solvent was removed *in vacuo* and the residual solid was recrystallised from DCM/hexane to give the product as a yellow solid. Yield: 85 mg, 65 %. ^1H NMR (400 MHz, CD_2Cl_2) δ : 7.84 (m, 4H, CH_{arom}), 7.55 (m, 8H, CH_{arom}), 7.41 (m, 6H, CH_{arom}), 7.29 (d, $J = 8$ Hz, CH_{arom}), 7.18 (d, $J = 8$ Hz, 2H, CH_{arom}), 6.74 (d, $J = 8$ Hz, 2H, CH_{arom}). $^{19}\text{F}\{^1\text{H}\}$ NMR (188 MHz) δ : -63.24 (s, 3F), -63.37 (s, 6F), -63.69 (s, 3F), -63.71 (s, 3F), -63.75 (s, 3F). Anal. Calcd. for $\text{C}_{60}\text{H}_{42}\text{F}_{18}$: C, 63.92; H, 2.38. Found: C, 63.36; H, 2.46 % (Submitted for HRMS). IR (KBr): $\nu_{(\text{CF}_3)}$ = 1327, $\nu_{(\text{arene ring})}$ = 1616, $\nu_{(\text{C}\equiv\text{C})}$ = 2212 cm^{-1} . Raman (solid): $\nu_{(\text{arene rings})}$ = 1363, 1509, 1539, 1616, $\nu_{(\text{C}\equiv\text{C})}$ = 2211 cm^{-1} . HRMS MALDI Calc. for $\text{C}_{54}\text{H}_{24}\text{F}_{18}$; m/z = 1014.15961; Found, 1014.15840 [M^+].

2.13 References

- 1) M. K. Nazeeruddin, R. Humphry-Baker, D. Berner, S. Rivier, L. Zuppidi, M. Graetzel, *J. Am. Chem. Soc.*, 2003, **125**, 8790.
- 2) C. Kaes, A. Katz, M. W. Hosseini, *Chem. Rev.*, 2000, **100**, 3553.
- 3) B. De Bruin, B. Eckhard, E. Bothe, T. Weyhermueller, K. Wieghardt, *Inorg. Chem.*, 2000, **39**, 2936.
- 4) V. V. Grushin, N. Herron, D. D. LeCloux, W. J. Marshall, V. A. Petrov, Y. Wang, *Chem. Commun.*, 2001, **16**, 1053.
- 5) J. P. Collman, J. W. Kang, W. F. Little, M. F. Sullivan, *Inorg. Chem.*, 1968, **7**, 1298.
- 6) Y. Wakatsuki, T. Kuramitsu, H. Yamazaki, *Tetrahedron Lett.*, **1974**, 4549.
- 7) V. Gandon, C. Aubert, M. Malacria, *Chem. Commun.*, 2006, 2209.
- 8) M. Lautens, W. Klute, W. Tam, *Chem. Rev.*, 1996, **96**, 49.
- 9) I. Ojima, M. Tzamarioudaki, Z. Li, R. J. Donovan, *Chem. Rev.*, 1996, **96**, 635.
- 10) E. T. Knight, L. K. Myers, M. E. Thompson, *Organometallics*, 1992, **11**, 3691.
- 11) H. G. Alt, H. E. Engelhardt, M. D. Rausch, L. B. Kool, *J. Organomet. Chem.*, 1987, **329**, 61.
- 12) M. Westerhausen, M. H. Digeser, C. Gückel, H. Nörg, J. Knizek, W. Ponikwar, *Organometallics*, 1999, **18**, 2491.
- 13) D. J. Sikora, M. D. Rausch, R. D. Rogers, J. L. Atwood, *J. Am. Chem. Soc.*, 1979, **101**, 5079.
- 14) J. L. Atwood, W. E. Hunter, H. Alt, M. D. Rausch, *J. Am. Chem. Soc.*, 1976, **98**, 2454.
- 15) H. tom Dieck, C. Munz, C. Müller, *J. Organomet. Chem.*, 1990, **384**, 243.
- 16) H. Suzuki, K. Itoh, Y. Ishii, K. Simon, J. A. Ibers, *J. Am. Chem. Soc.*, 1976, **98**, 8494.
- 17) B. Clarke, M. Green, F. G. A. Stone, *J. Chem. Soc. (A)*, 1970, 952.
- 18) C. S. Yi, J. R. Torres-Lubian, N. Liu, A. L. Rheingold, I. A. Guzei, *Organometallics*, 1998, **17**, 1257.
- 19) Y. Yamada, J. Mizutani, M. Kurihara, H. Nishihara, *J. Organomet. Chem.*, 2001, **637**, 80.
- 20) L. J. Canoira, J. L. Davidson, G. Douglas, K. W. Muir, *J. Organomet. Chem.*, 1989, **362**, 135.
- 21) T. V. Harris, J. W. Rathke, E. L. Muetterties, *J. Am. Chem. Soc.*, 1978, **100**, 6966.

- 22) R. Usón, J. Vicente, M. T. Chicote, P. G. Jones, G. M. Sheldrick, *J. Chem. Soc., Dalton Trans.*, 1983, 1131.
- 23) C. Bianchini, A. Mell, M. M. Peruzzini, A. Vacca, F. Vizza, *Organometallics*, 1991, **10**, 645.
- 24) H. Yamazaki, K. Yasufuku, Y. Wakatsuki, *Organometallics*, 1983, **2**, 726.
- 25) T. Shimura, A. Ohkubo, K. Aramaki, H. Uekusa, T. Fujita, S. Ohba, H. Nishihara, *Inorg. Chim. Acta*, 1995, **230**, 215.
- 26) Y. Wakatsuki, O. Nomura, K. Kitaura, K. Morokuma, H. Yamazaki, *J. Am. Chem. Soc.*, 1983, **105**, 1907.
- 27) M. I. Bruce, N. N. Zaitseva, B. W. Skelton, A. H. White, *Inorg. Chim. Acta*, 1996, **250**, 129.
- 28) J. P. Rourke, A. S. Batsanov, J. A. K. Howard, T. B. Marder, *Chem. Commun.*, 2001, 2626.
- 29) A. F. Hill, A. D. Rae, M. Schultz, A. C. Willis, *Organometallics*, 2006, submitted.
- 30) M. Horáček, I. Císařová, J. Kubišta, A. Spannenberg, K. Dallmann, U. Rosenthal, K. Mach, *J. Organomet. Chem.*, 2004, **689**, 4592.
- 31) V. V. Burlakov, A. Ohff, C. Lefeber, A. Tillack, W. Baumann, R. Kempe, U. Rosenthal, *Chem. Ber.*, 1995, **128**, 967.
- 32) U. Rosenthal, P.-M. Pellny, F. G. Kirchbauer, V. V. Burlakov, *Acc. Chem. Res.*, 2000, **33**, 119.
- 33) D. P. Hsu, W. M. Davis, S. L. Buchwald, *J. Am. Chem. Soc.*, 1993, **115**, 10394.
- 34) L. Pu, T. Hasegawa, S. Parkin, H. Taube, *J. Am. Chem. Soc.*, 1993, **115**, 2545.
- 35) A. Morneau, B. T. Donovan-Merkert, W. E. Geiger, *Inorg. Chim. Acta*, 2000, **300**, 96.
- 36) J. J. Eisch, A. M. Piotrowski, K. I. Han, C. Krüger, Y. H. Tsay, *Organometallics*, 1985, **4**, 224.
- 37) X. Zhang, G. B. Carpenter, D. A. Sweigart, *Organometallics*, 1999, **18**, 4887.
- 38) M. Retbøll, A. J. Edwards, A. D. Rae, A. C. Willis, M. A. Bennett, E. Wenger, *J. Am. Chem. Soc.*, 2002, **124**, 8348.
- 39) Z. Hou, A. Fujita, T. Koizumi, H. Yamazaki, Y. Wakatsuki, *Organometallics*, 1999, **18**, 1979.
- 40) Z. Lu, C.-H. Jun, S. R. de Gala, M. P. Sigalas, O. Eisenstein, R. H. Crabtree, *Organometallics*, 1995, **14**, 1168.

- 41) C. Perthuisot, B. L. Edelbach, D. L. Zubris, W. D. Jones, *Organometallics*, 1997, **16**, 2016.
- 42) C. Perthuisot, W. D. Jones, *J. Am. Chem. Soc.*, 1994, **116**, 3647.
- 43) B. C. Berris, G. H. Hovakeemian, Y.-H. Lai, H. Mestdaph, K. P. C. Vollhardt, *J. Am. Chem. Soc.*, 1985, **107**, 5670.
- 44) W.-Y. Yeh, S. C. N. Hsu, S.-M. Peng, G.-H. Lee, *Organometallics*, 1998, **17**, 2477.
- 45) A. Chehata, A. Oviedo, A. Arévalo, S. Bernès, J. J. García, *Organometallics*, 2003, **22**, 1585.
- 46) D. A. Vicic, W. D. Jones, *J. Am. Chem. Soc.*, 1997, **119**, 10855.
- 47) S. A. Gardner, H. B. Gordon, M. D. Rausch, *J. Organomet. Chem.*, 1973, **60**, 179.
- 48) B. L. Edelbach, R. J. Lachicotte, W. D. Jones, *J. Am. Chem. Soc.*, 1998, **120**, 2843.
- 49) C. Deuschel-Cornioley, A. von Zelewsky, *Inorg. Chem.*, 1987, **26**, 3354.
- 50) M. R. Plutino, L. M. Scolaro, A. Albinati, R. Romeo, *J. Am. Chem. Soc.*, 2004, **126**, 6470.
- 51) Y.-H. Chen, J. W. Merkert, Z. Murtaza, C. Woods, D. P. Rillema, *Inorg. Chim. Acta*, 1995, **240**, 41.
- 52) N. Shimhai, C. N. Iverson, B. L. Edelbach, W. D. Jones, *Organometallics*, 1999, **20**, 2759.
- 53) S. C. Cohen, A. G. Massey, *J. Organomet. Chem.*, 1967, **10**, 471.
- 54) M. D. Rausch, L. P. Klemann, *Chem. Commun.*, 1971, **7**, 354.
- 55) C. N. Iverson, R. J. Lachicotte, C. Müller, W. D. Jones, *Organometallics*, 2002, **21**, 5320.
- 56) H. Schwager, S. Spyroudis, K. P. C. Vollhardt, *J. Organomet. Chem.*, 1990, **382**, 191.
- 57) B. L. Edelbach, D. A. Vicic, R. J. Lachicotte, W. D. Jones, *Organometallics*, 1998, **17**, 4784.
- 58) C.-H. Jun, Z. Lu, R. H. Crabtree, *Tetrahedron Lett.*, 1992, **33**, 7119.
- 59) T. Satoh, W. D. Jones, *Organometallics*, 2001, **20**, 2916.
- 60) B. L. Edelbach, R. J. Lachicotte, W. D. Jones, *Organometallics*, 1999, **18**, 4040.
- 61) C. Müller, R. J. Lachicotte, W. D. Jones, *Organometallics*, 2002, **21**, 1975.
- 62) T. Schaub, U. Radius, *Chem. Eur. J.*, 2005, **11**, 5024.
- 63) C. N. Iverson, W. D. Jones, *Organometallics*, 2001, **20**, 5745.
- 64) C. B. Blanton, Z. Murtaza, R. J. Shaver, D. P. Rillema, *Inorg. Chem.*, 1992, **31**, 3230.
- 65) S. R. Stoyanov, J. M. Villegas, D. P. Rillema, *Inorg. Chem.*, 2003, **42**, 7852.

- 66) M. Maestri, D. Sandrini, V. Balzani, A. von Zelewsky, C. Deuschel-Cornioley, P. Jolliet, *Helv. Chim. Acta*, 1988, **71**, 1053.
- 67) G. Y. Zheng, D. P. Rillema, J. DePriest, C. Woods, *Inorg. Chem.*, 1998, **37**, 3588.
- 68) J. DePriest, G. Y. Zheng, N. Goswami, D. M. Eichhorn, C. Woods, D. P. Rillema, *Inorg. Chem.*, 2000, **39**, 1955.
- 69) G. Y. Zheng, D. P. Rillema, *Inorg. Chem.*, 1998, **37**, 1392.
- 70) G. Y. Zheng, D. P. Rillema, J. H. Reibenspies, *Inorg. Chem.*, 1999, **38**, 794.
- 71) M. Kurashina, M. Murata, T. Watanabe, H. Nishihara, *J. Am. Chem. Soc.*, 2003, **125**, 12420.
- 72) J.-C. Lee, A. Nishio, I. Tomita, T. Endo, *Macromolecules*, 1997, **30**, 5205.
- 73) H. Nishihara, T. Shimura, A. Ohkubo, N. Matsuda, K. Aramaki, *Adv. Mater.*, 1993, **5**, 752.
- 74) T. Shimura, A. Ohkubo, N. Matsuda, I. Matsuoka, K. Aramaki, H. Nishihara, *Chem. Mater.*, 1996, **8**, 1307.
- 75) S. S. H. Mao, F.-Q. Liu, T. D. Tilley, *J. Am. Chem. Soc.*, 1998, **120**, 1193.
- 76) Y. Koga, K. Ueno, K. Matsubara, *J. Poly. Sci. A, Polymer Chem.*, 2006, **44**, 4204.
- 77) S. Yamaguchi, K. Tamao, *J. Organomet. Chem.*, 2002, **653**, 223.
- 78) M. Hissler, P. W. Dyer, R. Réau, *Coord. Chem. Rev.*, 2003, **244**, 1.
- 79) K. Tamao, S. Yamaguchi, M. Shiro, *J. Am. Chem. Soc.*, 1994, **116**, 11715.
- 80) A. J. Boydston, Y. Yin, B. L. Pagenkopf, *J. Am. Chem. Soc.*, 2004, **126**, 3724.
- 81) J. G. Rodríguez, A. Lafuente, L. Rubio, J. Esquivias, *Tetrahedron Lett.*, 2004, **45**, 7061.
- 82) J. G. Rodríguez, J. Esquivias, A. Lafuente, L. Rubio, *Tetrahedron Lett.*, 2006, **62**, 3112.
- 83) S.-S. Sun, A. J. Lees, *J. Am. Chem. Soc.*, 2000, **122**, 8956.
- 84) T. S. Jung, J. H. Kim, E. K. Jang, D. H. Kim, Y.-B. Shim, B. Park, S. C. Shin, *J. Organomet. Chem.*, 2000, **599**, 232.
- 85) J. S. Siddle, R. M. Ward, J. C. Collings, S. R. Rutter, L. Porrès, L. Applegarth, A. Beeby, A. S. Batsanov, A. L. Thompson, J. A. K. Howard, T. B. Marder, submitted.
- 86) A. Beeby, I. Clark, K. S. Findlay, P. Matousek, A. W. Parker, R. E. Pearce, L. Porrès, S. R. Rutter, M. Towrie, in preparation.
- 87) P. Lind, C. Lopes, K. Öberg, B. Eliasson, *Chem. Phys. Lett.*, 2004, **387**, 238.
- 88) P. Lind, A. Eriksson, C. Lopes, B. Eliasson, *J. Phys. Org. Chem.*, 2005, **18**, 426.

- 89) R. Vestberg, C. Nilsson, C. Lopes, P. Lind, B. Eliasson, E. Malmstrom, *J. Polymer Science*, 2005, **43**, 1177.
- 90) S. H. Eichhorn, A. J. Paraskos, K. Kishikawa, T. M. Swager, *J. Am. Chem. Soc.*, 2002, **124**, 12742.
- 91) G. Heppke, D. Moro, *Science*, 1998, **279**, 1872.
- 92) H.-F. Hsu, C.-H. Kuo, C.-F. Chen, Y.-H. Lin, L.-Y. Husng, C.-H. Chen, K.-O. Cheng, H.-H. Chen, *Chem. Mater.*, 2004, **16**, 2379.
- 93) K. Kishikawa, M. C. Harris, T. M. Swager, *Chem. Mater.*, 1999, **11**, 867.
- 94) K. Sanechika, T. Yamamoto, A. Yamamoto, *Bull. Chem. Soc. Jpn.*, 1984, **57**, 752.
- 95) M. A. Penz, I. Perez, J. P. Sestelo, L. A. Sarandeses, *Chem. Commun.*, 2002, 2246.
- 96) A. Orita, F. Ye, G. Babu, T. Ikemoto, J. Otera, *Can. J. Chem.*, 2005, **83**, 716.
- 97) F. Freeman, D. S. H. Kim, *J. Org. Chem.*, 1992, **57**, 1722.
- 98) a) D. Zargarian, P. Chow, N. J. Taylor, T. B. Marder, *J. Chem. Soc., Chem. Commun.*, 1989, 540; b) P. Chow, D. Zargarian, N. J. Taylor, T. B. Marder, *J. Chem. Soc., Chem. Commun.*, 1989, 1545.
- 99) D. L. Thorn, *Organometallics*, 1985, **4**, 192.
- 100) X. Zhu, R. M. Ward, D. Albesa-Jové, J. A. K. Howard, L. Porrès, A. Beeby, P. J. Low, W.-K. Wong, T. B. Marder, *Inorg. Chim. Acta*, 2006, **359**, 2859.
- 101) M. van Leeuwen, R. M. Ward, T. B. Marder, unpublished results.
- 102) F. Seeler, A. S. Batsanov, T. B. Marder, unpublished results.
- 103) T. Haumann, J. Benet-Buchholz, R. Boese, *J. Mol. Struct.*, 1996, **374**, 299.
- 104) P. Nguyen, Z. Yuan, L. Agocs, G. Lesley, T. B. Marder, *Inorg. Chim. Acta*, 1994, **220**, 289.
- 105) P. Nguyen, S. Todd, D. van der Biggelaar, N. J. Taylor, T. B. Marder, F. Wittmann, R. H. Friend, *Synlett*, 1994, 299.
- 106) P. Nguyen, S. Todd, D. van den Biggelaar, N. J. Taylor, J. C. Collings, R. M. Ward, R. Ll. Thomas, A. S. Batsanov, D. S. Yufit, A. L. Thompson, J. A. K. Howard, O. F. Koentjoro, D. P. Lydon, P. J. Low, S. R. Rutter, K. S. Findlay, L. Porrès, A. Beeby, A. S. Scott, W. Clegg, S. W. Watt, C. Viney, T. B. Marder, in preparation.
- 107) C. Hansch, A. Leo, R. W. Taft, *Chem. Rev.*, 1991, **91**, 165.
- 108) W. Hübel, R. Merenyi, R. Vannieuwenhoven, *Chem. Ber.*, 1963, **96**, 930.
- 109) A. J. Chalk, R. A. Jerussi, *Tetrahedron Lett.*, 1972, **1**, 61.
- 110) R. S. Dickson, L. J. Michel, *Aust. J. Chem.*, 1975, **28**, 285.
- 111) J. R. Fritch, K. P. C. Volhardt, *Organometallics*, 1982, **1**, 590.

- 112) T. Sugihara, A. Wakabayashi, Y. Nagai, H. Takao, H. Imagawa, M. Nishizawa, *Chem. Commun.*, 2002, 567.
- 113) D. Wasserfallen, G. Mattersteig, V. Enklemann, K. Müllen, *Tetrahedron*, 2006, **62**, 5417.
- 114) S. Taniguchi, T. Yokoi, A. Izuoka, M. M. Matsushita, T. Sugawara, *Tetrahedron Lett.*, 2004, **45**, 2671.
- 115) Y. Kojima, M. Tsuji, T. Matsuoka, H. Takahashi, *Macromolecules*, 1994, **27**, 3735.
- 116) H.-Fu. Hsu, M.-C. Lin, W.-C. Lin, Y.-H. Lai, S.-Y. Lin, *Chem. Mater.*, 2003, **15**, 2115.
- 117) T. M. Fasina, J. C. Collings, J. M. Burke, A. S. Batsanov, R. M. Ward, D. Albesa-Jové, L. Porrès, A. Beeby, J. A. K. Howard, A. J. Scott, W. Clegg, S. W. Watt, C. Viney, T. B. Marder. *J. Mater. Chem.*, 2005, **15**, 690.
- 118) S. J. Greaves, E. L. Flynn, E. L. Fitcher, E. Wrede, D. P. Lydon, P. J. Low, S. R. Rutter, A. Beeby, *J. Phys. Chem. A*, 2006, **110**, 2114.
- 119) J. Nierle, D. Barth, D. Kuck, *Eur. J. Chem.*, 2004, **4**, 867.
- 120) K. Kondo, S. Yasuda, T. Sakaguchi, M. Miya, *J. Chem. Soc., Chem. Commun.*, 1995, **1**, 55.
- 121) K. Kobayashi, N. Kobayashi, *J. Org. Chem.*, 2004, **69**, 2487.
- 122) J. Q. Umberger, V. K. LaMer, *J. Am. Chem. Soc.*, 1945, 1099.
- 123) C. A. Parker, C. G. Hatchard, T. A. Joyce, *J. Mol. Spectroscopy*, 1964, **14**, 311.
- 124) D. Magde, J. H. Brannon, T. L. Cremers, J. Olmsted, *J. Phys. Chem.*, 1979, **83**, 696.
- 125) T. Karstens, K. Kobs, *J. Phys. Chem.*, 1980, **84**, 1871.
- 126) J. R. Lakowicz, *Principles of Fluorescence Spectroscopy*, Kluwer, New York, 1999, Second Edition.
- 127) W. H. Melhuish, *J. Phys. Chem.*, 1961, **65**, 229.
- 128) D. V. O'Connor, D. Phillips, *Time Correlated Single Photon Counting*, Academic Press, London, 1984.
- 129) D. V. O'Connor, W. R. Ware, J. C. Andre, *J. Phys. Chem.*, 1979, **83**, 1333.
- 130) G. M. Sheldrick, *SHELXTL*, version 6.14; Bruker-Nonius AXS, Madison, Wisconsin, U.S.A., 2003.

Chapter 3

Synthesis of Rh-diyne and -tolan π - complexes and a mechanistic proposal for rhodacycle formation

3.1 Introduction

Transition metal π -complexes of buta-1,3-dienes

Numerous 1,3-diyne complexes of polynuclear systems are known, wherein each $C\equiv C$ bond plays a $\mu\text{-}\eta^2\text{-}\eta^2$ role. Many of these compounds have been characterised by X-ray crystallography, and the area has been reviewed.¹

This section aims to introduce examples of mono-metallic π -complexes, with a single metal coordinated to one of the diyne $C\equiv C$ bonds (a), and examples of bi-metallic π -complexes in which each of the $C\equiv C$ bonds are coordinated to a single metal atom (b), particularly for those involving Rh (Figure 1).

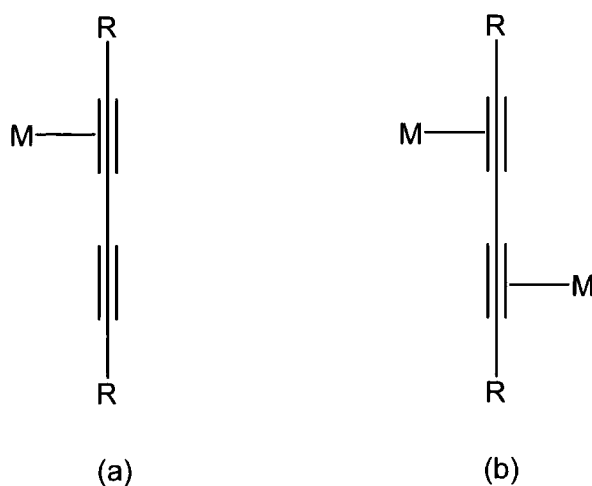


Figure 1. Mono-metallic (a) and bi-metallic (b) complexes of buta-1,3-diyne.

3.1.1 Mono-metallic complexes of buta-1,3-dienes

There are few Rh examples of this type. We have previously reported the *in situ* formation of $\text{Rh}(\text{PMe}_3)_3(\text{Cl})((1,2\text{-}\eta^2)\text{-4-F}_3\text{C-C}_6\text{H}_4\text{-C}\equiv\text{C-C}\equiv\text{C-C}_6\text{H}_4\text{-4-CF}_3)$ as a precursor to a relatively rare $\mu\text{-}(1,2\text{-}\eta^2):(3,4\text{-}\eta^2)$ bi-metallic species.² However, the closest analogues to these are four-coordinate, square planar Rh complexes containing η^2 -alkyne, halide and phosphine ligands simultaneously, prepared by Werner and co-workers.³ Of these, four of the complexes have been structurally characterised. All of them are 16-electron, square-

planar complexes of the form *trans*-XRh(PⁱPr₃)₂(η²-RC≡CR'), with the C≡C bond oriented perpendicular to the coordination plane (Figure 2). The group have also prepared the Ir analogue, [IrCl(η²-TMSC≡CC≡CTMS)(PⁱPr)₂] in 75 % yield, by reaction of [IrCl(COE)₂]₂ with TMS-C≡CC≡C-TMS in the presence of PⁱPr₃,^{3e} and they reported that the compound underwent thermal and photochemical conversion to the corresponding vinylideneiridium(I) compound, [Cl(PⁱPr₃)₂Ir=C=C(TMS)(C≡CTMS)]. Derivatives of the type RhCl(AsⁱPr₂CH₂CH₂OMe)(η²-RC≡CC≡CR) (R = Me, TMS), with substituted arsine ligands, in place of phosphine ligands were also prepared in almost quantitative yield, by the displacement of ethene from Rh(C₂H₄)Cl(AsPⁱPr₂CH₂CH₂OMe₂).^{3f}

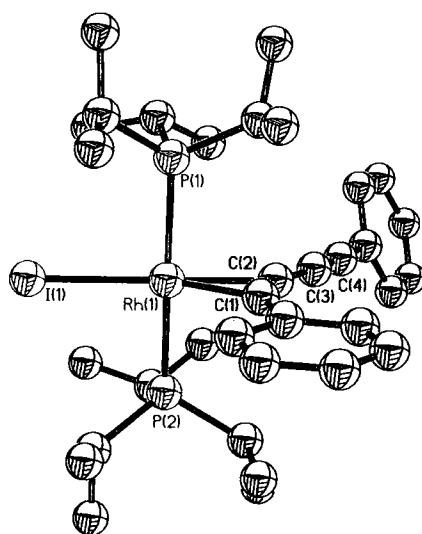


Figure 2. Example of a four-coordinate, square planar Rh complex containing η²-acetylenic, halide and phosphine ligands simultaneously. Hydrogen atoms are omitted for clarity and thermal ellipsoids are shown at 50 % probability.

In their synthesis of heteronuclear triangular cluster compounds, Yamazaki and co-workers have prepared [Pt(η²-PhC≡CC≡CPh)(PPh₃)₂] in quantitative yield by reaction of Pt(PPh₃)₄ with 1,4-diphenylbutadiyne⁴ and have obtained an X-ray structure which confirms the original proposal that only one of the C≡C bonds is coordinated to the metal.⁵ The compound was found to be almost planar, with the coordinated alkyne bond length increased to 1.305(11) Å from 1.197(9) Å in the free diyne.⁶ The group have also prepared the closely related compound Pt(η²-PhC≡CC≡CPh)(dppe)^{7,8} in 38 % yield, by a particularly interesting route that involved the homocoupling of two acetylide ligands on

$\text{Pt}(\text{C}\equiv\text{CPh})_2(\text{dppe})$ promoted by $\text{Ru}_3(\text{CO})_9(\text{PPh}_3)_3$ in refluxing toluene (Figure 3).⁹ A similar reaction occurs when $\text{PdCl}_2(\text{dppn})$ ($\text{dppn} = \text{Ph}_2\text{PC}_{10}\text{H}_6\text{PPh}_2$, $\text{C}_{10}\text{H}_6 = 1,8$ -naphthalenediyl) is treated with two equivalents of phenylacetylene in an ethanol/DCM mixture with NEt_3 base, giving $\text{Pd}(\eta^2\text{-PhC}\equiv\text{CC}\equiv\text{CPh})(\text{dppn})$ via a $(\text{dppn})\text{Pd}(\text{C}\equiv\text{CR})_2$ intermediate.¹⁰ The structure was characterised by X-ray crystallography which showed that the diyne lies in the PdP_2 plane with significant rotation of the diyne phenyl groups from co-planarity with the metallacycle.

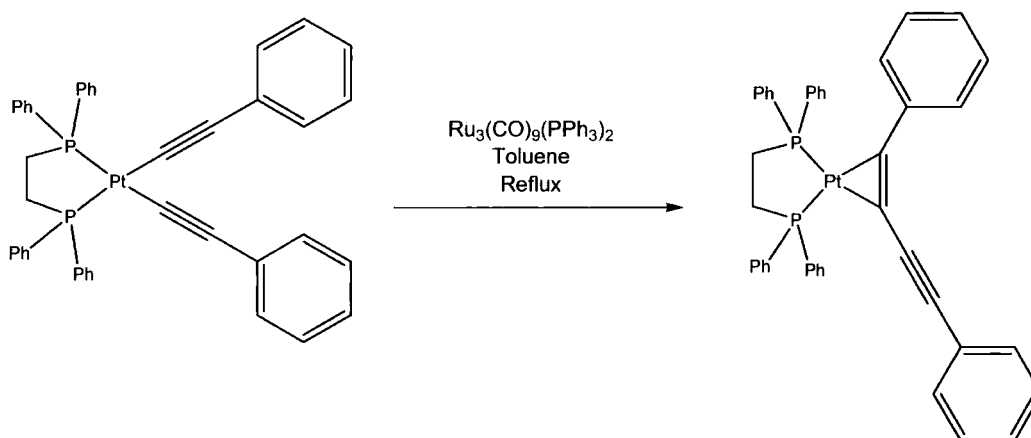


Figure 3. Formation of a Pt-diyne π -complex by homocoupling of two acetylide ligands.

The related compound $\text{Pt}(\eta^2\text{-PhC}\equiv\text{CC}\equiv\text{CPh})(\text{dppf})$ has also been reported.¹¹ The complex was formed by the facile conversion of a Pt bis(acetylide) into a π -coordinated diyne, assisted by an excess of electrophilic gold phosphine, $[\text{Au}(\text{PPh}_3)]^+$, and the product was characterised by X-ray crystallography. Bruce *et al.* have prepared the analogous compound $\text{Pt}(\eta^2\text{-TMSC}\equiv\text{CC}\equiv\text{CTMS})(\text{PPh}_3)_2$ in 86 % yield, from $\text{Pt}(\eta^2\text{-C}_2\text{H}_4)(\text{PPh}_3)_2$ and TMS-CC-CC-TMS ,¹² and Casey and co-workers have prepared a the very similar compound $\text{Pt}(\eta^2\text{-TMSC}\equiv\text{CC}\equiv\text{CTMS})(\text{PAr}_3)_2$ ($\text{Ar} = 4\text{-CH}_3\text{-C}_6\text{H}_4\text{-}$) and also $\text{Pt}(\eta^2\text{-MeC}\equiv\text{CC}\equiv\text{CMe})(\text{PAr}_3)_2$ by the same route.¹³ Casey studied protonation of these platinum diyne complexes with HBF_4 and $\text{CF}_3\text{CO}_2\text{H}$ which gave σ -2-butadienyl complexes via thermally unstable π -propargyl intermediates (Figure 4).

Complexes of 1,4-diphenylbutadiyne are also known for Ru ,¹⁴ W ,¹⁵ Mo ,¹⁵ Ti ,¹⁶ Nb ¹⁷ and Ta .¹⁸ Hill and co-workers have prepared $\text{Ru}(\eta^2\text{-PhC}\equiv\text{CC}\equiv\text{CPh})(\text{CO})_2(\text{PPh}_3)_2$ in 95 % yield, from $[\text{Ru}(\text{CO})_2(\text{PPh}_3)_3]$.¹⁴ If treated with an acid with a non-nucleophilic

anion, such as HBF_4 , HSbF_6 or HClO_4 , it was possible to protonate the diyne to form $\text{Ru}(\text{PhC}\equiv\text{C}-2\text{-C}=\text{CHPh})(\text{CO})_2(\text{PPh}_3)_2\text{X}$, ($\text{X} = \text{BF}_4^-$, SbF_6^- , ClO_4^-) (Figure 5).

Dehnicke *et al.* have prepared W and Mo diphenylbutadiyne complexes $[\text{WCl}_4(\eta^2\text{-PhC}\equiv\text{CC}\equiv\text{CPh})]_2$ and $[\text{MoCl}_4(\eta^2\text{-PhC}\equiv\text{CC}\equiv\text{CPh})]_2$ from WCl_6 (with C_2Cl_4 reducing agent) and MoCl_5 respectively.¹⁵ Reaction with PPh_4Cl in DCM in the presence of CCl_4 gave $\text{PPh}_4[\text{WCl}_5(\eta^2\text{-PhC}\equiv\text{CC}\equiv\text{CPh})]\text{CCl}_4$, which could be brominated in the *trans*-positions of the free alkyne bond to give $\text{PPh}_4[\text{WCl}_5(\eta^2\text{-PhC}\equiv\text{CC}(\text{Br})=\text{C}(\text{Br})\text{Ph})]\text{CCl}_4$. The group have also prepared similar compounds from $\text{Ph-C}\equiv\text{C-C}\equiv\text{C-TMS}$.

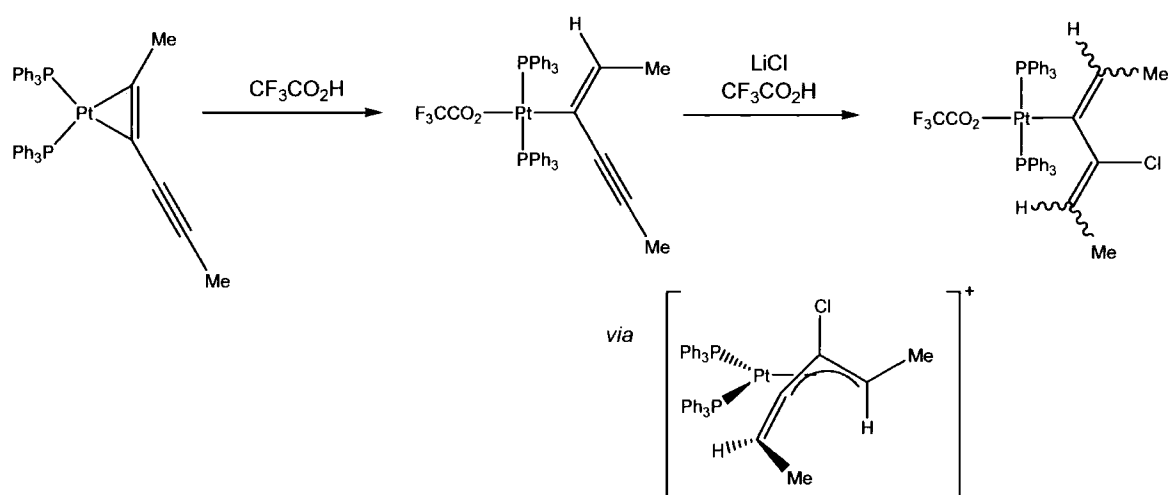


Figure 4. Synthesis of a Pt σ -2-butadienyl complex via a thermally unstable π -propargyl intermediate.

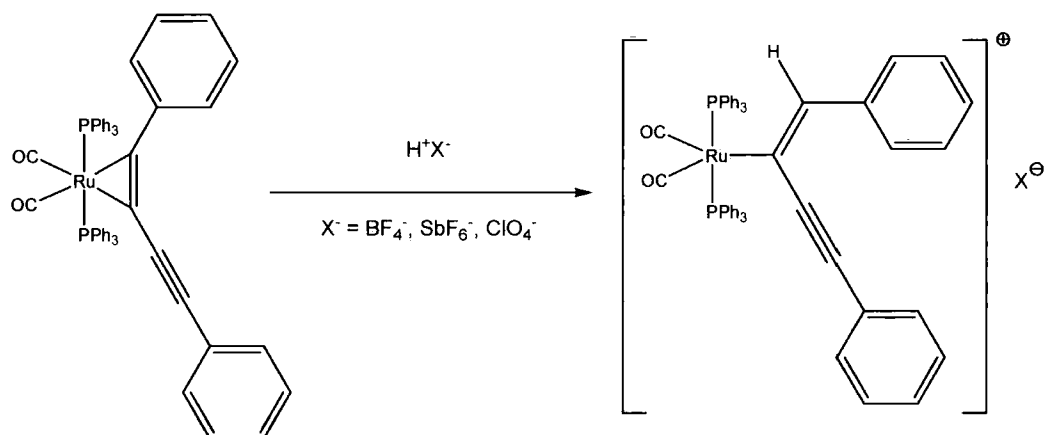


Figure 5. Protonation of $\text{Ru}(\eta^2\text{-PhC}\equiv\text{CC}\equiv\text{CPh})(\text{CO})_2(\text{PPh}_3)_2$ with non-nucleophilic acids.

During their attempts to prepare Ti bis(acetylide) complexes with porphyrin ligands, Woo *et al.* have prepared diphenylbutadiyne π -complexes from titanium porphyrin substrates by a number of methods.¹⁶ Reaction of (TTP)TiCl₂ (TTP = *meso*-5,10,15,20-tetratolylporphyrinato dianion) with two equivalents of PhC≡CLi for 20 hours, followed by crystallisation from toluene/hexane, gave [(TTP)Ti(η^2 -PhC≡CC≡CPh)] as a blue crystalline solid in 34 % yield. The product was characterised by X-ray crystallography and it was found that the C≡C bond had increased in length, from 1.197(9) Å in the free diyne to 1.316(4) Å. The same product was prepared by reaction of (TTP)TiCl with diphenylbutadiyne in the presence of NaBEt₃H (20 hours, 44 % yield) and also by the displacement of EtC≡CEt from (TTP)Ti(η^2 -EtC≡CEt) with diphenylbutadiyne (1 hour, no reported yield). The group found that if a solution of the product was exposed to air or treated with pyridine, then the diyne would dissociate to form oxidised (TTP)Ti=O and (TTP)Ti(py)₂ respectively. Ta porphyrin complexes with π -coordinated diphenylbutadiyne have also been prepared.¹⁸

Diyne containing niobocene complexes Nb(η^5 -C₅H₄SiMe₃)₂Cl(η^2 -(RC≡CC≡CR)) (R = Ph and SiMe₃) have been reported as *endo*- and *exo*-isomers by reaction of Nb(η^5 -C₅H₄SiMe₃)₂Cl with the respective diyne (Figure 6). The diphenylbutadiyne analogue was characterised by X-ray crystallography and the coordinated alkyne bond was found to have increased in length to 1.282(7) Å. The paramagnetic niobocene complex Nb(η^5 -C₅H₄SiMe₃)₂(η^2 -TMSC≡CC≡CTMS) was prepared from Nb(η^5 -C₅H₄SiMe₃)₂Cl(η^2 -(TMSC≡CC≡CTMS)), and subsequently oxidised in the presence of MeCN or ^tBuCN, to give the stable cationic d² derivatives [Nb(η^5 -C₅H₄SiMe₃)₂(η^2 -TMSC≡CC≡CTMS)(L)][BPh₄] (L = MeCN, ^tBuCN).¹⁷

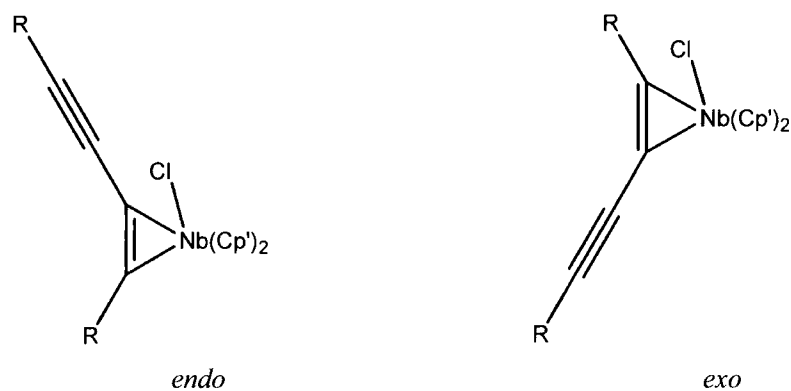


Figure 6. *Endo*- and *exo*- isomers of Nb(η^5 -C₅H₄SiMe₃)₂Cl(η^2 -(RC≡CC≡CR)), (R = Ph, TMS).

The Fe complex $\text{Fe}(\text{CO})_2(\text{PEt}_3)_2(\eta^2\text{-TMSC}\equiv\text{CC}\equiv\text{CTMS})$ is very similar to the proposed structures of $\text{Rh}(\text{PPh}_3)_3\text{Me}(\eta^2\text{-(RC}\equiv\text{CC}\equiv\text{CR)})$ ($\text{R} = \text{-C}_6\text{H}_4\text{-4-OMe}$, $\text{-C}_6\text{H}_4\text{-4-CF}_3$, $\text{-C}_6\text{H}_4\text{-4-CO}_2\text{Me}$) (*vide infra*) and has been synthesised and characterised by X-ray crystallography.¹⁹ The structure reveals a 5-coordinate, distorted trigonal bipyramid coordination around Fe, with the bent diyne lying in the $\text{Fe}(\text{CO})_2$ plane and the two phosphine ligands in the axial positions (Figure 7). The coordinated alkyne substituents are bent back between 140° and 150° indicating strong back bonding from Fe to the acetylenic unit. The IR spectrum clearly showed stretches corresponding to one $\text{C}\equiv\text{C}$ bond (2109 cm^{-1}) and one $\text{C}=\text{C}$ bond (1750 cm^{-1}).

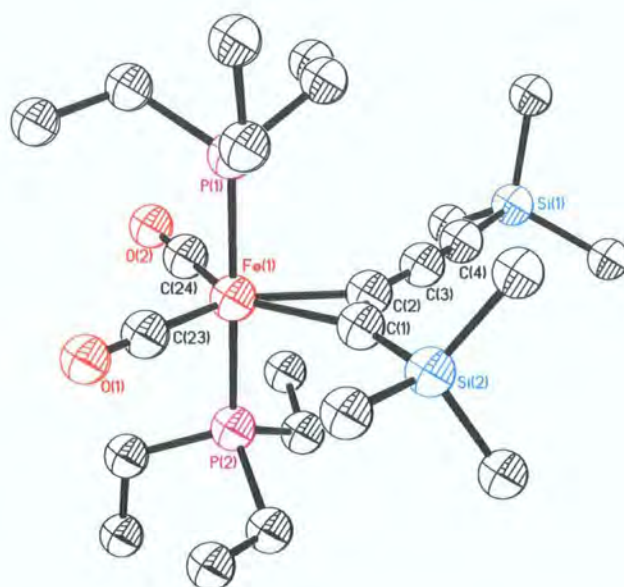


Figure 7. Molecular structure of $\text{Fe}(\text{CO})_2(\text{PEt}_3)_2(\eta^2\text{-TMSC}\equiv\text{CC}\equiv\text{CTMS})$. Hydrogen atoms are omitted for clarity and thermal ellipsoids are shown at 50 % probability.¹⁹

Rosenthal *et al.* have prepared interesting Ti and Zr metallocyclopentadienes that are fused with a nickelacyclopropene.²⁰ The unusual bicyclic compounds were prepared by reaction of $\text{Ni}(\text{PPh}_3)_2(\eta^2\text{-PhC}\equiv\text{CC}\equiv\text{CPh})$ with ‘ MCp_2 ’ ($\text{M} = \text{Ti, Zr}$) (Figure 8).

Bruce and co-workers have coordinated novel transition metal complexes of diphosphine butadiynes to ‘ $\text{Pt}(\text{PPh}_3)_2$ ’.²¹ They first prepared transition metal complexed diynes of the type $(\text{ML}_n\text{-PPh}_2\text{-C}\equiv\text{C-})_2$ ($\text{ML}_n = \text{Mo}(\text{CO})_5$, $\text{W}(\text{CO})_5$, $\text{Fe}(\text{CO})_4$) by reaction of $\text{Ph}_2\text{P-C}\equiv\text{CC}\equiv\text{C-PPh}_2$ with $\text{Mo}(\text{CO})_5(\text{NCMe})$, $\text{W}(\text{CO})_5(\text{THF})$ and $\text{Fe}_2(\text{CO})_9$ respectively.

These were subsequently reacted with $\text{Pt}(\text{C}_2\text{H}_4)(\text{PPh}_3)_2$ and the corresponding η^2 complex was formed by displacement of the coordinated ethene (Figure 9).

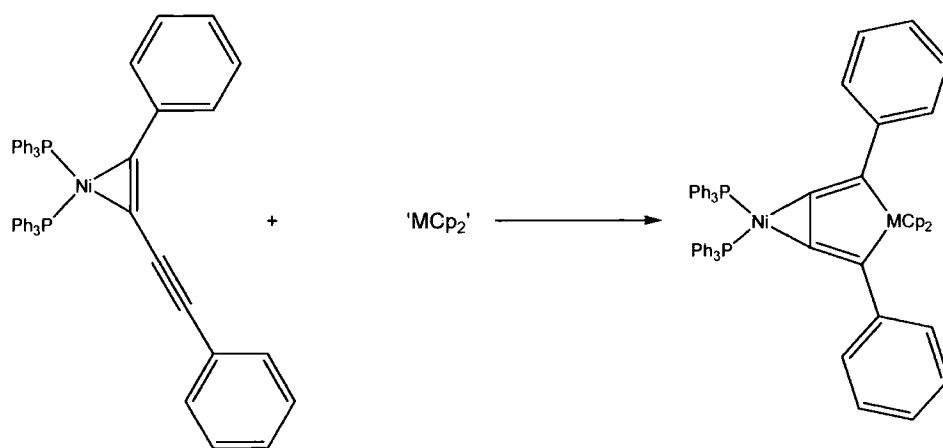


Figure 8. Formation of a fused bicyclic compound from $\text{Ni}(\text{PPh}_3)_2(\eta^2\text{-PhC}\equiv\text{CC}\equiv\text{CPh})$.

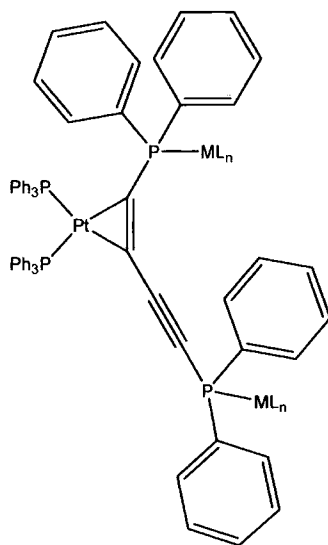


Figure 9. ' $\text{Pt}(\text{PPh}_3)_2$ ' complex with a novel transition metal complexed diphosphine butadiyne.

3.1.2 Bi-metallic complexes of buta-1,3-diyne

Bi-metallic diyne complexes, in which each C≡C bond coordinates to one metal atom, are scarce. The August 2006 version of the CSD²² contains 13 such complexes of 9 different transition metals. In $(\text{Cp}_2\text{Ti})_2(\text{Me}_3\text{SiC}\equiv\text{CC}\equiv\text{CPh})^{23}$ and $(\text{Cp}^*_2\text{La})_2(\text{RC}\equiv\text{CC}\equiv\text{CR})$ ($\text{R} = \text{'Bu}$ or Ph)²⁴ the bent diyne rod adopts a planar *trans*-configuration with both metal atoms lying in the same plane in *endo*, rather than *exo*, positions (Figure 10), which permits an η^3 coordination of the diyne with each metal atom. The remaining complexes exhibit η^2, η^2 diyne coordination. The complexes $(\text{PyCl}_4\text{W})_2(\text{TMS}\text{C}\equiv\text{CC}\equiv\text{CPh})$,²⁵ $(\text{Cp}_2\text{V})_2(\text{TMS}-\text{C}\equiv\text{C}-\text{C}\equiv\text{C}-\text{TMS})$,²⁶ and $[(\text{R}_2\text{PCH}_2\text{CH}_2\text{PR}_2)\text{Ni}]_2(\text{R}'\text{C}\equiv\text{CC}\equiv\text{CR}')$ where $\text{R} = \text{'Pr}$, $\text{R}' = \text{H}$,²⁷ or $\text{R} = \text{'Bu}$, $\text{R} = \text{Ph}$,²⁸ adopt a *gauche* conformation of the diyne moiety, with the $\text{C}\equiv\text{CC}\equiv\text{C}$ torsion angle $\tau = 74\text{--}98^\circ$ and the dihedral angle between two MC_2 planes $\theta = 69\text{--}102^\circ$. Unfortunately, these have been determined at low precision, with $\text{R}(\text{F}) = 8\text{--}16\%$, and the bond distances are not very accurate. The complex $[(2,6\text{-dimethylpyridine})\text{Ni}]_2(\text{TMS}-\text{C}\equiv\text{CC}\equiv\text{C}-\text{TMS})$ ²⁹ is intermediate between *gauche* and *cis*-conformations, with reported values of $\tau = 20$ and 34° , $\theta = 21$ and 39° in two ligands. However, the structure had been solved in the wrong space group (Figure 11).³⁰

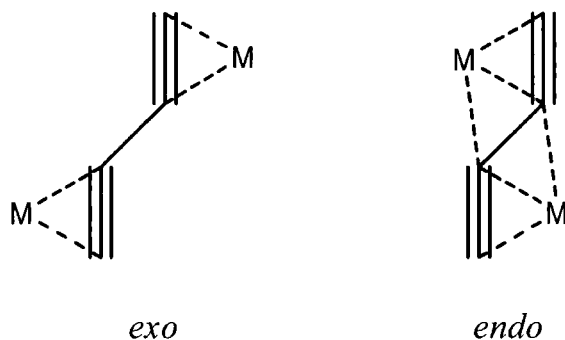


Figure 10. Bi-metallic coordination to butadiyne in *exo*- and *endo*-positions.

The complexes $[(\text{C}_5\text{H}_4\text{Me})\text{Mn}]_2(\text{MeC}\equiv\text{CC}\equiv\text{CMe})$,³¹ $\{(\text{Me}_2\text{N})\text{ZrC}_5\text{H}_4\text{-CMe}_2\text{-C}_2\text{B}_{10}\text{H}_{10}\}_2(\text{PhC}\equiv\text{CC}\equiv\text{CPh})$ ³² and the polymeric complex $\text{Cu}_2\text{Cl}_4\text{-(NH}_3\text{CH}_2\text{C}\equiv\text{CC}\equiv\text{CCH}_2\text{NH}_3)$ ³³ are also rigorously *trans* ($\tau = \theta = 0^\circ$) due to crystallographic C_i symmetry, the metal atoms lying in the diyne plane in *exo* positions (Figure 10). $(\text{Cp}_2\text{V})_2(\text{Ph}_2\text{PC}\equiv\text{CC}\equiv\text{CPh}_2)$ ²⁶ is approximately *trans*, without having any crystallographic symmetry ($\tau = 155^\circ$, $\theta = 166^\circ$).

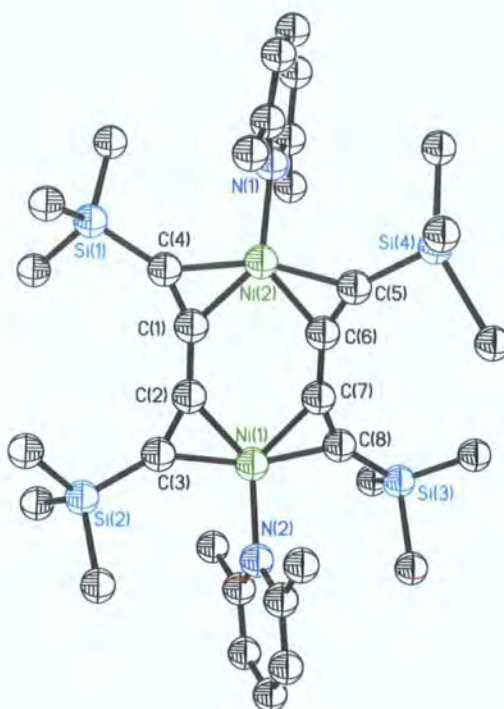


Figure 11. Molecular structure of $[(2,6\text{-dimethylpyridine})\text{Ni}]_2(\text{TMS-C}\equiv\text{C-C}\equiv\text{C-TMS})_2$. Hydrogen atoms are omitted for clarity and thermal ellipsoids are shown at 50 % probability.²⁹

We have previously reported $[\text{Rh}(\text{PMe}_3)_3(\text{Cl})]_2(\mu\text{-}(1,2\text{-}\eta^2):(3,4\text{-}\eta^2)\text{-}4\text{-F}_3\text{C-C}_6\text{H}_4\text{-C}\equiv\text{C-C}\equiv\text{C-C}_6\text{H}_4\text{-}4\text{-CF}_3)$ (*vide infra*),² which crystallised as two different solvates, each with crystallographic C_i symmetry, with the diyne ‘rod’ distorted towards a *trans*-butadiene structure through narrowing of the $\text{C}\equiv\text{C-C}$ angles. The only other di-rhodium compound in this class, $[\text{Rh}_2(\text{O}_2\text{CCF}_3)_4]_2(\text{Me}_2\text{CO})_2(\text{IC}\equiv\text{CC}\equiv\text{CI})$ ³⁴ has a most peculiar structure, containing $\text{Rh}_2(\text{O}_2\text{CCF}_3)_4$ units, weakly coordinated at one axial site by an acetone ligand (Rh-O 2.214(8) Å) and at the other axial site by a $\text{C}\equiv\text{C}$ bond of the diyne molecule, which lies at an inversion centre. The $\text{Rh}\cdots\text{C}$ distances of 2.604(13) Å and 2.632(13) Å are much longer than in $[\text{Rh}(\text{PMe}_3)_3(\text{Cl})]_2(\mu\text{-}(1,2\text{-}\eta^2):(3,4\text{-}\eta^2)\text{-}4\text{-F}_3\text{C-C}_6\text{H}_4\text{-C}\equiv\text{C-C}\equiv\text{C-C}_6\text{H}_4\text{-}4\text{-CF}_3)$ (2.212(2) Å and 2.051(2) Å in the benzene solvate). Small deviations of the diyne from linearity (angles I-C-C 166(2)° and C-C-C 173(2)°), permit $[\text{Rh}_2(\text{O}_2\text{CCF}_3)_4]_2(\text{Me}_2\text{CO})_2(\text{IC}\equiv\text{CC}\equiv\text{CI})$ to be regarded as an intermediate case between a π -complex and a co-crystal.

Evans and co-workers reported the first structurally characterised example of a 4f element coordinating in an η^2 mode to a $\text{C}\equiv\text{C}$ bond.³⁵ Reaction of two equivalents of $(\text{Cp}^*)_2\text{Sm}(\text{THF})_2$ with diphenylbutadiyne in THF gave $[(\text{Cp}^*)_2\text{Sm}]_2(\mu\text{-}(1,2\text{-}\eta^2):(3,4\text{-}\eta^2)\text{-PhC}\equiv\text{CC}\equiv\text{CPh})]$ as a red solid in 60 % yield. The structure has C_i symmetry, with a *trans*-

orientation of the metal atoms. The Cp* ligands are in an eclipsed arrangement which may be a result of the Cp*-methyl groups preferring not to reside over the C₁-C₂ multiple bond.

Pörschke *et al.* have reported the formation of $[\{(dippe)Pd\}_2(\mu-(1,2-\eta^2):(3,4-\eta^2)\text{-HC}\equiv\text{CC}\equiv\text{CH})]$, a bi-metallic Pd complex of the parent butadiyne, in the solid state;³⁶ however, in solution, the isomeric form, where both Pd(dippe) moieties coordinate to the same alkyne bond, is thermodynamically favoured (Figure 12).

Jones and co-workers have reported thermal and photochemical Si-C bond activation by donor-stabilised Pt(0)-diyne complexes.³⁷ The compound $[(Pt(COD))_2(\mu-(1,2-\eta^2):(3,4-\eta^2)\text{-TMS-C}\equiv\text{C-C}\equiv\text{C-TMS})]$ treated with two equivalents of Me₂NCH₂CH₂P^{*i*}Pr₂ (PN) gave the dinuclear Pt(II) complex $[(PN)Pt(TMS)\text{-C}\equiv\text{C-C}\equiv\text{C-Pt(TMS)(PN)}]$ under thermal conditions (70 °C, C₆D₆, 16 h) (Figure 13).

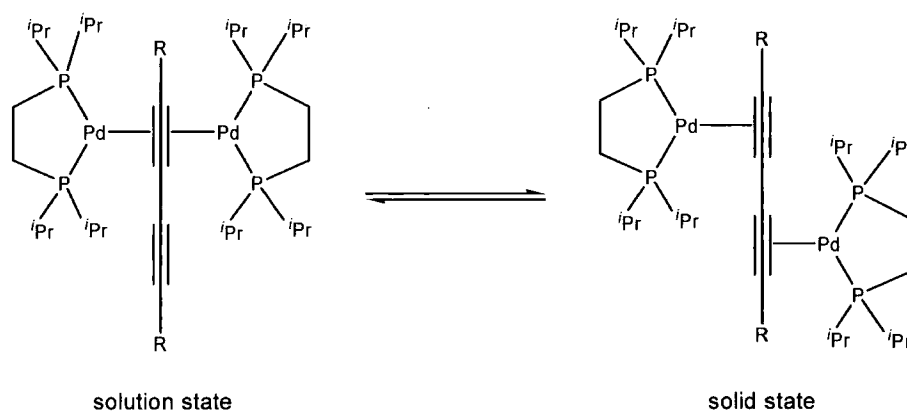


Figure 12. Reversible formation of $[\{(dippe)Pd\}_2(\mu-(1,2-\eta^2):(3,4-\eta^2)\text{-HC}\equiv\text{CC}\equiv\text{CH})]$.³⁶

The same group also observed the formation of the bi-metallic complex $[(Ni(PN))_2(\mu-(1,2-\eta^2):(3,4-\eta^2)\text{-Ph-C}\equiv\text{C-C}\equiv\text{C-Ph})]$ during their studies of the catalytic ring opening of biphenylene with Ni-alkyne complexes.³⁸ The closely related non-chelating, bis-phosphine complex, $[(Ni(PPh_3))_2(\mu-(1,2-\eta^2):(3,4-\eta^2)\text{-Ph-C}\equiv\text{C-C}\equiv\text{C-Ph})]$ has also been reported.³⁹

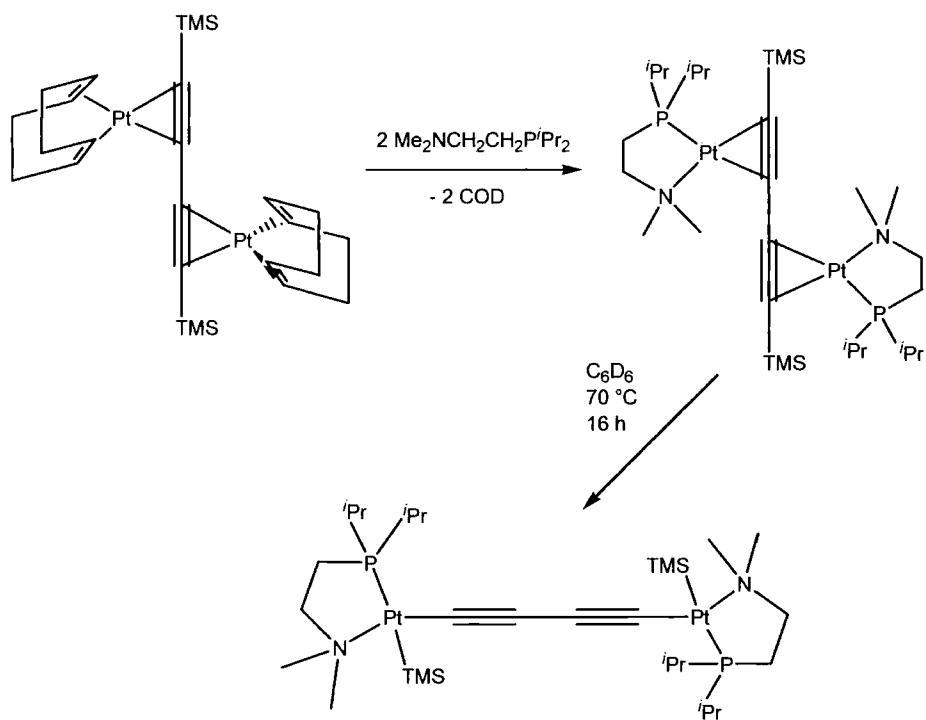


Figure 13. Thermal Si-C bond activation by a donor stabilised Pt(0) complex.

3.2 Results and Discussion

3.2.1 Intermediate π -complexes formed during Rh-Me-based rhodacycle synthesis

In the synthesis of rhodacyclopentadiene compounds based on $\text{Rh}(\text{PMe}_3)_4\text{Me}$, *in situ* $^{31}\text{P}\{^1\text{H}\}$ NMR spectroscopy, which was used to monitor the reactions, indicated that metallacycle formation did not occur with solvent cycling or without heating of the reaction mixture. Initially, there was rapid formation of an intermediate species, with three unique phosphine environments, indicated by a doublet of doublet of doublets, a doublet of triplets and a doublet of doublet of doublets, in a 1:1:1 ratio. The Rh-P coupling constants (138 Hz, 83 Hz and 127 Hz respectively), clearly indicate a Rh(I) species, which may be assigned to a complex formed from the π -coordination of one diyne $\text{C}\equiv\text{C}$ bond to Rh with displacement of a PMe_3 ligand. The sharp peaks and splitting observed in the $^{31}\text{P}\{^1\text{H}\}$ NMR spectra indicate that the complex is static, with no rotation around the Rh-alkyne bond (Figure 14).

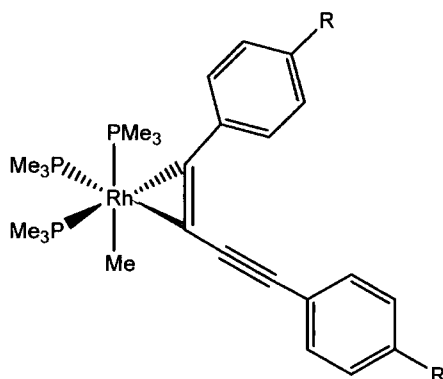


Figure 14. Proposed intermediate formed by π -coordination of diyne to $\text{Rh}(\text{PMe}_3)_4\text{Me}$.

As is expected, the Me group occupies an axial environment which, due to the unsymmetrical coordination of diyne, results in three inequivalent PMe_3 ligands. Rossi and Hoffmann showed that for 18-electron trigonal bipyramidal $d^8\text{-ML}_4\text{-X}$ systems, strong σ -donors prefer axial positions whereas strong π -acceptors bind in the equatorial plane.⁴⁰ The ^1H NMR spectrum supports the proposed structure, showing three unique PMe_3

environments and, for *para*-substituted diynes, four doublets corresponding to the four aromatic proton environments. The spectra also showed there to be one equivalent of free diyne present in solution. Compounds **1-3** were synthesised by reaction of one equivalent of diyne with $\text{Rh}(\text{PMe}_3)_4\text{Me}$, and gave identical ^1H and $^{31}\text{P}\{^1\text{H}\}$ NMR spectra (without the peaks associated with free diyne) under the above conditions (Figures 15 and 16). ^1H and $^{19}\text{F}\{^1\text{H}\}$ NMR spectra show that there are two different environments for the OMe, CO_2Me and CF_3 *para*-substituents, arising from the unsymmetrically bound diyne, and a complex second order, finely structured, approximate ‘doublet of quartets’ for the Rh-Me ligand (Figure 17).

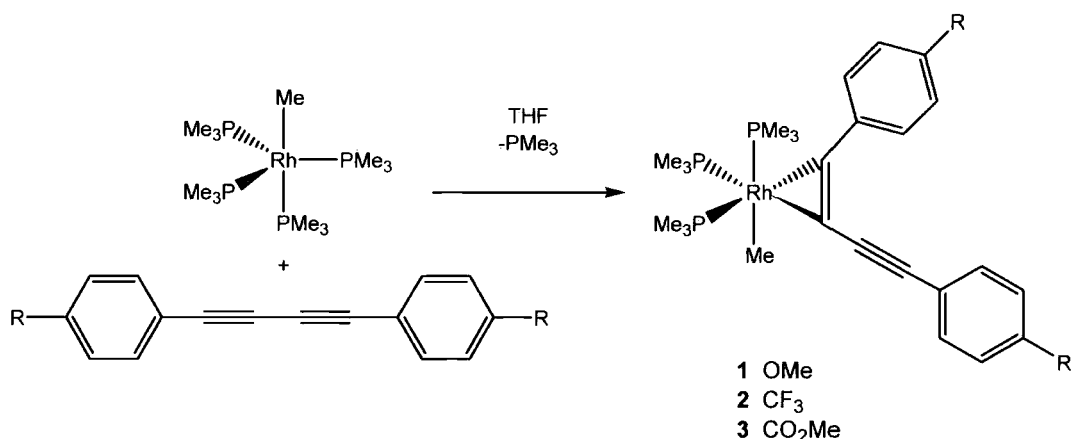


Figure 15. General reaction scheme for the formation of compounds **1-3**.

Although we were not successful in obtaining crystal structures to support the NMR spectroscopic evidence for the proposed intermediate, we successfully grew crystals of $\text{Rh}(\text{PMe}_3)_3\text{Me}(\eta^2\text{-MeO-4-C}_6\text{H}_4\text{-C}\equiv\text{C-C}_6\text{H}_4\text{-4-CN})$, **4**. In this compound, the unsymmetrical tolan, $\text{MeO-4-C}_6\text{H}_4\text{-C}\equiv\text{C-C}_6\text{H}_4\text{-4-CN}$, was used in place of the 1,4-bis(4-R-phenyl)buta-1,3-diyne and, due to the different *para*-substituents, formed an unsymmetrical π -complex with $\text{Rh}(\text{PMe}_3)_3\text{Me}$. Addition of one equivalent of the tolan to $\text{Rh}(\text{PMe}_3)_4\text{Me}$ in THF immediately formed the orange π -complex in quantitative yield. The X-ray structure (*vide infra*) confirms the axial position of the methyl ligand and hence the three mutually *cis* PMe_3 ligands. The ^1H NMR spectrum of **4** is very similar to those of compounds **1-3**. Due to the small chemical shift difference between the three PMe_3 environments in the spectrum of **4**, the $^{31}\text{P}\{^1\text{H}\}$ NMR spectrum, however, is not the same. Unlike the spectra for **1-3**, the spectrum of **4** does not show three individual peaks but

instead shows a complex second order pattern, although the integrals are clearly in a 1:1:1 ratio (Figure 18).

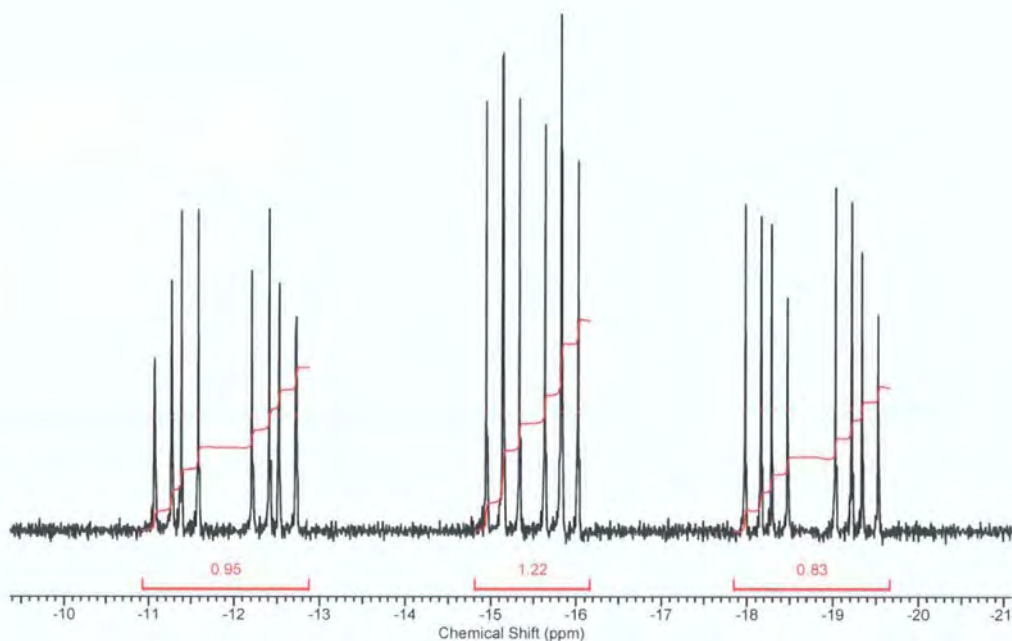


Figure 16. $^{31}\text{P}\{^1\text{H}\}$ NMR spectrum of compound 1.

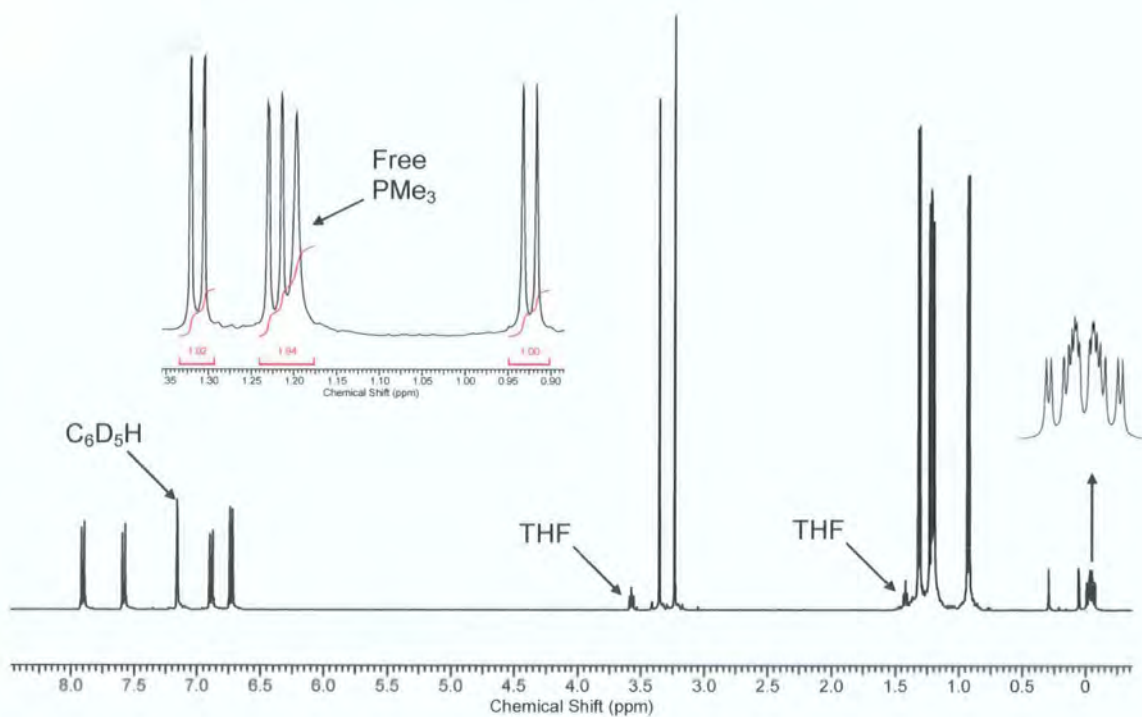


Figure 17. ^1H NMR spectrum of compound 1.

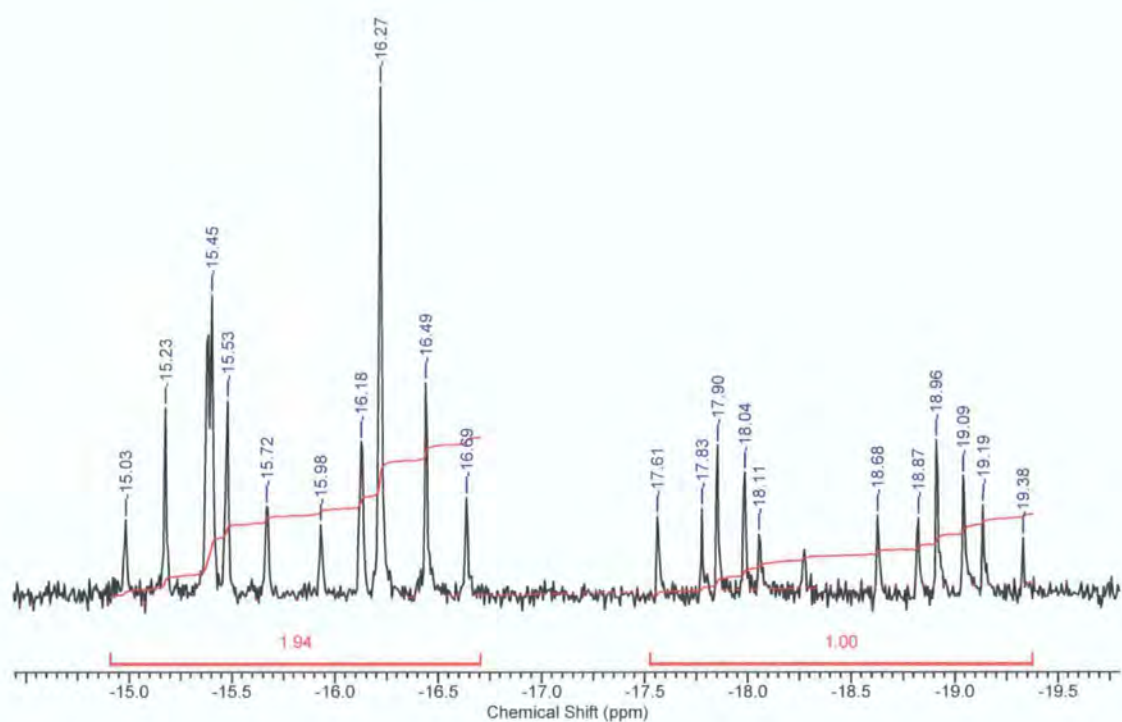


Figure 18. $^{31}\text{P}\{^1\text{H}\}$ NMR spectrum of compound **4**.

Reaction of one equivalent of the symmetrical tolan, 4-F₃C-C₆H₄C≡C-C≡CC₆H₄-4-CF₃ in THF with Rh(PMe₃)₄Me, gave Rh(PMe₃)₃Me(η²-4-F₃C-C₆H₄C≡C-C≡CC₆H₄-4-CF₃), **5**, the symmetrical analogue of **4**. The ¹H and ¹⁹F{¹H} NMR spectra of **5** clearly show that there are only two PMe₃ environments, in a 2:1 ratio, and a single *para*-substituent peak, further confirming the axial environment of the methyl ligand and supporting the formulation of **1-3**. As for **4**, the $^{31}\text{P}\{^1\text{H}\}$ NMR spectrum of **5** was heavily 2nd order due to the small chemical shift difference between the two phosphine environments.

3.2.2 Crystal structure of **4**

Crystallographic data for compound **4** is presented in Tables 1 and 2. Compound **4** was crystallised in a 5 mm diameter glass tube by slow diffusion of a layer of hexane into a THF solution.

Lengths	4	Angles	4
Rh-C(0)	2.138(3)	C(1)-C(2)-C(3)	141.0(3)
Rh-P(1)	2.3278(8)	C(1)-C(2)-C(3')	149.1(6)
Rh-P(2)	2.3209(9)	C(2)-C(1)-C(10)	142.6(3)
Rh-P(3)	2.3394(8)	C(1)-Rh-C(2)	35.68(11)
Rh-C(1)	2.107(3)	C(0)-Rh-P(3)	173.38(9)
Rh-C(2)	2.093(3)	P(1)-Rh-P(2)	102.33(3)
C(1)-C(2)	1.287(4)	RhC(1)C(2) vs. ring C(3)-C(8)*	35.3
C(2)-C(3)	1.440(5)	RhC(1)C(2) vs. ring C(3')-C(8')*	31.7
C(1)-C(10)	1.453(4)	RhC(1)C(2) vs. ring C(10)-C(15)*	8.0

Table 1. Selected bond lengths (Å) and angles (°) in compound 4. * Denotes interplanar angles.

Monoclinic crystals (space group = $P2_1/c$) were found to have a single molecule in the asymmetric unit with a distorted trigonal bipyramidal geometry around Rh and a mutually *cis* orientation of the three PMe_3 ligands, with P(1)Me_3 and P(2)Me_3 in equatorial environments and P(3)Me_3 in an axial environment [$\text{Rh-P(1)} = 2.3278(8)$ Å, $\text{Rh-P(2)} = 2.3209(9)$ Å, $\text{Rh-P(3)} = 2.3394(8)$ Å] (Figure 19). The Rh-C(1) and Rh-C(2) bond lengths are slightly shorter than Rh-C(0) [2.107(3) Å, 2.093(3) Å and 2.138(3) Å respectively] with the π -coordinated alkyne rotated only 10.3° with respect to the Rh-P(1)-P(2) plane. The P(1)-Rh-P(2) angle of $102.33(3)^\circ$ is smaller than expected for a trigonal bipyramid due to the steric bulk of the coordinated alkyne and the *trans* C(0)-Rh-P(3) angle is $173.38(9)^\circ$. The cyano phenyl ring, C(10)-C(15) is almost co-planar with the metallacycle [8.0°] whereas the disordered methoxyphenyl group C(3)-C(8) [and C(3')-C(8')] are rotated by 41.2° and 37.5° respectively to the C(10)-C(15) ring. The C(1)-C(2)-C(3) and C(10)-C(1)-C(2) angles are considerably less than 180° , being $141.0(3)^\circ$ and $142.6(3)^\circ$ respectively. In comparison, the corresponding angles in the free tolan⁴¹ are close to linearity, [$176.23(15)^\circ$ and $176.25(15)^\circ$ respectively] and the alkyne bond is lengthened from $1.198(2)$ Å to $1.287(4)$ Å. The methoxyphenyl group, O and C(3)-C(9) with attached hydrogens, are

disordered between two orientations with occupancies of 75 % and 25 % respectively. The ligand P(1)Me₃ is rotationally disordered between two positions, and C(17), C(18) and C(19) (with attached hydrogens) occupy two positions with the occupancies of 82 % and 18 %.

Molecule	4 - 06srv104
Empirical formula	C ₂₆ H ₄₁ NOP ₃ Rh
Formula Weight	579.42
Temperature (K)	120(2)
Crystal system	Monoclinic
Space Group	<i>P</i> 2 ₁ / <i>c</i>
a (Å)	9.3243(7)
b (Å)	15.5098(11)
c (Å)	19.7237(13)
α (°)	90.00
β (°)	100.78(1)
γ (°)	90.00
Volume (Å ³)	2802.1(3)
Z	4
Density (calculated) Mg/m ³	1.373
Absorption coefficient (mm ⁻¹)	0.799
Crystal size (mm)	0.38 x 0.19 x 0.10
Theta range for data collection (°)	2.22 to 28.85
Reflections collected	7425
Independent reflections	6454
Data / Restraints / Parameters	7425 / 74 / 345
Final R indices	R1 = 0.0429 wR2 = 0.0983
R indices (all data)	R1 = 0.0514 wR2 = 0.1019

Table 2. Summary of the crystallographic data for compound 4.

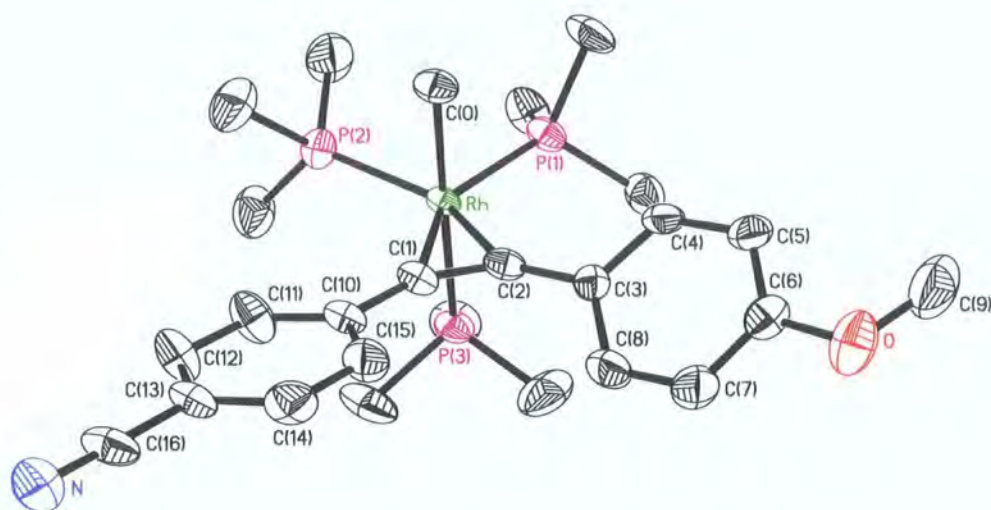


Figure 19. Molecular structure of $\text{Rh}(\text{PMe}_3)_3\text{Me}(\eta^2\text{-4-MeO-C}_6\text{H}_4\text{-C}\equiv\text{C-C}_6\text{H}_4\text{-4-CN})$. Disorder in $\text{P}(1)\text{Me}_3$ and the methoxyphenyl group, O' and $\text{C}(3)'\text{-C}(9)'$ and all hydrogen atoms are omitted for clarity and thermal ellipsoids are shown at 50 % probability.

3.3.3 Proposed reaction mechanism

From the NMR spectroscopic evidence, it is proposed that rhodacyclopentadiene formation occurs *via* a stepwise mechanism. Initially, one equivalent of diyne forms a π -complex with Rh, with the diyne lying in the equatorial plane, by displacement of one PMe_3 ligand. The sharp NMR spectra are consistent with a static complex or one in which any alkyne rotation, Berry pseudorotation or alkyne dissociation process must be extremely slow at best on the NMR timescale at room temperature. Before cyclisation can occur, a second PMe_3 must temporarily dissociate from Rh, so that a second equivalent of diyne can coordinate in the vacant site, forming a bis(π -complex) which can then go on to cyclise, forming the metallacycle (Figure 20). The coordination site left vacant upon rhodacyclopentadiene formation is then filled with the PMe_3 displaced in the second step. Removal of the first equivalent of PMe_3 *in vacuo*, will thus facilitate the reaction, as binding of the second diyne would be inhibited by the presence of excess PMe_3 .

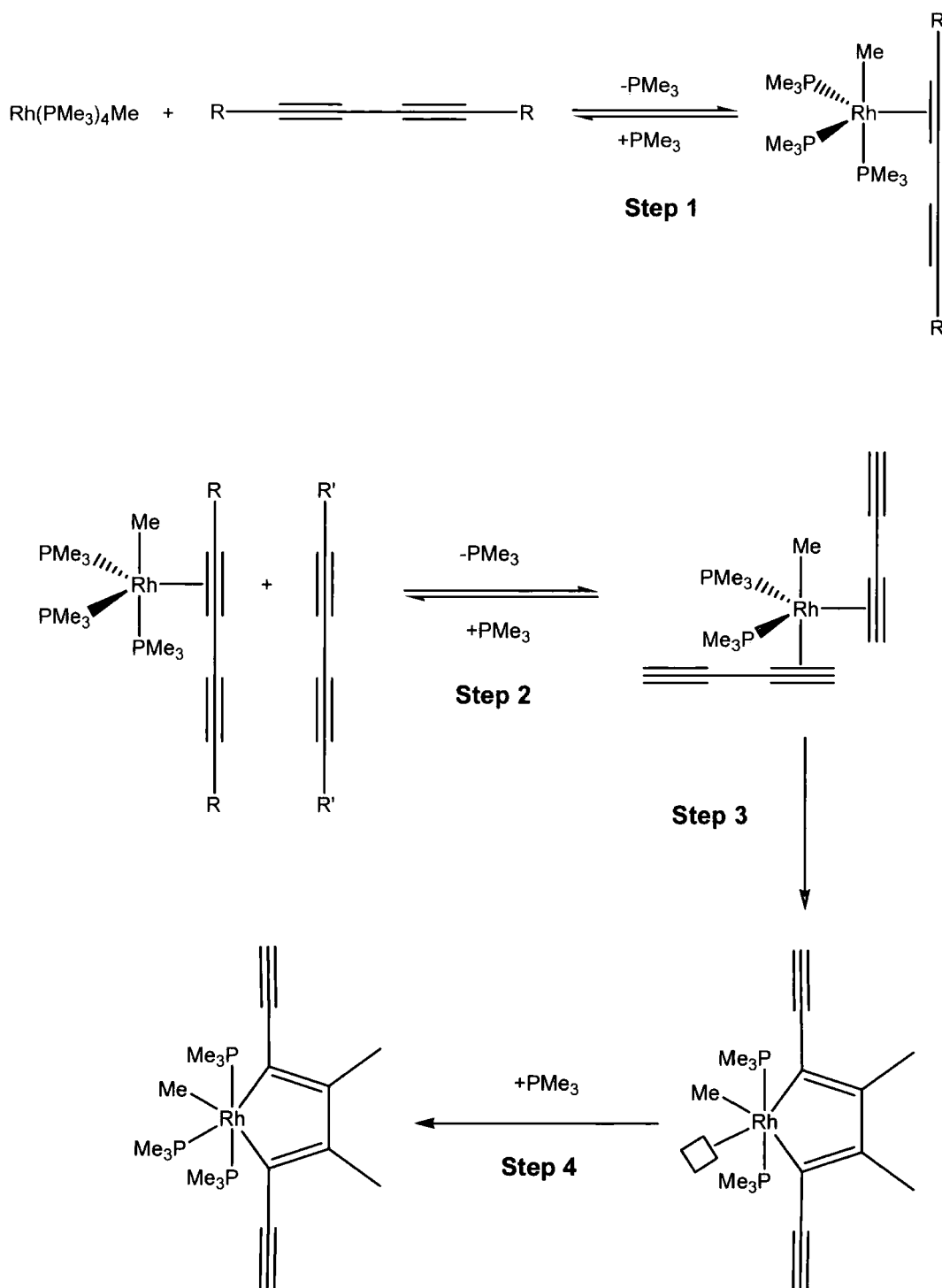


Figure 20. Proposed step-wise reaction mechanism.

As was noted in Chapter 2, in the synthesis of rhodacyclopentadienes, the cycling of THF solvent during synthesis aids binding of the second diyne and thus metallacycle formation by removing the liberated PMe_3 , encouraging the temporary dissociation of a second PMe_3 ligand. Given the strong *trans*-influence of the Me ligand (cf. $J_{\text{Rh-P trans to Me}} =$

83 Hz), it is most likely that PMe_3 dissociation occurs *trans* to the CH_3 group. Step 2 is a reversible step, such that either of the coordinated diynes may dissociate from the Rh before the cyclisation process occurs. If two different diynes are used in Step 1 and Step 2, then this results in scrambling, and a number of compounds are formed. To probe the mechanism, the sequential addition of two diynes with differing *para*-substituents to $\text{Rh}(\text{PMe}_3)_4\text{Me}$ was followed by *in situ* $^{31}\text{P}\{^1\text{H}\}$ NMR spectroscopy. Reaction of $\text{Rh}(\text{PMe}_3)_4\text{Me}$, first with one equivalent of $4\text{-F}_3\text{C-C}_6\text{H}_4\text{-C}\equiv\text{C-C}\equiv\text{C-C}_6\text{H}_4\text{-4-CF}_3$, gave compound **2** in quantitative yield. *In situ* reaction of this complex with one equivalent of $4\text{-MeO-C}_6\text{H}_4\text{-C}\equiv\text{C-C}\equiv\text{C-C}_6\text{H}_4\text{-4-OMe}$, resulted in the formation of four unique rhodacycles as shown by four sets of doublets of doublets with associated doublets of triplets in the $^{31}\text{P}\{^1\text{H}\}$ NMR spectrum (Figure 21). The peak intensities indicate two major products and two minor products in an approximate ratio of 12:15:65:76 (i.e. both major and minor products form in a ca. 1:1 ratio). It was possible to assign each of the minor isomers to the previously synthesised symmetrical CF_3 and OMe rhodacycles proving that some mixing does occur and that diyne coordination to Rh during Step 2, is reversible. However, the predominance of the unsymmetric products to the symmetric ones (ca. 5:1) suggests that diyne dissociation from the bis(diyne) intermediate is probably slower than cyclisation. In addition, quantitative formation of the mono-diyne π -complex shows that the second step must be significantly slower than the formation of the initial π -complex.

The two major products are proposed to be the two unsymmetrically substituted compounds formed by the reductive coupling of one equivalent of each diyne on Rh. The Me ligand in the environment *trans* to the rhodacycle results in the formation of two regioisomeric compounds (Figure 22), and the result was not dependent on the order in which the different diynes were added. Thus, addition of one equivalent of $4\text{-MeO-C}_6\text{H}_4\text{-C}\equiv\text{C-C}\equiv\text{C-C}_6\text{H}_4\text{-4-OMe}$ to $\text{Rh}(\text{PMe}_3)_4\text{Me}$ gave **1**; subsequent addition of one equivalent of $4\text{-F}_3\text{C-C}_6\text{H}_4\text{-C}\equiv\text{C-C}\equiv\text{C-C}_6\text{H}_4\text{-4-CF}_3$ to this complex gave the same mixture of four products in approximately the same ratio (10:17:65:72), indicating that both donor and acceptor substituted diynes are able to dissociate from the bis(π -complex) intermediate. Although the mixture was not separated, it has been shown that the luminescent TMSA-substituted rhodacycles are stable to chromatography on silica gel columns and so it may well be possible to separate the mixture by this method or even by preparative HPLC.

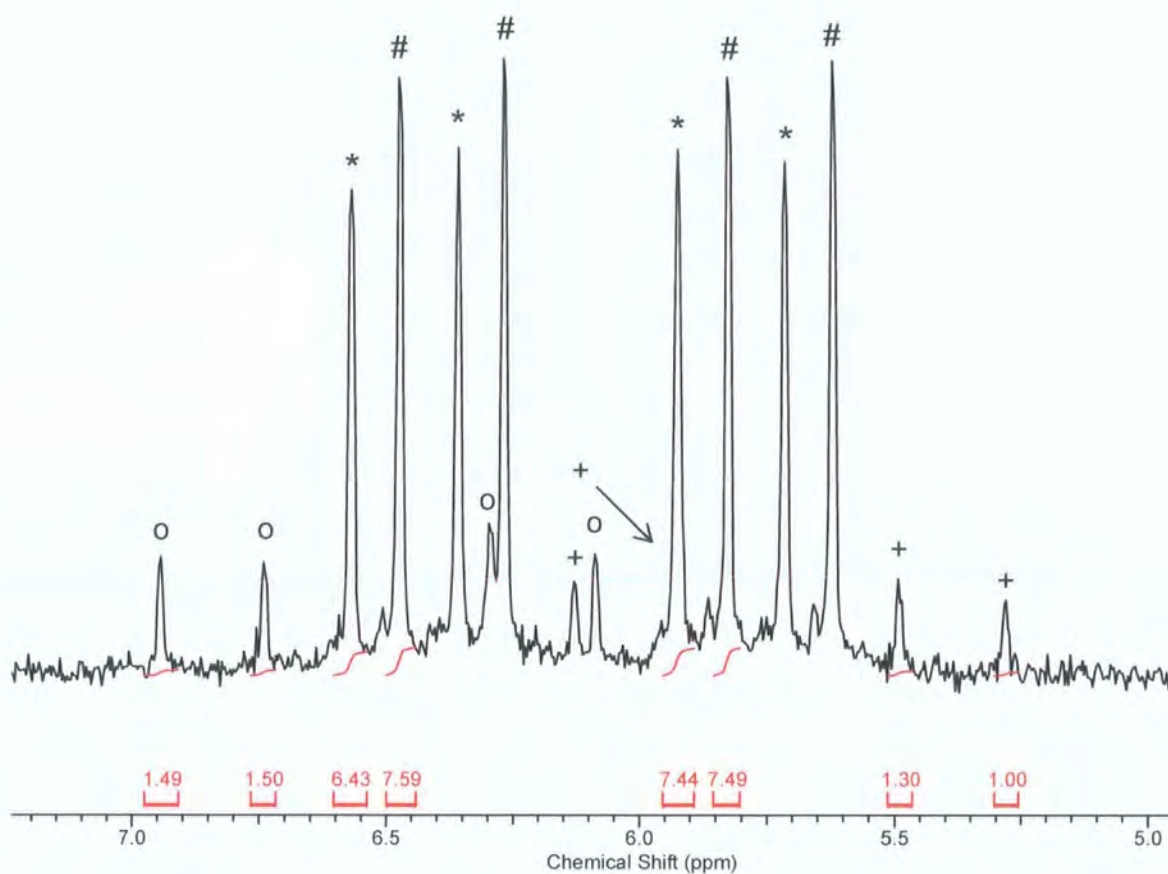


Figure 21. The doublet of doublet region of the *in situ* $^{31}\text{P}\{^1\text{H}\}$ NMR spectrum recorded after the addition of one equivalent of 4-MeO-C₆H₄-C≡C-C≡C-C₆H₄-4-OMe to compound **2**. The doublets of doublets for the four rhodacycle compounds are indicated by o, *, # and +.

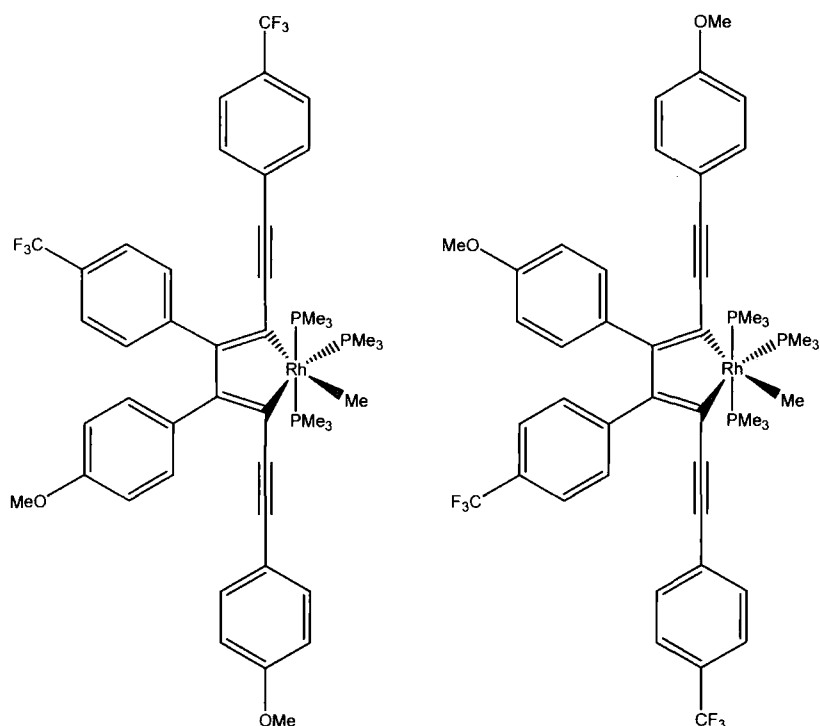


Figure 22. Two regioisomers formed by sequential reaction of $\text{Rh}(\text{PMe}_3)_4\text{Me}$ with 4-MeO-C₆H₄-C≡C-C≡C-C₆H₄-4-OMe and 4-F₃C-C₆H₄-C≡C-C≡C-C₆H₄-4-CF₃ in either order.

3.3.4 Intermediate π -complexes formed during attempts to synthesise a Rh-Cl-based rhodacycle

Two equivalents of 4-F₃C-C₆H₄-C≡C-C≡C-C₆H₄-4-CF₃ were added to a suspension of $[\text{Rh}(\text{PMe}_3)_4]\text{Cl}$ in THF and, over a period of several minutes, the RhCl salt gradually dissolved. Following the reaction by *in situ* $^{31}\text{P}\{^1\text{H}\}$ NMR spectroscopy showed that we had not formed the expected rhodacycle. The spectra instead showed two sets of doublet of doublets, -1.61 (dd, $^1J_{\text{RhP}} = 97$ Hz, $^2J_{\text{PP}} = 37$ Hz), -2.86 (dd, $^1J_{\text{RhP}} = 97$ Hz, $^2J_{\text{PP}} = 35$ Hz) with associated doublets of triplets, -11.36 (dt, $^1J_{\text{RhP}} = 141$ Hz, $^2J_{\text{PP}} = 35$ Hz), -16.49 (dt, $^1J_{\text{RhP}} = 135$ Hz, $^2J_{\text{PP}} = 37$ Hz). The magnitude of the $^1J_{\text{Rh-P}}$ coupling constants (>100 Hz for the doublet of triplets) clearly suggest Rh(I) rather than Rh(III). The relative intensities of the peaks indicated that those at -1.61 and -16.49 ppm represent two and one PMe_3 ligands respectively for one compound, whereas those at -2.86 and -11.36 ppm represent two and one PMe_3 ligands respectively for a second compound. *In situ* $^{19}\text{F}\{^1\text{H}\}$ NMR spectroscopy reveals that both compounds contain unsymmetrically bound diyne insofar as

each species gave rise to two singlets for the CF₃ peaks in a 1:1 ratio which can be assigned as two 1:1 regioisomers, **6** and **7**, due to the Cl being in an equatorial position (Figure 23).

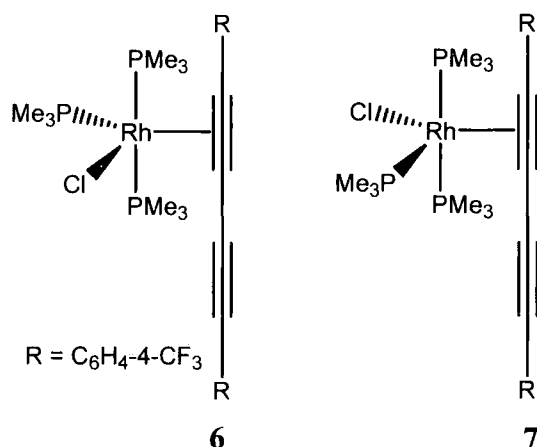


Figure 23. Two isomeric RhCl intermediates with diene lying in the RhPCL equatorial plane.

Initially, it was suggested that the intermediates formed were a mixture of **6** or **7** with a bi-metallic complex, **8** (Figure 24).² The ³¹P{¹H} and ¹⁹F{¹H} NMR spectroscopy and IR data supported this proposed structure and Pörschke *et al.* had shown closely related behaviour for [{(dippe)Pd}₂-(HC≡C-C≡CH)];³⁶ however, further work on alkyne π-complexes formed from [Rh(PMe₃)₄]Cl has since confirmed the formation of the two regioisomeric complexes **6** and **7** (*vide infra*).

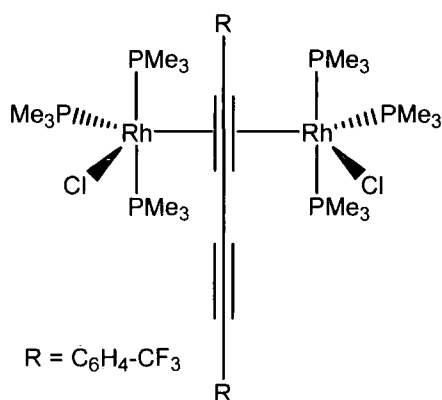


Figure 24. Incorrectly proposed bi-metallic intermediate, **8**.

Overnight, purple crystals suitable for X-ray analysis formed in 50 % yield from a C_6D_6/THF solution. Two single crystal structures obtained from two separate reactions carried out in different NMR tubes revealed that in contrast to what was observed in solution, the material which precipitated was a relatively rare μ -(1,2- η^2):(3,4- η^2) bi-metallic species in which each butadiyne triple bond is coordinated to a separate Rh centre, **9** (Figure 25). It is likely that the formation of **9** is not reversible, thus inhibiting the metallacycle cyclisation step and so hindering rhodacyclopentadiene formation. Attempts to prepare Rh-Me analogues of **9** were unsuccessful.

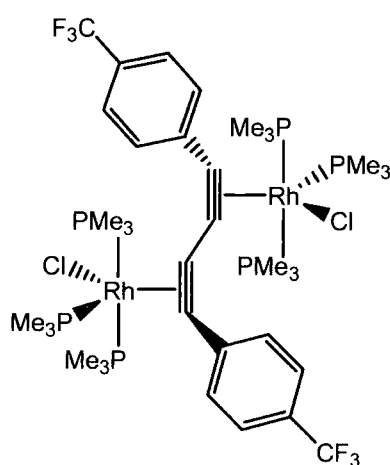


Figure 25. $[Rh(PMe_3)_3(Cl)]_2(\mu$ -(1,2- η^2):(3,4- η^2)-4-F₃C-C₆H₄-C≡C-C≡C-C₆H₄-4-CF₃), **9**.

3.3.5 Crystal structure of **9**

Compound **9** was characterised by single-crystal X-ray studies of two different solvates, namely **9**·5 C_6D_6 and **9**·2THF. In both structures, molecule **9** has crystallographic C_i symmetry and a similar geometry (Figure 26 and Tables 3 and 4). The former structure contains two independent C_6D_6 molecules in general positions and another at an inversion centre, whereas the latter has one THF molecule in a general position. The 18-electron Rh centre adopts a distorted trigonal bipyramidal geometry. The P(1) and P(3) atoms occupy apical positions and the C(1)≡C(2) bond lies in the equatorial plane, as defined by its midpoint and the atoms Rh, Cl, P(2), as expected (*vide supra*). The diyne ‘rod’ is distorted toward a ‘*trans*-butadiene’ structure through narrowing of the C≡C-C angles. In **9**·5 C_6D_6 ,

the whole butadiyne is substantially planar; all of its carbon atoms, as well as Rh, Cl, P(2) atoms and their equivalents, lie in one plane with a mean deviation of 0.02 Å. Note that in single crystals, 1,4-bis(4-CF₃-phenyl)buta-1,3-diyne is neither entirely planar nor linear; the two benzene rings form a dihedral angle of 10.7°, the C(aryl)-CF₃ bond directions differ by 10.0°, and the carbon atoms deviate from their mean plane by 0.13 Å on average.⁴² The π -coordinated C(1)≡C(2) bond in **7** (Table 1) is lengthened by 0.09 Å compared to 1.205(2) Å in the butadiyne; the adjacent bonds C(2)-C(3) [1.454(3) Å] and C(1)-C(1') [1.405(4) Å] in the more precise structure **9**·5C₆D₆ are also longer than the corresponding bonds in the diyne [1.434(2) and 1.372(2) Å respectively] as a result of lower s-character in the bonds. The Rh-C(1) and Rh-C(2) distances are considerably different, reflecting the greater *trans*-influence of PMe₃ compared to that of Cl. In **9**·5C₆D₆, the CF₃ group is rotationally disordered between orientations A (90 %) and B (10 %); the latter was refined in isotropic approximation with restraints to threefold symmetry.

	9 ·5C ₆ D ₆	9 ·2THF		9 ·5C ₆ D ₆	9 ·2THF
Rh-Cl	2.5339(6)	2.515(1)	π -Rh-P(2)	132.4(6)	133.3(1)
Rh-P(1)	2.3172(7)	2.314(1)	π -Rh-P(3)	90.6(6)	89.3(1)
Rh-P(2)	2.3260(7)	2.327(1)	P(1)-Rh-P(2)	93.97(2)	94.28(4)
Rh-P(3)	2.3135(6)	2.309(1)	P(1)-Rh-P(3)	168.90(2)	168.92(4)
Rh-C(1)	2.212(2)	2.212(4)	P(2)-Rh-P(3)	94.02(2)	93.45(4)
Rh-C(2)	2.051(2)	2.039(4)	P(1)-Rh-Cl	85.90(2)	86.27(4)
C(1)-C(2)	1.296(3)	1.292(5)	P(2)-Rh-Cl	95.29(2)	95.58(4)
C(1)-C(1')	1.405(4)	1.394(8)	P(3)-Rh-Cl	85.70(2)	85.09(4)
C(2)-C(3)	1.454(3)	1.449(5)	C(1')-C(1)-C(2)	146.8(3)	147.6(5)
π -Rh-Cl	132.3(6)	131.0(1)	C(1)-C(2)-C(3)	140.0(2)	139.3(4)
π -Rh-P(1)	89.7(6)	91.2(1)			

Table 3. Selected bond lengths (Å) and angles (°) in compound **9**·5C₆D₆ and **9**·2THF. π is the midpoint of the C(1)≡C(2) bond.

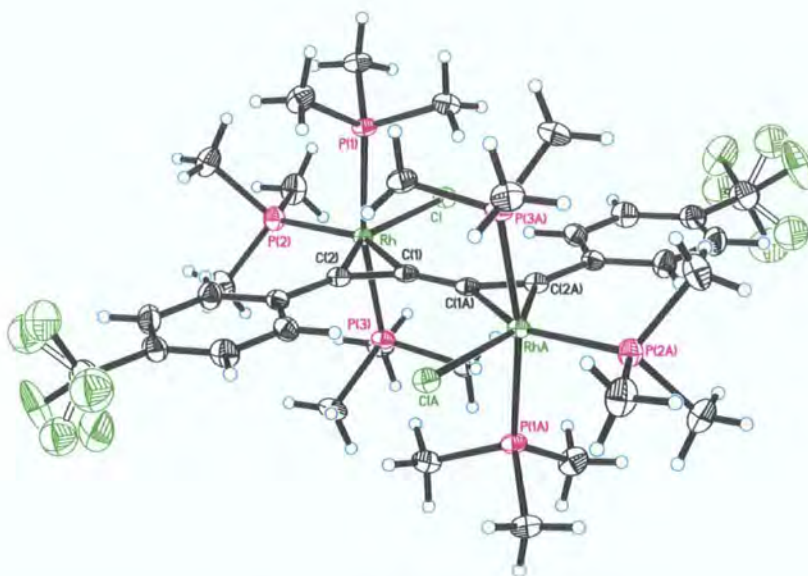


Figure 26. Molecular structure of $9 \cdot 5C_6D_6$. Solvent molecules have been omitted for clarity and the thermal ellipsoids are shown at 50 % probability.

3.3.6 Synthesis of $Rh(PMe_3)_3Cl$ π -complexes

To support the proposition that the Cl ligands in **6** and **7** lie in the equatorial plane and that coordination of an unsymmetrical alkyne (i.e. 1,4-bis(4-R-phenyl)buta-1,3-diyne) results in the formation of two regioisomers, we prepared the complex $Rh(PMe_3)_3Cl(\eta^2\text{-MeO-4-C}_6\text{H}_4\text{-C}\equiv\text{C-C}_6\text{H}_4\text{-4-CN})$, **10**, by reaction of one equivalent of MeO-4-C₆H₄-C \equiv C-C₆H₄-4-CN with a suspension of $[Rh(PMe_3)_4]Cl$ in THF. The tolan was employed rather than diyne to prevent the formation of the bi-metallic complex **9**. *In situ* 1H and $^{31}P\{^1H\}$ NMR spectroscopy revealed that the use of an unsymmetrical tolan gives rise to similar spectrum to that observed for the mixture of compounds **6** and **7**. The $^{31}P\{^1H\}$ NMR spectrum shows two pairs of overlapping doublets of doublets ($^1J_{RhP} = 101$ Hz and $^2J_{PP} = 40$ Hz) with associated doublets of triplets ($^1J_{RhP} = 133$ Hz and $^2J_{PP} = 40$ Hz) indicating two very closely related compounds. Eight sets of doublets in the aromatic region of the 1H NMR spectrum also support this.

Molecule	9·5C₆D₆ - 05srv250	9·2THF - 05srv290
Empirical formula	C ₃₆ H ₆₂ Cl ₂ F ₆ P ₆ Rh ₂ 5(C ₆ D ₆)	C ₃₆ H ₆₂ Cl ₂ F ₆ P ₆ Rh ₂ 2(C ₄ H ₈ O)
Formula Weight	1492.12	1215.60
Temperature (K)	120(2)	120(2)
Crystal system	Monoclinic	Monoclinic
Space Group	<i>P</i> 2 ₁ / <i>c</i>	<i>P</i> 2 ₁ / <i>n</i>
a (Å)	14.684(2)	17.014(2)
b (Å)	13.572(2)	10.046(1)
c (Å)	18.072(2)	17.835(2)
α (°)	90.0	90.00
β (°)	100.58(1)	112.72(1)
γ (°)	90.0	90.00
Volume (Å ³)	3540.4(8)	2811.9(5)
Z	2	2
Density (calculated) Mg/m ³	1.400	1.436
Absorption coefficient (mm ⁻¹)	0.730	0.905
Crystal size (mm)	0.22 x 0.20 x 0.09	0.19 x 0.07 x 0.02
Theta range for data collection (°)	1.41 to 29.98	1.41 to 27.50
Reflections collected	10317	6448
Independent reflections	7786	4645
Data / Restraints / Parameters	10317 / 6 / 409	6448 / 0 / 298
Final R indices	R1 = 0.0357 wR2 = 0.0767	R1 = 0.0466 wR2 = 0.1020
R indices (all data)	R1 = 0.0610 wR2 = 0.0860	R1 = 0.0757 wR2 = 0.1127

Table 4. Summary of the crystallographic data for compound **9**.

3.3.7 Crystal structure of **10b**

The crystallographic data for compound **10b** is presented in Tables 5 and 6. Compound **10b** was crystallised in a 5 mm diameter glass tube by slow diffusion of a layer of hexane into a toluene solution of a mixture of two regioisomers **10a** and **10b** (Figure 27).

Lengths	10b	Angles	10b
Rh-Cl	2.5187(5)	C(1)-C(2)-C(3)	146.79(15)
Rh-P(1)	2.3213(5)	C(2)-C(1)-C(10)	145.77(15)
Rh-P(2)	2.3428(4)	C(1)-Rh-C(2)	35.88(6)
Rh-P(3)	2.3130(5)	Cl-Rh-P(2)	96.381(15)
Rh-C(1)	2.0613(15)	P(1)-Rh-P(3)	170.516(15)
Rh-C(2)	2.1144(15)	RhC(1)C(2) vs. ring C(3)-C(8)*	11.5
C(1)-C(2)	1.287(2)	RhC(1)C(2) vs. ring C(10)-C(15)*	14.9
C(2)-C(3)	1.447(2)		
C(1)-C(10)	1.443(2)		

Table 5. Selected bond lengths (Å) and angles (°) in compound **10b**. * Denotes interplanar angles.

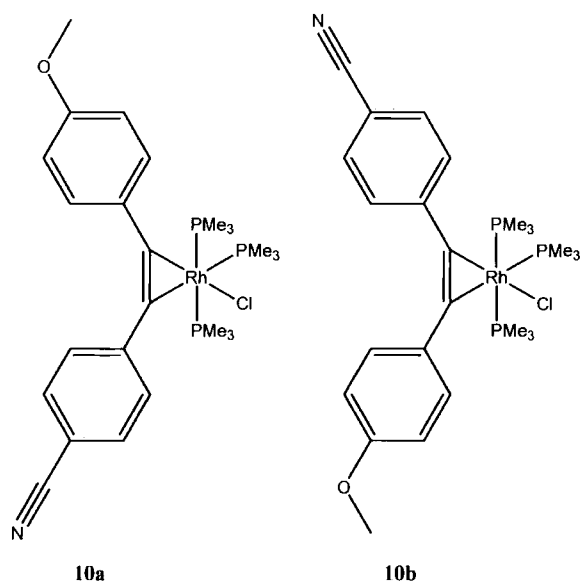


Figure 27. Diagram showing the two possible isomers of compound **10**.

Monoclinic crystals (space group = $P2_1/c$) were found to contain a single isomer of **10** with a distorted trigonal bipyramidal geometry around Rh with P(1)Me₃ *trans* to P(3)Me₃ and P(2)Me₃ and Cl in the equatorial plane [Rh-P(1) = 2.3213(5) Å, Rh-P(2) = 2.3428(4) Å, Rh-P(3) = 2.3130(5) Å and Rh-Cl = 2.5187(5) Å] (Figure 27). The Rh-C(1)

and Rh-C(2) bond lengths are 2.0613(15) Å and 2.1144(15) Å respectively, with the π -coordinated alkyne rotated by 2.0° out of the Rh-P(1)-P(2) plane.

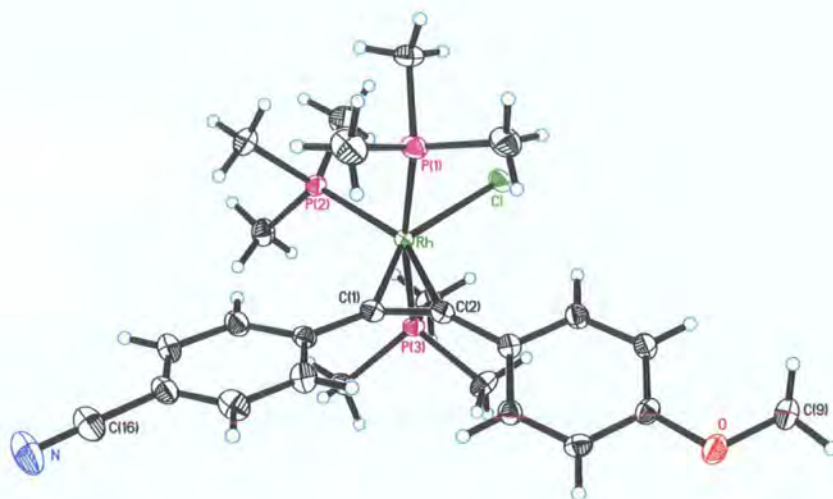


Figure 28. Molecular structure of $\text{Rh}(\text{PMe}_3)_3\text{Cl}(\eta^2\text{-MeO-4-C}_6\text{H}_4\text{-C}\equiv\text{C-C}_6\text{H}_4\text{-4-CN})$, **10b**. Thermal ellipsoids are shown at 50 % probability.

The P(1)-Rh-P(3) angle and the Cl-Rh-P(2) angles [170.516(15)° and 96.381(15)° respectively] are smaller than expected for a trigonal bipyramidal structure due to the steric effects. Both the methoxy-substituted phenyl ring, C(2)-C(7), and cyano-substituted phenyl ring, C(10)-C(15), are nearly co-planar with the metallacycle [interplanar angles being 11.5° and 14.9° respectively] and are thus rotated with respect to one another by 26.4°. The C(1)-C(2)-C(3) and C(10)-C(1)-C(2) angles are not linear at 146.79(15)° and 145.77(15)° respectively indicating substantial bend-back of the alkyne substituents due to the large degree of π -backbonding. In crystals of the free tolan⁴¹ the corresponding angles are close to 180°, [176.23(15)° and 176.25(15)° respectively]. The alkyne triple bond C(1)-C(2) is lengthened from 1.198(2) Å in the free tolan to 1.287(2) Å in the π -complex.

We also prepared $\text{Rh}(\text{PMe}_3)_3\text{Cl}(\eta^2\text{-CF}_3\text{-4-C}_6\text{H}_4\text{-C}\equiv\text{C-C}_6\text{H}_4\text{-4-CF}_3)$, **11**, to demonstrate that coordination of a symmetrical alkyne results in a single isomer only, with inequivalent CF₃ groups, due to the equatorial Cl ligand. Using variable temperature ¹⁹F{¹H} NMR spectroscopy, we studied the energy barrier to rotation around the Rh-alkyne π -bond. At room temperature, there are two CF₃ peaks with equal integrals.

Molecule	10b - 06srv041
Empirical formula	C ₂₅ H ₃₈ ClNOP ₃ Rh
Formula Weight	599.83
Temperature (K)	120(2)
Crystal system	Monoclinic
Space Group	<i>P</i> 2 ₁ / <i>c</i>
a (Å)	13.0598(14)
b (Å)	12.6394(13)
c (Å)	17.2022(18)
α (°)	90.00
β (°)	97.12(1)
γ (°)	90.00
Volume (Å ³)	2817.6(5)
Z	4
Density (calculated) Mg/m ³	1.414
Absorption coefficient (mm ⁻¹)	0.889
Crystal size (mm)	0.30 x 0.18 x 0.18
Theta range for data collection (°)	2.38 to 28.97
Reflections collected	7461
Independent reflections	6568
Data / Restraints / Parameters	7461 / 0 / 309
Final R indices	R1 = 0.0229 wR2 = 0.0516
R indices (all data)	R1 = 0.0294 wR2 = 0.0539

Table 6. Summary of the crystallographic data for compound **10b**.

Heating the sample to 56 °C resulted in coalescence of the two peaks (Figure 29) and corresponds to a ΔG^\ddagger of 16.4 ± 0.2 kcal/mol. It was also apparent that warming the solution resulted in the reversible dissociation of alkyne, although the peaks remained sharp, the rate of intermolecular exchange is slow.

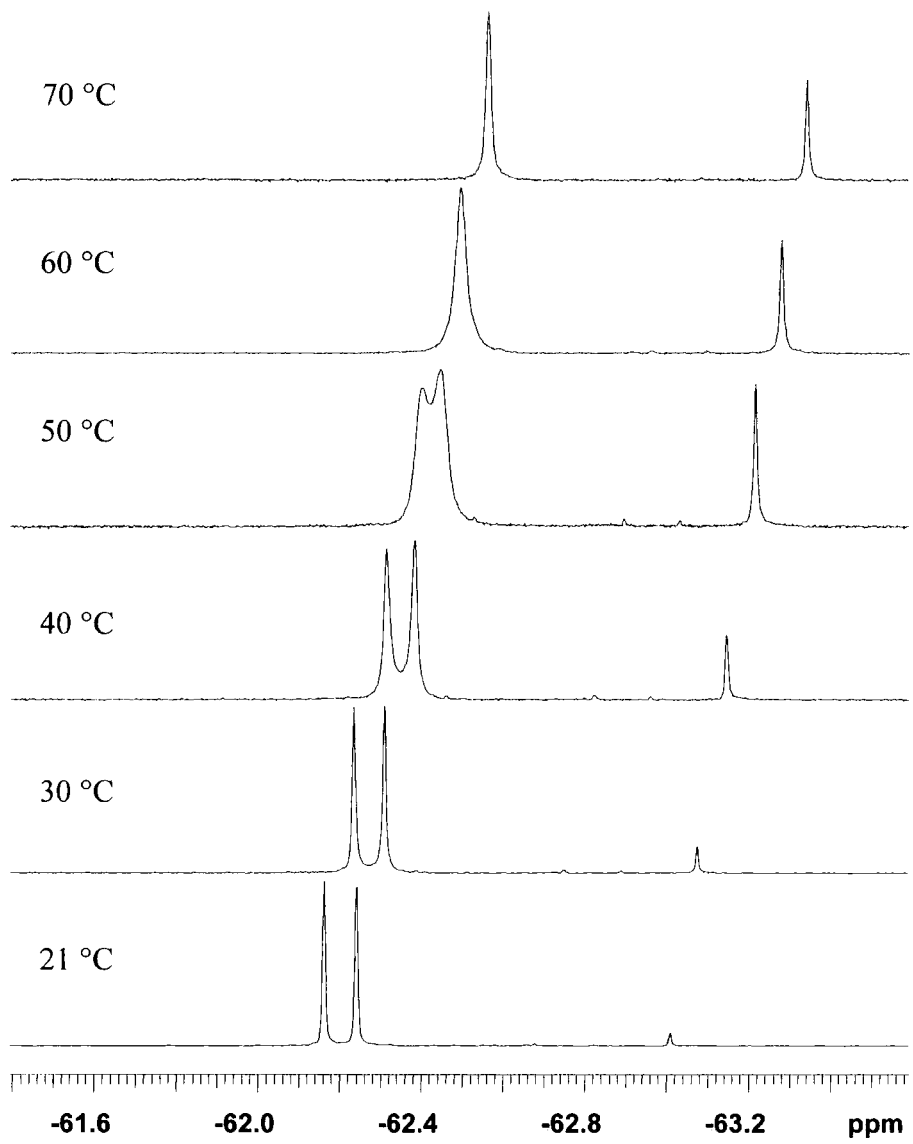


Figure 29. $^{19}\text{F}\{^1\text{H}\}$ NMR stack plot showing CF_3 group coalescence between 50-60 °C and an increased level of dissociation of tolan at higher temperature.

3.4 Conclusions

We have successfully prepared a number of 1:1 Rh(PMe₃)₃Me π -complexes with 1,4-bis(4-R-phenyl)buta-1,3-diyne, that we had previously observed as intermediates in our synthesis of rhodacyclopentadienes. We have also synthesised related Rh-Me π -complexes of 4-R-C₆H₄-C \equiv C-C₆H₄-4-R' tolans, **4** and **5**, to compare these to the proposed intermediates for the Rh-diyne compounds. We have characterised compound **4** by X-ray crystallography which confirms the axial methyl ligand and supports the proposed unsymmetrical coordination of diyne in the RhP₂ plane, **1-3**.

To investigate the intermediates observed during attempts to synthesise rhodacyclopentadienes based on [Rh(PMe₃)₄]Cl, we prepared a number complexes with diynes and tolans and obtained X-ray data on compounds **9** and **10b** which confirm the formation of rotamers **6** and **7**. We have also isolated the unusual centrosymmetric compound [Rh(PMe₃)₃(Cl)]₂(μ -(1,2- η^2): (3,4- η^2)-4-F₃C-C₆H₄-C \equiv C-C \equiv C-C₆H₄-4-CF₃), which crystallises reproducibly and in good yield as two different solvates from THF/C₆D₆ solution.

3.5 Experimental

3.5.1 General

All reactions were carried out using standard Schlenk techniques or in an Innovative Technology Inc. N₂ filled glove box. Solvents were dried before use with appropriate drying agents. The reagents used in synthesis were purchased from commercial suppliers and tested for purity by GC-MS before use. The 1,4-bis(*p*-R-phenyl)buta-1,3-diyne were prepared by Pd/Cu catalysed oxidative homocoupling as described in Chapter 1.

NMR spectra were recorded on Varian Mercury-200, Unity-300 and Inova 500 and Bruker Avance-400 spectrometers at the following frequencies: ¹H – 200, 300, 400, 500 MHz, ¹³C{¹H} – 100 MHz, ³¹P{¹H} – 80, 121, 202 MHz, ¹⁹F{¹H} – 188, 282 MHz in C₆D₆ solvent unless otherwise stated.

Elemental analyses were performed using an Exeter Analytical E440 machine by departmental services at Durham University.

IR spectra were recorded as KBr discs using either a Perkin-Elmer Spectrum 100 series FT-IR spectrometer. Raman spectra were recorded on solid samples using a Horiba Jobin-Yvon LabRamHR Raman microscope with the laser set at 785 nm.

Single-crystal diffraction experiments were carried out on Bruker 3-circle diffractometers with CCD area detectors APEX (4), SMART 6K (9·5C₆D₆, 9·2THF), or SMART 1K (10), using graphite-monochromated Mo-*K*_α radiation ($\lambda = 0.71073 \text{ \AA}$) and Cryostream (Oxford Cryosystems) open-flow N₂ cryostats. The structures were solved by direct methods and refined by full-matrix least squares against F^2 of all data, using SHELXTL software.⁴³ Non-H atoms were refined in anisotropic and H atoms in isotropic approximation.

3.5.2 Synthesis of Rh(PMe₃)₃Me-diyne and -tolan π -complexes

1 - Rh(PMe₃)₃Me(η^2 -1,4-bis(4-methoxyphenyl)buta-1,3-diyne)

The compound 1,4-bis(4-methoxyphenyl)buta-1,3-diyne (0.047 mmol, 12 mg) was dissolved in THF (2 ml) and added dropwise to a stirred solution of Rh(PMe₃)₄Me (0.047 mmol, 20 mg) in THF (1 ml). The solution was stirred for 5 min and then the solvent was removed *in vacuo* to yield a yellow solid which was recrystallised from THF/hexane. Yield: 25 mg, 87 %. ¹H NMR (400 MHz) δ : 7.90 (d, J = 8 Hz, 2H, CH_{arom}), 7.58 (d, J = 9 Hz, 2H, CH_{arom}), 6.89 (d, J = 8 Hz, 2H, CH_{arom}), 6.73 (d, J = 9 Hz, 2H, CH_{arom}), 3.36 (s, 3H, OMe), 3.23 (s, 3H, OMe), 1.31 (d, J = 6 Hz, 9H, PMe₃), 1.22 (d, J = 6 Hz, 9H, PMe₃), 0.92 (d, J = 6 Hz, 9H, PMe₃), -0.01 (m, 3H, Me). ³¹P{¹H} NMR (121 MHz) δ : -12.00 (ddd, ¹ J_{RhP} = 139 Hz, ² J_{PP} = 38 Hz, ² J_{PP} = 24 Hz, 1P_{eq}), -15.60 (dt, ¹ J_{RhP} = 84 Hz, ² J_{PP} = 24 Hz, 1P_{ax}), -18.90 (ddd, ¹ J_{RhP} = 127 Hz, ² J_{PP} = 38 Hz, ² J_{PP} = 24 Hz, 1P_{eq}). Anal. Calcd. for C₂₈H₄₄RhP₃O₂: C, 55.27; H, 7.29. Found: C, 55.42; H, 7.41 %. IR (KBr): ν (arene ring) = 1599, ν (C=C) = 1727, ν (C \equiv C) = 2123 cm⁻¹.

2 - Rh(PMe₃)₃Me(η^2 -1,4-bis(4-trifluoromethylphenyl)buta-1,3-diyne)

The compound 1,4-bis(4-trifluoromethylphenyl)buta-1,3-diyne (0.047 mmol, 16 mg) was dissolved in THF (2 ml) and added dropwise to a stirred solution of Rh(PMe₃)₄Me (0.047 mmol, 20 mg) in THF (1 ml). The solution was stirred for 5 min and then the solvent was removed *in vacuo* to yield an orange/red solid which was recrystallised from hexane. Yield: 28 mg, 87 %. ¹H NMR (400 MHz) δ : 7.74 (d, J = 8 Hz, 2H, CH_{arom}), 7.47 (d, J = 8 Hz, 2H, CH_{arom}), 7.37 (d, J = 8 Hz, 2H, CH_{arom}), 7.25 (d, J = 8 Hz, 2H, CH_{arom}), 1.22 (d, J = 6 Hz, 9H, PMe₃), 1.12 (d, J = 7 Hz, 9H, PMe₃), 0.81 (d, J = 6 Hz, 9H, PMe₃), -0.01 (m, 3H, Me). ³¹P{¹H} NMR (162 MHz) δ : -11.30 (ddd, ¹ J_{RhP} = 138 Hz, ² J_{PP} = 30 Hz, ² J_{PP} = 24 Hz, 1P_{eq}), -16.50 (dt, ¹ J_{RhP} = 83 Hz, ² J_{PP} = 24 Hz, 1P_{ax}), -18.00 (ddd, ¹ J_{RhP} = 127 Hz, ² J_{PP} = 30 Hz, ² J_{PP} = 24 Hz, 1P_{eq}). ¹⁹F{¹H} NMR (188) δ : -62.0 (s, 3F), -62.6 (s, 3F). Anal. Calcd. for C₂₈H₃₈RhP₃F₆: C, 49.14; H, 5.60. Found: C, 48.73; H, 5.67 %. IR (KBr): ν (CF₃) = 1320, ν (arene ring) = 1600, ν (C=C) = 1756, ν (C \equiv C) = 2114 cm⁻¹.

3 - Rh(PMe₃)₃Me(η²-1,4-bis(4-carbomethoxyphenyl)buta-1,3-diyne)

The compound 1,4-bis(4-carbomethoxyphenyl)buta-1,3-diyne (0.047 mmol, 15 mg) was dissolved in THF (2 ml) and added dropwise to a stirred solution of Rh(PMe₃)₄Me (0.047 mmol, 20 mg) in THF (1 ml). The solution was stirred for 5 min and then the solvent was removed *in vacuo* to yield a red solid which was recrystallised from THF/hexane. Yield: 28 mg, 90 %. ¹H NMR (400 MHz) δ: 8.23 (d, *J* = 8 Hz, 2H, CH_{arom}), 8.09 (d, *J* = 8 Hz, 2H, CH_{arom}), 7.87 (d, *J* = 8 Hz, 2H, CH_{arom}), 7.49 (d, *J* = 8 Hz, 2H, CH_{arom}), 3.52 (s, 3H, CO₂Me), 3.47 (s, 3H, CO₂Me), 1.20 (d, *J* = 6 Hz, 9H, PMe₃), 1.11 (d, *J* = 6 Hz, 9H, PMe₃), 0.81 (d, *J* = 6 Hz, 9H, PMe₃), -0.01 (m, 3H, Me). ³¹P{¹H} NMR (121 MHz) δ: -11.40 (ddd, ¹*J*_{RhP} = 137 Hz, ²*J*_{PP} = 31 Hz, ²*J*_{PP} = 24 Hz, 1P_{eq}), -16.44 (dt, ¹*J*_{RhP} = 83 Hz, ²*J*_{PP} = 24 Hz, 1P_{ax}), -18.20 (ddd, ¹*J*_{RhP} = 126 Hz, ²*J*_{PP} = 31 Hz, ²*J*_{PP} = 24 Hz, 1P_{eq}). Anal. Calcd. for C₃₀H₄₄RhP₃O₄: C, 54.22; H, 6.67. Found: C, 54.34; H, 6.92 %. IR (KBr): ν_(arene ring) = 1591, ν_(C=C) = 1714, ν_(C≡C) = 2119 cm⁻¹.

4 - Rh(PMe₃)₃Me(η²-MeO-4-C₆H₄-C≡C-C₆H₄-4-CN)

A solution of 4-MeO-C₆H₄-C≡C-C₆H₄-4-CN (0.118 mmol, 28 mg) in THF (1 ml) was added to a rapidly stirred solution of Rh(PMe₃)₄Me (0.118 mmol, 50 mg) in THF (2 ml) and the resulting solution was stirred for 5 min after which the THF was removed *in vacuo*. The resulting solid was washed with hexane and dried *in vacuo* to give the product as an orange solid. Yield: 67 mg, 98 %. A small amount of the product was dissolved in toluene and the solution was layered with hexane yielding single crystals suitable for X-ray analysis. ¹H NMR (400 MHz) δ: 7.55 (d, *J* = 8 Hz, 2H, CH_{arom}), 7.42 (d, *J* = 8 Hz, 2H, CH_{arom}), 7.15 (d, *J* = 8 Hz, 2H, CH_{arom}), 6.86 (d, *J* = 8 Hz, 2H, CH_{arom}), 1.14 (d, ²*J* = 6 Hz, 9H, PMe₃), 1.08 (d, ²*J* = 6 Hz, 18H, PMe₃), 0.77 (d, *J* = 6 Hz, 9H, PMe₃), -0.23 (m, 3H, Me). ³¹P{¹H} NMR (121 MHz) δ: -15.86 (m, 2P), -18.50 (m, 1P). Anal. Calcd. for C₂₅H₃₅F₆P₃ClRh₂: C, 53.89; H, 7.13; N, 2.42. Found: C, 53.41; H, 7.21; N, 2.79 %. IR (KBr): ν_(arene ring) = 1585, ν_(C=C) = 1749, ν_(C≡N) = 2215 cm⁻¹. Raman (solid): ν_(arene ring) = 1579, ν_(coord C≡C) = 1752, ν_(C≡N) = 2211 cm⁻¹.

5 - Rh(PMe₃)₃Me(η²-4-F₃C-C₆H₄-C≡C-C₆H₄-4-CF₃)

The compound Rh(PMe₃)₄Me (0.118 mmol, 50 mg) was dissolved in THF (2 ml). To this, 4,4'-bis(4-trifluoromethyl)tolan (0.118 mmol, 37 mg) in THF (2 ml) was added dropwise and the resulting solution was stirred for 5 min after which the THF was removed *in vacuo*. The resulting solid was washed with hexane and dried *in vacuo* to give analytically pure product as a yellow solid. Yield: 71 mg, 91 %. ¹H NMR (400 MHz) δ: 7.48 (d, (AB), *J* = 8 Hz, 4H, CH_{arom}), 7.42 (d, (AB), *J* = 8 Hz, 4H, CH_{arom}), 1.07 (s, 18H, PMe₃), 0.74 (d, *J* = 6 Hz, 9H, PMe₃), -0.16 (m, 3H, Me). ³¹P{¹H} NMR (162 MHz) δ: -17.36 (m, 3P). ¹⁹F{¹H} NMR (188 Hz) δ: -61.89 (s, 6F, CF₃). Anal. Calcd. for C₂₆H₃₈F₆P₃Rh: C, 47.29; H, 5.80. Found: C, 47.55; H, 5.83 %. IR (KBr): ν_(CF₃) = 1320, ν_(arene ring) = 1600, ν_(C=C) = 1756 cm⁻¹. Raman (solid): ν_(arene ring) = 1596, ν_(coord C=C) = 1757 cm⁻¹.

3.5.3 Synthesis of Rh(PMe₃)₃Cl-diyne and -tolan π-complexes

9 - [Rh(PMe₃)₃(Cl)]₂(μ-(1,2-η²):(3,4-η²)-4-F₃C-C₆H₄-C≡C-C≡C-C₆H₄-4-CF₃)

The compound [Rh(PMe₃)₄]Cl (20 mg, 0.045 mmol) was suspended in THF (1 ml). To this, 1,4-bis(4-trifluoromethylphenyl)buta-1,3-diyne (15 mg, 0.045 mmol) in THF (2 ml) was added dropwise and the resulting solution was stirred for 5 min after which the THF was removed *in vacuo*. A further portion of THF (2 ml) was added and the solution was stirred for an additional 5 min and again evacuated to dryness. This cycle was repeated two more times to remove dissociated PMe₃. Most of the sample was dissolved in C₆D₆ and a ¹H NMR spectrum (400 MHz) was recorded. δ: 8.15 (d, *J* = 8 Hz, CH_{arom}), 7.65 (d, *J* = 8 Hz, CH_{arom}), 7.54 (d, *J* = 8 Hz, CH_{arom}), 7.90 (d, *J* = 8 Hz, CH_{arom}), 7.39-7.21 (m, CH_{arom}), 1.38 (d, *J* = 7 Hz, PMe₃), 1.36 (d, *J* = 7 Hz, 2PMe₃), 1.22 (vt, *J* = 3 Hz, 2PMe₃), 1.18 (vt, *J* = 3 Hz, 2PMe₃). The solvent was removed and the entire sample was redissolved in THF/C₆D₆ and the ³¹P{¹H} and ¹⁹F{¹H} NMR were recorded. ³¹P{¹H} NMR (121 MHz) δ: -1.61 (dd, ¹*J*_{RhP} = 97 Hz, ²*J*_{PP} = 37 Hz), -2.86 (dd, ¹*J*_{RhP} = 97 Hz, ²*J*_{PP} = 35 Hz), -11.36 (dt, ¹*J*_{RhP} = 141 Hz, ²*J*_{PP} = 35 Hz), -16.49 (dt, ¹*J*_{RhP} = 135 Hz, ²*J*_{PP} = 37 Hz). ¹⁹F{¹H} NMR (188 Hz) δ: -62.32 (s, CF₃), -62.40 (s, CF₃), -62.76 (s, CF₃), -62.90 (s, CF₃). Crystals precipitated on standing overnight. Isolated yield of 4: 12 mg, 50 % based

on Rh. Anal. Calcd. for $C_{36}H_{62}F_6P_6Cl_2Rh_2 \cdot C_6D_6$: C, 43.65; H, 6.45. Found: C, 43.59; H, 6.50 %. Note that the analysis is excellent for a solvate containing one molecule of C_6D_6 but we observe two different solvates in the single crystals. It is thus not clear what or exactly how much solvent is contained in the elemental analysis sample as inclusion of two molecules of THF also gives a reasonable but not quite as good fit to the observed data. IR of reaction solution (THF): $\nu_{(\text{free } C\equiv C)} = 2177, 2139$, $\nu_{(\text{arene ring})} = 1598 \text{ cm}^{-1}$. IR of crystalline solid (KBr): $\nu_{(\text{coord } C\equiv C)} = 2134$ (w), $\nu_{(\text{arene ring})} = 1598 \text{ cm}^{-1}$. Raman of crystalline solid (KBr): $\nu_{(\text{coord } C\equiv C)} = 1731$, $\nu_{(\text{arene ring})} = 1599 \text{ cm}^{-1}$.

10 - $Rh(PMe_3)_3Cl(\eta^2\text{-MeO-4-C}_6\text{H}_4\text{-C}\equiv\text{C-C}_6\text{H}_4\text{-4-CN})$

The compound MeO-4-C₆H₄-C≡C-C₆H₄-4-CN (0.045 mmol, 11 mg) in THF (1ml) was added dropwise to a rapidly stirred suspension of $[Rh(PMe_3)_4]Cl$ (0.045 mmol, 20 mg) in THF (2 ml). The resulting solution was stirred for 5 min and then the solvent was removed *in vacuo*. The residual solid was washed with hexanes and then dried *in vacuo*. The subsequent NMR spectroscopy experiments showed there to be two isomers, A and B, formed in ca. 3:2 ratio. Layering of a toluene solution of the mixture with hexane in a 5 mm glass tube allowed for the formation of a few single-crystals. X-ray analysis of these crystals revealed them to be of a single isomer. Isomer A - ¹H NMR (400 MHz) δ : 8.20 (d, $J = 8$ Hz, 2H, CH_{arom}), 7.51 (d, $J = 8$ Hz, 2H, CH_{arom}), 7.25 (d, $J = 8$ Hz, 2H, CH_{arom}), 7.09 (d, $J = 8$ Hz, 2H, CH_{arom}), 3.36 (s, 3H, OMe), 1.28 (d, $J = 6$ Hz, 9H, PMe₃ *trans* C), 0.91 (vt, $J = 4$ Hz, 18H, PMe₃ *trans* PMe₃). ³¹P{¹H} NMR (162 MHz) δ : -0.43 (dd, ¹ $J_{Rh-P} = 100$ Hz, ² $J_{P-P} = 40$ Hz, 2P, P *trans* to P), -18.68 (dt, ¹ $J_{Rh-P} = 133$ Hz, ² $J_{P-P} = 40$ Hz, 1P, P *trans* to C). Isomer B - ¹H NMR (400 MHz) δ : 8.36 (d, $J = 8$ Hz, 2H, CH_{arom}), 7.37 (d, $J = 8$ Hz, 2H, CH_{arom}), 6.89 (d, $J = 8$ Hz, 2H, CH_{arom}), 6.82 (d, $J = 9$ Hz, 2H, CH_{arom}), 3.34 (s, 3H, OMe), 1.27 (d, $J = 6$ Hz, 9H, PMe₃ *trans* C), 0.91 (t, $J = 4$ Hz, 18H, PMe₃ *trans* PMe₃). ³¹P{¹H} NMR (162 MHz) δ : -1.05 (dd, ¹ $J_{Rh-P} = 101$ Hz, ² $J_{P-P} = 40$ Hz, 2P, P *trans* to P), -19.61 (dt, ¹ $J_{Rh-P} = 132$ Hz, ² $J_{P-P} = 40$ Hz, 1P, P *trans* to C). IR (KBr): $\nu_{(\text{arene ring})} = 1587$, $\nu_{(C=C)} = 1764$, $\nu_{(C\equiv N)} = 2215 \text{ cm}^{-1}$. Raman (solid): $\nu_{(\text{arene ring})} = 1601$, $\nu_{(C\equiv N)} = 2215 \text{ cm}^{-1}$.

11 - Rh(PMe₃)₃Cl(η²-F₃C-4-C₆H₄-C≡C-C₆H₄-4-CF₃)

The compound [Rh(PMe₃)₄]Cl (0.113 mmol, 50 mg) was suspended in THF (2 ml). To this, 4,4'-bis(4-trifluoromethyl)tolan (0.113 mmol, 36 mg) in THF (2 ml) was added dropwise and the resulting solution was stirred for 5 min after which the THF was removed *in vacuo*. The resulting solid was washed with hexanes and dried *in vacuo* to give pure product as an orange solid. Yield: 66 mg, 86 %. ¹H NMR (400 MHz) δ: 8.28 (d, *J* = 8 Hz, CH_{arom}, 2H), 7.50 (d, *J* = 8 Hz, 2H, CH_{arom}), 7.46 (d, (AB)', *J* = 8 Hz, 2H, CH_{arom}), 7.41 (d, (AB)', *J* = 8 Hz, 2H, CH_{arom}), 1.24 (d, *J* = 6 Hz, 9H, PMe₃), 0.86 (vt, *J* = 3 Hz, 18H, PMe₃). ³¹P{¹H} NMR (121 MHz) δ: -2.32 (dd, ¹*J*_{Rh-P} = 98 Hz, ²*J*_{P-P} = 40 Hz, 2P, P *trans* to P), -20.12 (dt, ¹*J*_{Rh-P} = 133 Hz, ²*J*_{P-P} = 40 Hz, 1P, P *trans* to C). ¹⁹F{¹H} NMR (188 Hz) δ: -62.18 (s, 3F, CF₃), -62.26 (s, 3F, CF₃). Anal. Calcd. for C₂₅H₃₅F₆P₃ClRh: C, 44.10; H, 5.18. Found: C, 43.85; H, 5.37 %. IR (KBr): ν_(CF₃) = 1319, ν_(arene ring) = 1602, ν_(C=C) = 1780 cm⁻¹. Raman (solid): ν_(arene ring) = 1600, ν_(coord C=C) = 1784 cm⁻¹.

3.6 References

- 1) P. J. Low, M. I. Bruce, *Adv. Organomet. Chem.*, 2001, **48**, 71.
- 2) R. M. Ward, A. S. Batsanov, J. A. K. Howard, T. B. Marder, *Inorg. Chim. Acta*, 2006, **359**, 3671.
- 3) (a) T. Rappert, O. Nurnberg, H. Werner, *Organometallics*, 1993, **12**, 1359; (b) H. Werner, O. Gevert, P. Steinert, J. Wolf, *Organometallics*, 1995, **14**, 1786; (c) H. Werner, M. Schafer, J. Wolf, K. Peters, H. G. von Schnering, *Angew. Chem. Int. Ed.*, 1995, **34**, 191; (d) H. Werner, O. Gevert, P. Haquette, *Organometallics*, 1997, **16**, 803; (e) H. Werner, R. W. Lass, O. Gevert, J. Wolf, *Organometallics*, 1997, **16**, 4077; (f) H. Werner, P. Schaub, *J. Chem. Soc., Dalton Trans.*, 1994, **23**, 3415.
- 4) S. Yamazaki, A. J. Deeming, D. M. Speel, *Organometallics*, 1998, **17**, 775.
- 5) J. B. B. Hayns, F. G. A. Stone, *J. Organomet. Chem.*, 1978, **160**, 335.
- 6) J. K. D. Surette, M.-A. MacDonald, M. J. Zaworotko, R. D. Singer, *J. Chem. Cryst.*, 1994, **24**, 715.
- 7) N. E. Leadbeater, *J. Organomet. Chem.*, 1999, **573**, 211.
- 8) N. E. Leadbeater, P. R. Raithby, *J. Coord. Chem.*, 2001, **53**, 311.
- 9) S. Yamazaki, Z. Taira, T. Yonemura, A. J. Deeming, *Organometallics*, 2005, **24**, 20.
- 10) H. S. Huh, Y. K. Lee, S. W. Lee, *J. Mol. Struct.*, 2006, **789**, 209.
- 11) C. V. Ursini, G. H. M. Dias, M. Hörner, A. J. Bortoluzzi, M. K. Morigaki, *Polyhedron*, 2000, **19**, 2261.
- 12) M. I. Bruce, P. J. Low, A. Werth, B. W. Skelton, A. H. White, *J. Chem. Soc., Dalton Trans.*, 1996, **8**, 1551.
- 13) C. P. Casey, S. Chung, Y. Ha, D. R. Howell, *Inorg. Chim. Acta*, 1997, **265**, 127.
- 14) N. W. Alcock, A. F. Hill, R. P. Melling, A. R. Thompsett, *Organometallics*, 1993, **12**, 641.
- 15) a) K. Stahl, F. Weller, K. Dehnicke, *Z. Anorg. Allg. Chem.*, 1990, **591**, 125; b) A. Werth, K. Dehnicke, D. Fenske, G. Baum, *Z. Anorg. Allg. Chem.*, 1984, **518**, 175.
- 16) J. Chen, I. A. Guzei, L. K. Woo, *Inorg. Chem.*, 2000, **39**, 3715.
- 17) C. Garcia-Yebra, F. Carrero, C. Lopez-Mardomingo, M. Fajardo, A. Rodriguez, A. Antindo, A. Otero, D. Lucas, Y. Mugnier, *Organometallics*, 1999, **18**, 1287.
- 18) B. Castellano, E. Solari, C. Floriani, N. Re, A. Chiesi-Villa, C. Rizzoli, *Chem. Eur. J.*, 1999, **5**, 722.

- 19) C. Gauss, D. Veghini, H. Berke, *Chem. Ber.*, 1997, **130**, 183.
- 20) S. Pulst, P. Arndt, B. Heller, W. Baumann, R. Kempe, U. Rosenthal, *Angew. Chem.*, 1996, **35**, 1112.
- 21) C. J. Adams, M. I. Bruce, E. Horn, E. R. T. Tiekink, *J. Chem. Soc., Dalton Trans.*, 1992, **7**, 1157.
- 22) F. H. Allen, R. Taylor, *Chem. Soc. Rev.*, 2004, **33**, 463.
- 23) U. Rosenthal, S. Pulst, P. Arndt, A. Ohff, A. Tillack, W. Baumann, R. Kempe, V. V. Burlakov, *Organometallics*, 1995, **14**, 2961.
- 24) C. M. Forsyth, S. P. Nolan, C. L. Stern, T. J. Marks, A. L. Rheingold, *Organometallics*, 1993, **12**, 3618.
- 25) M. Kersting, K. Dehnicke, D. Fenske, *J. Organomet. Chem.*, 1986, **309**, 125.
- 26) R. Choukroun, B. Donnadiou, I. Malfant, S. Haubrich, R. Frantz, C. Guerin, B. Henner, *Chem. Commun.*, 1997, 2315.
- 27) W. Bonrath, K.-R. Pörschke, G. Wilke, K. Angermund, C. Kruger, *Angew. Chem.*, 1998, **27**, 833.
- 28) D. J. Mindiola, R. Waterman, D. M. Jenkins, G. L. Hillhouse, *Inorg. Chim. Acta*, 2003, **345**, 299.
- 29) U. Rosenthal, S. Pulst, R. Kempe, K.-R. Pörschke, R. Goddard, B. Proft, *Tetrahedron*, 1998, **54**, 1277.
- 30) R. E. Marsh, *Acta Crystallogr. Sect. B*, 2002, **58**, 893.
- 31) G. G. Cash, R. C. Pettersen, *J. Chem. Soc., Dalton Trans.*, 1979, 1630.
- 32) Y. Wang, H.-P. Wang, H. Wang, H.-S. Chan, Z. Xie, *J. Organomet. Chem.*, 2003, **683**, 39.
- 33) G. V. Noshchenko, B. M. Mychalichko, V. N. Davydov, *Koord. Khim.*, 2003, **29**, 280.
- 34) E. V. Dikarev, N. S. Goroff, M. A. Petrukhina, *J. Organomet. Chem.*, 2003, **683**, 337.
- 35) a) W. J. Evans, R. A. Keyer, H. Zhang, J. L. Atwood, *Chem. Commun.*, 1987, 837; b) W. J. Evans, R. A. Keyer, J. W. Ziller, *Organometallics*, 1990, **9**, 2628.
- 36) F. Schager, W. Bonrath, K.-R. Pörschke, M. Kessler, C. Kruger, K. Seevogel, *Organometallics*, 1997, **16**, 4276.
- 37) C. Müller, R. J. Lachiotte, W. D. Jones, *Organometallics*, 2002, **21**, 1190.
- 38) C. Müller, R. J. Lachiotte, W. D. Jones, *Organometallics*, 2002, **21**, 1975.
- 39) A. Tillack, S. Pulst, H. Baudisch, K. Kortus, U. Rosenthal, *J. Organomet. Chem.*, 1997, **532**, 117.
- 40) A. R. Rossi, R. Hoffmann, *Inorg. Chem.*, 1975, **14**, 365.

- 41) F. Somera, A. Scott, W. Clegg, T. B. Marder, unpublished results.
- 42) A. S. Batsanov, J. C. Collings, I. J. S. Fairlamb, J. P. Holland, J. A. K. Howard, Z. Lin, T. B. Marder, A. C. Parsons, R. M. Ward, J. Zhu, *J. Org. Chem.*, 2005, **70**, 703.
- 43) G. M. Sheldrick, *SHELXTL*, version 6.14; Bruker-Nonius AXS, Madison, Wisconsin, U.S.A., 2003.

Chapter 4

Conclusions and suggestions for future work

4.1 Conclusions

This thesis has reported the synthesis and characterisation of a number of novel, luminescent rhodacyclopentadienes, formed by the regiospecific reductive coupling of two equivalents of 1,4-bis(4-R-phenyl)buta-1,3-diyne with $\text{Rh}(\text{PMe}_3)_4\text{X}$ ($\text{X} = -\text{CCTMS}$, $-\text{C}\equiv\text{C}-\text{C}_6\text{H}_4-4-\text{NMe}_2$, $-\text{C}\equiv\text{C}-\text{C}_6\text{H}_4-\text{C}\equiv\text{C}-\text{C}_6\text{H}_4-4-\text{NHex}_2$, $-\text{C}\equiv\text{C}-\text{C}\equiv\text{C}-\text{C}_6\text{H}_4-4-\text{NPh}_2$, Me, Cl) to give the *mer,cis*-[tris(trimethylphosphine)-X-2,5-bis(4-R-phenylethynyl)-3,4-bis(4-R-phenyl)rhodacyclopenta-2,4-diene] isomer exclusively. A range of substituted diynes have been utilised and their effect on the optical properties of the compounds is reported. The metallacycles are found to absorb in the UV-vis region, with absorption maxima between 453 nm and 544 nm and these chromophores are also luminescent at room temperature in solution in the range 496-631 nm, with fluorescent lifetimes indicative of emission from a singlet state. Both donor and acceptor R substituents shift the absorption and emission maxima bathochromically, and the effect of acceptor groups is found to be significantly greater than that for donors. Changing the $\text{C}\equiv\text{C}-\text{TMS}$ ligand to an acetylide with increased conjugation had little effect on the overall optical properties, which is related to unfavourable steric interactions between the ligand and the metallacycle. This is supported by the numerous structures which have been characterised by single-crystal X-ray crystallography. The Cl derivative was found to have similar absorption and emission properties to the acetylide-substituted rhodacycles, however, unlike these, the Me analogues are not luminescent at room temperature in solution. Slight shifts to lower energy for the absorption maxima for the Me and Cl derivatives are consistent with the stronger donation of the Me and Cl ligands compared to an acetylide which is also supported by the $J_{\text{Rh-P}}$ values in the $^{31}\text{P}\{^1\text{H}\}$ NMR spectrum. The shift in absorption and emission with different ligand types demonstrates that the metal does have a role in the overall photophysical properties of the system and is not solely acting as a tether for the organic fragment.

It has also been shown that slowly, and under forcing conditions only, the rhodacycles will react with additional diyne, forming 1,2,4-tris(4-R-phenylethynyl)-3,5,6-tris(4-R-phenyl)benzenes regiospecifically. The cyclotrimers are highly luminescent, and

the optical properties are reported and shown to be significantly different to the rhodacycles. The X-ray structure of the parent compound, 1,2,4-tris(phenyl)-2,5,6-tri(phenyl)benzene confirms the regioselectivity of cyclotrimer formation.

We have observed intermediates during the synthesis of the Rh-Me and Rh-Cl-based rhodacycles and these diyne π -complexes, along with related symmetrical and unsymmetrical tolan π -complexes, have been isolated and these are used to propose a mechanism for rhodacycle formation. We have also demonstrated that it is possible to form unsymmetrical rhodacycles by reaction of a 1:1 Rh-diyne π -complex with a second equivalent of a different diyne; however, due to the reversible nature of the bis(diyne) π -complex formation, the compounds are formed as a mixture of isomers. In our work on Rh-Cl-based rhodacycles, we have isolated the unusual centrosymmetric $[\text{Rh}(\text{PMe}_3)_3(\text{Cl})]_2(\mu-(1,2-\eta^2):(3,4-\eta^2)-4\text{-F}_3\text{C-C}_6\text{H}_4\text{-C}\equiv\text{C-C}\equiv\text{C-C}_6\text{H}_4\text{-4-CF}_3)$ bi-metallic complex which has been characterised by X-ray crystallography.

4.2 Suggestions for future work

This thesis has primarily looked at the effect of the *para*-substituent of the 1,4-bis(4-R-phenyl)buta-1,3-diyne on the photophysical properties of a number of rhodacyclopentadienes which are shown to have dramatic controlling effects on absorption and emission. We have also studied the effect of changing the ligand on Rh from acetylides of varying conjugation length to Me and Cl. Increasing conjugation length of acetylide ligands had little effect on the optical properties of the compounds due to unfavourable arene-arene interactions which result in decoupling of the conjugation between ligand and metallacycle. Although we see no emission from the Rh-Me analogues, use of Me and Cl ligands which are stronger donors than the acetylides does result in a shift in the absorption and, in the Rh-Cl case, emission maxima to lower energy. This strongly suggests that the metal does have a role in the controlling the photophysical properties of the rhodacycles and does not act solely as a tether for the

organic fragment, thus, it is worth pursuing alternatives that not only increase electron density at Rh, but also to increase the degree of conjugation within the system.

It may be possible to use $-\text{C}\equiv\text{C}-\text{OEt}$ as a ligand on Rh and this is important for two reasons; a) The OEt group is not as big as a phenyl ring and as such, should not interfere with the co-planarity of phenyl ring *ii* (see Chapter 2 for schematic for ring numbering system) with the metallacycle; indeed, favourable arene $\text{CH}\cdots\text{O}$ interactions should actually favour a planar rhodacycle geometry. The Et group should not cause any steric problems as this would not be directed towards the rhodacycle, and b) Lone pair electrons on oxygen should be able to conjugate with the metallacycle *via* the acetylide, thus increasing the overall conjugation within the system (Figure 1).

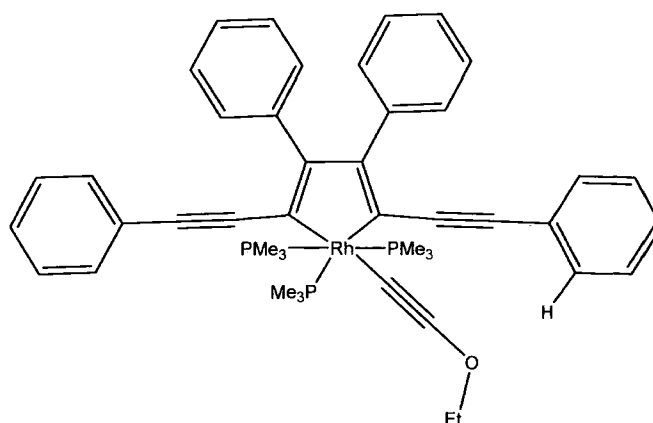


Figure 1. Substituted rhodacycle with favourable $\text{CH}\cdots\text{O}$ interactions.

The synthesis and characterisation of a rhodacycle prepared from 1,4-bis(4-dicyanovinylphenyl)buta-1,3-diyne should be re-examined. Initial results are promising, and it may be possible that the rhodacycle can be successfully prepared under suitable conditions. Solubility of both diyne and subsequent adducts was a problem with the TMSA derivative and so using $\text{Rh}(\text{PMe}_3)_4-(\text{C}\equiv\text{C}-\text{C}_6\text{H}_4)_n-4-\text{NHEx}_2$ ($n = 1, 2$) could reduce this problem.

The diynes used have so far been restricted to those with two butadiyne linked phenyl rings, $R-4-C_6H_4-C\equiv C-C\equiv C-C_6H_4-4-R$. Using the recently developed chemistry of $HCC-C_6H_4-CC-TMS$, however, we are easily able to prepare longer diynes with four aryl rings, $R-4-C_6H_4-C\equiv C-C_6H_4-C\equiv C-C\equiv C-C_6H_4-C\equiv C-C_6H_4-4-R$, in conjugation. These diynes can be derivatised with groups such as $-CF_3$, $-NHex_2$ and $-CO_2C_8H_{17}$, such that solubility should not be a problem and, if reductively coupled on Rh, these products should offer a greatly increased conjugation length within the rhodacycles (Figure 2) and hence have a dramatic effect on the observed luminescence. Increasing conjugation length, even with donor *para*-substituents, may also result in luminescence that is red-shifted to an energy that is comparable with that of the strong acceptors.

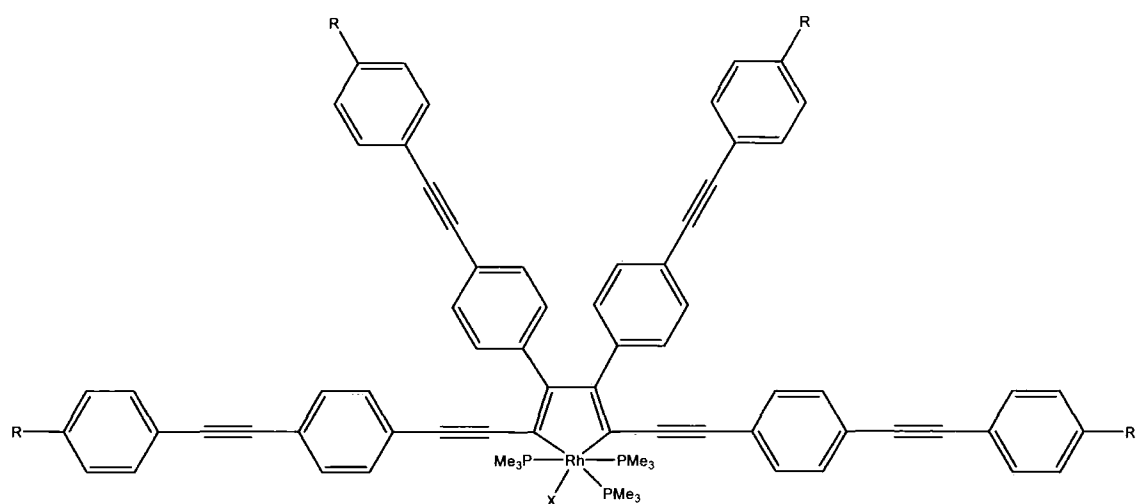


Figure 2. Rhodacycle prepared by reductive coupling of two equivalents of $R-4-C_6H_4-C\equiv C-C_6H_4-C\equiv C-C\equiv C-C_6H_4-C\equiv C-C_6H_4-4-R$ with $R(PMe_3)_4X$.

Chapter 3 discusses the mechanism of rhodacycle formation and illustrates that if one equivalent of diyne is added to a preformed Rh-diyne π -complex, a mixture of products, and not a single rhodacycle is observed. Use of column chromatography or HPLC could mean that it is possible to separate the mixture to obtain the four different rhodacycles that were formed. Further work into the compatibility of the rhodacycles

with silica gel and HPLC columns could result in the isolation of unsymmetrical donor-acceptor rhodacyclopentadienes, and their optical properties could then be examined.

All of the rhodacycles synthesised for this thesis have been formed from the reductive coupling of symmetrical diynes on Rh. There are a number of routes to unsymmetrical donor-acceptor diynes and so it would be interesting to synthesise rhodacycles from diynes of this type. A number of possible products could be formed and so separation by chromatographic means may well be necessary. Assuming the metallacycle formation reaction proceeds with the same regioselectivity with unsymmetrical diynes as it does with symmetrical diynes, the diyne $\text{O}_2\text{N}-4\text{-C}_6\text{H}_4\text{-C}\equiv\text{C-C}\equiv\text{C-C}_6\text{H}_4\text{-4-OR}$ ($\text{R} = \text{C}_8\text{H}_{17}$) offers two advantages; a) the NO_2 group is a strong acceptor and the OR group is a moderate donor and so combinations of NO_2/NO_2 (A), OR/OR (B), NO_2/OR (C) and OR/ NO_2 (D) (Figure 3) should result in optical properties that are different for each of the isomers, as only the substituents at the 2,5-bis(*p*-R-arylethynyl) positions are conjugated with the metallacycle, as steric crowding results in the rotation of the aryl rings at the 3 and 4 positions, and b) the long alkyl groups will increase the solubility of the system.

It would be of particular interest to study the emission properties of the rhodacycles at low temperature and in degassed solutions, to probe whether any emission from the triplet state is observed. In solution at room temperature, only singlet lifetimes were observed although this may be due to triplet quenching by traces of molecular oxygen and/or energy loss from the triplet state by vibrational relaxation (internal conversion).

It is important to attempt to apply the chemistry developed for the Rh system to other metals such as Ir and Pt. Use of 3rd row transition metals greatly increases the possibility of intersystem crossing to the triplet state and hence phosphorescent emission, important in applications such as OLEDs.

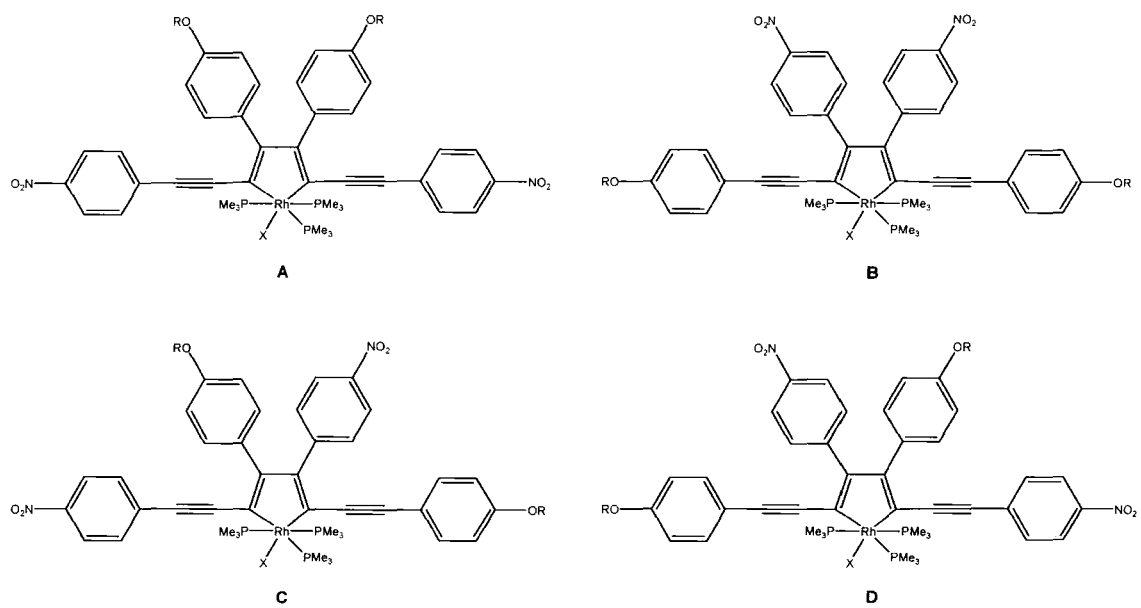


Figure 3. Four possible regioisomers formed by the reductive coupling of two equivalents of an unsymmetrical diyne with $\text{Rh}(\text{PMe}_3)_4\text{X}$.